

Tsim, Selina (2018) *Diagnostic and prognostic biomarkers of malignant pleural mesothelioma*. PhD thesis.

<https://theses.gla.ac.uk/30687/>

Copyright and moral rights for this work are retained by the author

A copy can be downloaded for personal non-commercial research or study, without prior permission or charge

This work cannot be reproduced or quoted extensively from without first obtaining permission in writing from the author

The content must not be changed in any way or sold commercially in any format or medium without the formal permission of the author

When referring to this work, full bibliographic details including the author, title, awarding institution and date of the thesis must be given

Diagnostic and Prognostic Biomarkers of Malignant Pleural Mesothelioma

Selina Tsim MBChB MRCP(UK)

**Submitted in fulfilment of the requirements for the degree of
Doctor of Philosophy**

Institute of Cancer Sciences

College of Medical and Veterinary Life Sciences

University of Glasgow

March 2018

Summary

Malignant Pleural Mesothelioma (MPM) is an aggressive intrathoracic malignancy with an overall poor prognosis. MPM is associated with asbestos exposure but has a long latency period between exposure and disease development. Incidence of MPM in the UK is therefore still rising, predicted to reach a peak in 2020. The majority of patients with MPM present with breathlessness, frequently due to a pleural effusion and/or chest pain. Diagnosis of MPM can be difficult.

Radiological detection of early stage MPM in particular can be challenging, as pleural tumour, nodularity or significant pleural thickening may not be evident. Diagnosis is further complicated by the low yield of pleural fluid cytology examination in MPM and pleural biopsy is therefore usually required to allow definitive diagnosis. This can be achieved under image guidance, at surgical thoracoscopy or at local anaesthetic thoracoscopy (LAT). A significant number of patients are either elderly or have co-morbidity precluding general anaesthesia and surgical thoracoscopy. Image-guided pleural biopsy is not always feasible, particularly in the absence of significant pleural thickening. LAT remains a limited resource in the UK.

A non-invasive biomarker of MPM, which could be performed early in the patient's presentation, and that could be available to most hospitals, would therefore be a major clinical advance, allowing clinicians to direct appropriate patients to specialist centres with access to LAT and specialist MDT input where MPM appears likely. There have been several potential blood biomarkers identified in the mesothelioma literature, including the most widely studied, Mesothelin, and more recently Fibulin-3 and SOMAscan™. Unfortunately study results have been variably limited by retrospective study design, inconsistent sampling time points, inconsistent results and lack of external validation, therefore despite initial promising results, none of these biomarkers have entered routine clinical practice for diagnosis. Similarly, utility of imaging biomarkers such as perfusion Computed Tomography (CT), Positron Emission Tomography (PET) and Dynamic Contrast Enhanced Magnetic Resonance Imaging (DCE-MRI) has been limited by high radiation dose, limited availability, and requirement for bulky (and therefore late stage) disease for assessment respectively.

In chapter 2, study design, recruitment and preliminary results of the DIAPHRAGM (Diagnostic and Prognostic Biomarkers in the Rational Assessment of Mesothelioma) study are reported. A prospective, multi-centre study was designed, recruiting patients with suspected pleural malignancy (SPM) at initial presentation to secondary care services, from a mixture of academic and more clinical units in the UK and Ireland, in addition to asbestos-exposed control subjects. In one of the largest biomarker studies in mesothelioma to date, 639 patients with SPM and 113 asbestos-exposed control subjects were recruited over three years. Data cleaning is being finalised by the Cancer Research UK Clinical Trials Unit Glasgow at the time of writing. Preliminary results reveal that 26% (n=154) patients recruited to the SPM cohort were diagnosed with MPM, 33% (n=209) had secondary pleural malignancy and 34% (n=218) were diagnosed with benign pleural disease. A final diagnosis is awaited in 7% (n=47) at the time of writing. SOMAscan™ and Fibulin-3 biomarker analyses are ongoing and DIAPHRAGM will definitively answer the question of diagnostic utility of these blood biomarkers in routine clinical practice, in a ‘real-life’ MPM population, relative to that of Mesothelin.

In chapter 3, contrast-enhanced MRI was performed in patients with suspected MPM and a novel MRI biomarker of pleural malignancy defined (Early Contrast Enhancement - ECE). ECE was defined as a peak in pleural signal intensity at or before 4.5 minutes after intravenous Gadobutrol administration. ECE assessment was successfully performed in all patients who underwent contrast-enhanced MRI. This included patients with pleural thickening <10mm (49/58 (84%)), the mean pleural thickness of all patients was 5mm. ECE demonstrated good overall diagnostic performance for the detection of pleural malignancy (sensitivity 83% (95% CI 61 - 94), specificity 83% (95% CI 68 - 91%), positive predictive value 68% (95% CI 47 - 84%), negative predictive value 92% (95% CI 78 - 97%)), comparable to morphology assessment at CT morphology and MRI morphology by experienced thoracic radiologists. In addition, ECE demonstrated good reproducibility (inter-observer $\kappa = 0.864$), superior to subjective morphology assessment at CT and MRI. Mean signal intensity gradient (MSIG), a marker of patient’s contrast enhancement pattern, correlated with tumour Microvessel Density (MVD) using Factor VII immunostain (Spearman’s $\rho = 0.43$, $p=0.02$). Additionally, a high

MSIG ($>0.533\text{AU/s}$), indicative of high tumour vascularity, was associated with poor median overall survival (12 months vs. 20 months, $p=0.047$).

Staging of MPM represents an additional challenge to clinicians. This is due to the complex morphology and often rind-like growth pattern of MPM. In addition, delineation of pleural disease from adjacent structures such as intercostal muscle and diaphragm can be difficult to assess, particularly at CT, which is the most commonly used imaging modality for diagnostic and staging assessment in MPM. Current clinical staging frequently underestimates extent of disease, with a significant proportion of patients being upstaged at time of surgery, and is limited by high inter-observer variability. Recent studies have reported the prognostic significance of CT-derived tumour volume; however, many of these studies have been limited by the laborious or complex nature of tumour segmentation, significant inter-observer variability or challenges encountered in separating pleural tumour from adjacent structures, which are often of similar density. MRI is superior to CT in the detection of invasion of the chest wall and diaphragm in MPM. In Chapter 4, MRI was used to quantitatively assess pleural tumour volume in 31 patients with MPM using novel semi-automated segmentation methodology. Four different segmentation methodologies, using Myrian[®] segmentation software were developed and examined. Optimum methodology was defined, based on the accuracy of volume estimates of an MRI phantom, visual-based analysis, intra-observer agreement and analysis time. Using the optimum methodology, there was acceptable error around the MRI phantom volume (3.6%), a reasonable analysis time (approximately 14 minutes), good intra-observer agreement (intra-class correlation coefficient (ICC) 0.875) and excellent inter-observer agreement (ICC 0.962). Patients with a high MRI-estimated tumour volume ($\geq 300\text{cm}^3$) had a significantly poorer median overall survival (8.5 months vs. 20 months) and was a statistically significant prognostic variable on univariate (HR 2.273 (95% CI 1.162 - 4.446), $p=0.016$) and multivariate Cox proportional hazards model (HR 2.114 (95% CI 1.046 - 4.270), $p=0.037$).

Table of Contents

Summary	1
Table of Contents	4
List of Tables	10
List of Figures	14
Acknowledgements	19
Declaration	20
List of Abbreviations	21
Publications relating to this thesis	27
Presentations to Learned Societies	28
CHAPTER 1: INTRODUCTION	29
1 Chapter 1: Introduction	30
1.1 General Introduction	30
1.2 Anatomy and Physiology of the Pleural Space	30
1.3 Pathophysiology of Pleural Effusion.....	31
1.4 Pleural Effusion in malignancy	32
1.5 Malignant Pleural Mesothelioma	33
1.6 Asbestos-induced Carcinogenesis in Malignant Pleural Mesothelioma	34
1.7 Current diagnostic pathway.....	35
1.7.1 Clinical presentation.....	35
1.7.2 Initial investigations	37
1.7.3 Pleural Biopsy.....	38
1.7.4 Histological findings	40
1.8 Imaging.....	41
1.8.1 Computed Tomography (CT).....	41
1.8.2 PET-CT	45
1.8.3 Magnetic Resonance Imaging (MRI)	47
1.9 Basic Magnetic Resonance Theory	47
1.9.1 Nuclear Magnetic Resonance	47
1.9.2 T1 Relaxation (Spin-Lattice relaxation)	49

1.9.3 T2 Relaxation (Spin-Spin relaxation)	49
1.9.4 Spatial Localisation of Tissue.....	50
1.9.5 K-space	50
1.10 MRI in the detection and differentiation of MPM	51
1.11 Staging of MPM.....	58
1.11.1 CT	62
1.11.2 PET-CT	63
1.11.3 MRI	64
1.12 Blood Biomarkers	64
1.12.1 Mesothelin	64
1.12.2 Megakaryocyte Potentiating Factor.....	65
1.12.3 Osteopontin	65
1.12.4 HMGB-1	66
1.12.5 SOMAscan™ Proteomic Classifier	67
1.12.6 Fibulin-3	73
1.13 Biomarker Reproducibility	81
1.13.1 Patient and Specimen Factors.....	81
1.13.2 Specimen processing and storage	82
1.13.3 Assay performance and validation	82
1.14 Summary	83
1.15 Aim of thesis and hypotheses tested.....	85
CHAPTER 2: DIAPHRAGM.....	87
2 Chapter 2: DIAPHRAGM - Diagnostic and Prognostic Biomarkers for the	
Rational Assessment of Mesothelioma	88
2.1 INTRODUCTION	88
2.2 AIM AND OBJECTIVES	89
2.3 METHODS	91
2.3.1 Ethical Approval	91
2.3.2 Study design and setting	91
2.3.3 Study Set-Up	93
2.3.4 Study Population	97
2.3.5 Glasgow Recruitment	99
2.3.6 Study Procedures.....	101
2.3.7 Statistical Analysis	108
2.3.8 Biomarker Sampling, Processing and Storage	110

2.3.9	Biomarker Analyses	112
2.3.10	Data Storage.....	113
2.3.11	Laboratory Activity - Fibulin-3 assay validation	113
2.4	RESULTS.....	118
2.4.1	Site recruitment.....	118
2.4.2	Patient recruitment.....	118
2.4.3	Patient Population	123
2.4.4	Fibulin-3 validation	129
2.5	DISCUSSION	131
2.5.1	Study Design	131
2.5.2	Challenges of recruiting in a multi-centre study	131
2.5.3	Challenges of recruiting a suspected pleural malignancy cohort	133
2.5.4	Strategies to improve study recruitment	135
2.5.5	Use of electronic health records for screening	137
2.5.6	Review of preliminary results	138
2.5.7	Fibulin-3 Validation	140
2.6	CONCLUSION	140
CHAPTER 3:	EARLY CONTRAST ENHANCEMENT	142
3	Chapter 3: Early Contrast Enhancement (ECE)	143
3.1	INTRODUCTION	143
3.1.1	Tumour Angiogenesis	144
3.1.2	Imaging of Angiogenesis.....	144
3.2	AIM AND OBJECTIVES	147
3.3	METHODS	149
3.3.1	Ethical Approval	149
3.3.2	Study Population	149
3.3.3	Clinical Assessment	150
3.3.4	Sample Size and Assumptions	151
3.3.5	Imaging acquisition	152
3.3.6	Imaging Analysis	160
3.3.7	Assessment of Tissue Microvessel Density	168
3.3.8	Statistical Analysis	169
3.4	RESULTS.....	169
3.4.1	Patient Demographics	169
3.4.2	Imaging results	173

3.4.3 Overall Diagnostic Performance	180
3.4.4 Post-hoc Analyses regarding ROI Signal Intensity Gradient	183
3.4.5 Mean Signal Intensity Gradient (MSIG)	184
3.4.6 Reproducibility	184
3.4.7 Tissue Microvessel Density	187
3.4.8 Relationship between MRI Perfusion Data and Tissue Microvessel Density in patients with MPM	187
3.4.9 Relationship between Tissue MVD and survival in MPM	188
3.4.10 Relationship between MRI perfusion data and survival in MPM....	190
3.5 DISCUSSION	190
3.5.1 Early Contrast Enhancement	190
3.5.2 ECE - An Imaging Biomarker of Pleural Malignancy	192
3.5.3 CT and MRI Morphology in Pleural Malignancy	196
3.5.4 Reproducibility	198
3.5.5 The Biological Basis of Early Contrast Enhancement	199
3.5.6 Potential clinical implications.....	202
3.5.7 Limitations of this study	203
3.6 CONCLUSION	204
CHAPTER 4: VOLUMETRIC ASSESSMENT OF MALIGNANT PLEURAL MESOTHELIOMA.....	205
4 Chapter 4: Volumetric Assessment of Malignant Pleural Mesothelioma	206
4.1 INTRODUCTION	206
4.1.1 Staging of Malignant Pleural Mesothelioma	206
4.1.2 Imaging Modalities for the Staging of MPM.....	208
4.1.3 Volumetric Assessment of MPM	210
4.2 AIM AND OBJECTIVES	213
4.3 METHODS	215
4.3.1 Ethical Approval	215
4.3.2 Study Population	215
4.3.3 Pleural Diagnostics and Staging	215
4.3.4 MR Image Acquisition	216
4.3.5 MRI Phantom	216
4.3.6 Image Analysis	217
4.3.7 Segmentation using Myrian®	221
4.3.8 Reproducibility	230

4.3.9	Defining Optimum Segmentation Methodology	230
4.3.10	Inter-observer agreement.....	231
4.3.11	Statistical Analysis	231
4.4	RESULTS.....	232
4.4.1	Patient Population	232
4.4.2	MRI Volume Analyses.....	234
4.4.3	Methodology Ranking	237
4.4.4	Reproducibility	238
4.4.5	Relationship between primary tumour volume and clinical T-stage	238
4.4.6	Relationship between disease volume and survival.....	239
4.5	DISCUSSION	243
4.5.1	Prognostic significance of tumour volume	245
4.5.2	Tumour volume and disease stage.....	250
4.5.3	Implementation and Future Testing.....	251
4.5.4	Possible Clinical Implications.....	253
4.5.5	Study Limitations.....	254
4.6	CONCLUSION	255
CHAPTER 5:	CONCLUSIONS.....	256
5	Chapter 5: Conclusions.....	257
5.1	Blood biomarkers in Malignant Pleural Mesothelioma	257
5.1.1	The DIAPHRAGM study	258
5.2	Imaging biomarkers in Malignant Pleural Mesothelioma	259
5.2.1	Early Contrast Enhancement at MRI	260
5.3	Staging of Malignant Pleural Mesothelioma	261
5.3.1	Volumetric Assessment of Malignant Pleural Mesothelioma	262
5.4	Future Work.....	263
	Appendix 1 Site Feasibility Questionnaire.....	265
	Appendix 2 Suspected Pleural Malignancy Cohort Patient Information Sheet	266
	Appendix 3 DIAPHRAGM invitation letter to Clydeside Action on Asbestos members.....	271
	Appendix 4 Asbestos-exposed Control Cohort Patient Information Sheet ..	272
	Appendix 5 MRI Substudy Patient Information Sheet.....	275

Appendix 6 Baseline Information Case Report Form	279
Appendix 7 MPM Follow-up Visit Case Report Form	287
Appendix 8 MPM Long-term Follow-up Case Report Form.....	291
Appendix 9 Diagnostic Review Case Report Form.....	294
Appendix 10 Asbestos-exposed Control Case Report Form	297
Appendix 11 Asbestos Exposure Questionnaire	302
Appendix 12 MRI Safety Questionnaire	304
References	306

List of Tables

Chapter 1

Table 1.1	Differential diagnosis of exudative pleural effusion.....	36
Table 1.2	IMIG/TNM 7 th Edition staging system for Malignant Pleural Mesothelioma.....	60
Table 1.3	TNM 8 th Edition staging system for Malignant Pleural Mesothelioma.....	61
Table 1.4	13 proteins that comprise the SOMAscan™ assay.....	69
Table 1.5	Summary of previous studies of Fibulin-3 in Malignant Pleural Mesothelioma.....	79

Chapter 2

Table 2.1	Research objectives and related outcome measures of the DIAPHRAGM study.....	90
Table 2.2	Schedule of assessments for participants recruited to the Suspected Pleural Malignancy cohort of the DIAPHRAGM study.....	102
Table 2.3	Schedule of assessments for participants recruited to the asbestos-exposed control cohort of the DIAPHRAGM study via invitation by Clydeside Action on Asbestos (CAA).....	105
Table 2.4	Schedule of assessments for participants recruited to the Asbestos-exposed control cohort of the DIAPHRAGM study after identification at respiratory outpatient clinic.....	106
Table 2.5	DIAPHRAGM recruiting centres and initial projected recruitment numbers provided by each site Principal Investigator.....	119

Table 2.6	Details of recruitment to the Suspected Pleural Malignancy cohort by site in the DIAPHRAGM study.....	121
Table 2.7	Preliminary results of final pleural diagnoses for patients recruited to the SPM cohort of the DIAPHRAGM study.....	126
Table 2.8	Fibulin-3 levels measured in conditioned medium from three different Mesothelioma cell lines.....	130
Table 2.9	Fibulin-3 levels measured in conditioned medium from benign mesothelial cell line (LP9), Phosphate Buffered Solution and distilled water.....	130
Chapter 3		
Table 3.1	Study objectives and outcome measures of the Early Contrast Enhancement study.....	148
Table 3.2	Magnetic Resonance Imaging (MRI) protocols for patients recruited to the Early Contrast Enhancement study.....	157
Table 3.3	Summary of pleural diagnoses in 58 patients with suspected pleural malignancy recruited to the Early Contrast Enhancement study.....	172
Table 3.4	Summary of demographics, diagnosis and imaging results in 36 patients diagnosed with pleural malignancy who underwent contrast-enhanced MRI for ECE assessment, contrast-enhanced CT scanning and pleural biopsy. False negative (*) and false positive (†) results are highlighted.....	176
Table 3.5	Summary of demographics, diagnosis and imaging results in 23 patients diagnosed with benign pleural disease who underwent contrast-enhanced MRI for ECE assessment, contrast-enhanced CT scanning and pleural biopsy. False negative (*) and false positive (†) results are highlighted.....	178

Table 3.6	The diagnostic performance and reproducibility of CT morphology, MRI morphology and MRI-Early Contrast Enhancement (ECE) assessed in 58 patients with suspected Pleural Malignancy.....	181
Table 3.7	2 x 2 Contingency tables describing results of Computed Tomography (CT) Morphology, Magnetic Resonance Imaging (MRI) Morphology, Early Contrast Enhancement (ECE) at MRI and Combined MRI Morphology-ECE assessment in 58 patients with suspected pleural malignancy.....	182
Table 3.8	Discordant cases at CT Morphology Assessment by two thoracic radiologists. False negatives (*) and false positives (†) are highlighted.....	185
Table 3.9	Discordant cases at MRI Morphology Assessment by two thoracic radiologists. False negatives (*) and false positives (†) are highlighted.....	185
Table 3.10	Discordant cases at MRI Early Contrast Enhancement by two respiratory physicians. False negatives (*) and false positives (†) are highlighted.....	186
Table 3.11	Discordant cases at MRI Early Contrast Enhancement at repeated (intra-observer) testing. False negatives (*) and false positives (†) are highlighted.....	186

Chapter 4

Table 4.1	Summary of results of previous studies assessing the prognostic significance of imaging-derived tumour volume in patients with Malignant Pleural Mesothelioma.....	212
Table 4.2	Research Objectives and Outcome Measures for the MRI Volumetry study.....	214

Table 4.3	Pleural tumour volumes for 31 patients with Malignant Pleural Mesothelioma measured at contrast-enhanced Magnetic Resonance Imaging using four different semi-automated segmentation methodologies.....	235
Table 4.4	Intra-observer agreement of four different methodologies tested in the volumetric assessment of 15/31 patients with Malignant Pleural Mesothelioma.....	236
Table 4.5	Inter-item Correlation Matrix between four different methodologies tested in the volumetric assessment of 31 patients with Malignant Pleural Mesothelioma.....	236
Table 4.6	Scoring matrix to define optimum methodology between four different methodologies in the volumetric assessment of patients with Malignant Pleural Mesothelioma.....	237
Table 4.7	Prognostic factors for 31 patients with Malignant Pleural Mesothelioma (MPM) analysed in a univariate Cox proportional hazards model.....	241
Table 4.8	Prognostic factors for 31 patients with Malignant Pleural Mesothelioma (MPM) analysed in a backwards stepwise multivariate Cox proportional hazards model.....	242

List of Figures

Chapter 1

Figure 1.1	Axial contrast-enhanced CT images of a patient with Malignant Pleural Mesothelioma.....	42
Figure 1.2	Axial contrast-enhanced CT images of a patient with Malignant Pleural Mesothelioma and thoracoscopic images for the same patient.....	44
Figure 1.3	Axial ^{18}F FDG-PET-CT image of a patient with Malignant Pleural Mesothelioma, demonstrating intense ^{18}F FDG uptake within pleural tumour.....	47
Figure 1.4	Schematic representation of net magnetisation vector of tissue protons orientated in the same plane as the main magnetic field (B_0) (longitudinal/Z axis) and tipping of net magnetisation into the transverse plane (X-Y axis) in response to a 90° excitatory radiofrequency (RF) pulse.....	49
Figure 1.5	T1-weighted axial and coronal MR images of a patient with pleural effusion.....	52
Figure 1.6	T2-weighted axial and coronal MR images of a patient with pleural effusion, demonstrating enhancing pleural tumour and nodular pleural thickening with chest wall invasion.....	53
Figure 1.7	T1-weighted MR images of two patients with Malignant Pleural Mesothelioma.....	55

Chapter 2

Figure 2.1	Study flowchart for participants recruited to Suspected Pleural Malignancy cohort of the DIAPHRAGM study.....	92
------------	---	----

Figure 2.2	Study flowchart for participants recruited to the Asbestos-exposed Control cohort of the DIAPHRAGM study.....	93
Figure 2.3	Recruiting centre opening process.....	96
Figure 2.4	Summary of recruitment to the Suspected Pleural Malignancy (SPM) cohort of the DIAPHRAGM study.....	120
Figure 2.5	Summary of recruitment to the Asbestos-exposed control (AEC) cohort of the DIAPHRAGM study.....	120
Figure 2.6	Summary of recruitment of cases of Malignant Pleural Mesothelioma (MPM) within the Suspected Pleural Malignancy cohort of the DIAPHRAGM study.....	123
Figure 2.7	Study flowchart summarising recruitment to the Suspected Pleural Malignancy (SPM) cohort of the DIAPHRAGM study.....	124
Figure 2.8	Study flowchart summarising recruitment to the Asbestos-exposed Control (AEC) cohort of the DIAPHRAGM study.....	128
Figure 2.9	Standard curves measuring Fibulin-3 levels across 9 plates.....	129

Chapter 3

Figure 3.1	Example of a non-contrast enhanced MRI scan, acquired in separate axial blocks, and their corresponding sagittal and coronal images, early in the process of developing imaging protocols for the Early Contrast Enhancement study.....	154
Figure 3.2	Isotropically-acquired, contrast-enhanced MR images acquired over time pre- and post- intravenous administration of Gadobutrol.....	156
Figure 3.3	Example of ROI placed on macro-nodular pleural disease at contrast-enhanced MRI.....	162

Figure 3.4	Example of ROI placed on representative pleura in the absence of macro-nodular disease at contrast-enhanced MRI.....	164
Figure 3.5	Example of signal intensity (SI)/time curves measured from up to 15 ROI placed on representative pleura at contrast-enhanced MRI.....	165
Figure 3.6	Example of mean signal intensity (SI)/time curves summarising ROI SI/time curves for individual patients at contrast-enhanced MRI.....	166
Figure 3.7	Contrast-enhanced, T1-weighted coronal MR image with a ROI placed on extra-corporeal air, used to correct for background signal noise.....	166
Figure 3.8	Paraffin-embedded representative pleural biopsies stained with CD34 and Factor VIII immunostain and corresponding images where computer software has detected the immunostain to calculate Microvessel Density.....	168
Figure 3.9	Study flowchart of patients recruited to the MRI sub-study in the Early Contrast Enhancement study.....	171
Figure 3.10	Contrast-enhanced, coronal T1-weighted MR images and ROI signal intensity/time curves in patients with obvious macro-nodular disease (Panel A) demonstrating ECE (Panels B - C), in patients with effusion-dominant, low volume pleural disease (Panel D) but at least one ROI demonstrating ECE (Panels E - F) and where no single ROI demonstrated ECE (Panels G - H).....	175
Figure 3.11	ROC curves of ROISIG measured in 58 patients with suspected pleural malignancy using contrast-enhanced MRI.....	183
Figure 3.12	Correlation between mean signal intensity gradient (MSIG) and tumour Microvessel Density (MVD) measured using Factor VIII and CD34 immunostain.....	187

Figure 3.13	Kaplan-Meier curves demonstrating the relationship between tumour Microvessel Density (MVD) and median overall survival using Factor VIII and CD34 immunostain.....	189
Figure 3.14	Kaplan-Meier curves demonstrating the relationship between patient mean signal intensity gradient (MSIG) and median overall survival.....	190
Chapter 4		
Figure 4.1	MRI phantom. Panel A is a photograph of the MRI phantom containing a precise volume of water. Panels B and C demonstrate MRI phantom imaged at T1-weighted MRI in coronal (Panel B) and axial (Panel C) planes.....	217
Figure 4.2	Example of mean signal Intensity/time curves for ROI placed on pleura and adjacent structures in a patient with MPM.....	218
Figure 4.3	Manual delineation of pleural volume at contrast-enhanced MRI using OsiriX software.....	219
Figure 4.4	Semi-automated volume segmentation at contrast-enhanced MRI using the MIAlite plugin for OsiriX.....	220
Figure 4.5	Contour mask of pleural volume in axial and coronal planes, created semi-automatically using Myrian [®] software.....	222
Figure 4.6	Semi-automated, threshold-based segmentation of pleural volume at contrast-enhanced MRI using Methodology 1.....	226
Figure 4.7	Semi-automated, threshold-based segmentation of pleural volume at contrast-enhanced MRI using Methodology 2.....	227
Figure 4.8	Semi-automated, threshold-based segmentation of pleural volume at contrast-enhanced MRI using Methodology 3.....	228

Figure 4.9	Semi-automated, threshold-based segmentation of pleural volume at contrast-enhanced MRI using Methodology 4.....	229
Figure 4.10	MRI Volumetry study flowchart.....	233
Figure 4.11	Bland-Altman analysis comparing volume measurements performed by ST and GC.....	238
Figure 4.12	Relationship between clinical T-stage and measured pleural tumour volume at contrast-enhanced MRI.....	239
Figure 4.13	Kaplan-Meier curves demonstrating median overall survival based on MRI-estimated tumour volume in patients with MPM.....	240

Acknowledgements

The work reported in this thesis was performed under the supervision of Dr Kevin Blyth and Professor Anthony Chalmers. I would like to thank Dr Kevin Blyth for the opportunity to work at the Glasgow Pleural Disease Unit. I will be eternally grateful to him for his mentorship in clinical work, academia and life. I would like to thank Professor Anthony Chalmers for his guidance in this thesis.

I would like to thank the Chief Scientist Office Scotland for funding the DIAPHRAGM study and my first two years as a Clinical Research Fellow and the West of Scotland Lung Cancer Research Group for funding my final year as a Clinical Research Fellow.

This work would not have been possible without the support and hard work of the Cancer Research UK Clinical Trials Unit Glasgow, particularly the DIAPHRAGM TMG - Laura Clark, Caroline Kelly, Ann Shaw and Stephen Clark, who were infallible in their organisation and running of this study and in their positivity.

I am thankful to Dr John Foster for his invaluable lessons in MR physics and Rosie Woodward and Evonne McLennan for all of their time spent teaching me and helping me to acquire the MRI scans in this thesis. I would like to thank Carol McCormick and Fiona Thomson at the Translational Pharmacology Unit for their mentorship during my short time in the lab. I am grateful to the DIAPHRAGM recruiting teams and the Clinical Research Facility Glasgow, particularly Tricia Clark, for their hard work in recruiting to DIAPHRAGM.

A special thanks to my friend, Dr Jo Simpson, whose company in the library, the gym and in front of the DJ box have kept me smiling in the process of writing every chapter of this thesis.

I am indebted to the patients who gave up their precious time to participate in the studies in this thesis.

Finally, I dedicate this thesis to my husband Graeme, who has been eternally patient and encouraging throughout this entire project and my parents for their unwavering love and support.

Declaration

The work presented in this thesis was undertaken during my tenure as a Clinical Research Fellow at the Glasgow Pleural Disease Unit, Queen Elizabeth University Hospital, Glasgow and at the Institute of Cancer Sciences, College of Medical and Veterinary Life Sciences, at the University of Glasgow. I was supervised by Dr Kevin Blyth and Professor Anthony Chalmers.

All of the work reported in this thesis was undertaken by me, with the assistance of a number of colleagues who have been formally acknowledged in the previous section. The statistical analysis plan and sample size calculation for the DIAPHRAGM study were done by the Jim Paul and Caroline Kelly, statisticians at the Cancer Research UK Clinical Trials Unit Glasgow. All remaining statistical analyses in this thesis were done by me.

Work relating to this thesis has been published in or submitted to peer-reviewed journals and presented at national and international conferences.

The writing of this thesis constitutes my own work, written solely by me.

Signed

Selina Tsim, March 2018

List of Abbreviations

3D	3-dimensional
ADC	Apparent Diffusion Co-efficient
AEC	Asbestos-exposed Control
AJCC	American Joint Committee on Cancer
ANOVA	Analysis of Variance
AU	Arbitrary Units
AUC	Area Under the Curve
BAPE	Benign Asbestos Pleural Effusion
BTS	British Thoracic Society
CAA	Clydeside Action on Asbestos
CAD	Coronary artery disease
CALGB	Cancer and Leukaemia Group B
CRUK	Cancer Research United Kingdom
CRF	Case Report Form
CT	Computed Tomography
CTPA	Computed Tomography Pulmonary Angiogram
CTU	Clinical Trials Unit
CXR	Chest radiograph

DCE-MRI	Dynamic Contrast Enhanced Magnetic Resonance Imaging
DIAPHRAGM	Diagnostic and Prognostic Biomarkers in the Rational Assessment of Mesothelioma
DNA	Deoxyribonucleic acid
DWI	Diffusion Weighted Imaging
ECE	Early Contrast Enhancement
ECM	Extracellular Matrix
ECOG	Eastern Cooperative Oncology Group
EDTA	Ethylenediaminetetraacetic acid
eGFR	Estimated Glomerular Filtration Rate
EHR	Electronic health record
ELISA	Enzyme-Linked Immunosorbent Assay
EORTC	European Organisation for Research and Treatment of Cancer
EPP	Extrapleural pneumonectomy
FFPE	Formalin-fixed paraffin-embedded
FISH	Fluorescence in situ hybridisation
FDG	Fluoro-Deoxy-Glucose
GRE	Gradient Echo Sequence
HGF	Hepatocyte Growth Factor
HMGB-1	High Mobility Group Box-1

IASLC	International Association for the Study of Lung Cancer
IGF	Insulin-like Growth Factor
HU	Hounsfield Units
ICC	Intraclass Correlation Coefficient
IMIG	International Mesothelioma Interest Group
IQR	Interquartile range
kel	Elimination rate constant
kep	Redistribution rate constant
LAT	Local Anaesthetic Thoracoscopy
LDH	Lactate Dehydrogenase
MDT	Multi-disciplinary Team
MMP	Matrix metalloproteinase
MPF	Megakaryocyte Potentiating Factor
MRI	Magnetic Resonance Imaging
MPM	Malignant Pleural Mesothelioma
MSIG	Mean Signal Intensity Gradient
MTV	Metabolic Tumour Volume
MVD	Microvessel Density
NCRI	National Cancer Research Institute

NPV	Negative Predictive Value
NSCLC	Non-Small Cell Lung Cancer
PACS	Picture Archiving and Communication System
PBS	Phosphate Buffered Solution
P/D	Pleurectomy/Decortication
PDGF	Platelet-derived Growth Factor
PET	Positron Emission Tomography
PIS	Patient Information Sheet
PM	Pleural Malignancy
PMMA	Polymethyl methacrylate
PPV	Positive Predictive Value
PS	Performance Status
QEUH	Queen Elizabeth University Hospital
R&D	Research and Development
RCT	Randomised Controlled Trial
RECIST	Response Evaluation Criteria in Solid Tumours
RF	Radiofrequency
RNS	Reactive Nitrogen Species
ROC	Receiver Operating Characteristic

ROI	Region of Interest
ROISIG	Region of Interest Signal Intensity Gradient
ROS	Reactive Oxygen Species
SD	Standard deviation
SI	Signal Intensity
SMR	Standardised Mortality Ratio
SOMAmers™	Slow Off-rate Modified Aptamers
SPECT	Single Photon Emission Computed Tomography
SPM	Suspected Pleural Malignancy
SUV	Standardised Uptake Value
SV40	Simian Virus 40
TB	Tuberculosis
TE	Echo Time
TGF- β	Transforming Growth Factor- β
TGV	Total Glycolytic Volume
TLG	Total Lesion Glycolysis
TMG	Trial Management Group
TNF- α	Tumour Necrosis Factor- α
TNM	Tumour Node Metastasis

TPL	Translational Pharmacology Laboratory
TR	Repetition Time
UICC	Union for International Cancer Control
US	Ultrasound
VATS	Video-assisted Thoracoscopic Surgery
VEGF	Vascular Endothelial Growth Factor
VIBE	Volumetric interpolated breath-hold examination
WCC	White Cell Count
WoS	West of Scotland

Publications relating to this thesis

1. Early Contrast Enhancement: A novel magnetic resonance imaging biomarker of pleural malignancy

S Tsim, CA Humphreys, GW Cowell, DB Stobo, C Noble, R Woodward, CA Kelly, L Alexander, JE Foster, C Dick, KG Blyth

Lung Cancer April 2018;118:48-56

2. Diagnostic and Prognostic Biomarkers in the Rational Assessment of Mesothelioma (DIAPHRAGM) study: a protocol of a prospective, multicentre, observational study

S Tsim, C Kelly, L Alexander, C McCormick, F Thomson, R Woodward, JE Foster, DB Stobo, J Paul, NA Maskell, A Chalmers, KG Blyth

BMJ Open Nov 2016;6(11):e013324

3. Imaging in Pleural Mesothelioma: A Review of the 13th International Conference of the International Mesothelioma Interest Group

SG Armato III, KG Blyth, JJ Keating, S Katz, S Tsim, J Coolen, E Gudmundsson, I Opitz, AK Nowak

Lung Cancer Nov 2016;101:48-58

Presentations to Learned Societies

1. Preliminary results of the Diagnostic and Prognostic Biomarkers in the Rational Assessment of Mesothelioma (DIAPHRAGM) study

S Tsim, C Kelly, M Evison *et al.*

Accepted for oral presentation at the American Thoracic Society International Conference May 2018

2. Novel MRI methodology for the assessment of tumour volume in MPM

S Tsim, GW Cowell, R Woodward *et al.*

Accepted for oral presentation at the International Conference of the International Mesothelioma Interest Group May 2018

3. Optimisation of the methods for Early Contrast Enhancement (ECE) - Magnetic Resonance Imaging in patients with Mesothelioma

S Tsim, CA Humphreys, DB Stobo *et al.*

Oral presentation at the International Conference of the International Mesothelioma Interest Group 2016

4. Early Contrast Enhancement: A perfusion-based Magnetic Resonance Imaging biomarker of pleural malignancy

S Tsim, CA Humphreys, DB Stobo *et al.*

Oral presentation at the British Thoracic Society Winter Meeting 2015

5. Contrast-enhanced Magnetic Resonance Imaging as a marker of tumour angiogenesis in Malignant Pleural Mesothelioma

S Tsim, CA Humphreys, DB Stobo *et al.*

Runner-up prize for best poster presentation, British Thoracic Oncology Group annual meeting 2015

CHAPTER 1: INTRODUCTION

1 Chapter 1: Introduction

1.1 General Introduction

Malignant Pleural Mesothelioma (MPM) is an invasive thoracic malignancy associated with inherent diagnostic difficulties. It frequently presents as an emergency admission with breathlessness associated with a pleural effusion and has a poor median survival of 9.5 months. Local anaesthetic thoracoscopy (LAT) allows examination of the pleural cavity, multiple biopsies to be taken and therapeutic talc poudrage pleurodesis. However, access to LAT in the UK remains limited and therefore referral to specialist centres providing this service is often needed. A non-invasive biomarker to direct appropriate patients to these services is urgently required. The general aim of this thesis is to examine the true clinical utility of existing blood biomarkers in the existing MPM literature and to generate novel imaging biomarkers of MPM.

1.2 Anatomy and Physiology of the Pleural Space

The pleura is a fibrous membrane structure consisting of a single layer of mesothelial cells with underlying connective tissue layers, blood vessels, nerves and lymphatics. (1) The pleura folds back on itself to form a double membrane structure lining the surface of the lung, including the interlobar fissures (visceral pleura) and the chest wall, diaphragm and mediastinum (parietal pleura). The parietal and visceral pleura are continuous at the lung hilum via the pulmonary ligament. (2) The visceral pleura receives its blood supply from the bronchial circulation and the parietal pleura receives its blood supply from the intercostal arteries. (3) The thin space between the parietal and visceral pleura is known as the pleural cavity. In healthy humans, the pleural space contains a small volume of pleural fluid (approximately 0.3 ml/kg body mass). (4) Pleural fluid is filtered from systemic capillaries to the pleural space via the parietal pleural interstitium down a relatively small pressure gradient. Pleural fluid circulates within the pleural space, where the intra-pleural pressure is subatmospheric at approximately -8cmH₂O at end-inspiration. Pleural fluid is drained via parietal pleural stomata and pleural lymphatics. Pleural fluid resorption is an active process, mediated by pulsatile smooth muscle activity within the lymphatic walls

and pressure oscillations secondary to respiration. (4) This process normally increases in response to an increase in pleural fluid volume, however the degree to which pleural lymphatic flow can increase in response to increased pleural fluid filtration is limited. (4) The principal function of pleural fluid in health is to maintain close apposition of the parietal and visceral pleural membranes during respiration and to provide lubrication to allow frictionless movement of the two pleural surfaces. (5)

1.3 Pathophysiology of Pleural Effusion

A pleural effusion is an excess accumulation of fluid within the pleural space. This can result from one of several different mechanisms interrupting the balance between pleural fluid filtration and pleural fluid drainage. Pleural effusions can be classified as a transudate or an exudate. An exudative pleural effusion can be distinguished from a transudate with an accuracy of 93% (6) using Light's criteria, where the effusion is defined as an exudate if one or more of the following are true: Pleural fluid protein concentration divided by serum protein concentration >0.5 ; pleural fluid lactate dehydrogenase (LDH) concentration divided by serum LDH concentration >0.6 ; pleural fluid LDH concentration $>2/3$ upper limit of laboratory normal reference range for serum LDH concentration. (7) Whether a pleural effusion is a transudate or an exudate is a result of the mechanism of disruption between filtration and drainage of pleural fluid:

1. Changes in microvascular hydrostatic or oncotic pressure (8) - resulting in a transudative pleural effusion, as occurs in heart failure, liver failure and hypoalbuminaemia, which can result from systemic illness and nephrotic syndrome
2. Reduction in pleural pressure (8) - resulting in a transudative pleural effusion, as occurs in atelectasis, which can occur secondary to bronchial obstruction in lung cancer, and trapped lung
3. Changes in mesothelial and capillary endothelial permeability (5) - resulting in an exudative pleural effusion as occurs in inflammatory disorders, such as rheumatoid pleurisy, parapneumonic effusions and effusions secondary to

pulmonary embolism or malignancy, where malignant infiltration of the pleura can increase mesothelial permeability and infiltration of blood vessels or tumour-mediated release of pro-inflammatory cytokines and vasoactive mediators can increase endothelial permeability (8,9)

4. Impaired lymphatic drainage (8) - resulting in an exudative effusion.

Lymphatic obstruction can result from tumour in malignancy or inflammatory debris in inflammatory conditions or parapneumonic effusions. Impaired lymphatic drainage due to malignant infiltration of mediastinal lymph nodes is one of the commonest mechanisms for pleural effusion in malignancy. (10,11) Lymphatic abnormalities, as found in yellow nail syndrome can also result pleural effusion via impaired lymphatic drainage

1.4 Pleural Effusion in malignancy

Malignancy is one of the most common causes of pleural effusion, accounting for approximately 30% of all pleural effusions (12) and has an estimated incidence of 50,000 per year in the UK. (13) Lung cancer accounts for approximately 35% of all metastatic pleural effusions, with breast cancer (approximately 25%), lymphoma (approximately 10%) and ovarian cancer (approximately 5%) being the next most common causes of metastatic malignant pleural effusion. (11) Malignant pleural effusion is indicative of advanced stage malignancy and associated with poor survival outcomes, with a median survival of 192 days in breast cancer and a median survival of only 74 days in lung cancer. (14) However, where it will affect management, pleural metastases, defined as parietal pleural tumour deposits or positive effusion cytology should be confirmed, as pleural effusion can occur in malignancy without any evidence of pleural involvement. In lung cancer, pleural effusion can be parapneumonic secondary to bronchial obstruction, or can result from atelectasis associated with bronchial obstruction. (11) This is an important distinction, as patients with pleural effusion but no pleural metastases can still potentially be radically treatable and have a significantly better survival than those with malignant pleural effusion. (15) MPM is a primary pleural tumour in which pleural effusion is found in approximately 90% of cases. (13)

1.5 Malignant Pleural Mesothelioma

MPM is an invasive primary pleural malignancy with 2515 mesothelioma deaths reported in Great Britain in 2014. (16) The main MPM histologic subtypes are epithelioid (associated with the best prognosis), sarcomatoid (associated with the worst prognosis) and biphasic (a combination of epithelioid and sarcomatoid features). MPM is strongly associated with asbestos exposure, (17) with a history of asbestos exposure elicited in approximately 80 - 85% of patients. (18,19) Asbestos is a group of naturally occurring silicate fibres, which can be divided into two major groups - serpentine asbestos, which typically have short, curly fibres (chrysotile) and amphibole asbestos, which is characterised by straighter and longer fibres (amosite, crocidolite, actinolite, anthophyllite and tremolite). (1) Asbestos, most commonly chrysotile, was widely used in several industries in the UK, particularly in the early to mid-twentieth century. (16) High risk occupations therefore include shipyard workers, motor industry workers, carpenters, plumbers, electricians and painter and decorators. (20) Low level non-occupational exposure to asbestos via a relative or spouse, or environmental exposure in the household or neighbourhood is also associated with MPM. (21) Several years after the initial identification of the link between asbestos exposure and MPM in the 1950s (22), industry regulations were put in place in the late 1960s, requiring employers to limit asbestos exposure and provide protective clothing. The importation and industrial use of amosite and crocidolite asbestos was banned in 1985 and chrysotile asbestos was banned from industrial use in 1999 in the UK. (23) However, there is a long latency period, with an average period of approximately 40 years between exposure and MPM development. (18) Predictive models therefore estimate that there will be approximately 2500 deaths per year ongoing until around 2020 in the UK when rates will begin to decline, (24) with the total number of deaths in Great Britain from mesothelioma predicted to be approximately 90,000 by 2050. (25) Unfortunately, there is an estimated 2 million tons of asbestos still being used globally each year, particularly in Asia and India. (26) This ongoing use of asbestos means that MPM will continue to be a burdensome disease for several decades to come. Due to its strong association with asbestos exposure, MPM is considered an industrial disease. Patients in the UK can therefore claim for compensation and all cases in the UK require reporting to the procurator fiscal

at time of patient death. (27) Inadequate histological confirmation of a diagnosis of MPM in life typically requires post-mortem confirmation at death. This can be stressful for the patient's family and result in funeral delays.

1.6 Asbestos-induced Carcinogenesis in Malignant Pleural Mesothelioma

As discussed in the previous section, there is a strong association between asbestos exposure and MPM. There have also been reports of an association between ionising radiation from external beam radiotherapy, simian virus 40 (SV40) in historic polio vaccines and a genetic predisposition with MPM. (1,28,29) However, by far the strongest association is asbestos exposure, with approximately 80 - 85% of patients with MPM having a history of asbestos. (18,19) Amphibole asbestos fibres are considered to be more carcinogenic than the shorter serpentine asbestos fibres. (30) Asbestos fibres reach the pleura following inhalation, either directly via alveoli and the visceral pleura or via lymphatic vessels. (31) The mechanism of asbestos-induced carcinogenesis in MPM is not entirely clear. However, previous studies have demonstrated that asbestos induces a chronic inflammatory reaction, with macrophage accumulation in the pleura, where asbestos fibres undergo frustrated phagocytosis by macrophages. In response, there is release of numerous cytokines, including Tumour Necrosis Factor- α (TNF- α), and reactive oxygen species (ROS) and reactive nitrogen species (RNS). Asbestos fibres can also directly induce human mesothelial cells to express TNF- α receptor 1 (TNF-R1) and to secrete TNF- α . (32) Release of ROS and RNS contribute to asbestos-mediated deoxyribonucleic acid (DNA) damage and aneuploidy. However, instead of undergoing apoptosis, these cells continue to divide. This is in part mediated by the NF- κ B pathway, which is activated by the binding of TNF- α and its receptor TNF-R1. (33) Activation of NF- κ B results in the activation of apoptosis inhibitors, promoting cellular proliferation. (34) Activation of the phosphoinositide-3 kinase (PI3K)/Akt pathway also promotes cellular proliferation and inhibits apoptosis in MPM. (35) Continued division of cells with DNA strand breaks and chromosomal aberrations eventually results in the emergence of malignant cell clones. (36) In addition, numerous other cytokines have been implicated in the pathogenesis of MPM. Expression of vascular

endothelial growth factor (VEGF), a potent stimulator of tumour neovascularisation, necessary for tumour growth and metastasis, has been shown to be increased in MPM cell lines. (37) Similarly, expression of insulin-like growth factor (IGF), platelet-derived growth factor (PDGF), transforming-growth factor beta (TGF- β), hepatocyte growth factor (HGF) and interleukins 6 and 8 is elevated in MPM, contributing to tumour growth, cell proliferation and migration, tumour neoangiogenesis and tumour invasiveness. (32,36,38)

1.7 Current diagnostic pathway

1.7.1 Clinical presentation

MPM most commonly presents with breathlessness and/or chest pain as a result of a pleural effusion. (18) Patients may also present with weight loss, sweats or lethargy as a result of the systemic effects of malignancy. (18,39) Right-sided disease tends to predominate and bilateral disease is extremely rare (previously recorded in 3% of patients). (40,41) Infrequently, patients may have palpable lymph nodes and/or digital clubbing. Emergency presentation is common (42,43) and prompt initial diagnostic sampling and relief of symptomatic pleural effusion is often required. MPM is typically associated with an exudative pleural effusion.

However, there are often few features to distinguish MPM from other causes of pleural effusion, of which there are many (see Table 1.1). Presenting symptoms of breathlessness and chest pain are common to many causes of pleural effusion other than MPM, including pulmonary thromboembolism and parapneumonic effusion. (44) In addition, multiple cancers can metastasise to the pleura causing pleural effusion and are associated with systemic features of malignancy, such as weight loss and sweats, which is often found in patients with MPM. A history of occupational exposure to asbestos in a patient presenting with pleural effusion always raises the possibility of MPM, however, asbestos exposure is also associated with benign asbestos pleural effusion (BAPE) and an increased risk of lung cancer. (17) Additionally, up to 12% of patients diagnosed with BAPE, based on the finding of fibrinous pleuritis at pleural biopsy, will prove to have MPM on subsequent follow-up. (45)

Table 1.1 Differential diagnosis of exudative pleural effusion

Malignancy
Primary pleural malignancy e.g. Mesothelioma Secondary pleural malignancy
Infection
Parapneumonic effusion Tuberculosis
Inflammatory
Rheumatoid arthritis Other autoimmune pleuritis e.g. systemic lupus erythematosus Benign asbestos pleural effusion Sarcoidosis
Reactive
Secondary to lung collapse Post thoracic surgery e.g. coronary artery bypass graft Post myocardial infarction Pancreatitis Pulmonary embolism
Other
Drugs e.g. amiodarone, nitrofurantoin, tyrosine kinase inhibitors, dantrolene Lymphatic disorders e.g. Yellow Nail Syndrome or lymphangioleiomyomatosis

1.7.2 Initial investigations

Current diagnostic pathways start with clinical assessment, radiographic imaging and ultrasound-guided pleural aspiration. (44) Appearances on chest radiography (CXR) that are typically found in MPM include pleural effusion, loss of hemithoracic volume, nodular pleural thickening, irregular fissural thickening or a localised mass lesion. The presence of non-calcified and calcified pleural plaques may alert the clinician to prior asbestos exposure, even in the absence of an obvious exposure history. However, pleural plaques are not specific to MPM and may occur after low-level asbestos exposure. (46,47) The sensitivity and specificity of CXR findings for MPM are unsurprisingly poor (14 - 43%) (39,48) and further imaging is required in all patients.

A blood-stained appearance of fluid at initial pleural aspiration can indicate pleural malignancy as a potential diagnosis. (49) However, pulmonary infarction secondary to pulmonary thromboembolism, trauma and parapneumonic effusions can also cause a blood-stained pleural effusion. (49,50)

Cytological examination of pleural fluid is diagnostic in approximately 60% of cases of malignancy. (44) However, the sensitivity of pleural fluid cytology in the diagnosis of MPM is much lower (0 - 16%). (51) While centres with expert cytopathology available have reported sensitivities of 73%, (52) the practice of diagnosing MPM on pleural fluid cytology alone remains controversial. (53,54) Cytological appearances can be relatively bland or resemble reactive mesothelial proliferation and conversely benign reactive mesothelial proliferation can exhibit striking cytological atypia with often many overlapping cytological features. (54,55) In addition, sarcomatoid MPM does not typically exfoliate cells into pleural fluid and a diagnosis of sarcomatoid MPM is rarely achievable on pleural fluid cytology. (56,57)

Demonstration of invasion by the mesothelial cell population is therefore often key to making a diagnosis of MPM, (57) and this is not possible with pleural fluid specimens alone. Repeated pleural aspiration beyond two pleural fluid specimens does not significantly improve diagnostic yield (58) and should be

avoided to prevent extensive fibrin deposition, (59) which may preclude effective thoracoscopic assessment, and procedure tract metastasis, which is a known complication in MPM. (60) If a diagnosis is not established following pleural aspiration, further investigation with additional imaging and pleural biopsy is recommended. Imaging is discussed further in section 1.8.

1.7.3 Pleural Biopsy

Pleural biopsy techniques available include blind closed needle biopsy, image-guided percutaneous pleural biopsy, local anaesthetic thoracoscopy (LAT), video-assisted thoracoscopic surgery (VATS) and open pleural biopsy. Open pleural biopsy is rarely utilised now that thoracoscopy is available and is associated with intractable chest wall pain and high rates of tract metastases. (51)

Blind closed needle biopsies (frequently known as Abrams biopsy) are widely available and can be performed under local anaesthetic. However, it frequently yields tissue specimens <10mm and has a poor overall sensitivity for diagnosis of MPM with sensitivity previously reported to be as low as 16 - 30%. (54,61) Asbestos fibre deposition and MPM disease distribution is heterogeneous, and at early stages disease is frequently concentrated in the costophrenic gutter, (62) not easily accessible with an Abrams biopsy needle, which may account for the low diagnostic yield with blind closed needle biopsy.

Image-guided percutaneous pleural biopsy is also widely available and can be performed under local anaesthetic. A retrospective study of ultrasound-guided cutting needle biopsy in 70 patients with suspected MPM reported diagnostic sensitivity of 77% and negative predictive value of 57% (95% confidence intervals not reported). (63) Maskell *et al* conducted a prospective, randomised trial comparing Computed Tomography (CT)-guided pleural biopsy with Abram's pleural biopsy in 50 patients with suspected pleural malignancy and at least one negative pleural cytology sample. Sensitivity of CT-guided biopsy was significantly higher than Abram's pleural biopsy for the detection of pleural malignancy in this study (sensitivity 87% versus 47%; difference in sensitivity 47% (95% CI 10 - 69%), $p=0.02$). Results were similar in the subgroup of patients with MPM (CT-guided biopsy sensitivity 88% and Abram's pleural biopsy sensitivity

55%). (64) Image-guided percutaneous pleural biopsy is frequently employed in patients with a visible pleural mass, however it does not allow for definitive pleural fluid management in patients with symptomatic pleural effusion and these patients would therefore require additional pleural intervention. In addition, it does not allow direct inspection of the pleural cavity.

Adequate inspection and sampling of the pleural space is important given the heterogeneous disease distribution and also to allow accurate subtyping of MPM. There is a significant survival difference between histologic subtypes, with a median survival in epithelioid, biphasic and sarcomatoid MPM of 13.1, 8.4 and 4 months respectively. (65) Inadequate sampling may result in failure to identify prognostically significant sarcomatoid elements, which would constitute biphasic disease. LAT and VATS are both techniques that allow direct visual inspection of the pleural cavity in addition to therapeutic drainage of pleural effusion and talc poudrage within a single procedure.

VATS has excellent diagnostic sensitivity for pleural malignancy, reported to be 95% in one retrospective case series of 182 consecutive patients (66) and 100% in a small prospective series, in which 23/25 patients were diagnosed with MPM. (67) VATS utilises dual ports, making breakdown of adhesions in a multi-loculated pleural space more feasible to allow adequate visualisation of the pleural surfaces. However, VATS requires referral to a thoracic surgeon and fitness for general anaesthesia. It is therefore not suitable for patients with reduced performance status or significant co-morbidity, (44) which is frequently the case in patients with suspected MPM, who are often in their 7th or 8th decade of life given the long latency period between asbestos exposure and disease development.

LAT, also known as medical thoracoscopy, does not require a general anaesthetic and can be performed under local anaesthetic or conscious sedation, (68) making it accessible to a wider population than VATS. It utilises a single port and a rigid or semi-rigid thoracoscope and has excellent diagnostic sensitivity for MPM, reported to be 96 - 98.4% in two prospective case series, (69,70) with a low major complication rate. (71) LAT is therefore recommended in patients who do not have a diagnosis following pleural aspiration as an alternative to image-guided biopsy, particularly in patients who require talc poudrage pleurodesis. If

the pre-test probability of MPM is high, some centres may use LAT earlier in the diagnostic pathway to prevent multiple pleural interventions. (71) While the number of centres providing a LAT service in the UK is increasing, (71) it is currently limited to approximately 40 centres. Patient access to LAT therefore frequently requires referral to tertiary centres who offer this service.

1.7.4 Histological findings

There are three main histological subtypes of mesothelioma - epithelioid, sarcomatoid and biphasic (mixed epithelioid and sarcomatoid features). Epithelioid MPM accounts for approximately 60% of all mesotheliomas. Morphologically, it typically consists of well-formed papillary structures, frequently with fibrovascular cores, formed by cuboidal cells with uniform, round nuclei that have small to medium-sized nucleoli. These cuboidal cells can mimic reactive mesothelial cells. (72) Similarly, many features frequently demonstrated in reactive mesothelial proliferation can resemble a neoplastic process, including high cellularity, high mitotic activity, necrosis and formation of papillary groups, with entrapment of mesothelial cells within fibrosis often mimicking invasion. (54) Pancytokeratin staining to assess the overall mesothelial architecture can help to demonstrate regularity of growth and respect of mesothelial boundaries in reactive mesothelial proliferation to distinguish it from mesothelioma. (54) Immunohistochemistry can help distinguish epithelioid MPM from metastatic lung adenocarcinoma. A panel including positive mesothelial markers (e.g. Calretinin, Cytokeratin 5/6, Wilms Tumour-1) and negative adenocarcinoma markers (e.g. TTF1, CEA, Ber-Ep4) is typically demonstrated. (54,72) Sarcomatoid MPM is characterised by a hypercellular spindle-cell proliferation, with elongated nuclei, numerous mitotic figures and eosinophilic cytoplasm. Approximately 30% of sarcomatoid MPM will have desmoplastic features, which are predominantly hypocellular with scattered atypical cells among dense collagenous tissue. (73) Desmoplastic mesothelioma can resemble benign fibrinous pleuritis and expression of mesothelial markers on immunohistochemistry can be inconsistent or absent. (73) Recently, studies have highlighted potential clinical utility of p16 chromosomal deletion detected using Fluorescence in situ hybridisation (FISH). One study demonstrated hemi- or homozygous deletion in 67% of epithelioid,

87.5% of biphasic, 100% of sarcomatoid MPM and no cases of benign fibrinous pleurisy. (74) Demonstration of invasion into submesothelial tissue or underlying fat, skeletal muscle, rib or lung is however still considered key in the diagnosis of MPM. (54) Clinical history and imaging findings should also be reviewed in conjunction with pathologic findings before confirming a diagnosis of MPM.

1.8 Imaging

Detection of Malignant Pleural Mesothelioma

Imaging plays a major role in the assessment of all patients with pleural disease. Imaging in pleural malignancy and in particular early stage MPM can be difficult as morphological features of pleural malignancy and pleural thickening may be minimal or absent. There are also often few features that differentiate MPM from secondary pleural malignancy, which can often be diagnosed without the need for LAT.

1.8.1 Computed Tomography (CT)

CT imaging is established as the key imaging test in patients with MPM and is recommended in all patients with suspected pleural malignancy and in patients with an undiagnosed exudative pleural effusion. (44) Optimal CT assessment of the pleura requires post-contrast imaging at an interval of 60 - 90 seconds. (75) The imaged volume should include the thorax and abdomen to allow accurate assessment of disease extent and stage, including the most inferior borders of the costophrenic sulci. CT features of pleural malignancy have been widely reported and include pleural enhancement, infiltration of the chest wall, mediastinum or diaphragm, nodular or mediastinal pleural thickening and interlobar fissural nodularity (see Figure 1.1 for an example). (76,77) The detection of one or more of these features on CT was associated with a sensitivity of 96% and specificity of 80% for malignancy (although not MPM specifically). (77)

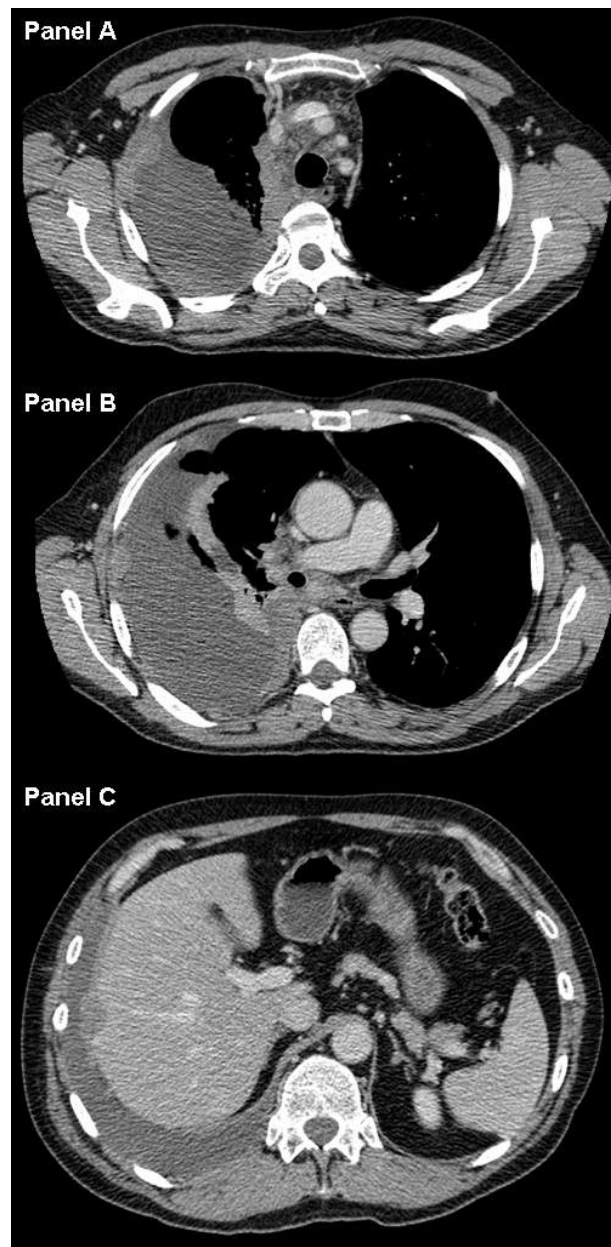


Figure 1.1 Axial contrast-enhanced CT images of a patient with MPM, taken at the Queen Elizabeth University Hospital 2015, demonstrating enhancing pleural mass lesions, nodular pleural thickening and mediastinal pleural thickening (Panels A and B) and infiltration of the diaphragm (Panel C).

Pleural effusion and pleural thickening are common but non-specific features, and are frequently demonstrated in benign pleural disease, including BAPE. (78) The concomitant presence of pleural calcification has been reported as more commonly associated with benign pleural disease, (76) but pleural plaques are frequently visualised in MPM (in up to 53% of patients). (40) No CT features reliably differentiate MPM from metastatic pleural malignancy, although enhancement of the interlobar fissures was reported more frequently in MPM in

a single study (39% in MPM versus 0% in other malignancies) (79). Moreover, CT cannot reliably distinguish between histological MPM subtypes, although ipsilateral volume loss, interlobar fissural involvement and mediastinal pleural involvement are reported more frequently in patients with sarcomatoid disease. (40,80) Metintas *et al* reported circumferential pleural thickening in 70% of MPM patients but only 15% of patients with metastatic pleural malignancy, resulting in a MPM sensitivity, specificity and odds ratio of 70%, 85%, and 3.17 (95% CI 1.67 - 6.01). (81) The same study reported mediastinal pleural involvement more frequently in MPM than metastatic pleural malignancy (85% versus 33% respectively), resulting in an MPM sensitivity of 85% and specificity of 67% for this feature. (81) In this study, the stage of the patients included was not reported, but it is important to note that features such as circumferential pleural thickening are frequently absent in early stage disease. In addition, CT imaging can grossly underestimate macroscopic disease visible at thoracoscopy and can occasionally fail to identify nodular pleural thickening what is often diffuse at thoracoscopy (see Figure 1.2). It is also important to note that all of the above features are subjective and therefore operator dependent. This is perhaps reflected in the heterogeneity in reported overall diagnostic performance of CT for pleural malignancy in the literature. While previous research have reported sensitivities of 70 - 93% and specificity of 87 - 96%, (77,81) Hallifax *et al* reported lower diagnostic performance (sensitivity 68% (95% CI 62 - 75%) and specificity 78% (95% CI 72 - 84%) in a retrospective review of 370 patients referred for LAT. (82) Similarly, our own research group has reported sensitivity of 58% (95% CI 51 - 65%) and specificity of 80% (95% CI 72 - 87%), resulting in a positive predictive value (PPV) of 83% (95% CI 75 - 89%) and a negative predictive value (NPV) of 54% (95% CI 46 - 61%), in 315 patients presenting with suspected pleural malignancy, reflecting the lower diagnostic performance of CT in 'real-life' clinical practice. (83) This is clearly an important difference, research studies typically adhere to strict imaging protocols, with optimised contrast timings, and utilise study specific reporting with thoracic specialty radiologists. In our study, 50% of patients presented as an emergency to secondary care services and almost 1 in 5 of these patients had a CT pulmonary angiogram (CTPA) performed to exclude concomitant pulmonary thromboembolism. In these patients, the diagnostic sensitivity of CTPA for detecting pleural malignancy was significantly lower than those who had venous

phase CT performed (sensitivity 27% (95% CI 9 - 53%) versus 61% (95% CI 53 - 68%) respectively, $p=0.0056$). In addition, only 37% of the scans performed in this study were reported by a thoracic radiologist (defined as radiologists with a primary subspecialty interest in chest imaging, including involvement in a thoracic oncology multidisciplinary team). CT scans that were reported by a non-thoracic radiologist had lower diagnostic sensitivity (53% (95% CI 44 - 62%)) than those reported by a thoracic radiologist (69% (95% CI 55 - 79%) $p=0.0488$), reflecting the subjectivity of CT assessment. (83)

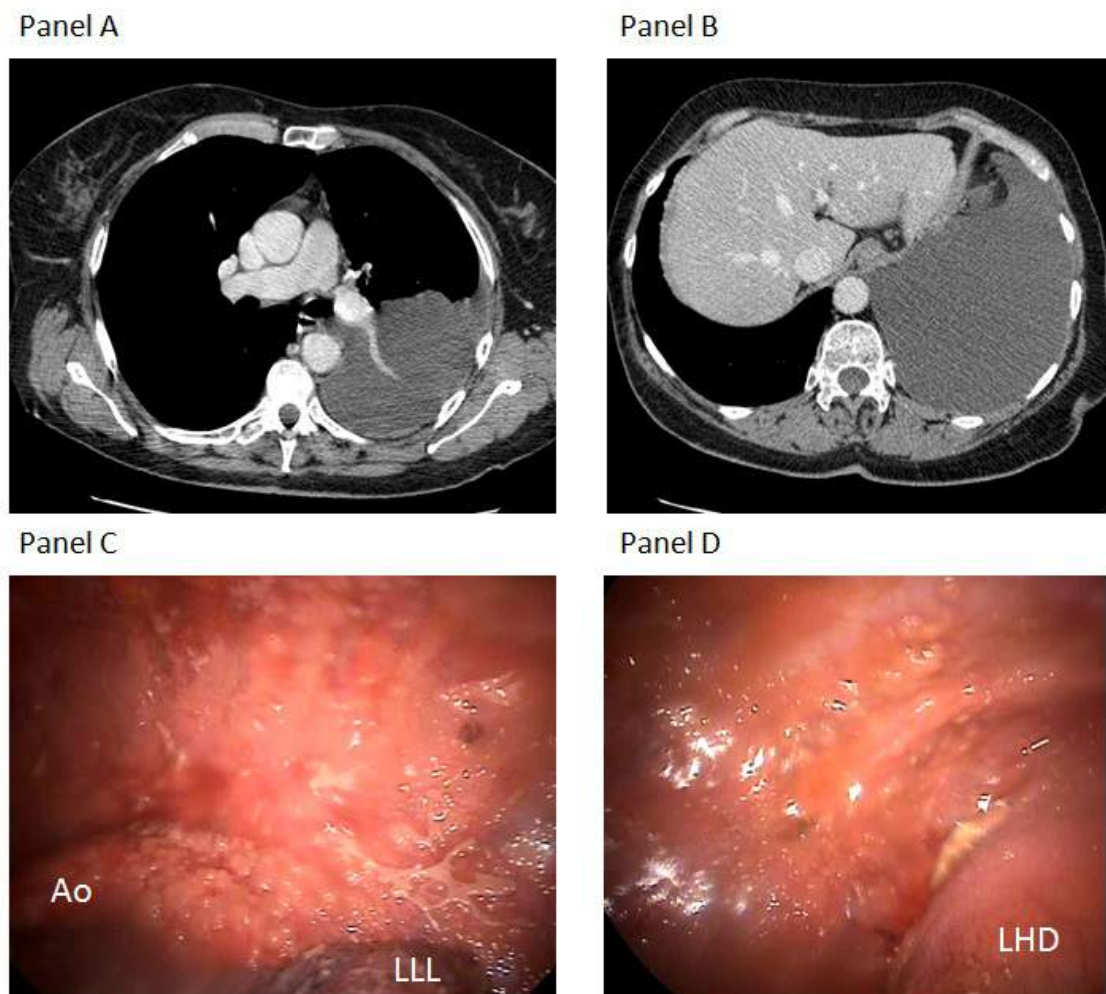


Figure 1.2 Axial contrast-enhanced CT images of a patient with Malignant Pleural Mesothelioma demonstrating a large left sided pleural effusion but little in the way of pleural thickening or nodularity (Panels A and B). Thoracoscopic findings in the same patient (Panels C and D) demonstrate diffuse nodular pleural tumour affecting the costal pleura, aorta (Ao), left lower lobe (LLL) and left hemidiaphragm (LHD) despite lack of obvious tumour at CT imaging. Reproduced with permission. (84)

1.8.2 PET-CT

Positron Emission Tomography (PET) exploits increased uptake of radioactive metabolic tracers (e.g. ^{18}F Fluoro-Deoxy-Glucose (FDG)) by cancer cells. Integrated PET-CT overcomes the poor spatial resolution of PET by combining metabolic PET data with high resolution CT data. Patients are typically fasted for 4 - 6 hours before injection of 3.5 - 5.2 MBq/kg of ^{18}F FDG 60 - 120 minutes prior to scanning.

In pleural malignancy, increased FDG uptake is typically visualised at sites of pleural tumour, lymph node involvement and distant metastases (see Figure 1.3). SUV values are typically higher in MPM (reported mean SUVmax 6.5 +/- SD 3.4) than in benign pleural disease (reported mean SUVmax 0.8 +/- SD 0.6), however some overlap in these values has been demonstrated in previous single-centre prospective case series. (85) (86) An SUVmax threshold of >2.0 has been found to reliably differentiate MPM from benign pleural disease with a sensitivity of 88 - 97% and specificity of 88 - 100%, based on single-centre prospective studies. (85-87) Importantly, SUV values are influenced by patient characteristics, including weight, blood glucose levels and respiratory motion, as well as technical factors such as scanner variability and parameter variability including field of view. (88) Additionally, SUV values are calculated over identified Regions of Interest and may not reflect the overall biology of the pleura or disease, particularly in MPM where disease distribution can be markedly heterogeneous. Visual-based assessment is therefore recommended in combination with SUV values when assessing patients. False negatives have been reported in patients with small lesions or a low proliferative index, which may be found in patients with early stage MPM. Additionally, false positives in patients with inflammatory disorders, such as rheumatoid pleuritis and tuberculous pleurisy, and in patients with prior talc pleurodesis has been well reported. (89-91). This is highlighted by the low specificity (35%) reported in one study that included patients with prior talc pleurodesis. (90) Recent meta-analyses regarding FDG-PET are somewhat contradictory, reporting differing pooled sensitivities/specificities in differentiating MPM from benign pleural

disease. Treglia reported a sensitivity of 95% (95% CI 92 - 97%) and specificity of 82% (95% CI 76 - 88%) (89), while Porcel *et al* reported a sensitivity of only 81% (95% CI 66 - 91%) and a specificity of 74% (95% CI 58 - 85%) for semi-quantitative interpretation using PET-CT. (92) There are no specific PET-CT features that differentiate MPM from other causes of pleural malignancy. One single centre study demonstrated a tendency for epithelioid MPM to have a lower SUV value to sarcomatoid MPM (mean SUV 3.78 versus 6.16), however this was not statistically significant. (86) In general PET-CT is not routinely used for imaging detection of MPM but may be useful in identifying suitable targets for image-guided pleural biopsy. This is currently being examined in a UK multi-centre randomised controlled trial (TARGET trial, ISRCTN 14024829). (93)

Dual time point FDG-PET imaging has been evaluated as a means of improving the specificity of PET-CT. The technique involves imaging at two separate time points following a single administration of ^{18}F FDG. Previous studies reported rising SUV values in malignant tumours for several hours post-administration in contrast to inflammatory disorders. (94,95) Mavi *et al* demonstrated a significantly higher SUVmax at both time points (early and delayed) in patients with MPM in comparison to patients with benign pleural disease. In addition, they observed increasing SUVmax values in patients with MPM in contrast to static or decreasing SUVmax values in patients with benign disease. (94) Similarly, Yamamoto *et al* demonstrated increased FDG uptake between early and delayed phased FDG-PET in patients with MPM but no increase in patients with benign pleural disease. (95) However, dual time point imaging clearly requires longer scan times and therefore expense and availability may limit its clinical utility.

More recently, novel PET tracers targeting tumour hypoxia and angiogenesis have recently been developed. ^{18}F -fluoromisonidazole (FMISO) is one example of a PET tracer that can be used to assess tumour hypoxia, and has recently been examined multiple solid tumours, including NSCLC, prostate cancer and head and neck cancer. (96) (97) Similarly, ^{18}F -fluciclatide is a novel angiogenesis PET tracer, which is targeted to integrin $\alpha_v\beta_3$ and has been studied in NSCLC, colorectal cancer and breast cancer. (97) (98)

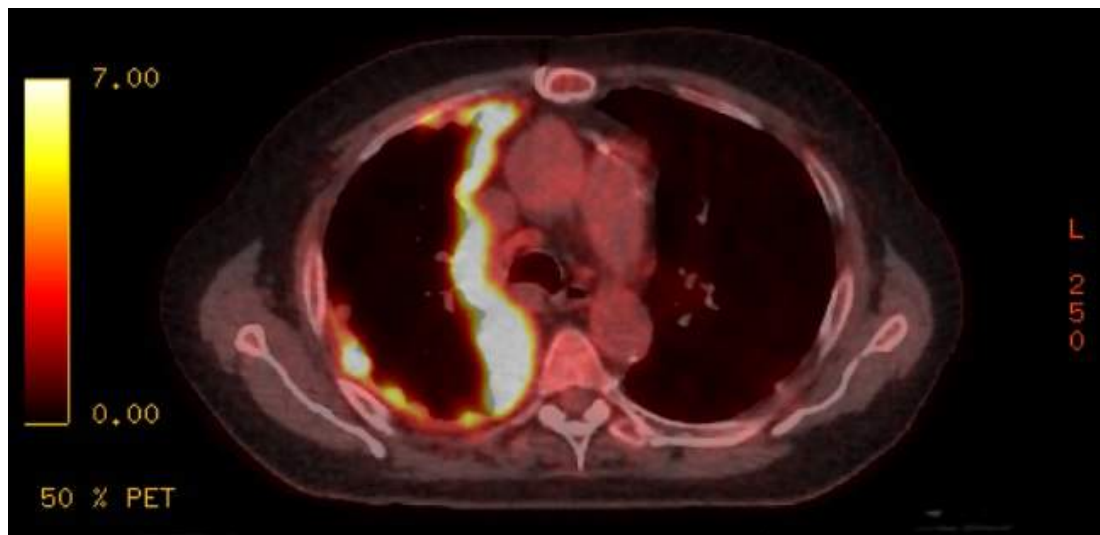


Figure 1.3 Axial ^{18}F FDG-PET-CT image of a patient with Malignant Pleural Mesothelioma, taken at the West of Scotland PET centre 2013, demonstrating intense ^{18}F FDG uptake within pleural tumour

1.8.3 Magnetic Resonance Imaging (MRI)

Magnetic Resonance Imaging (MRI) utilises resistive electromagnets to generate a magnetic field, with modern MRI systems having the ability to generate field strengths of up to 7-Tesla. Current clinical systems typically operate at 1.5 to 3-Tesla. MRI has advantages of not utilising ionising radiation and provides excellent contrast and spatial resolution for anatomic information in addition to functional information that can provide insight into underlying disease biology. Basic magnetic resonance theory is discussed here before discussing the role of MRI in the detection and differentiation of MPM.

1.9 Basic Magnetic Resonance Theory

1.9.1 Nuclear Magnetic Resonance

Magnetic resonance (MR) images are constructed from the dissipation of energy absorbed by the nuclei of Hydrogen atoms in response to a radiofrequency (RF) pulse, when a patient is placed in a magnetic field. Hydrogen consists of a single proton nucleus, orbited by one electron and is the most abundant element in the human body. For simplicity, the Hydrogen atom can be referred to as a proton.

Each proton spins around its own axis in a random orientation. When a magnetic field (B_0) is applied, the protons align with the magnetic field, either in parallel or in anti-parallel, and 'precess' at the Larmour frequency. The Larmour or precessional frequency is dependent on the strength of the magnetic field and the gyromagnetic ratio, which is constant for any given nucleus (42.57 MHz/Tesla for H^+). More protons are aligned parallel (low energy state) with B_0 than anti-parallel (high energy state), resulting in a net longitudinal magnetisation in the direction of the magnetic field (Z axis, see figure 1.4). In response to an excitatory RF pulse, protons spinning at the same precessional frequency as the frequency of the RF pulse will 'flip', rotating the net magnetisation into the transverse plane (X-Y, see figure 1.4). The degree that net magnetisation rotates into the transverse plane (flip angle) is dependent on the amplitude and duration of the RF pulse.

Once the excitatory RF pulse ends, the protons begin to relax back to their original state (equilibrium), resulting in rotation of the net magnetisation back from the transverse plane to the longitudinal axis. Relaxation depends on protons releasing the absorbed energy from the RF pulse, resulting in an MR signal. Relaxation can be divided into two independent but simultaneous processes, T1 relaxation and T2 relaxation.

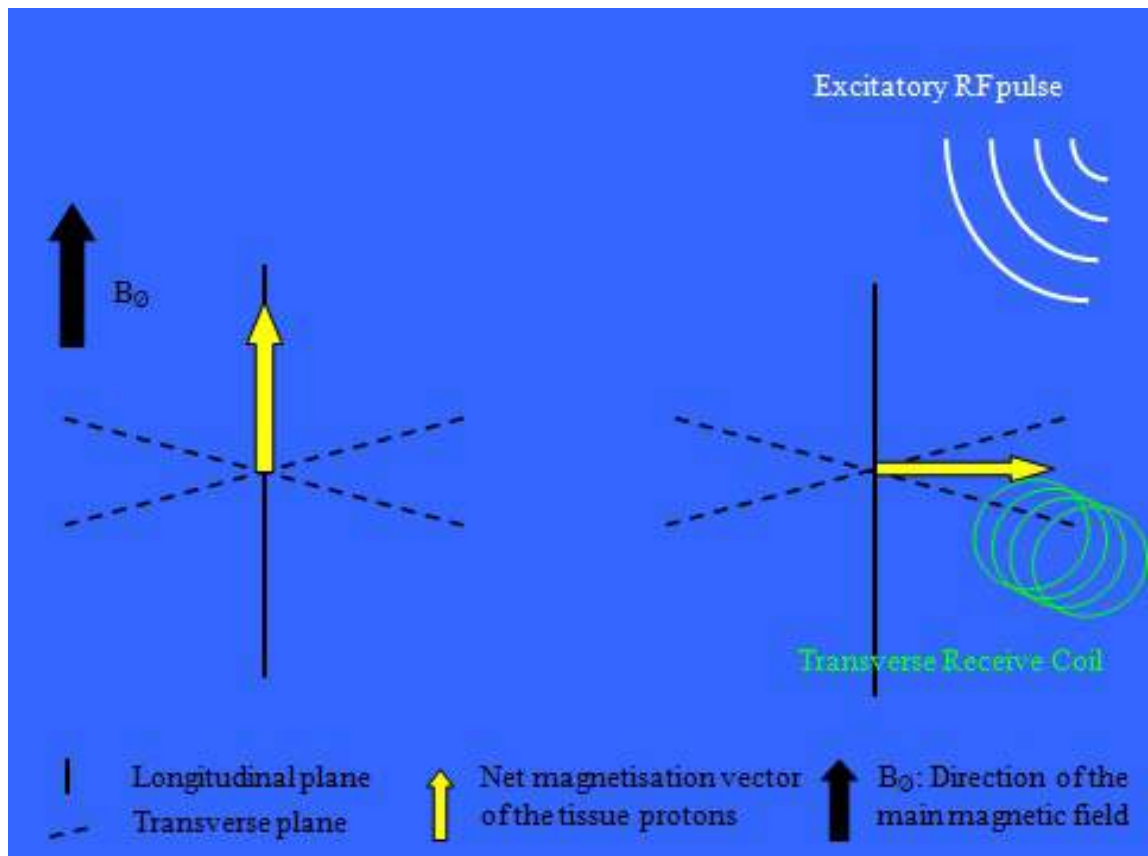


Figure 1.4 Schematic representation of net magnetisation vector of tissue protons orientated in the same plane as the main magnetic field (B_0) (longitudinal/Z axis) and tipping of net magnetisation into the transverse plane (X-Y axis) in response to a 90° excitatory radiofrequency (RF) pulse. Reproduced with the permission of Dr Kevin Blyth

1.9.2 T1 Relaxation (Spin-Lattice relaxation)

T1 relaxation describes the recovery of the longitudinal net magnetisation at the end of the RF pulse, with release of energy into the surrounding tissues (lattice). The T1 relaxation time is defined as the time it takes for the longitudinal magnetisation to recover to 63% of its original magnetisation at equilibrium. This T1 relaxation time is different for different tissues, depending on the proton's surrounding environment.

1.9.3 T2 Relaxation (Spin-Spin relaxation)

T2 relaxation describes the decay of transverse magnetisation produced by an excitatory RF pulse. Each individual proton spins around its own axis with no

phase coherence (out-of-phase). In response to a RF pulse, the protons start spinning in the same direction (in-phase). When the RF pulse is switched off, the protons will start to de-phase, resulting in decay of transverse magnetisation and release of energy amongst individual protons. T2 relaxation time is defined as the time it takes for the spins to de-phase to 37% of the original value. T2 relaxation is also tissue dependent and occurs much faster than T1 relaxation.

Contrast between tissues in MRI is a result of different T1 and T2 characteristics of adjacent tissues. Alterations in MRI pulse sequences can be made to optimise contrast between adjacent tissues of interest, producing T1- or T2-weighted images. T1-weighted images can be produced by reducing the time in between repeated excitatory RF pulses (the Repetition Time (TR)). T2-weighted images can be produced by increasing TR and increasing the Echo Time (TE). Echo time is the time from the RF pulse to the resulting MR signal (the echo).

1.9.4 Spatial Localisation of Tissue

Gradient coils are embedded in the inner core of the main electromagnet in the MRI scanner. They are arranged in sagittal, coronal and axial planes to the main magnetic field (B_0), creating additional small magnetic fields in their own plane. These gradient coils are used to create a Slice Encoding Gradient, a Phase Encoding Gradient, and a Frequency Encoding Gradient, which allows MR signal to be localised to an individual voxel within an individual block of tissue.

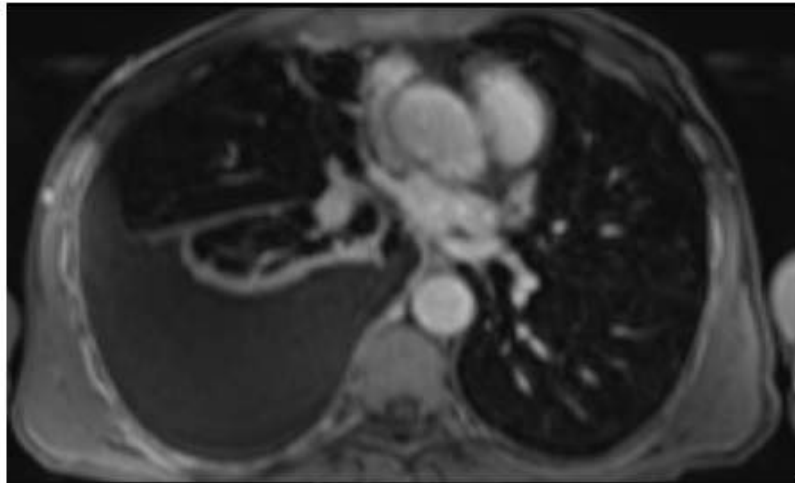
1.9.5 K-space

K-space is made up of the raw, unprocessed MRI signals. Low frequency signals are arranged in the centre of *k*-space, containing information about signal and tissue contrast. High frequency signals are arranged around the periphery of *k*-space and contains information about spatial resolution. The unprocessed MRI signals within *k*-space are transformed into interpretable images by the computer using a mathematical process known as Fourier Transformation.

1.10 MRI in the detection and differentiation of MPM

Pleural fluid appears dark on T1-weighted images due to the slower T1 relaxation of free water solutions in comparison to tissue such as fat (which has a fast T1 relaxation and therefore appears bright), see Figure 1.5. This effect is enhanced using paramagnetic contrast agents such as gadolinium. On T2-weighted imaging, free fluid such as pleural effusion appears bright, in contrast to lung and muscle. T2-weighted imaging can be useful for detecting septations within pleural fluid (which can also be identified using thoracic ultrasound). This is important when considering patients for local anaesthetic thoracoscopy, where significant loculation can preclude effective examination of the pleural cavity (see Figure 1.6).

Panel A



Panel B

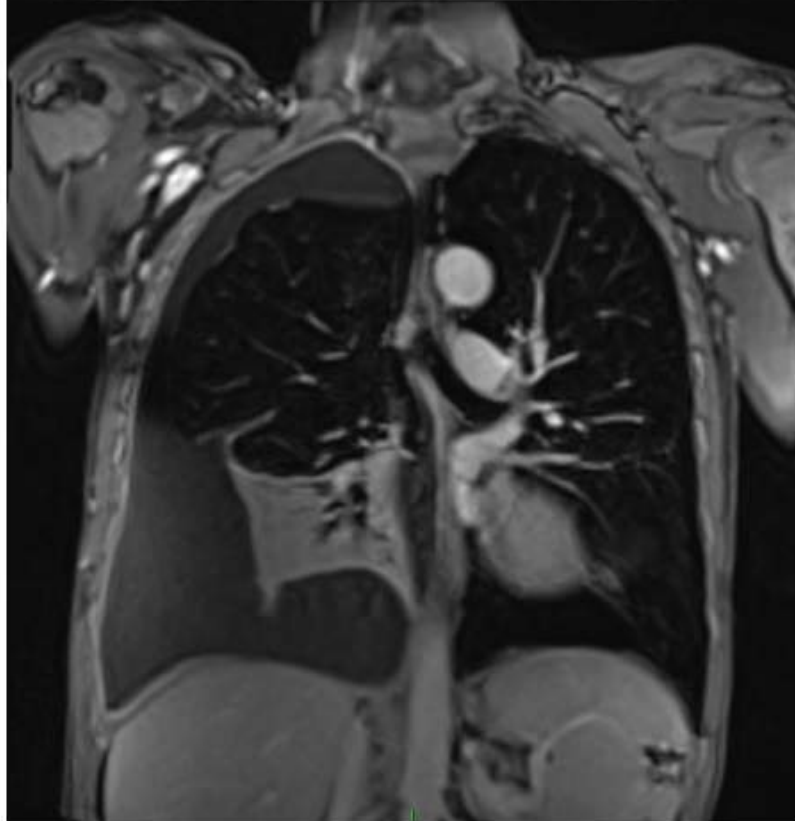
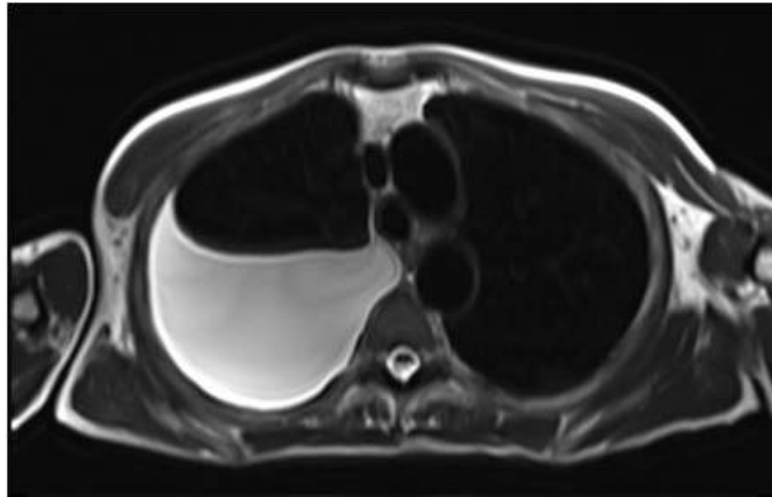
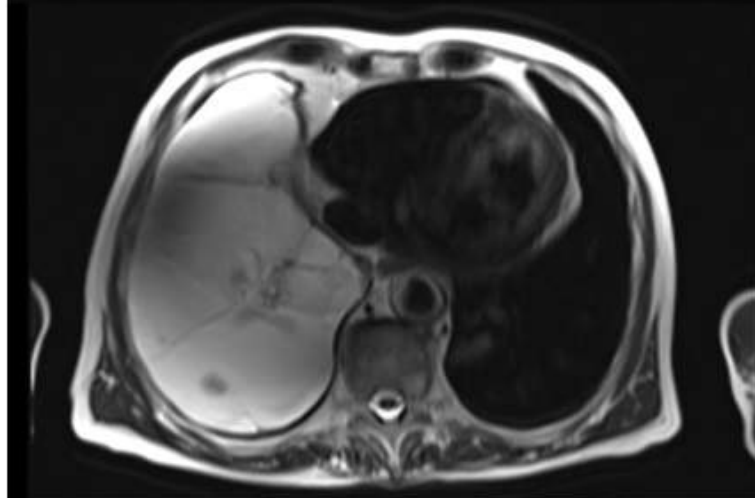


Figure 1.5 T1-weighted axial (Panel A) and coronal (Panel B) fat-saturated VIBE images of a patient with pleural effusion, taken post-contrast using a 3T Siemens Magnetom PRISMA[®] MR scanner at the Glasgow Clinical Research Imaging Facility, QEUH

Panel A



Panel B



Panel C

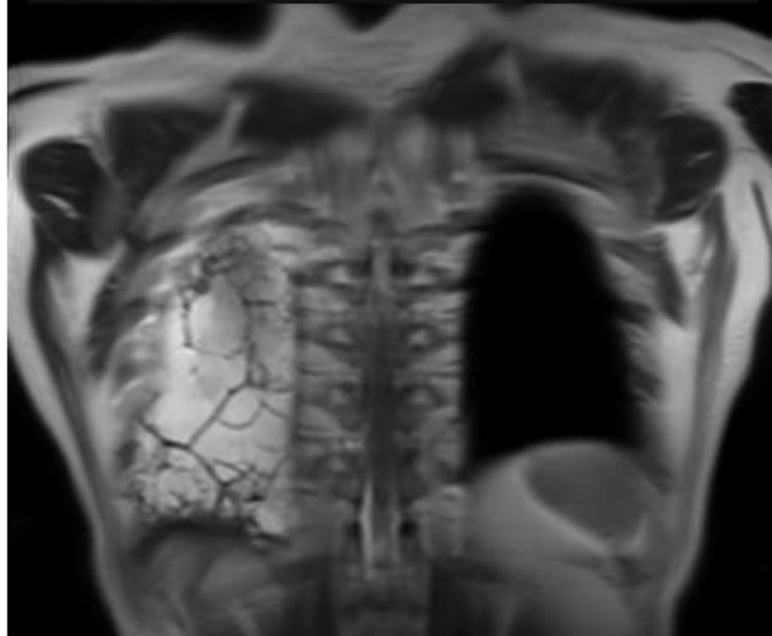


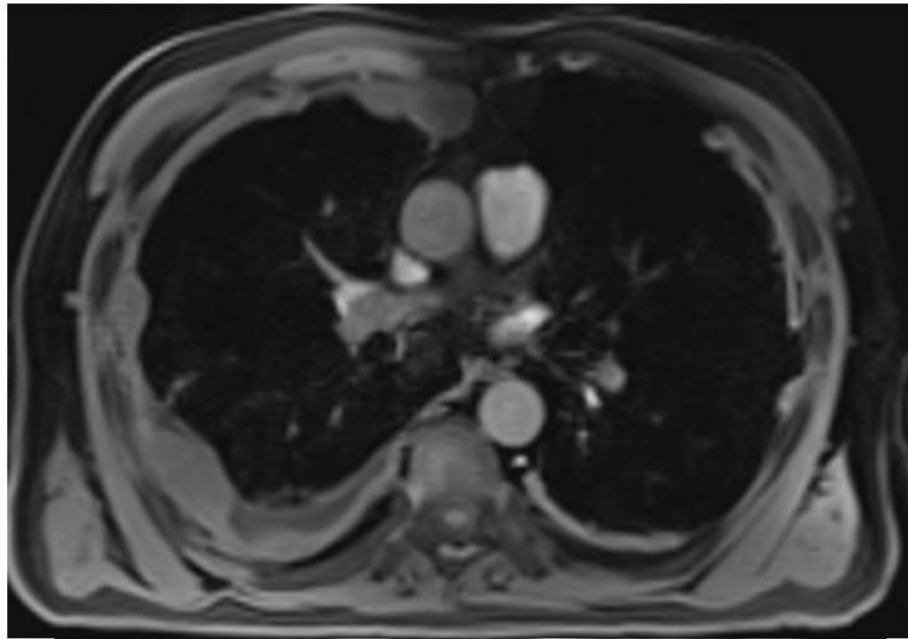
Figure 1.6 T2-weighted axial (Panels A and B) and coronal (Panel C) HASTE images of a patient with pleural effusion, taken pre-contrast using a 3T Siemens Magnetom PRISMA[®] MR scanner at the Glasgow Clinical Research Imaging Facility, QEUH. Panels B and C clearly demonstrate multiple septations (appearing dark) within pleural fluid (bright)

Features of malignancy previously described such as nodular pleural thickening, mediastinal pleural involvement and infiltration of the chest wall or diaphragm are all demonstrable on MRI (see Figure 1.7). The presence of these features at MRI resulted in a sensitivity of 96% and specificity of 80% for pleural malignancy in one retrospective series (95% confidence intervals not reported). (77) The same study reported findings of increased signal intensity of malignant pleural lesions in comparison to intercostal muscles at both T2-weighted and contrast-enhanced T1-weighted imaging, with a resulting sensitivity of 91% and 93% and specificity of 80% and 73% respectively (95% confidence intervals not reported). When combining this signal intensity data with the described morphological findings, the authors reported an overall sensitivity of 100% and specificity of 93% for pleural malignancy (95% confidence intervals not reported). (77)

Boraschi *et al* reported increased signal intensity at T1 and T2-weighted imaging in patients with MPM and low signal intensity within benign pleural plaques. (99)

Similarly, Falaschi *et al* reported pleural hyperintensity in comparison to intercostal muscle at T1-weighted imaging, differentiating between malignant and benign pleural lesions with a sensitivity of 100% and specificity of 60% (95% confidence interval not reported). Patients with TB pleuritis demonstrated falsely elevated pleural hyperintensity on both T1 and T2-weighted imaging in this study. (100)

Panel A



Panel B



Figure 1.7 T1-weighted axial (Panel A) and coronal (Panel B) fat-saturated VIBE images of two patients with Malignant Pleural Mesothelioma, taken post-contrast using a 3T Siemens Magnetom Verio® MR scanner at the BHF Glasgow Cardiovascular Imaging Facility (Panel A) and a 3T Siemens Magnetom PRISMA® MR scanner at the Glasgow Clinical Research Imaging Facility, QEUH (Panel B). Panel A demonstrates enhancing pleural tumour and Panel B demonstrates nodular pleural thickening with chest wall invasion

MRI examination of patients with pleural malignancy using diffusion-weighted MRI (DWI-MRI) has also been described. DWI-MRI is based on the random motion of water protons within tissue. (101) The Apparent Diffusion Co-efficient (ADC), measured at DWI-MRI is a quantitative measure of the diffusion of water molecules, and can provide information about tissue such as tissue cellularity (increased cellularity resulting in a lower ADC) and oedema (associated with a higher ADC). (102) DWI-MRI is well established in neuro-imaging, in particular assessment of acute cerebral ischaemia (103) and has also been used to assess renal lesions (104) and prostate cancer. (105) Changes in MPM at DWI-MRI have previously been reported by Gill *et al*, who reported lower ADC levels in MPM in comparison to patients with benign pleural disease, indicating increased cellularity causing restricted water diffusion. (106) In addition, it has been reported that patients with epithelioid subtype exhibit significantly higher ADC values than patients with sarcomatoid MPM. (107,108) However, Gill *et al* were unable to compute ADC values for 12% (n=7) of the patients included in their study as a result of significant image distortion. (106) Coolen *et al* also demonstrated significantly lower ADC values at DWI-MRI in patients with MPM in comparison to patients with benign disease and reported a sensitivity of 71% and specificity of 100% at an optimum ADC cut-off of $1.52 \times 10^{-3} \text{mm}^2/\text{sec}$ (95% confidence intervals not reported). (90) Pleural pointillism is a more recently described visual analogue of ADC at DWI-MRI, which does not require software calculation of a quantitative value. This describes inhomogeneous pleural hyperintensity at high b value imaging (b value $1000 \text{ sec}/\text{mm}^2$) representing areas of low diffusion. In a single-centre, prospective study of 100 consecutive patients with suspected MPM, the presence of pleural pointillism was detectable in patients with pleural malignancy with a sensitivity of 92.5% (95% CI 83.7 - 96.8%) and specificity of 78.8% (95% CI 62.2 - 89.3%). (109)

Dynamic-Contrast Enhanced MRI (DCE-MRI) is based on assessment of tissue microvasculature and vascular permeability. Sequential MR images are acquired in the first few seconds after contrast injection (typically intravenous gadolinium), imaging the temporal passage of contrast material through tissue and thus providing information about tissue perfusion. (110) Utilising DCE-MRI, pharmacokinetic parameters characterising perfusion (redistribution rate

constant (K_{el}) and microvascular permeability (elimination rate constant (K_{ep})) can be calculated. K_{el} is a measure of the rate of Gadolinium transfer between the extracellular space and the vascular space. K_{ep} is a measure of the rate of Gadolinium elimination from the intravascular space. DCE-MRI has previously been studied in multiple tumour types, including breast (111-113), hepatocellular (114) and prostate cancer. (115,116) In addition, DCE-MRI has previously been studied in MPM. Giesel *et al* performed DCE-MRI in 19 patients with predominantly stage IV MPM, measuring pharmacokinetic parameters (amplitude, redistribution rate constant (k_{ep}) and elimination rate constant (k_{el})) following intravenous Gadolinium contrast administration. They demonstrated areas of intense contrast enhancement within pleural tumour (high amplitude) in addition to a rapid washout pattern (positive k_{el}) within 'hot spots' of the tumour and slow contrast elimination (negative k_{el}) within the remaining tumour. (117) The same authors went on to report a moderate correlation ($r=0.5$) between total tumour Amplitude (increase of signal intensity post-contrast relative to pre-contrast signal intensity) and Microvessel Density measured in formalin-fixed, paraffin-embedded pleural tumour, using CD34 immunostain. (118)

Coolen *et al* subsequently corroborated these findings, performing DCE-MRI in addition to DWI-MRI in a small prospective cohort study with a combined sensitivity of 93% and specificity 94% (95% confidence intervals not reported) for pleural malignancy. (90) These studies highlight the potential of DCE-MRI for detection of MPM, however, successful measurement of pharmacokinetic parameters is difficult to achieve in patients who do not have bulky (and therefore typically advanced) tumour. In addition, DCE-MRI is limited by the compromise between spatial resolution and temporal resolution (119), which is significant in a morphologically complex disease such as MPM. A limited number of slices and therefore volume can be included in DCE-MRI, due to the limited acquisition time, resulting in localised, 'hot-spot' sampling rather than acquiring information about the entire volume of pleura. This results in a risk of sampling error, where the region sampled is not representative of the entire tumour, (120) which is significant in MPM, which has a heterogeneous and often widespread disease distribution. This limits clinical utility as a diagnostic

biomarker, particularly in early stage detection of MPM but highlights its potential as a predictive biomarker of anti-angiogenic chemotherapy response.

1.11 Staging of MPM

Staging of MPM is difficult due to its unusual rind-like growth pattern, different to the expansile mass growth of most other tumours. Until recently, the International Mesothelioma Interest Group (IMIG) recommended Tumour Node Metastasis (TNM) 7th edition staging system was the mostly widely accepted current staging system for MPM (see Table 1.2). (121) However, these recommendations were based largely on expert consensus and data from small retrospective surgical series. In addition, Tumour (T) staging reflected anatomical surfaces involved or invaded into, rather than the size of the primary tumour, and these judgements were best made at time of surgery, rather than on imaging. It was therefore difficult to use in clinical practice, where the majority of patients do not undergo surgery. In addition, nodal (N) staging was based on the N descriptors in Non-Small Cell Lung Cancer (NSCLC) staging. The lymphatic drainage of the pleura differs from that of the lung, with evidence of direct mediastinal drainage in previous studies. (122) (123) As a result, patterns of nodal spread in MPM almost certainly differ to those in lung cancer. (124)

The International Association for the Study of Lung Cancer (IASLC) Mesothelioma database, was established as part of the Mesothelioma Staging Project in 2011. This incorporated retrospective data, from multiple (largely surgical) centres, including data from patients diagnosed between 1995 to 2009. Initial review of 3101 patients, 3017 (97%) of whom were surgical, included in the database highlighted inadequacies in the current staging system. In particular, there were discrepancies between clinical and pathological staging, with frequent upstaging following surgery, and no statistically significant difference in survival between T1 versus T2 patients nor between N1 versus N2 patients. (125) The Prospective Staging Project in Malignant Pleural Mesothelioma was therefore initiated by the IASLC in 2010. Subsequent review of a database of 3519 MPM cases (1566 prospectively collected and 1953 retrospectively collected) from 29 centres across four continents has informed the 8th edition of TNM staging, (see Table 1.3) and includes a larger number of non-surgical patients. (126) (127) (128)

Review of T staging in 1987/3519 MPM cases demonstrated poor discrimination in survival between clinically staged T1a and T1b categories (HR 0.99, $p=0.95$). (126) Furthermore, review of N staging in 2173/3519 MPM cases demonstrated poor discrimination in survival between pathologically staged N1 and N2 categories (HR 0.99, $p=0.99$). (127) Updated 8th edition T-staging therefore collapses 7th edition T1a and T1b into a single T1 category. (126) Similarly, updated 8th edition N-staging collapses 7th edition N1 and N2 into a single N1 category, comprising ipsilateral, intrathoracic nodal metastases, with the 7th edition N3 now being reclassified as N2. (127)

At the time of recruitment of patients to the studies outlined in this thesis, the previous edition of TNM staging was being used and therefore all staging reported in the following chapters is done so according to the 7th edition TNM staging system. Review of the mesothelioma database has demonstrated a survival disadvantage with increasing maximal pleural thickness (patients with a maximal pleural thickness $<5.1\text{mm}$ had a 24-month survival of 51% versus 39% for patients with a maximal pleural thickness $\geq 5.1\text{mm}$) and increasing total pleural thickness (patients with a total pleural thickness $<13\text{mm}$, 13 - 60mm and $\geq 60\text{mm}$ had a 24-month survival of 55%, 40% and 30% respectively). Increasing pleural thickness was also associated with an increased rate of nodal involvement. (126) Quantifying disease using pleural thickness measurements or volumetric assessment therefore has the potential to be used in the future as an alternative or addition to T staging. The need for this has been highlighted by the significant difficulty in accurate clinical staging in MPM using current imaging modalities, with 80.8% of stage I and 69.5% of stage II patients being upstaged following surgical staging. (125) Here I discuss the current roles of CT, PET-CT and MRI in the staging of MPM.

Table 1.2 IMIG/TNM 7th Edition staging system for Malignant Pleural Mesothelioma

Primary Tumour (T)

Tx	Not assessable
T0	No evidence of primary tumour
T1a	Tumour limited to the ipsilateral parietal pleura, including mediastinal and diaphragmatic pleura, no involvement of visceral pleura
T1b	Tumour involving ipsilateral parietal and visceral pleura
T2	Invasion of tumour into the underlying lung or involvement of the diaphragmatic muscle
T3	Locally advanced but potentially resectable tumour Invasion of tumour into endothoracic fascia or mediastinal fat Solitary focus of tumour invading chest wall Non-transmural pericardial involvement
T4	Locally advanced, technically unresectable tumour Diffuse or multi-focal chest wall involvement, with or without rib destruction Trans-diaphragmatic extension of tumour into peritoneum Extension of tumour to the contralateral pleura, spine or one or more mediastinal organs, including transmural pericardial involvement, with or without pericardial effusion, or tumour involving the myocardium

Regional Lymph Nodes (N)

Nx	Not assessable
N0	No regional lymph node metastases
N1	Ipsilateral intrapulmonary or hilar lymph node metastases
N2	Ipsilateral mediastinal lymph node metastases, including ipsilateral internal mammary or para-aortic lymph node metastases
N3	Contralateral intrapulmonary, hilar or mediastinal lymph node metastases, or any (ipsilateral or contralateral) supraclavicular lymph node metastases

Distant Metastasis (M)

MX	Not assessable
M0	No distant metastasis
M1	Distant metastasis present

Table 1.3 TNM 8th Edition staging system for Malignant Pleural Mesothelioma**Primary Tumour (T)**

Tx	Not assessable
T0	No evidence of primary tumour
T1	Tumour limited to parietal (including mediastinal and diaphragmatic pleura) +/- involvement of the visceral pleura
T2	Invasion of tumour into the underlying lung or involvement of the diaphragmatic muscle
T3	Locally advanced but potentially resectable tumour Invasion of tumour into endothoracic fascia or mediastinal fat Solitary focus of tumour invading chest wall Non-transmural pericardial involvement
T4	Locally advanced, technically unresectable tumour Diffuse or multi-focal chest wall involvement, with or without rib destruction Trans-diaphragmatic extension of tumour into peritoneum Extension of tumour to the contralateral pleura, spine or one or more mediastinal organs, including transmural pericardial involvement, with or without pericardial effusion, or tumour involving the myocardium

Regional Lymph Nodes (N)

Nx	Not assessable
N0	No regional lymph node metastases
N1	Ipsilateral intrapulmonary, hilar or mediastinal lymph node metastases, including ipsilateral internal mammary or para-cardiac lymph nodes
N2	Contralateral intrapulmonary, hilar or mediastinal lymph node metastases, or any (ipsilateral or contralateral) supraclavicular lymph node metastases

Distant Metastasis (M)

MX	Not assessable
M0	No distant metastasis
M1	Distant metastasis present

1.11.1 CT

Despite its widespread use in clinical practice for the detection of pleural malignancy and MPM, CT performs poorly as a staging tool in comparison to alternative imaging techniques such as PET-CT and MRI.

CT features that suggest disease is not technically resectable include: invasion of extrapleural fat, infiltration or displacement of ribs by tumour, bony destruction and invasion or tumour encasement of the diaphragm. (110) However, CT has limitations in the assessment of infiltration of the chest wall and diaphragm, (129,130) with one study reporting 75% of cases with chest wall infiltration precluding surgical resection not being identified on preceding CT imaging. (131) The sensitivity of CT for nodal metastases has previously been reported as 56% with a specificity of 39% (95% confidence intervals not reported). (130) This is insufficient, particularly given the significant survival differences between patients with N0 versus N1 and N2 disease (HR 1.26, $p=0.0071$ and HR 1.40, $p<0.0001$ respectively). (125) Distant metastases, including pulmonary metastases can be identified on CT (132) However, previous studies have demonstrated frequent up-staging of disease following further evaluation with PET-CT. One study reported up-staging in 37% of patients who underwent CT and PET-CT, with 77% of cases reflecting distant metastases identified on PET-CT that were not identified on CT. (133)

Volumetric assessment of tumour burden has previously been studied utilising CT for prognostic and treatment response purposes. Pass *et al* assessed pre-operative tumour volumes in 48 MPM patients undergoing extrapleural pneumonectomy or pleurectomy/decortication. They reported a significant difference in survival based on pre-operative CT-based tumour volumes. Patients with tumour volumes $<100\text{cm}^3$ had a median overall survival of 22 months, compared to 9 months in patients with tumour volumes $>100\text{cm}^3$. In addition, progressively higher post-operative IMIG stage was associated with higher median pre-operative CT tumour volume in this study. (134) Similarly, Gill *et al* retrospectively measured pre-operative CT-based tumour volume in 88 patients with epithelioid MPM undergoing extrapleural pneumonectomy. The median

tumour volume was 319cm³ in this study and increasing tumour volume was associated with worse survival (tumour volume $\leq 500\text{cm}^3$ had a median overall survival of 24.4 months versus a median overall survival of 12 months for tumour volume $> 500\text{cm}^3$). (135) While CT volumetry appears to be a promising technique of assessing tumour burden, its application in clinical practice is currently still limited, principally due to the time consuming nature of free-hand volumetric measurements. Studies have utilised a semi-automated method of measuring tumour volume to overcome this, based on differential Hounsfield Units (HU). (136) (137) (138) However, MPM is morphologically complex, with an unusual growth pattern and delineation of pleural tumour from adjacent structures, such as intercostal muscle and pleural fluid, with a similar density represents a significant challenge in this regard.

1.11.2 PET-CT

Based on prior data, integrated PET-CT should be utilised rather than isolated PET since the sensitivity of the latter for N2 disease has previously been reported as 11% in patients undergoing surgical resection with lymph node dissection, whereas the sensitivity and specificity of integrated PET-CT for predicting N2 disease has been reported as 60% and 80% respectively. (139) Plathow *et al* assessed the accuracy of CT, PET-CT and MRI for the selection of patients with potentially-operable disease (earlier than Stage III) by acquiring all scans prior to surgery in 54 patients (52 of whom subsequently underwent surgery). They concluded that PET-CT offered the highest diagnostic accuracy, for example in stage III disease, diagnostic accuracy rates for CT, MRI and PET-CT were 75% (sensitivity 75%, specificity 100%), 90% (sensitivity 91%, specificity 100%) and 100% (sensitivity 100%, specificity 100%), respectively. (140) This performance largely reflected better detection of nodal and extra-thoracic metastases. However, PET-CT has been shown to underestimate T staging in up to 29% of patients in previous studies, largely due to under-identification of chest wall and diaphragmatic invasion. (141) PET-CT provided accurate T staging in only 14/24 (63%) of patients in comparison to pathological staging in patients enrolled in a single-centre, prospective feasibility study of EPP followed by intensity-modulated radiation therapy. (141) In one other small study, 24% (n=7) of patients had extra-thoracic metastases demonstrated on PET-CT not

previously identified utilizing conventional CT. (141) (142) Although integrated PET-CT is the best imaging modality for detecting nodal and extra-thoracic metastases, (143) its limitations in MPM should also be appreciated, particularly in the assessment of locally invasive T4 disease. (141) Therefore, PET-CT has important limitations but definite utility in the staging of patients who are being considered for radical therapies or trials.

1.11.3 MRI

In previous studies, MRI has been shown to be superior to CT in detecting invasion of chest wall, diaphragm and bony structures, which was best visualised on T1-weighted images, and important for both detection and staging of MPM. (79,144) Stewart *et al* performed contrast-enhanced 1.5-Tesla MRI scans on 69 patients with apparently resectable MPM following contrast-enhanced CT scanning. MRI detected the presence of technically non-resectable disease in 17/69 (22%) of these patients not previously demonstrated on CT. This included mediastinal involvement, diaphragmatic invasion, chest wall infiltration and contralateral pleural disease. (145) Therefore MRI has clinical utility in MPM staging and assessment of the presence of infiltrative disease that would preclude surgical resection.

1.12 Blood Biomarkers

A diagnostic biomarker is a quantifiable substance, involving measurements on biological material, such as blood, or on imaging that can be used to accurately, reproducibly and objectively differentiate a pathological state from an alternative controlled state (such as a normal biological state). (146,147) An ideal diagnostic biomarker in oncology would be measurable non-invasively and detectable at an early disease stage. In MPM, biomarkers are most frequently measured in blood and pleural fluid. Previously published data regarding the most widely studied and/or promising blood biomarkers are summarised below.

1.12.1 Mesothelin

Mesothelin is a cell-adhesion glycoprotein that is over-expressed in MPM (in addition to pancreatic and ovarian cancer). (148,149) Serum mesothelin levels

(also known as serum mesothelin related protein (SMRP)) are elevated in patients with MPM in comparison to asbestos-exposed controls. (150,151) In a meta-analysis, Hollevoet *et al* performed a ROC regression analysis on serum mesothelin levels in MPM patients versus controls and reported that the highest AUC was obtained when differentiating patients with advanced stage (III/IV) epithelioid MPM (AUC 0.84) and the lowest AUC was demonstrated in patients with early stage (I/II) sarcomatoid MPM (AUC 0.56). (152) Previous authors have reported sensitivities for MPM ranging from 56-77% at 95% specificity. (149-151) However the meta-analysis by Hollevoet *et al*, incorporating data from 4491 individuals (1026 with MPM) reported substantial between-study heterogeneity in results, with sensitivity ranging between 19 - 68% and specificity ranging between 88 - 100%. The summary estimate of sensitivity was only 47% (95% prediction interval 26 - 70%) and specificity 96% (95% prediction interval 85 - 99%). (152) This is insufficient for diagnostic purposes and Mesothelin is not currently part of assessment algorithms. (44) (143)

1.12.2 Megakaryocyte Potentiating Factor

Megakaryocyte Potentiating Factor (MPF) is a cleavage product of the Mesothelin Precursor Protein, the other being Mesothelin/SMRP. Increased serum levels have been reported in MPM cases, relative to asbestos-exposed controls and patients with pleural plaques and/or asbestosis. (150) Creaney *et al* reported a sensitivity of 34% at 95% specificity in a study involving 66 MPM patients and inferior performance compared to serum Mesothelin in the same cohort. (150) Hollevoet *et al* later reported a MPF sensitivity of 64% at 95% specificity, which was equivalent to Mesothelin (68% at 95% specificity) in a larger prospective study, which included 85 MPM patients. (153) MPF therefore offers no advantage over Mesothelin.

1.12.3 Osteopontin

Osteopontin is a glycoprotein overexpressed in several cancers, including MPM, lung cancer, ovarian cancer and malignant melanoma. Pass *et al* reported higher serum Osteopontin levels in 76 MPM patients relative to asbestos-exposed normal controls, with a MPM sensitivity of 78% at 86% specificity. Diagnostic accuracy was similar in patients with early and late stage MPM, leading the authors to

propose a potential future role as an early detection marker in asbestos-exposed individuals. (154) However, these results were not validated externally, with a sensitivity of 47% at 95% specificity subsequently reported by Creaney *et al* (150), possibly related to protein instability due to thrombin cleavage. Osteopontin therefore has no current clinical role as a MPM biomarker.

1.12.4 HMGB-1

High Mobility Group Box-1 (HMGB-1) is secreted by active monocytes/macrophages and passively released by cells undergoing necrosis. (155) It is pro-inflammatory and overexpressed in a number of different tumour cells including colorectal cancer, melanoma, breast cancer and pancreatic cancer. (156) In human mesothelial cells, asbestos exposure results in necrosis and release of HMGB-1 (non-acetylated isoform) into the extracellular space, triggering activation and accumulation of macrophages and resultant active secretion of pro-inflammatory mediators, including HMGB-1 (hyper-acetylated isoform) and Tumour Necrosis Factor (TNF α). (157,158) In a retrospective series, Tabata *et al* reported increased serum HMGB-1 (isoform not specified) in patients with MPM (n=61) relative to patients with pleural plaques and asbestosis (n=26) and healthy asbestos-exposed controls (n=19). Between these groups they reported a sensitivity of 34% (at 100% specificity), however they found no difference in HMGB1 levels between MPM cases and 11 additional patients with secondary pleural malignancy (159). This greatly limits the clinical applicability of these findings. More recently, Napolitano *et al* reported increased serum levels of hyper-acetylated HMGB-1 in patients with MPM (n=22) in comparison to asbestos-exposed (n=20) and healthy controls (n=20). A cut-point of 2.0ng/ml differentiated these groups perfectly (sensitivity 100%, specificity 100% (AUC 1.000). Serum HMGB-1 performed less well in the differentiation of MPM from benign effusions (n=13) or non-mesothelioma malignant effusions (n=25, AUC 0.86 for total HMGB-1 and AUC 0.84 for hyper-acetylated HMGB-1). (158) These results are promising and should be prospectively validated in external populations in future studies.

1.12.5 SOMAscan™ Proteomic Classifier

SOMAscan™ is a 13-protein classifier developed by SomaLogic Inc. (Boulder, Colorado, USA), using a novel proteomics-based biomarker detection technique based on SOMAmers™ (Slow Off-rate Modified Aptamers). (160) Proteomics is the study of the whole complement of proteins produced by an organism in order to gain better understanding of its underlying biology. The SOMAscan™ assay has the capability of measuring >1000 proteins from a small biological sample such as serum. (161) SOMAmers™ are polyanion-single-stranded DNA molecules (aptamers) (162) that have been chemically modified with the addition of protein-like functional groups, allowing them to bind to an increased number of proteins and peptides with high specificity. SOMAmers™ with slow dissociation rates (half-life >30 minutes) are selected to further improve specificity, where non-specific protein binding interactions have faster dissociation kinetics (half-life of a few minutes or less) following challenging by an anionic competitor, e.g. dextran sulfate. (160,161)

Ostroff *et al* measured over 800 candidate proteins using the Somascan™ proteomic assay in the serum of 117 MPM patients and 142 asbestos-exposed controls. The study was retrospective, using archived serum and all samples were drawn at surgical MPM centres in the US between 1996 and 2011. They identified 64 candidate biomarkers, which were ranked by their Gini importance and constructed a 13-protein random forest classifier model containing the highest ranked markers. Using a cut-off classifier score of 0.5, the 13-protein classifier was able to differentiate MPM from controls with an overall sensitivity (in combined training, verification and validation cohorts) of 93.2% (95% CI 88.6 - 97.7%) at a specificity of 90.8% (95% CI 86.1 - 95.6%). (163). Sensitivity of the classifier for detecting stage I/II disease was 88%. However, MPM specificity was lower in patients with non-MPM pleural effusion, with 30/32 patients with non-MPM pleural effusion having false positive results (specificity 6%). (163)

The 13 proteins that comprise the Somascan™ classifier are either up-regulated (n=9) or down-regulated (n=4) in MPM vs. asbestos-exposed control (see Table 1.4). The up-regulated proteins include: C9, encoded by C9, CKbeta8-1, encoded by CCL23, Cyclin-dependent kinase-5 (CDK5), encoded by CDK5/CDK5R1, B-lymphocyte chemoattractant (BLC) encoded by CXCL13, Coagulation factor

encoded by F1, Ficolin-2 (FCN2), encoded by FCN2, Soluble Intercellular Adhesion Molecule-2 (sICAM-2), encoded by ICAM2, Midkine, encoded by MDK and CD30, encoded by TNFRSF8. The down-regulated proteins include: Apolipoprotein A-1 (Apo A-1), encoded by APOA1, Fibronectin encoded by FN1, Stem Cell Factor soluble receptor (SCF-sR), encoded by KIT and Kallistatin, encoded by SERPINA4.(163) These proteins are principally involved in inflammation and regulation of cellular proliferation. (163) The roles of these 13 proteins are discussed briefly here.

Table 1.4. 13 proteins that comprise the SOMAscan assay, which are either up-regulated or down-regulated in Malignant Pleural Mesothelioma (MPM) relative to Asbestos-exposed controls (AEC)

Protein Target	Encoding Gene	Function	MPM vs. AEC*	Previously identified in MPM
Complement 9	C9	Adaptive immune response	Up	No
Ck- β 8-1	CCL23	Cellular ion homeostasis, inflammatory response	Up	No
Cyclin-dependent kinase5/p35	CDK5	Cell morphogenesis	Up	No
B-lymphocyte chemoattractant	CXCL13	Immune system development	Up	No
Coagulation Factor IX	F9	Coagulation cascade	Up	No
Ficolin-3	FCN2	Immune effector	Up	No
Intecellular Adhesion Molecule-2	ICAM2	Cell adhesion	Up	No
Midkine	MDK	Regulation of cell division	Up	No
CD30	TNFRSF8	Regulation of cytokines & cell proliferation	Up	Yes
Fibronectin	FN1	Cell morphogenesis	Down	Yes
Stem Cell Factor	KIT	Immune system development, receptor tyrosine kinase	Down	Yes
Kallistatin	SERPINA4	Serine protease inhibitor	Down	No
Apolipoprotein-A1	APOA1	Lipd transport	Down	No

MPM; Malignant Pleural Mesothelioma, AEC; Asbestos-exposed control

*Up or down-regulated in MPM relative to AECs

CD30 is a member of the Tumour Necrosis Factor (TNF)-receptor family, it is a type 1 transmembrane glycosylated protein. (164) It is expressed in activated T cells and activated B cells producing Th2-type cytokines (165) and Hodgkin's and Reed-Sternberg cells. (164) Elevated serum levels of soluble CD30 is found in autoimmune conditions, including systemic lupus erythematosus and mixed connective tissue disease, (166) viral infections including Human Immunodeficiency Virus (HIV) and Epstein-Barr Virus (EBV) infection and malignancy, including Hodgkin's disease and anaplastic large cell lymphoma. (167-169) Cross-linking of CD30, mediated by TNFR-associated factor (TRAF) proteins, results in activation of NF-kappa B, resulting in induction of IL-2, IL-6 and TNF-alpha. (167) CD30 positive immunohistochemistry staining has also previously been demonstrated in MPM. (170)

CKbeta8-1/CCL23 is a chemokine which interacts with CCR1 receptor, which is expressed on monocytes, dendritic cells, lymphocytes and endothelial cells. (171) It augments endothelial cell migration and differentiation (172) and mediates monocyte chemotaxis. (173) Serum levels of CKbeta8-1 have been reported to be elevated in inflammatory disorders such as Systemic Sclerosis. (174)

Cyclin-dependent kinase-5 (CDK5) is a widely expressed enzyme, found in pancreatic cells and lens epithelial cells. It is principally expressed in neuronal tissues where it regulates neuronal migration and axonal growth in the developing central nervous system. (175) Dysregulation of CDK5 has been implicated in neurodegenerative disorders including Alzheimer's disease and Motor Neuron Disease and it is upregulated in nociceptive neurons during peripheral inflammation. (175) CDK5 is activated by p35 in response to inflammation and this has been shown to be regulated by TNF alpha-induced NF kappa B signalling pathways. (176)

B-lymphocyte chemoattractant (BLC) is a chemokine that mediates B-cell migration to lymphoid follicles and the spleen. (177) Induction of BLC is regulated by NF-kappa B signalling pathways (178,179) and its expression has been shown to be upregulated in breast cancer. (180) This is associated with increased serum levels of BLC in patients with metastatic breast cancer. (180)

Complement 9 (C9) is a part of the complement system that forms a membrane attack complex (MAC) along with complement proteins C5b, C6, C7 and C8 (C5b-9 complex). The MAC interacts with the cell membrane, forming pores which ultimately result in cell lysis. However, if insufficient channels are formed in the cell membrane, the C5b-9 complex can induce cellular proliferation instead of lysis (181) by activating signal transduction pathways and transcription factors. (182,183) Resistance to complement-dependent cell death is also mediated by the NF-kappa B pathway. (184) C5b-9 expression has previously been shown to be upregulated in gastric adenocarcinoma (185) and breast cancer. (186)

Ficolin-2 (FCN2) is a protein synthesised in the liver and found in serum. (187) It can activate complement via the lectin pathway (188) and binds to and opsonises a number of microbial pathogens including *Streptococcus pneumoniae* and *Pseudomonas aeruginosa*. (187)

Intercellular Adhesion Molecule-2 (ICAM2) is a transmembrane glycoprotein that is a member of the immunoglobulin superfamily. It is expressed on resting lymphocytes, vascular endothelial cells and haematopoietic progenitor cells (189) and has roles in lymphocyte trafficking, and neutrophil migration. (190,191) ICAM-2 has previously been reported to inhibit cancer cell migration, limiting the metastatic potential of neuroblastoma cells. (192)

Midkine is a heparin-binding growth factor which has roles in migration of inflammatory cells, angiogenesis, cell growth and carcinogenesis (193) There is increased expression of midkine in a number of malignancies, (194) including gastric cancer, (195) hepatocellular carcinoma, (196) oesophageal cancer, pancreatic cancer, lung cancer (197), breast cancer (198) and neuroblastoma. (199) This increased expression is associated with increased circulating levels of midkine. (194) Cell-free midkine mRNA levels have also been demonstrated to be elevated in malignant effusions from lung cancer patients, (200) however there has been no previously reported association between midkine levels and MPM.

Apolipoprotein A-1 (Apo A-1) is the major protein component of human plasma high density lipoprotein (HDL), synthesised in the liver and small intestine. (201)

It has roles in the transportation of cholesterol to the liver and intestine and is involved in the uptake of lipoproteins by tissues. (202) It has also been reported to inhibit inflammation, tumour growth and metastasis. (203) Low levels of Apo A-1 have been shown to be associated with increased risk of lung cancer, (204) oesophageal cancer (205) and breast cancer, (206) and is associated with a poorer prognosis in lung cancer. (206)

Fibronectin is an extracellular matrix (ECM) glycoprotein synthesised in the liver with roles in cell adhesion, cell migration and wound healing through ECM remodelling. (207) In cancer, alternatively spliced fibronectin is up-regulated within tumour stroma and is associated with epithelial-mesenchymal transition of cancer cells, enhanced neoangiogenesis and tumour invasion and a stiffened ECM. (208) Low fibronectin expression in multiple mesothelioma cell lines *in vitro* has been reported. (209) However, high plasma and pleural fluid fibronectin levels have previously been demonstrated in MPM, metastatic lung cancer and tuberculous effusions. (210,211)

Stem Cell Factor (SCF), also known as kit ligand or mast cell growth factor, is a cytokine that exists in soluble and transmembrane forms. It is the ligand for the tyrosine kinase receptor c-kit and has roles in haematopoiesis, germ cell maturation, melanocyte development and mast cell proliferation. (212) SCF-deficient mutant mice exhibit increased sensitivity to lethal irradiation, (213) highlighting the potential role of SCF in inhibiting apoptosis and stimulating cell cycle progression. (212,214) Upregulation of c-kit receptor and SCF has previously been reported in chemoresistant mesothelioma cell lines *in vitro*. (215)

Kallistatin is a serine protease inhibitor initially identified in human lung fibroblasts as a kallikrein-binding protein. (216) Kallikrein enzymatically releases kinin from kinogen. Kinin is a vasoactive peptide that mediates smooth muscle contractility, vasodilation and vascular permeability. (216) Kallistatin as additional roles in regulation of blood pressure and inhibition of angiogenesis, inflammation and tumour growth. (217,218) Kallistatin suppression of tumour angiogenesis has been reported to be via inhibition of TNF alpha-induced NF kappaB pathways and reduced expression of VEGF. (219)

Many of the proteins that make up this SOMAscan™ signature have not previously been associated with MPM and may lead to novel drug or diagnostic targets. Importantly, several of these proteins are inflammatory mediators and their relationships with talc pleurodesis, which is known to produce an acute systemic inflammatory response, (220,221) and prognostically important inflammatory biomarkers, including neutrophil-to-lymphocyte ratio and the modified Glasgow Prognostic Score (mGPS) (222,223) need to be assessed.

1.12.6 Fibulin-3

Structure and Function

Fibulin-3 is a secreted extracellular glycoprotein encoded by the gene EFEMP1 (EGF-containing fibulin-like extracellular matrix protein 1) located on chromosome 2p16. (224,225) It is a short fibulin, with a molecular mass of 55kDA, (225) characterised by 6 repeated calcium-binding epidermal growth factor (EGF)-like modules followed by a fibulin-type module at the C terminal region. (224,226) Fibulin-3 is expressed in human fibroblasts and is up-regulated in senescent fibroblasts. (224,227) In adult humans, it is widely distributed including to cartilage, bone, subretinal pigment epithelium, skin and capillaries, (226) localised to the basement membrane in epithelial and endothelial cells. (225) Fibulin-3 binds to the elastin precursor, tropoelastin. Elastic fibres, consisting of elastin and microfibrils, together with collagen fibres, contribute to the integrity of the basement membrane in connective tissues. (228-230) EFEMP1 knockdown mice exhibit premature aging and atrophy of fat and muscle, with loss of body mass, formation of hernias and a reduced lifespan. (231) In contrast, mice transfected with EFEMP1, demonstrate an upregulation of vascular endothelial growth factor (VEGF) expression and an accumulation of Fibulin-3 protein in the endoplasmic reticulum of retinal pigment epithelial cells, resulting in vision loss similar to age-related macular degeneration. (232)

Fibulin-3 in malignancy

The level of Fibulin-3 expression varies between solid tumours. It is down-regulated in breast, (233,234) colorectal, (235) non-small cell lung cancer

(NSCLC), (236,237) nasopharyngeal, (238) and hepatocellular carcinoma, (239) where it has been reported to function as a tumour suppressor. Paradoxically, it has been found to be up-regulated in glioma, (240,241) cervical cancer (242) and pancreatic cancer, (232) where it has been reported to promote tumour growth and invasion.

Fibulin-3 has been shown to inhibit the expression and activity of matrix metalloproteinase (MMP)-2, MMP-3 and MMP-9, and increase the expression and activity of MMP antagonists - tissue inhibitor of metalloproteinase (TIMP)-1 and TIMP-3. (225,243) This results in inhibition of cell migration, cell growth, endothelial cell proliferation, angiogenesis and invasion *in vitro* and inhibits tumour angiogenesis *in vivo*, demonstrated in a fibrosarcoma mouse model. (228,238,243)

In breast cancer, EFEMP1 has been reported to be down-regulated in approximately 60% of breast cancer tissues (233) and this has been found to be more exaggerated in advanced stage (IV) breast cancer. (234) Fibulin-3 expression has also been shown to be downregulated in hepatocellular carcinoma cell lines and colorectal carcinoma tissue in comparison to normal colonic tissue and colonic adenomatous tissue as a result of epigenetic silencing through hypermethylation in the promotor region of Fibulin-3. (228,235,239) Comparable to previous studies in breast cancer, (234) Tong *et al*, demonstrated that Fibulin-3 down-regulation was more marked in advanced stage (III/IV) tumours. (235) Similarly, there was a significantly higher rate of EFEMP1 promotor methylation in aggressive NSCLC cell lines in comparison to less invasive NSCLC cell lines (244) and in NSCLC tumour tissue samples in comparison to non-tumour tissue samples. (236) This was reported to be associated with poor tumour differentiation, advanced tumour stage and lymph node metastasis. (236,237)

In contrast, EFEMP1 was found to be up-regulated in aggressive, pro-angiogenic pancreatic carcinoma cell lines in comparison to non-aggressive pancreatic tumour cell lines, in addition to human pancreatic ductal carcinoma tissue specimens. (232) It has been reported that EFEMP1 expression indirectly stimulates tumour growth through activation of epidermal growth factor

receptor (EGFR) (245) and tumour angiogenesis by increasing vascular endothelial growth factor (VEGF) secretion. (232)

Similarly, Fibulin-3 expression is up-regulated in glioma cells, where it is associated with a more aggressive, metastatic phenotype, (240) with increased cancer cell adhesion and migration *in vitro* and increased tumour invasion *in vivo* in a glioma mouse model. Fibulin-3 expression was shown to promote tumour invasion and survival in glioblastoma cells. (240) These tumours also demonstrated increased expression of MMP-2 and MMP-9, (241) in direct contrast to the findings in other cancers. (225,243)

Cervical carcinoma cells have also been reported to show higher levels of Fibulin-3 expression in comparison to normal cervical squamous epithelium. This was associated with lymph node metastasis and vascular invasion, with a positive correlation between EFEMP1 expression and microvessel density, a surrogate marker of tumour vascularity, measured using CD34 immunostaining of tumour tissue. (242)

Fibulin-3 as a Blood Biomarker in Mesothelioma

Davidson *et al* initially reported increased EFEMP1 gene expression in a small study, which included 5 patients with Malignant Peritoneal Mesothelioma. (246) Fibulin-3 was subsequently first highlighted as a potential biomarker in Malignant Pleural Mesothelioma by Pass *et al*. In this retrospective study, Fibulin-3 was measured by a Fibulin-3 ELISA (USCN Life Science Inc., Houston, Texas, USA) on archived plasma and pleural fluid samples from patients with MPM, asbestos-exposed controls and patients with non-MPM pleural effusions in two cohorts (Detroit and New York) and a blinded external validation set (Toronto cohort). Mean plasma Fibulin-3 levels were significantly higher in patients with MPM in comparison to asbestos-exposed controls and patients with non-MPM pleural effusion ($112.9 \pm 7.6\text{ng/ml}$, $24.3 \pm 1.4\text{ng/ml}$, $44.7 \pm 3.4\text{ng/ml}$ respectively, $p < 0.001$) in the New York cohort. At an optimum Fibulin-3 threshold of 52 ng/ml, sensitivity was 97% (at 95% specificity) for distinguishing MPM from all other controls (AUC 0.99 (95% CI 0.974 - 0.997). However, in the blinded external validation set, measured plasma Fibulin-3 levels in patients with MPM was lower

(mean 66.4 ± 7.2 ng/ml) and sensitivity was below 40% (at 95% specificity), AUC 0.87 (95% CI 0.805 - 0.921). (247)

Creaney *et al* subsequently reported lower plasma Fibulin-3 levels (median 28.0 ng/ml (interquartile range (IQR) 20 - 47) in patients with MPM, a lower optimum threshold of 29 ng/ml and overall inferior diagnostic performance (sensitivity 21% at 95% specificity, AUC 0.671) than previously reported by Pass *et al*. They found that the diagnostic performance of Fibulin-3 was inferior to that of Mesothelin measured in the same cohort of patients. (151) This study was performed using archived samples that were drawn within 1 month of diagnosis and this is therefore likely to include patients who have had significant pleural intervention, including thoracoscopic biopsy and talc pleurodesis. This is significant as talc pleurodesis has previously been reported to be associated with increased Fibroblast Growth Factor-beta (FGFb) levels with resultant stimulation of fibroblast proliferation. (248) It is therefore likely that talc pleurodesis would result in elevated Fibulin-3 levels, even in non-MPM effusions.

A small Italian study subsequently found no difference in Fibulin-3 levels between patients with MPM (mean 25.2 ± 1.8 ng/ml) and asbestos-exposed controls (mean 20.7 ± 1.3), p value not reported. However, this study utilised serum rather than plasma and the asbestos-exposed control group had asbestosis rather than benign asbestos-related pleural disease. (249) Serum levels have previously been demonstrated to be significantly lower than plasma levels (mean 87.3 ± 17.6 ng/ml vs. 110.8 ± 21.1 ng/ml, $p=0.006$). (247) Following this, in a small Egyptian study using an unspecified Fibulin-3 assay and internally defined cut-points, Agha *et al* reported 100% sensitivity and 78% specificity in differentiating MPM (n=25) from non-malignant pleural disease (n=9), and 88% sensitivity at 82% specificity in differentiating MPM from secondary pleural malignancies (n=11). (250) No combined sensitivity was reported and the study was limited by small patient numbers. Demir *et al* also assessed serum Fibulin-3 levels in patients with MPM, asbestos-exposed controls and healthy controls. They reported significantly higher levels in MPM (mean 168.1 ± 165.1 ng/ml) in comparison to healthy controls (mean 76.4 ± 39.6 ng/ml) and asbestos-exposed controls, which consisted largely of patients with pleural plaques (mean 87.4 ± 53.5 ng/ml), $p=0.001$. They defined an optimum Fibulin-3 cut-off of 51.41 ng/

providing a sensitivity of 88.1%, specificity 66.7%. (251) Similarly, Kaya *et al* reported significantly higher serum Fibulin-3 levels in patients with MPM (n=43) compared to healthy controls with no known asbestos exposure (n=40) (mean 90.3 ± 42.1 ng/ml vs. 17.8 ± 12.7 ng/ml respectively, $p < 0.001$). Overall diagnostic performance for serum Fibulin-3 in this study was high, with an AUC 0.976 and an optimum cut-off point of 26.6ng/ml providing a sensitivity of 93% at 90% specificity, confidence intervals were not reported. (252) However, this study did not include asbestos-exposed subjects or patients with pleural disease as controls and its clinical relevance is therefore limited.

Finally, Kirschner *et al* measured Fibulin-3 expression and secretion in vitro using cell-conditioned medium collected from several human MPM cell lines (including H28, H226, H2452 and MSTO) and benign mesothelial cells lines (LP9 and MeT-5A) and in vivo in MPM mouse models utilising using a Fibulin-3 ELISA (USCN Life Science Inc.). In vitro, both MPM cell lines and benign mesothelial cell lines expressed Fibulin-3 with no significant difference between the two groups ($p=0.093$) and there was a strong correlation between cellular Fibulin-3 expression and Fibulin-3 protein secretion (Spearman's $\rho=0.78$, $p=0.017$). In vivo, Fibulin-3 was measurable in plasma (but not serum) samples from H226 and MSTO-xenografts. (253) The same group then assessed Fibulin-3 levels in archived blood taken from patients with MPM prior to diagnostic video-assisted thoracoscopic surgical biopsy (VATS) or extrapleural pneumonectomy. Blood samples from patients with benign pleural disease (pleural plaques and pleuritis), non-MPM malignancy (lung, breast, endometrial, colonic adenocarcinoma) and patients with coronary artery disease (CAD) undergoing cardiac surgery were also used as control samples. Archived pleural fluid samples from patients with and without MPM were also assessed for fibulin-3 levels. This was done in two separate cohorts (Sydney, which included 37 patients with MPM and 32 non-MPM controls, and Vienna, which included 47 MPM and 24 non-MPM). Fibulin-3 levels in patients with MPM was significantly higher in patients with MPM than patients with pleural plaques or CAD in the Sydney cohort (mean level 16.10 ± 1.87 ng/ml vs. 10.92 ± 1.54 ng/ml, $p=0.039$) but not in the Vienna cohort (mean level 11.51 ± 1.73 ng/ml vs. 11.97 ± 3.56 ng/ml, $p=0.897$). AUC was 0.63 (95% CI 0.50 - 0.76) and 0.56 (95% CI 0.47 - 0.71) for the Sydney and Vienna cohorts respectively, (253) significantly lower than originally

reported by Pass *et al* (AUC 0.99). (247) Confidence intervals were wide, reflecting the low patient number included in this study. This study was also limited by its retrospective nature and utilisation of blood samples from patients with CAD as a major contributor to the control arm, who did not have evidence of asbestos exposure or pleural disease.

Results from these previous studies are summarised in Table 1.5.

Table 1.5. Summary of previous studies of Fibulin-3 in Malignant Pleural Mesothelioma

Author	Patient Cohort	Sample type	Fibulin-3 Assay	Fibulin-3 level (ng/ml)	Cut-off (ng/ml)	Sensitivity (95% CI)	Specificity (95% CI)	AUC (95% CI)
Pass <i>et al</i> (247)	Detroit	Plasma	ELISA (USCN Life Science Inc.)	Mean 105 ± 71	32.9	100% (90.5 - 100%)	100% (91.4 - 100%)	1 (NR)
	MPM n=78			Mean 13.9 ± 1.2*				
	AEC n=41			Not measured				
	non-MPM effusion n=53							
	New York	Plasma	ELISA (USCN Life Science Inc.)	Mean 112.9 ± 7.6	52.8	94.6% (84.9 - 98.9%)	95.7% (89.6 - 98.8%)	0.99 (NR)
	MPM n=64			Mean 24.3 ± 1.4*				
	AEC n=95			Mean 44.7 ± 3.4**				
	non-MPM effusion n=40							
	Toronto (blinded external validation)	Plasma	ELISA (USCN Life Science Inc.)		28.96	72.9% (NR)	88.5% (NR)	0.87 (0.805 - 0.921)
	MPM n=48			Mean 66.4 ± 7.2				
	AEC n=96			Mean 13.9 ± 2.1*				
Creaney <i>et al</i> (254)	MPM n=82	Plasma	ELISA (USCN Life Science Inc.)	Median 28.0 (IQR 20 - 47)	29	48% (NR)	71% (NR)	0.671 (0.606 - 0.732)
	AEC n=49			Median 29.3 (IQR 21 - 41)				
	non-MPM effusion (benign) n=35			Median 17.4 (IQR 12 - 22)*				
	non-MPM effusion (malignant) n=36			Median 17.1 (IQR 12 - 21)*				
Kirschner <i>et al</i> (253)	Sydney	Plasma	ELISA (USCN Life Science Inc.)	Mean 16.1 ± 1.87	29	13.5% (NR)	96.9% (NR)	0.63 (0.51 - 0.76)
	MPM n=37			Mean 10.92 ± 1.54†				
	non-MPM n=32							
	Vienna	Plasma		Mean 11.51 ± 1.73	29	12.7% (NR)	87.5% (NR)	

	MPM non-MPM	n=47 n=24		ELISA (USCN Life Science Inc.)	Mean 11.97 ± 3.56				0.56 (0.41 - 0.71)
Agha <i>et al</i> (250)	MPM non-MPM (malignant) non-MPM (benign)	n=25 n=11 n=9	Serum	ELISA (specific assay NR)	Mean 96.64 ± 32.64 Mean 58.45 ± 27.01‡ Mean 30.11 ± 33.72§	18†† 66.5‡‡	100% (NR)†† 88% (NR)‡‡	77.8% (NR)†† 81.8% (NR)‡‡	0.897 (NR)†† 0.776 (NR)‡‡
Corradi <i>et al</i> (249)	MPM Asbestosis NSCLC Controls	n=14 n=14 n=23 n=23	Serum	ELISA (USCN Life Science Inc.)	Mean 25.2 ± 1.8 Mean 20.7 ± 1.3 Mean 13.2 ± 1.5§§ Mean 16.7 ± 1.5¶¶	NR	NR	NR	NR
Demir <i>et al</i> (251)	MPM AEC Healthy control	n=42 n=48 n=41	Serum	ELISA (Shanghai Sunred BioTech Co., Ltd.)	Mean 168.1 ± 165.1 Mean 87.4 ± 53.5* Mean 76.4 ± 39.6¶¶¶¶	51.4	88.1% (NR)	66.7% (NR)	NR
Kaya <i>et al</i> (252)	MPM Healthy control	n=43 n=40	Serum	ELISA (specific assay NR)	Mean 90.3 ± 42.1 Mean 17.8 ± 12.7¶¶¶¶	36.6	93% (NR)	90% (NR)	0.976 (NR)
Hooper <i>et al</i> (255)	MPM	n=73	Plasma	NR	Median 21.17 (IQR 13.46 - 34.41)	NR	NR	NR	NR

95% CI; 95% Confidence Interval, MPM; Malignant Pleural Mesothelioma, AEC; Asbestos Exposed Control, non-MPM, non-Malignant Pleural Mesothelioma diagnosis, ELISA; Enzyme Linked Immunosorbent Assay, IQR; Interquartile Range, SD; Standard Deviation, NR; Not reported, * p < 0.001 for the comparison between MPM and AEC groups, ** p < 0.001 for the comparison between MPM and non-MPM effusion groups, † p < 0.05 for the comparison between MPM and non-MPM groups, ‡ p < 0.001 for the comparison between MPM and non-MPM (malignant) groups, § p < 0.001 for the comparison between MPM and non-MPM (benign) groups, †† for differentiation between MPM and benign cases, ‡‡ for differentiation between MPM and non-MPM (malignant) cases, §§ p < 0.01 for the comparison between MPM and NSCLC groups, ¶ p < 0.05 for the comparison between MPM and control groups, ¶¶ p < 0.001 for the comparison between MPM and healthy control groups

1.13 Biomarker Reproducibility

One of the major challenges with biomarker development in cancer is reproducibility. A multitude of factors can affect biomarker reproducibility and this would need to be assessed before applicability to routine clinical practice can be determined. Human specimens are often subject to marked variations in pre-analytical factors such as specimen collection, processing and storage that can significantly alter their molecular composition and consistency, which can in turn affect assay outcomes and reproducibility. (256) It is therefore vital that these variables are recorded and their effect on experimental outcomes assessed. (256)

1.13.1 Patient and Specimen Factors

Experimental assessment of any biomarker should reflect its intended purpose. (146) Timing of specimen collection from patients within biomarker research studies should be uniform and replicate when it would be used in clinical practice. In MPM, there are significant diagnostic challenges, and patients should ideally be referred to a specialist centre with access to appropriate diagnostics including local anaesthetic thoracoscopy early in their journey. This would avoid unnecessary repeated pleural aspirations or blind pleural biopsies, which is associated with a risk of tumour seeding along intervention tracts and undue delays in diagnosis of MPM, which can preclude access to important clinical trials. A diagnostic biomarker for MPM would therefore be best placed as early as possible in the patient journey, such as at presentation.

Many previous biomarker studies in MPM have been limited by their retrospective nature or recruitment from surgical centres. Patients have frequently had specimens taken for biomarkers after a diagnosis of MPM has been made and therefore by definition after pleural biopsy and often pleurodesis has been performed. In addition, many archived samples taken from surgical centres that have been used in previous biomarker studies have been taken post-operatively, and in some cases after chemotherapy has been initiated. As a result, it is

difficult to quantify the effect of pleural biopsy, surgery, chemotherapy and pleurodesis on measured biomarkers from the current literature. In addition, other patient factors such as body weight, age, co-morbidities, concomitant medications, renal function and liver function are all potential confounders that may alter the measurement of a biomarker. (147) The magnitude of the effect of these factors need to be known to allow appropriate interpretation of results in clinical practice.

1.13.2 Specimen processing and storage

As MPM is a relatively rare malignancy, many biomarker studies in MPM utilise archived biological samples. Specimens are therefore likely to have been subject to different processing and storage procedures to that of the assay manufacturer's instructions. Longterm biomarker stability in plasma or serum is critical when using stored samples in biomarker studies. (147)

To be valuable in routine clinical practice, where specimens will often be taken in an outpatient clinical setting, biomarker levels need to remain stable at room temperature, as it would be difficult to achieve immediate transportation and processing, especially at low temperatures (such as 2-8°C as is required in the Fibulin-3 assay kit manufacturer's instructions), to the laboratory in 'real life' clinical practice.

1.13.3 Assay performance and validation

Analytical factors can also affect biomarker reproducibility, it is therefore vital to examine the analytic performance of any assay being used in a biomarker study. Precision, reproducibility, linearity and analytic sensitivity and specificity are all important assessments of an assay's performance. Given the significant variation in measured Fibulin-3 levels and diagnostic performance of Fibulin-3 previously reported in MPM studies, rigorous internal validation of the FBLN3 assay kit (Cloud-Clone Corp., formerly ISCN Life Science, Houston, Texas, USA) was performed as part of the DIAPHRAGM study.

1.14 Summary

Malignant Pleural Mesothelioma is a rare invasive thoracic malignancy with a poor median overall survival of 9.5 months, and one-year survival rate of 41% and three-year survival rate of 12%. (65) Patients can therefore spend a significant amount of their remaining time following initial presentation in hospital. This is due to the symptomatic burden of pleural effusion frequently resulting in emergency presentation requiring hospital admission, followed by the potential requirement for multiple investigations and pleural procedures due to the much poorer sensitivity of investigations such as pleural aspiration in comparison to other pleural malignancies. This is associated with the potential for deterioration in the patient's performance status, which can then preclude them from treatment, risk of procedural complications, such as tract metastases and emotional distress of the patient and their family resulting from diagnostic uncertainty. In addition, some patients are unable to have a diagnosis of MPM confirmed during life, which results in the requirement for a post-mortem examination due to medicolegal implications of the diagnosis.

The variable and often subtle imaging abnormalities typical of early stage MPM result in significant challenges in detection and staging. In particular, differentiating early stage MPM from BAPE, where pleural effusion and minimal pleural thickening may be the only visible change on imaging. Similarly differentiating MPM from secondary pleural malignancy such as lung cancer can be difficult. The rind like spread of MPM and heterogeneous disease distribution makes assessment of volume of disease challenging, and this is reflected in the limitations of current staging systems and frequent finding of underestimation of clinical disease stage in published literature. Despite advances in imaging technology, there remains significant limitations in the non-invasive assessment of MPM in current clinical practice.

Due to the inherent difficulties surrounding MPM diagnostics, non-invasive biomarkers are urgently required to direct appropriate patients to specialist centres offering timely diagnostic investigations, such as LAT, and access to specialist mesothelioma MDTs, where diagnosis and staging can be reviewed and an up to date clinical trials portfolio is maintained.

Ideally, biomarkers would offer sufficient sensitivity at high specificity (mandatory given the relative rarity of MPM) to improve diagnostic accuracy in patients presenting with possible MPM. A positive biomarker test could then direct specialist referral to a thoracoscopy centre, ensuring that diagnostic delays and unnecessary repeated pleural interventions are avoided.

Despite promising results in discovery studies no MPM biomarker has been sufficiently validated. Studies to date have been limited by their retrospective design and use of selected MPM cohorts (e.g. late stage patients referred to tertiary centres rather than unselected patients at first presentation). Many studies have also used control subjects with little or no relevance to the significant current clinical challenges health professionals face when managing a patient with potential MPM. In particular, the evidence surrounding the utility of Fibulin-3 as a diagnostic biomarker in MPM is conflicting, with 3 studies reporting diagnostic performance >80% sensitivity and >80% specificity (250,252,257) and 3 studies concluding insufficient diagnostic performance of Fibulin-3 to be used in routine clinical practice. (151,251,253) In addition, there appears to be variation in the levels of Fibulin-3 measured in plasma from patients with MPM between studies, (mean levels ranging from 11.51ng/ml to 112.9ng/ml), despite the vast majority of studies using ELISA assay kits from the same manufacturer (USCN Life Science, Houston, Texas, USA).

As highlighted by studies of Fibulin-3, there are frequently inconsistent sampling protocols, assay methodology and optimum thresholds reported between studies. It is therefore important to consider factors that may have affected reproducibility of the original results, including patient factors and analytical factors. An appropriately designed prospective trial and a robust assay validation process are both pertinent.

1.15 Aim of thesis and hypotheses tested

The overall aim of this thesis is to examine the diagnostic performance, reproducibility and prognostic value of blood and novel Magnetic Resonance Imaging biomarkers in Malignant Pleural Mesothelioma. To address this aim, I have undertaken three separate studies in a large and well-characterised patient cohort, and tested three specific hypotheses.

Chapter 2: ‘DIAPHRAGM - Diagnostic and Prognostic Biomarkers in the Rational Assessment of Mesothelioma’

SOMAscan™ and Fibulin-3 are blood biomarkers that have initially shown promise as diagnostic biomarkers of MPM. However, studies have been retrospective in nature, utilising archived specimens, largely from patients at surgical centres, and frequently from patients who already had a confirmed diagnosis of MPM (and therefore were post-biopsy +/- pleurodesis) and therefore not in the population where a novel biomarker is most urgently required (i.e. at presentation). The principal hypothesis of this study was that SOMAscan™ and Fibulin-3 provide clinically useful diagnostic and prognostic information related to MPM in an intention to diagnose population.

Chapter 3: ‘Early Contrast Enhancement as a non-invasive imaging biomarker of pleural malignancy’

Novel, non-invasive imaging biomarkers of pleural malignancy and MPM are urgently required. Ideally, these should not rely on anatomical/morphological features of malignancy, since these are frequently minimal or absent in early stages of disease. Previous MRI studies have utilised DWI-MRI and DCE-MRI to detect changes in the tumour microenvironment (tumour cellularity with DWI-MRI and tumour vascularity with DCE-MRI). However, these techniques have been limited due to issues with image distortion (DWI-MRI) or applicability in early stage patients without bulky imaging abnormalities (DCE-MRI). The principal hypothesis of this study was that a novel contrast-enhanced MRI protocol, exploiting neo-vascularisation in the pleural tumour micro-environment, could

distinguish benign from malignant pleural disease with sufficient diagnostic accuracy to be of utility in clinical practice, including in patients with early stage MPM and minimal pleural thickening.

Chapter 4: 'Volumetric assessment of Malignant Pleural Mesothelioma'

The need for better non-invasive techniques to accurately assess disease burden in MPM is clear. Volumetric assessment of MPM has previously been studied utilising CT. However, MRI may provide a more accurate assessment of disease burden due to its inherent advantages over CT in terms of contrast resolution and therefore tumour boundary delineation. The principal hypothesis of this study was that primary tumour volume can be accurately, reproducibly and practically assessed in patients with MPM using novel, semi-automated methodology at contrast-enhanced MRI.

CHAPTER 2: DIAPHRAGM

2 Chapter 2: DIAPHRAGM – Diagnostic and Prognostic Biomarkers for the Rational Assessment of Mesothelioma

2.1 INTRODUCTION

As previously discussed in Chapter 1, a reliable, non-invasive diagnostic biomarker for MPM would be a major clinical advance. This would allow clinicians to reliably differentiate likely MPM from secondary pleural malignancies (e.g. lung or breast cancer), which may present with similar clinical and imaging features but require less evolved diagnostic pathways. This reflects the improved sensitivity of pleural cytology in these diseases and the frequent option of alternative sites for tissue biopsy. A positive MPM biomarker test could facilitate early referral to a thoracoscopy centre and avoid unnecessary diagnostic delay (e.g. due to repeated pleural aspirations), minimising the risk of subsequent needle-tract metastases and maximizing opportunity for clinical trial enrolment.

Biomarker results should correlate with disease extent, which is difficult in MPM given the previously described difficulties in MPM disease quantification and staging, and have defined relationships with potential confounders including the effect of pleural interventions. This is important because the precedent has been established in prostate and breast cancer, that recent sampling, resection or peri-tumoural inflammation may affect biomarker expression. This is particularly relevant to MPM where biopsies are frequently large and often combined with pleurodesis.

Previously studied biomarkers are not currently used in routine clinical practice as a diagnostic tool, largely due to insufficient diagnostic performance in early stage MPM. Two recently reported blood biomarkers, SOMAscan™ (163) and Fibulin-3 (247) show promise as diagnostic biomarkers of MPM, but studies have been limited by their retrospective nature, inconsistent (and often late) sampling time-points, and in the case of Fibulin-3 inconsistent results. (151,250,253)

This chapter examines the design and set-up of the DIAPHRAGM study, clinical activity and recruitment of patients to the study and my laboratory activity in the study.

2.2 AIM AND OBJECTIVES

The aim of the DIAPHRAGM study was to prospectively evaluate the diagnostic and prognostic performance of the SOMAscan™ classifier and Fibulin-3 in an intention to diagnose population. A robust Fibulin-3 assay validation process was incorporated given previously discussed inconsistent results between studies.

The principal hypothesis was that with an adequate sample size and appropriate clinical trial design, the diagnostic performance of SOMAscan™ and/or Fibulin-3 would have sufficiently high sensitivity (>90% and >80% respectively) at high specificity (>90% for both) to be of routine clinical value in the diagnosis of MPM.

Study objectives and their related outcome measures are presented in Table 2.1.

Table 2.1 Research objectives and related outcome measures of the DIAPHRAGM study

Research Objective	Outcome Measures
Primary To determine whether SOMAscan™ results and/or Fibulin-3 levels in blood at presentation can differentiate MPM from asbestos-exposed controls and patients with other causes of pleural effusion with a sufficient degree of sensitivity and specificity to be of routine clinical value	Serum SOMAscan™ Plasma Fibulin-3 Final diagnosis reached
Secondary To determine whether: 1. SOMAscan™ results and/or Fibulin-3 levels at presentation provide clinically useful prognostic information in MPM patients 2. early changes in Fibulin-3 levels after diagnosis (at 3 months) are associated with a poorer prognosis in MPM	Serum SOMAscan™ & plasma Fibulin-3 at presentation Survival (from registration) Plasma Fibulin-3 at presentation and 3 months post-diagnosis Survival (from registration)
Exploratory To determine whether: 1. there is a correlation between SOMAscan™ and/or Fibulin-3 levels in blood and tumour volume, defined by MRI 2. there is a correlation between SOMAscan™ and/or Fibulin-3 levels in blood and tumour angiogenesis (as defined by perfusion-based MRI biomarkers) 3. there is a correlation between SOMAscan™ and/or Fibulin-3 levels in blood and pleural fluid at presentation in patients with MPM	Serum SOMAscan™ Plasma Fibulin-3 MPM tumour volume at MRI, defined using Myrian intrasense™ software Serum SOMAscan™ Plasma Fibulin-3 MRI Early Contrast Enhancement SOMAscan™ and Fibulin-3 at presentation and at 1 month post-biopsy +/- drainage and pleurodesis

2.3 METHODS

DIAPHRAGM was funded by the Chief Scientist Office (CSO) Scotland (ETM/285) in March 2013. At the time of grant application, I was a full-time trainee in Respiratory and General Internal Medicine, working with Dr Kevin Blyth, who was the principal grant applicant. While I was not involved in writing the grant application, I was involved in discussions regarding the study protocol and logistics of recruiting to the study with Dr Blyth during the grant application process. When DIAPHRAGM was funded in March 2013, I applied for a 3-year period 'out-of-programme for research' to the Postgraduate Dean. This was approved from September 2013 and I commenced my time as a Clinical Research Fellow in November 2013, the first 2 years of which was funded through the DIAPHRAGM study grant award.

2.3.1 Ethical Approval

The study was approved by the West of Scotland Research Ethics Committee on 26th November 2013 (Ref: 13/WS/0240). NHS Greater Glasgow & Clyde acted as the study sponsor.

2.3.2 Study design and setting

DIAPHRAGM was a prospective, multi-centre observational study. It included a Suspected Pleural Malignancy (SPM) group and an asbestos-exposed control (AEC) group. Overall study design for the SPM cohort is summarised in Figure 2.1. Overall study design for the AEC cohort is summarised in Figure 2.2. The biomarker sampling windows were designed to replicate when the biomarker would be used in routine clinical practice, i.e. at initial presentation with suspected pleural malignancy, and were therefore drawn prior to a diagnosis of MPM being made. In addition to better replicating the future use of these potential biomarkers, this avoided the potential confounding effect of pleural biopsy and/or pleurodesis on biomarker results. In order to maximise the potential population of SPM patients, the study design allowed for biomarkers to be drawn after simple diagnostic pleural aspiration had been performed. However, exact timing of the biomarker draw relative to pleural aspiration was recorded in every case to assess any confounding effect this intervention may

have on biomarker results. Identical processing and storage protocols were used in both SPM and AEC cohorts. Potential additional confounders including renal function, inflammatory indices and drugs was also recorded. An exploratory, cross-sectional MRI sub-study was performed to determine whether there was any correlation between blood biomarker levels and MPM tumour volume. Tumour volume was measured at contrast-enhanced MRI, which is described in detail in Chapter 4.

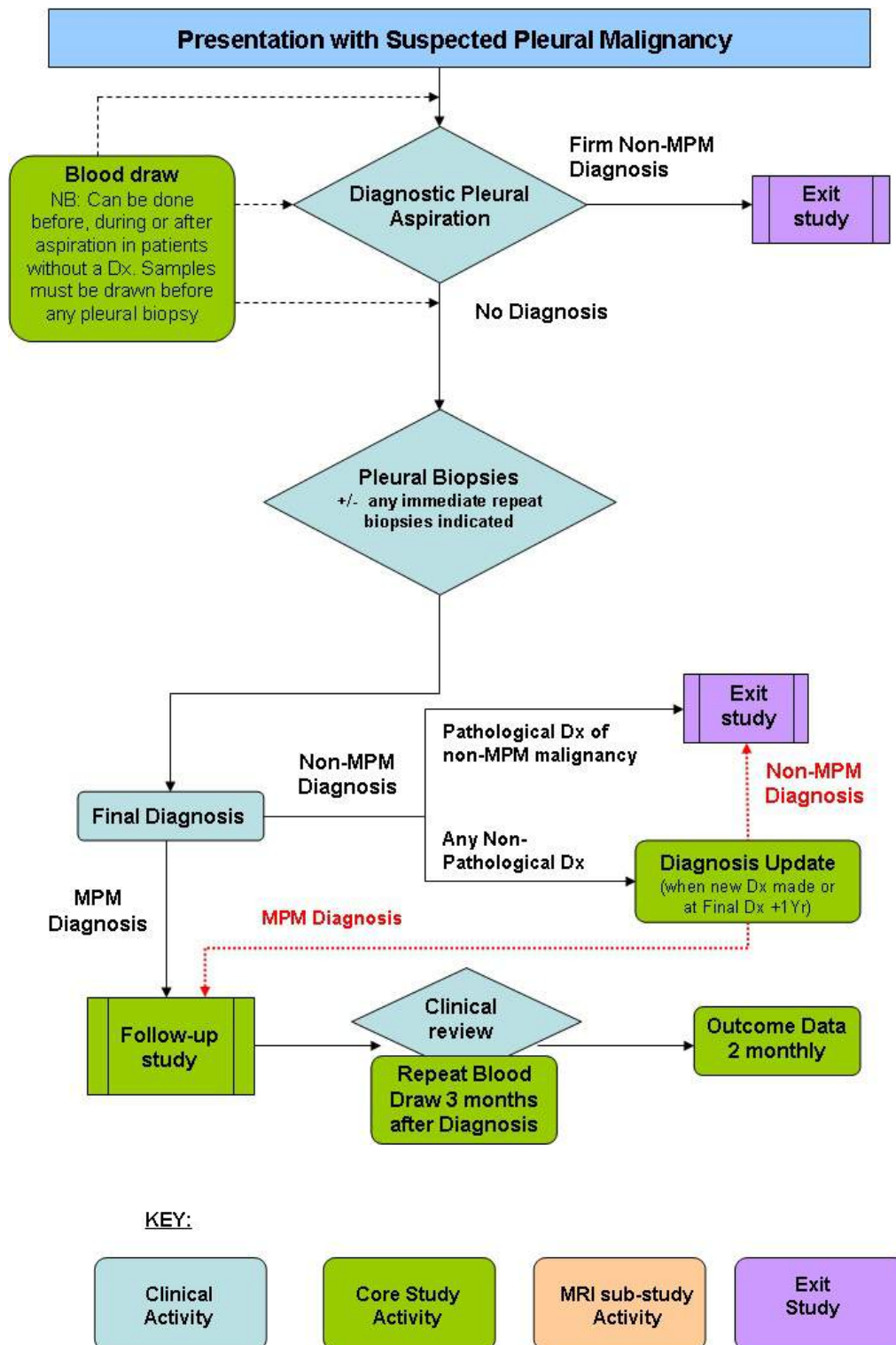


Figure 2.1 Study flowchart for participants recruited to Suspected Pleural Malignancy cohort of the DIAPHRAGM study

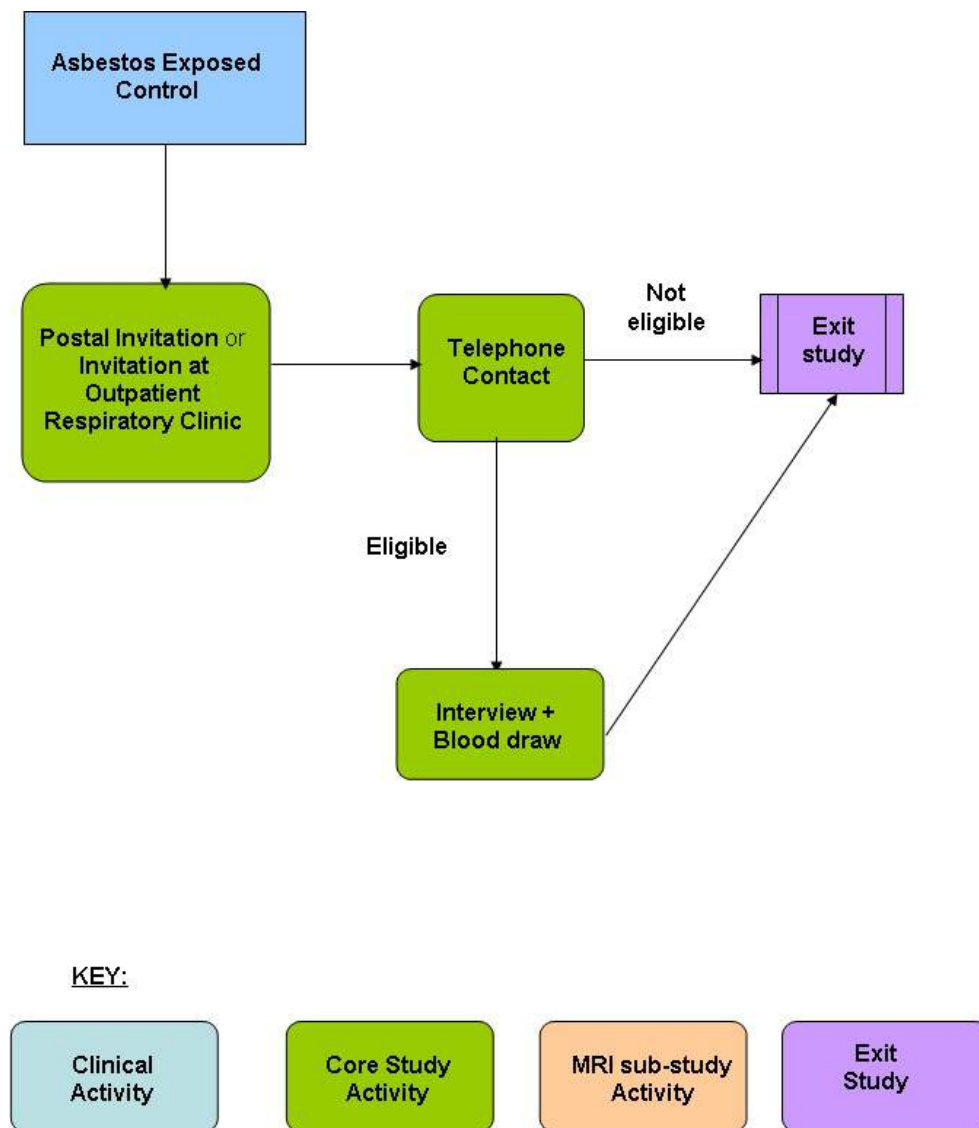


Figure 2.2 Study flowchart for participants recruited to the Asbestos-exposed Control cohort of the DIAPHRAGM study

2.3.3 Study Set-Up

2.3.3.1 Overall

A trial management group (TMG), which included the study Chief Investigator (Dr Kevin Blyth), the CRUK Clinical Trials Unit Glasgow team (project manager, clinical trial co-ordinator, trial statistician and trial monitor) and myself (as Clinical Research Fellow) was formed. TMG responsibilities included study site selection and set up, development of study documentation, monitoring of trial

activities and communication with sites. Importantly, the TMG met on a monthly basis to review recruitment, including overall recruitment numbers, recruitment at each site, site screening logs and mesothelioma numbers. Study documentation, including patient information sheets and case report forms were drafted by me and approved by Dr Blyth and the other members of the DIAPHRAGM TMG. DIAPHRAGM newsletters were sent to each recruiting site with the aim of providing recruitment updates, reminders about protocol updates and gratitude and encouragement for ongoing study participation.

The study was supported by the National Cancer Research Institute (NCRI) and is registered on the ISRCTN registry (ISRCTN10079972), a searchable clinical trial registry. In addition, details of the study were made available on the Cancer Research UK website, the Experimental Cancer Medicine Centre (ECMC) website and the Mesothelioma UK website and newsletters. The study was also highlighted at the 'British Thoracic Oncology Group (BTOG)/Mesothelioma UK Managing Mesothelioma in the UK' Meeting in 2014, in order to promote national and international awareness of the study and encourage potential recruiting centres to approach the TMG if interested in contributing.

2.3.3.2 Site Selection

The SPM group was recruited from 22 centres in the U.K. and Republic of Ireland. Recruiting centres were deliberately a mixture of academic and more clinically-orientated units, making results of the study generalisable to patients presenting with SPM to acute hospital services. 11/22 (50%) of these centres were concentrated in a geographical location with a MPM standardised mortality ratio (SMR) >100. (258)

Sites interested in participating as a recruiting centre were asked to complete a site 'Confirmation of Interest and Feasibility' form (see Appendix 1). All principal investigators had a declared interest in pleural disease and each centre had sufficiently evolved pleural diagnostic services to deliver a reliable diagnosis. Specifically, access to on-site thoracoscopy (ideally including LAT) and a regional mesothelioma multi-disciplinary team (MDT) meeting (for diagnostic review and staging) was required. In addition, all centres were required to have

access to research nurses, a centrifuge and a -80°C freezer, and most centres had a history of successful multi-centre research collaboration.

Centres opened to recruitment in a staggered fashion over a period of 2.5 years. All centres completed standard procedures before opening to recruitment (see Figure 2.3). The Queen Elizabeth University Hospital (QEUH) opened in June 2015 merging 3 individual sites, which closed at that point to form the QEUH, these being the Southern General Hospital, Victoria Infirmary and Gartnavel General Hospital. While outpatient clinics continued to be based at the original hospitals, all in-patient services were moved to QEUH. These centres will be referred to as West of Scotland (WoS) centres for the remainder of this thesis. The AEC group and the MRI sub-study cohort were recruited from West of Scotland centres only.

Site training was done myself, either remotely (utilising PowerPoint slides, e-mail correspondence +/- telephone conference) or in person at a site visit. On-site initiation visits were conducted at all WoS centres, Aberdeen Royal Infirmary, Southmead Hospital (Bristol), University Hospital of South Manchester, Northern General Hospital (Sheffield), Royal Alexandra Hospital (Paisley), Forth Valley Royal Hospital (Falkirk), Inverclyde Royal Hospital (Greenock) and University Hospital Galway.

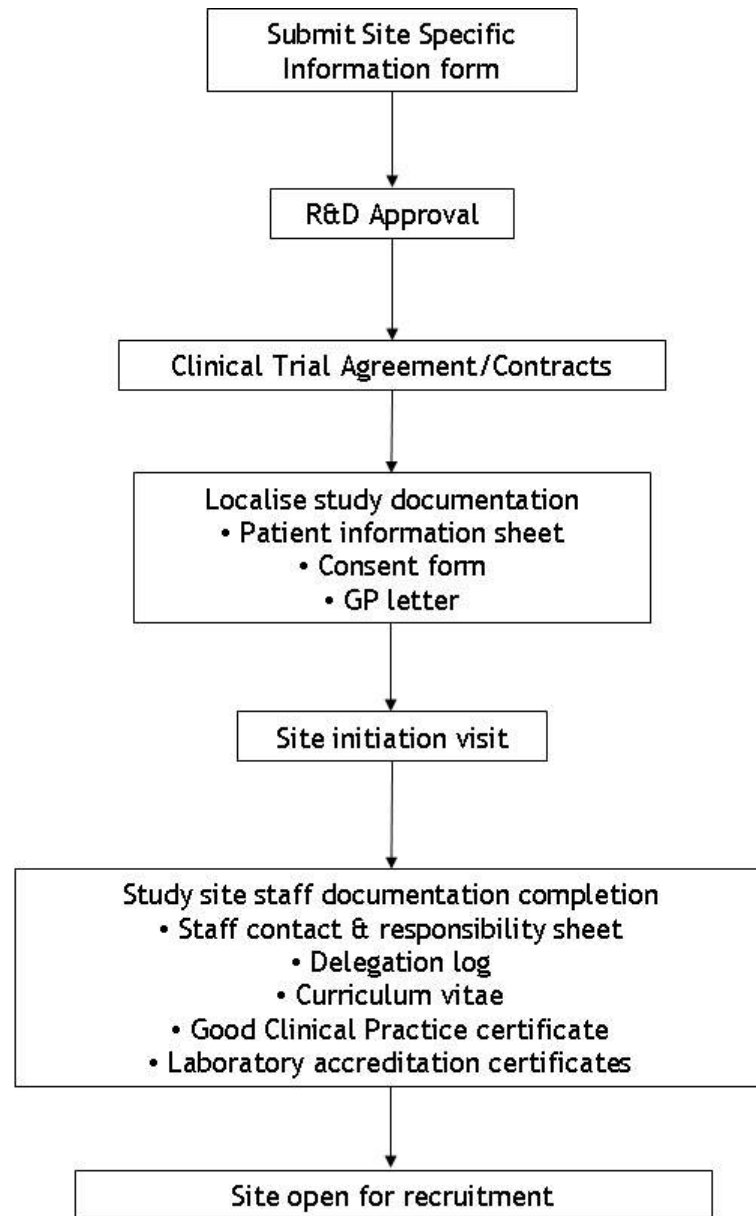


Figure 2.3 Recruiting centre opening process

2.3.4 Study Population

2.3.4.1 Suspected Pleural Malignancy Cohort

Patients with suspected PM were identified on presentation to a Respiratory out-patient clinic or acute hospital admissions unit. Eligibility criteria for the SPM cohort were as follows:

Inclusion Criteria

1. Suspected pleural malignancy, defined by a unilateral pleural effusion or pleural mass lesion
2. Sufficient fitness for diagnostic sampling (site investigator's clinical judgment)
3. Informed written consent

Exclusion Criteria

1. Insufficient fitness (based on site investigator's clinical judgement)
2. Intercostal chest drain in-situ
3. Intercostal chest drain inserted within the previous 3 months

2.3.4.2 Asbestos-exposed Control Cohort

Eligibility for the asbestos-exposed control cohort were as follows:

Inclusion Criteria:

1. Documented history of asbestos exposure and associated radiological evidence of asbestos exposure, e.g. pleural plaques, asbestosis or diffuse pleural thickening
2. Willing and able to travel to a research clinic interview in Glasgow

3. Informed written consent

Exclusion Criteria:

1. Known Malignant Pleural Mesothelioma
2. Known or suspected other thoracic malignancy under investigation
3. Known pleural effusion of any cause

2.3.4.3 Cross-sectional MRI sub-study Cohort

In order to address the study's exploratory objectives, a cross-sectional MRI sub-study was performed. Eligibility for the MRI sub-study were as follows:

Inclusion Criteria:

1. Pleural histological sampling (by LAT/image-guided biopsy) indicated to investigate suspected pleural malignancy following a non-diagnostic pleural aspiration
2. Recruited in a West of Scotland centre

Exclusion Criteria:

1. Unable to undergo MRI (due to claustrophobia or known contraindications such as pacemaker, ferrous metal implants or metallic foreign body)
2. Allergy to Gadolinium contrast
3. Renal impairment (eGFR <30ml/min)
4. Pregnancy

2.3.5 Glasgow Recruitment

Suspected Pleural Malignancy Cohort

Patients in WoS centres (n=4) were identified, screened and recruited by myself. Patients in the Royal Alexandra Hospital (RAH) and Inverclyde Royal Hospital (IRH) were identified and screened by myself and recruited by a research nurse based at the Glasgow Clinical Research Facility. At these centres, potential patients were identified by myself using an electronic Healthcare Information System (Trakcare[®], InterSystems Corporation, Massachusetts, USA). This system is used by NHS Greater Glasgow & Clyde health board (which incorporates all of the WoS centres, RAH and IRH) and includes details of all hospital out-patient appointments and in-patient admissions, which can be sorted by individual hospital consultants or services and in-patient wards. I could review patients' electronic case records as a member of the clinical team. Previous electronic case records (including referral letters, clinic letters, discharge letters and previous laboratory results) are available via Trakcare[®]. In addition, patients' images (including chest radiographs and CT scans) were accessible using an electronic picture archiving and communication system (PACS v11.4, Carestream Health, NY, USA).

Utilising these systems, I identified potential study participants by reviewing all new out-patient referrals to all of the respiratory consultants (n=30) at each hospital. This included review of the referral letter and any available previous clinic letters and radiology. In addition, I screened all new patient admissions to the acute medical receiving units and respiratory inpatient wards on a daily basis, reviewing any available investigations and radiology. After initial identification using this methodology, potential participants were further assessed for their eligibility based on history and examination, attained via personal review and/or communication with the patient's responsible consultant. Any potentially eligible patients were provided with the study Patient Information Sheet (PIS), see Appendix 2, by myself or the patient's responsible consultant and given sufficient time to read and consider it and ask any questions prior to providing informed written consent. Respiratory

consultants in WoS centres were provided with a diagnostic pleural aspiration service by myself so that any patients with suspected PM not identified at the time of Trakcare[®] review had a second opportunity to be identified and screened, when they attended for their diagnostic pleural aspiration. In the vast majority of cases, patients were consented and blood biomarkers were drawn on the same date as their diagnostic pleural aspiration.

Asbestos-Exposed Control Cohort

AEC subjects were initially recruited via invitations sent by Clydeside Action on Asbestos (CAA), an advocacy body based in Glasgow with a database of over 600 clients, see Appendix 3. An additional population of potential AEC subjects was identified via respiratory outpatient clinics at WoS centres from 17th October 2014 to study completion.

Subjects invited by CAA were asked to contact either myself or a research nurse based at the Glasgow Clinical Research Facility if they were interested in taking part. If eligible, an AEC PIS (see Appendix 4) was posted out to the subject and telephone contact made the following week to confirm ongoing interest in participation and a single research clinic visit scheduled.

Potential subjects were identified from respiratory outpatient clinics by myself in a similar fashion to the method described in section 2.3.5. I reviewed clinic letters and any available recent imaging of all new and returning patients attending respiratory out-patient clinics at WoS centres. If potentially eligible, a research nurse would aim to attend the clinic, provide the patient with the AEC PIS and recruit the patient if confirmed as eligible. If this was not possible, either due to research nurse availability or if the patient did not have sufficient time to consider the PIS, they were invited to attend a separate single research clinic visit at a later date. Transportation from the subject's home to the research clinic at the Glasgow Clinical Research Facility was provided if required in an attempt to minimise participant burden. All participants were given sufficient time to read and consider the PIS and ask any questions prior to providing informed written consent

Cross-sectional MRI sub-study Cohort

All patients included in the MRI sub-study were recruited by myself from WoS centres. Patients were identified by reviewing the results of their pleural aspiration, MDT discussion and referral for further investigation. Patients were approached at the clinical visit where the non-diagnostic pleural aspiration results, and the need for further investigation (e.g. thoracoscopy or image-guided biopsy), were discussed. Subjects were provided with a separate MRI sub-study PIS (see Appendix 5) and given sufficient time to read and consider it and given the opportunity to ask questions. If willing, they were asked to provide additional informed written consent when they attended for the MRI scan.

All MRI scans were performed at the Glasgow Clinical Research Imaging Facility. This was initially based at the British Heart Foundation (BHF) Glasgow Cardiovascular Imaging Facility, University Avenue, University of Glasgow, which was located separate to the WoS recruiting hospitals. Return transportation from the subject's home was provided if required in order to minimise patient burden. From August 2015, the Glasgow Clinical Research Imaging Facility was based at the QEUEH. Following this, patients were generally consented and underwent MRI examination on the same date that they were electively admitted for LAT or image-guided biopsy (both of which were performed at QEUEH).

2.3.6 Study Procedures

The schedule of assessments for each SPM subject recruited to the DIAPHRAGM study is presented in Table 2.2. The schedule of assessments for each AEC subject recruited to the DIAPHRAGM study (depending on whether they were invited by CAA or identified via respiratory out-patient clinics) is presented in Table 2.3 and Table 2.4 respectively.

2.3.6.1 Patient Registration

All patients were registered to the study and provided with a unique study identification number by the Clinical Trials Unit Glasgow following confirmation of eligibility.

Review eligibility criteria	X	X*								
Introduce study if eligible	X	X*								
Provide with PIS	X	X*								
Discussion and informed consent		X	X*							
Register patient with CTU		X	X*							
Complete asbestos questionnaire		X	X*							
Record clinical history		X	X*							
Clinical examination		X	X*					X		
Record all diagnostic test results (including any repeats)		X	X*			X				
Record concomitant medications		X	X*					X		
Blood draw		X	X*					X		
Research pleural fluid draw (MRI sub-study only)		X								
Update relevant imaging results								X		
Outcome assessment								X	X	
Diagnosis update										X
MRI Sub-study Activity										
Review eligibility criteria			X							
Introduce study if eligible			X							
Provide separate sub-study PIS			X							
X-ray orbits if indicated			X							
MRI safety questionnaire			X	X*						
Discussion and informed consent				X						
Register patient with CTU				X						
Pleural MRI scan				X						

Retain or discard research pleural fluid sample				X						
Blood draw							X			
Clinical examination							X			
Record relevant imaging results							X			
Record concomitant medications							X			

*If not previously done, Dx; Diagnosis

⁽¹⁾ At visit 3, where the results of the diagnostic pleural aspiration are reviewed, there are 3 possible outcomes:

I. If any non-MPM diagnosis is made: subject will exit study. No further blood draws or follow-up visits are required but a Diagnosis Review 1 year from the date of Final Diagnosis will be required in patients with a non-pathological diagnosis. This will include all patients diagnosed with a non-MPM illness after a pleural aspiration alone, EXCEPT those with a cytological diagnosis of non-MPM malignancy

II. If no diagnosis is made: a pleural biopsy will be arranged, if clinically indicated (e.g. Thoracoscopy or image-guided pleural biopsy). If a West of Scotland patient, these patients may be considered for the MRI sub-study

III. If diagnosis is confirmed as MPM (unlikely based on cytology): subject will enter follow-up with a 3 month blood draw

*If not previously done

Table 2.3 Schedule of assessments for participants recruited to the asbestos-exposed control cohort of the DIAPHRAGM study via invitation by Clydeside Action on Asbestos (CAA)

CAA identified patients			
Visit Number	Screening	Visit 1	Visit 2
Approximate Day*	0	7-14	14-28
Postal Invitation	X		
Post PIS	X	X (if not already done)	
Telephone contact		X	
Eligibility screening		X	
Discussion & Informed consent			X
Register subject with CTU			X
Record medical history			X
Record Medications			X
Asbestos exposure history questionnaire			X
Blood draw			X

*The exact dates will depend on when/if each study participant responds to the postal invitation and when they can attend for interview and blood draw

Table 2.4 Schedule of assessments for participants recruited to the Asbestos-exposed control cohort of the DIAPHRAGM study after identification at respiratory outpatient clinic

Hospital Identified Patients			
Visit Number	Screening	Visit 1 (Telephone contact if eligibility screening not performed at screening visit)	Visit 2
Approximate Day*	0	1-7	7-28
Introduce Study	X		
Eligibility screening	X	X (if not previously performed)	
Provide PIS	X	X (will be posted out if not provided at screening)	
Opportunity for discussion	X	X	X
Discussion & Informed consent			X
Register subject with CTU			X
Record medical history			X
Record Medications			X
Asbestos exposure history questionnaire			X
Blood draw			X

*The exact dates will depend on when in the hospital encounter each study participant is given the PIS and when they can attend for interview and blood draw

2.3.6.2 Case Report Forms

Suspected Pleural Malignancy Cohort

All patients in the SPM cohort had a Baseline Information Form (see Appendix 6) completed. Patients who had a final diagnosis of MPM had a Follow-up Visit Form (see Appendix 7) completed at 3 months after diagnosis and a Long Term Follow-up Form (see Appendix 8) completed at 2 monthly intervals post-diagnosis.

Patients without a cytological or histological diagnosis, and patients with a benign diagnosis (even if histologically confirmed, e.g. BAPE based on benign fibrinous pleurisy at pleural biopsy) had a Diagnostic Review Form (see Appendix 9) completed at the 12-month anniversary of the original diagnosis, or as soon as a new pleural diagnosis was made. The purpose of this was to capture any false negative diagnostic tests from the initial pathway, acknowledging the major diagnostic challenges posed by pleural malignancies, particularly MPM, which is associated with a false negative pleural biopsy rate of up to 12% reported in previous case series. (45)

Asbestos-Exposed Control Cohort

All participants in the AEC cohort had an Asbestos-Exposed Controls Case Report Form (CRF) (see Appendix 10) completed. This form included a review of any unexplained breathlessness, chest wall pain or breathlessness experienced within the preceding 6 months reported by the subject at the research visit. The purpose of this was to ensure that any recent development of concerning clinical features that may indicate new, undiagnosed pleural malignancy would be detected. If this was the case, then the subject was referred for clinical investigation as appropriate and excluded from the AEC cohort. The subject's available imaging was also reviewed and recorded.

2.3.6.3 Asbestos Exposure Questionnaire

Detailed asbestos exposure histories were taken from all participants in both the SPM cohort and the AEC cohort using an asbestos exposure questionnaire derived

from the Health and Safety Executive asbestos survey (259) (see Appendix 11). This questionnaire included recording of the nature of occupational exposure(s), which can be correlated to likely fibre exposure. The duration and first year of exposure was also recorded. Non-occupational sources of exposure were also recorded (e.g. the washing of an occupationally exposed spouse's work clothes or environmental exposure from the household or surrounding environment).

2.3.7 Statistical Analysis

2.3.7.1 Sample Size Calculation

SOMAscan™ assay

Sample size calculations were performed by the Cancer Research UK (CRUK) Clinical Trials Unit Glasgow statisticians based on the previously published sensitivity of 93.2% (95% CI 88.6 - 97.7%) and specificity of 90.8% (95% CI 86.1 - 95.6%) for SOMAscan™. (163) As MPM is a relatively rare disease, it would be clinically important for the biomarker test to have high sensitivity at high specificity. With an MPM sample size of 120, the study will be able to distinguish a sensitivity of <80% from a sensitivity >90% with 93% power, at the 5% one-sided level of significance. Initial projected incidence of MPM in the target population of patients presenting with suspected PM was 20%. The target overall sample size was therefore 600 patients with suspected pleural malignancy. However, as the study was designed to recruit patients at presentation with suspected PM, the final number of patients included in the study with a final diagnosis of MPM will not be known until study completion. The precision around the reported sensitivity from this study will therefore depend on the final number of MPM patients included but the standard error in the estimated sensitivity will be <5%, provided at least 120 MPM cases are recruited and their samples are available for analyses.

109 asbestos-exposed control subjects will distinguish a specificity of <80% from a specificity of >90% with 88% power, at the 5% one-sided level of significance. The standard error in the estimated specificity will be <5%.

The study data will be used to estimate the AUC for SOMAscan™ for distinguishing patients with MPM from non-MPM patients in the suspected pleural malignancy cohort. Assuming 120 patients in the MPM group and 120 in the non-MPM group, the AUC can be estimated with a 95% CI width of 0.120 - 0.168 (assuming a cut-point exists with a reasonable sensitivity of 80% and a modest specificity of 40%). if more sensitive/specific cut-points exist, the width of the 95% CI will be much reduced.

Fibulin-3

With a MPM sample size of 120, the study will be able to distinguish a sensitivity of >80% from a sensitivity of <70% with 80% power, at the 5% one-sided level of statistical significance. The precision around the reported sensitivity will depend on the final number of MPM patients included but the standard error in the estimated sensitivity will be <5%.

In order to achieve 90% power to distinguish a specificity of >90% from a specificity <85%, at the 5% one-sided level of statistical significance, a random sample of 378 non-MPM samples will be analysed. The standard error in the estimated specificity will be <2.3%.

2.3.7.2 Primary analysis plan

Statistical analysis will be performed by the CRUK Clinical Trials Unit Glasgow statisticians. Sensitivity and specificity at pre-specified cut-offs (0.5 for SOMAscan™ and 52ng/ml for Fibulin-3) will be estimated using 2 x 2 contingency tables. The overall diagnostic performance of each biomarker will be assessed using ROC curves. Logistic regression will be used to estimate a diagnostic model using biomarker results and clinical or radiological variables. Cross-validation will be used to provide robust estimates of AUC and specificity at fixed sensitivity rates of 80%, 90% and 95%.

2.3.7.3 Secondary analysis plan

A prognostic model will be developed using Cox proportional hazard techniques. The modelling process will incorporate biomarker measurements at presentation (both biomarkers) and at 3 months (Fibulin-3 only due to cost restraints

associated with SOMAscan™ analyses) and other known prognostic features. This will include performance status and tumour histology.

2.3.7.4 Exploratory analysis plan

The association between SOMAscan™ results and Fibulin-3 in blood and tumour volume/measures of tumour angiogenesis will be estimated by Pearson or Spearman correlation, depending on the normality of the distribution of the data. The same methods will be used to test the association between Fibulin-3 in blood and pleural fluid. Changes in Fibulin-3 levels before and after histological sampling will be compared using a paired t-test or Wilcoxon signed rank-sum test, depending on the normality of the distribution of the data.

2.3.8 Biomarker Sampling, Processing and Storage

2.3.8.1 Biomarker Sampling

Materials for blood sampling

- Tourniquet
- Alcohol wipe
- 21-gauge needle (BD Medical, UK)
- 20 ml syringe (BD Medical, UK)
- 2 x 5 ml vacutainer tube containing SST clot activator (Greiner Bio-One)
- 1 x 9 ml (or 2 x 4 ml) vacutainer tube containing EDTA (Greiner Bio-One)

Materials for pleural fluid sampling

- Sterile gloves and gown
- Antiseptic solution
- Dressing pack with sterile drape

- 1% lidocaine
- Occlusive dressing
- 2 x 21-gauge needle (BD Medical, UK)
- 1 x 25-gauge needle (BD Medical, UK)
- 1 x 10 ml syringe (BD Medical, UK)
- 1 x 60 ml syringe (BD Medical, UK)
- 1 x 20 ml universal container (ThermoFisher Scientific)

Methods for biomarker sampling

Blood samples were taken from participants by a competent member of the study team. Sufficient blood was collected to allow duplicate samples of serum and plasma to be collected for all measurements at all visits, ensuring redundancy in case of loss or damage to samples during transportation. 9 ml of venous blood was collected first into a vacutainer tube containing SST clot activator. A further 9 ml of venous blood was then collected into a second vacutainer tube containing EDTA.

In WoS centres, 20 ml pleural fluid was collected by myself at the time of initial diagnostic or therapeutic aspiration into a plain universal container. All pleural aspirations were performed under ultrasound guidance and aseptic technique, following consent. If pleural fluid was not collected at this initial time, then a further opportunity was allowed immediately prior to thoracoscopy if the patient was registered in the MRI sub-study.

2.3.8.2 Sample Processing and Storage

Materials for sample processing and storage

- 500 µL cryovials (ThermoFisher Scientific)

- 1 ml pipette
- Centrifuge
- Cryolabels
- Cryobox
- -80°C freezer

Methods for sample processing and storage

Serum samples (collected in the vacutainer tube containing SST clot activator) was allowed to clot for 30 minutes before centrifugation. Plasma samples (collected in the vacutainer tube containing EDTA) and pleural fluid samples could be centrifuged immediately. All samples were centrifuged at 2200g for 15 minutes at room temperature. These were the processing instructions provided by SOMAlogic® at study commencement.

For all samples, the supernatant was withdrawn by pipette immediately following centrifugation and aliquoted into a minimum of 4 cryovials of at least 250µL volume, labelled with the patient's study ID, sample details (i.e. serum, plasma or pleural fluid) and the sampling date, before being placed in a cryobox and into a -80°C freezer within 2 hours of initial blood draw.

2.3.9 Biomarker Analyses

The diagnostic performance of SOMAscan™ and Fibulin-3 will be assessed using cut-points determined in the relevant original studies (SOMAscan™ classifier cut-off score of >0.5 and Fibulin-3 cut-off of 52ng/ml) and compared to the currently best studied MPM biomarker, Mesothelin using the MESOMARK® ELISA (Fujirebio Diagnostics Inc, PA, USA).

SomaLogic® are performing all SOMAscan™ analyses, utilising SOMAmer™ reagents to specifically bind to protein targets in serum as discussed in Chapter 1. Fibulin-3 and Mesothelin levels are being measured by the Translational Pharmacology

Unit (Wolfson Wohl Cancer Research Centre, UK) according to GCP guidelines. Fibulin-3 levels in plasma and pleural fluid is being measured using the commercially available ELISA (Cloud-Clone Corp., formerly USCN Life Science Inc, Houston, Texas, USA) as in the original study. (247) Mesothelin is being measured using the MESOMARK® ELISA (Fujirebio Diagnostics, Inc, PA, USA).

2.3.10 Data Storage

All data for the DIAPHRAGM study was recorded on paper Case Report Forms. This data was then entered into a password encrypted electronic database by the CRUK Clinical Trials Unit Glasgow team (ORACLE database version 11g, Oracle Corporation, California, USA).

2.3.11 Laboratory Activity - Fibulin-3 assay validation

Pre-validation testing of the most widely used Fibulin-3 assay (FBLN3 assay, Cloud-Clone Corporation, Houston, Texas, USA) was undertaken by the Translational Pharmacology Laboratory, formerly Analytical Services Unit (University of Glasgow, UK). These tests highlighted possible manufacturing inconsistencies between batches of the FBLN3 assay kit (Cloud-Clone Corp., Houston, Texas, USA). Initial standard curves from lot number L141204141 were successful, with coefficient of variation (CV%) <20%. However, the quality control sample provided by the manufacturer did not produce a result within the range of the standard curve. on two separate occasions. This experiment was repeated using lot number L150714373. However, the standard curve failed on 4 separate occasions (with CV% of up to 119%). It was then noticed that the standard diluent and assay diluent A appeared cloudy. Further kits from the original lot number (L141204141) were therefore ordered from the manufacturer. Unfortunately, further quality control samples could not be provided by the kit manufacturer. In order to validate the assay, we therefore had to establish alternative positive and negative control samples. This was done by myself under the direct supervision of Caroline McCormick (Research Assistant) and Fiona Thomson (Director/Senior Research Fellow) at the Translational Pharmacology Laboratory (TPL), Wolfson Wohl Cancer Research Centre, Institute of Cancer Sciences, University of Glasgow. The establishment of these positive and negative control samples is summarised in Sections

2.3.11.1 - 2.3.11.2. Subsequent assay validation was not performed by me and is not described here; this was completed by the TPL.

2.3.11.1 Materials

Cell lines

Mesothelioma cell lines HP1 and H2595, and the benign mesothelial cell line LP9, were sourced from Dr Harvey Pass at NYU Langone Medical Center by Dr Kevin Blyth. Mesothelioma cell line H226 was sourced from the Beatson Institute for Cancer Research by Dr Kevin Blyth.

Culture medium

- Dulbecco's Modified Eagle Medium (DMEM) (ThermoFisher Scientific, Massachusetts, USA)
- Penicillin (10,000 units/ml) and Streptomycin (10,000 micrograms/ml) (Gibco, Life Technologies, UK)
- Heat-activated Foetal Bovine Serum (FBS) (Gibco, Life Technologies, UK)

Equipment

Fibulin-3 assay kit was purchased from Cloud-Clone Corporation, formerly USCN Life Science, Houston, Texas, USA. Materials included in the kit were:

- Pre-coated 96-well strip plate
- Plate sealer for 96 wells
- Stock standard
- Standard diluent
- Detection reagent A

- Assay diluent A
- Detection reagent B
- Assay diluent B
- Tetramethylbenzadine (TMB) substrate
- Stop solution

Additional equipment used included:

- Microplate reader with $450 \pm 10\text{nm}$ filter - SpectraMax[®] Plus 384 and SoftMax[®] Pro 6.4 (Molecular Devices Corp., California, USA)
- Multi-channel, high precision pipettes with disposable tips (Gilson Inc, Wisconsin, USA)
- Table top centrifuge suitable for 2 ml tubes
- Incubator at 37°C
- CASY[®] cell counter and analyser (Roche, Germany)

Additional Solutions

- Trypsin (Gibco, Life Technologies, UK)
- CASYton solution (Roche, Germany)
- Dimethyl sulfoxide (DMSO) (ThermoFisher Scientific, Massachusetts, USA)
- Distilled water for use as wash buffer
- 0.01mmol/l Phosphate Buffered Saline (PBS), pH 7.4 (ThermoFisher Scientific, Massachusetts, USA)

2.3.11.2 Experimental Procedures

Cell culture

Mesothelioma cell lines HP1 and H2595 and H226 were grown in culture medium solution, (Dulbecco's Modified Eagle Medium (DMEM), supplemented with Penicillin and Streptomycin (10,000 micrograms/ml) and heat-activated Foetal Bovine Serum (FBS)). Cells were grown in 75cm² flasks with 20mls culture medium incubated at 37°C and 10% CO₂.

To split cells, culture media was removed by me and cells were dissociated with 3ml trypsin and the flask returned to the incubator for 10 minutes until the cells had become detached from the flask. 10ml of culture media was then re-added to the flask. 200µl of media and the cells in suspension were removed from the flask into a universal container. 9.8ml of CASYton solution was added to the container before being placed into a cell counter. Based on the cell count per ml, I calculated the volume of culture media with the cell suspension required to be added to a 75cm² flask. A volume of fresh culture media was then added by me to make the total volume up to 20ml, prior to re-incubation at 37°C and 10% CO₂.

Once an adequate supply of cells had been established, one flask from each cell line was used for further experimentation. Once cells in each flask reached 80% confluence (assessed by me under the supervision of Carol McCormick), culture medium was replaced with 2ml serum-free medium (consisting of DMEM and Penicillin/Streptomycin) and re-incubated for 24 hours. Cell-conditioned medium was then collected into a universal container and spun at 1200rpm for 5 minutes at 21°C (i.e. room temperature) for 5 minutes. The supernatant was collected by me into eppendorfs and frozen at -80 °C.

Fibulin-3 Assay

The assay used to measure Fibulin-3 levels is a sandwich Enzyme-linked Immunosorbent Assay (ELISA). The assay was performed by me, under the direct supervision of Carol McCormick, as per manufacturer's instructions. A 96-well microplate is pre-coated with a Fibulin-3-specific capture antibody (by the

manufacturer) to which samples (antigen) were added prior to incubation for one hour at 37°C. The microplate was then washed using distilled water to remove any unbound antigen before a second, independent antibody specific to Fibulin-3, which is conjugated to Horseradish Peroxidase (HRP) was then added. The microplate was again incubated for 30 minutes at 37°C before being washed with distilled water to again remove any unbound conjugated antibody-antigen complexes. TMB substrate was then added to the microplate. The substrate was hydrolysed in proportion to the amount of conjugated antibody-antigen complexes present in the each well of the microplate, with a resultant colour change (blue). Stop solution (Sulphuric acid) was then added after a 15 - 20 minute incubation period to terminate the enzyme-substrate reaction, resulting in a further colour change (yellow). The optical density of this colour change was measured spectrophotometrically at a wavelength of 450nm \pm 10nm, using SpectraMax[®] Plus 384 spectrophotometer (Molecular Devices Corp., California, USA).

Standard Curve

A 7-point standard curve was produced using the Stock Standard and Standard Diluent provided in with the FBLN3 kit by me under the direct supervision of Carol McCormick. The concentration at each point of the standard curve was 100ng/μl, 50 ng/μl, 25 ng/μl, 12.5 ng/μl, 6.25 ng/μl, 3.12 ng/μl, 1.56 ng/μl.

To assess the validity of the standard curve, back calculated concentrations were compared with the known concentration of the standard solution at all 7 dilutions. In order to be valid, the back calculated concentration needed to be within 20% of the known concentration (25% for the lower two concentrations).

I then assessed the reproducibility of the standard curve by repeating this in duplicate on nine separate plates.

Establishing Positive Control Samples

I measured Fibulin-3 levels using supernatant collected from conditioned media from the Mesothelioma cell lines H226, H2595 and HP1 at 3 concentrations (undiluted, 1:1 dilution and 1:4 dilution). PBS was used as the diluent.

Establishing Negative Control Samples

I measured Fibulin-3 levels using supernatant collected from conditioned media from benign mesothelial cell line LP9 at 3 concentrations (undiluted, 1:1 dilution and 1:4 dilution). PBS was used as the diluent. PBS and distilled water were run alongside as a quality control sample.

2.4 RESULTS

2.4.1 Site recruitment

The TMG was approached by 13 hospital sites following study promotion with an interest in becoming a participating centre. Following review of each site's estimated new number of patients diagnosed with MPM, recruitment target and access to facilities such as LAT, a mesothelioma MDT and research nurses, 7/13 (54%) of these sites were selected as DIAPHRAGM recruiting centres. An additional 11 hospital sites (not including the 4 WoS centres) were approached directly by the TMG to participate in DIAPHRAGM. The mean time taken to open a recruiting centre was 22 (SD 11) weeks. Site set up was completed in a significantly shorter period of time in the WoS centres in comparison to the non-WoS centres (median 81 days versus 154 days, $p=0.0029$). Projected recruitment numbers per site ranged between 2 - 75 patients, see Table 2.5.

2.4.2 Patient recruitment

Median time from site opening to recruitment of the first study participant was 31.5 (IQR 11.5 - 66.5) days. 26% ($n=5$) centres achieved their initial projected recruitment target, with WoS centres recruiting 125% of their original projected recruitment and University Hospital of South Manchester achieving 124% of their original projected recruitment. The remaining centres achieved between 10 - 67.5% of their recruitment target, see Table 2.6. The overall rate of recruitment to the SPM and AEC cohort is summarised in Figure 2.4 and Figure 2.5 respectively.

Table 2.5 DIAPHRAGM recruiting centres and initial projected recruitment numbers provided by each site Principal Investigator

Recruiting Centre	Opening process initiated	Opened for recruitment	Initial projected total recruitment
Glasgow Royal Infirmary, Glasgow	11/10/2013	31/12/2013	75
Gartnavel General Hospital, Glasgow	11/10/2013	31/12/2013	75
Southern General Hospital, Glasgow	11/10/2013	31/12/2013	75
Victoria Infirmary, Glasgow	11/10/2013	31/12/2013	75
Aberdeen Royal Infirmary, Aberdeen	20/12/2013	23/05/2014	30
Southmead Hospital, Bristol	20/12/2013	18/06/2014	50
St. James's University Hospital, Leeds	28/02/2014	03/07/2014	50
University Hospital Galway, Galway	20/12/2013	22/09/2014	40
Northern General Hospital, Sheffield	20/12/2013	17/10/2014	10
Glenfield Hospital, Leicester	28/05/2014	19/01/2015	20
Basildon University Hospital, Basildon	17/09/2014	19/01/2015	10
Royal Preston Hospital, Lancashire	17/09/2014	16/03/2015	30
Royal Gwent Hospital, Newport	17/09/2014	08/04/2015	30
Forth Valley Royal Hospital, Larbert	23/04/2014	22/04/2015	40
Royal Alexandra Hospital, Paisley	20/01/2015	21/05/2015	30
Inverclyde Royal Hospital, Greenock	20/01/2015	21/05/2015	40
Aintree University Hospital, Liverpool	08/04/2015	03/06/2015	5
Huddersfield Royal Infirmary, Huddersfield	04/02/2015	10/06/2015	5
University Hospital South Manchester, Manchester	24/02/2015	10/06/2015	50
Kings Mill Hospital, Sutton-in-Ashfield	09/04/2015	22/07/2015	10
John Radcliffe Hospital, Oxford	17/11/2015	19/04/2016	15
Derriford Hospital, Plymouth	23/03/2016	12/10/2016	2

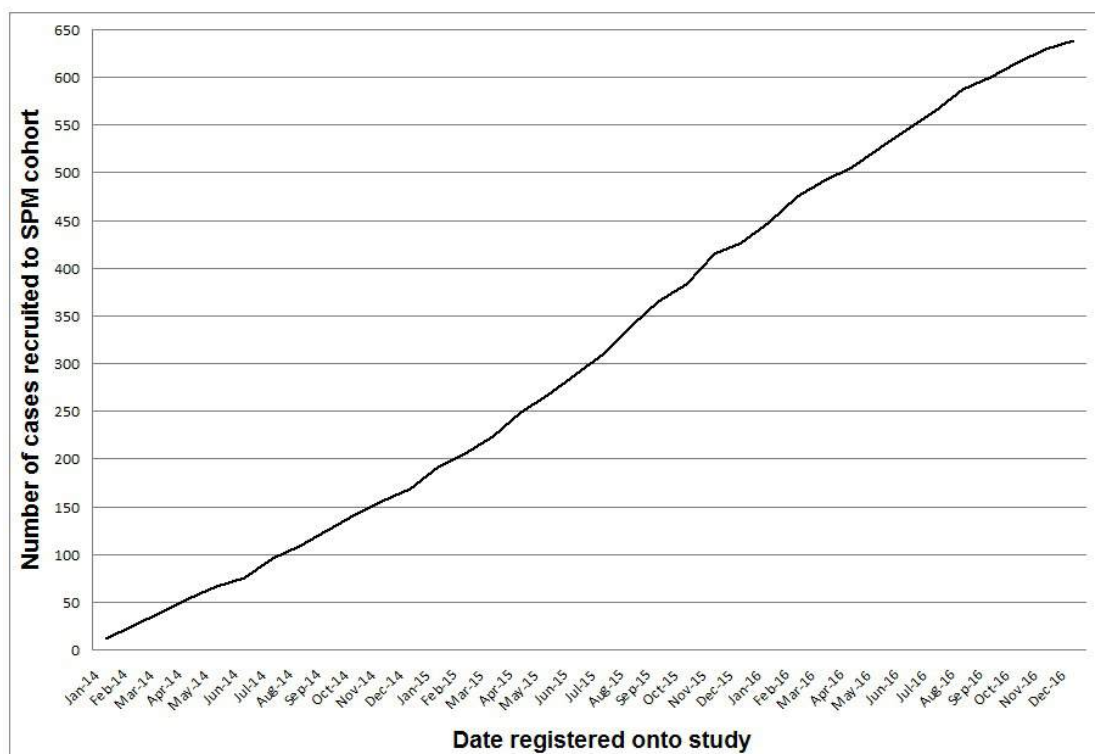


Figure 2.4 Summary of recruitment to the Suspected Pleural Malignancy (SPM) cohort of the DIAPHRAGM study

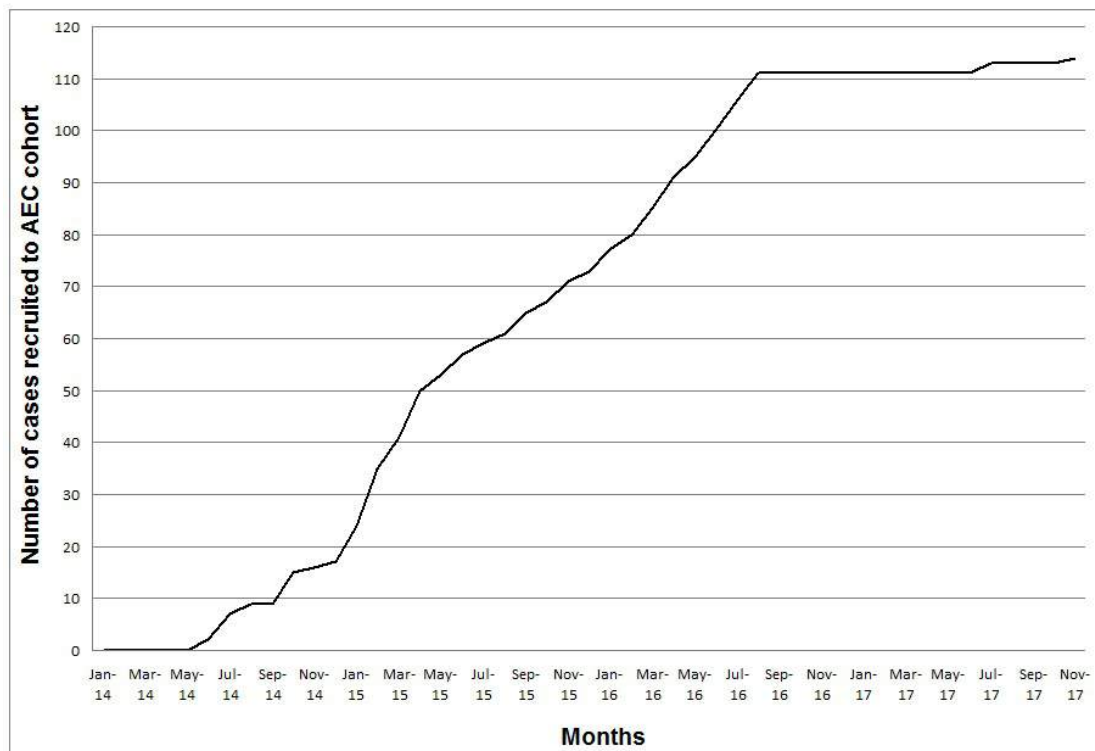


Figure 2.5 Summary of recruitment to the Asbestos-exposed control (AEC) cohort of the DIAPHRAGM study

Table 2.6 Details of recruitment to the Suspected Pleural Malignancy cohort by site in the DIAPHRAGM study

Recruiting Centre	Initial projected total recruitment	Actual number of patients recruited	Recruitment target achieved
WoS centres, Glasgow	300	376	Yes
Aberdeen Royal Infirmary, Aberdeen	30	7	No
Southmead Hospital, Bristol	50	24	No
St. James's University Hospital, Leeds	50	13	No
University Hospital Galway, Galway	40	20	No
Northern General Hospital, Sheffield	10	5	No
Glenfield Hospital, Leicester	20	2	No
Basildon University Hospital, Basildon	10	8	No
Royal Preston Hospital, Lancashire	30	2	No
Royal Gwent Hospital, Newport	30	20	No
Forth Valley Royal Hospital, Larbert	40	27	No
Royal Alexandra Hospital, Paisley	30	18	No
Inverclyde Royal Hospital, Greenock	40	12	No
Aintree University Hospital, Liverpool	5	20	Yes
Huddersfield Royal Infirmary, Huddersfield	5	5	Yes
University Hospital South Manchester, Manchester	50	62	Yes
Kings Mill Hospital, Sutton-in-Ashfield	10	6	No
John Radcliffe Hospital, Oxford	15	10	No
Derriford Hospital, Plymouth	2	2	Yes

Patient recruitment - Mesothelioma case accrual

The mesothelioma rate following 24 months of recruitment was lower than initially estimated at 13% (original estimate 20%). The implication of this was that the target number of MPM cases (n=120) would not be achieved by planned study closure. This was identified by the TMG and a successful application was made to the Chief Scientist Office Scotland for a 12-month, no-cost, study extension to allow recruitment to complete. Selected centres (Southmead Hospital, University Hospital South Manchester and Oxford) were asked to focus recruitment efforts on patients requiring local anaesthetic thoracoscopy in an effort to enrich the mesothelioma population within the SPM cohort. This is because the prevalence of MPM in a population of patients undergoing LAT is higher than that of a population undergoing initial diagnostic pleural aspiration, as patients with underlying pathology diagnosed at pleural aspiration, e.g. secondary pleural malignancy diagnosed at pleural cytology, are removed from the cohort, leaving a more concentrated population. Centres were also encouraged to submit diagnostic update case report forms for any DIAPHRAGM patients who had an updated diagnosis of MPM at the time the diagnosis was made rather than waiting until the form was due at 12 months. These measures steadily improved the mesothelioma rate from 13% to 23% over the following 12 months of recruitment (see Figure 2.6). This rate was kept under regular close review by the TMG.

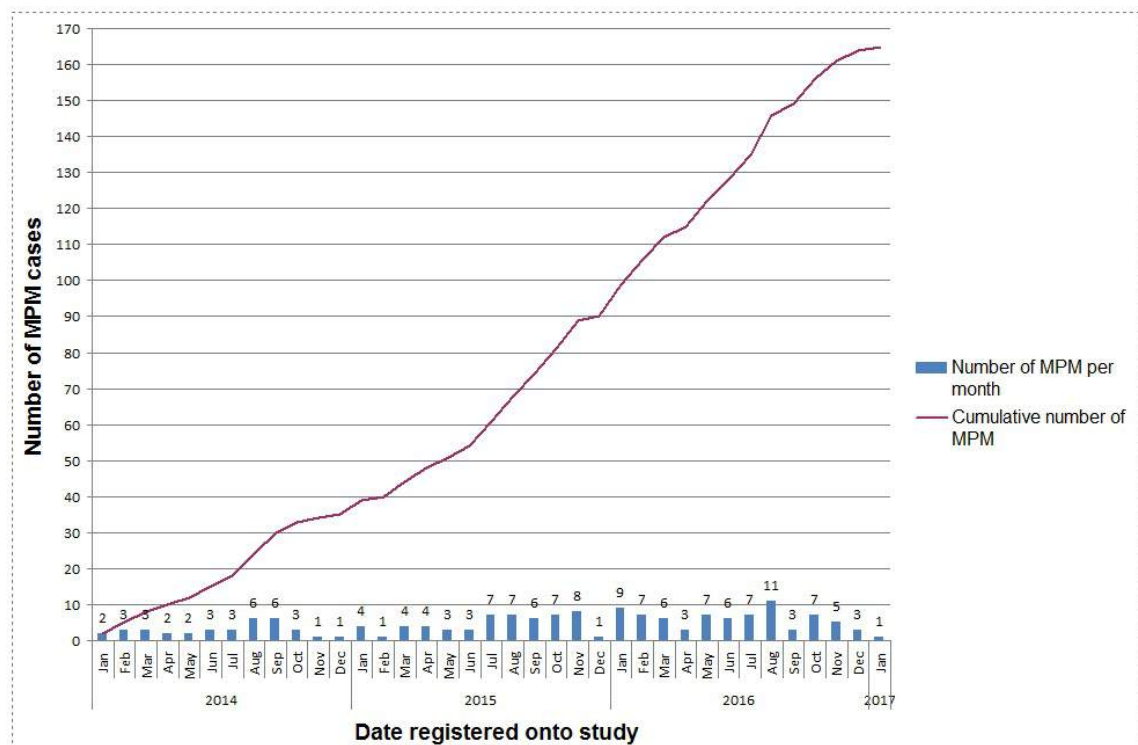


Figure 2.6 Summary of recruitment of cases of Malignant Pleural Mesothelioma (MPM) within the Suspected Pleural Malignancy cohort of the DIAPHRAGM study

2.4.3 Patient Population

Suspected pleural malignancy cohort

1143 patients were screened and 639 patients (107% of target) were recruited to the SPM cohort between December 2013 - December 2016. 44% (n=504) of screened patients were not recruited. 75% (n=380) were deemed ineligible, 7.5% (n=38) declined to participate due to being unhappy with the proposed protocol, 12.5% (n=63) declined to participate for another reason and 5% (n=23) were not given the PIS for another reason (see Figure 2.7).

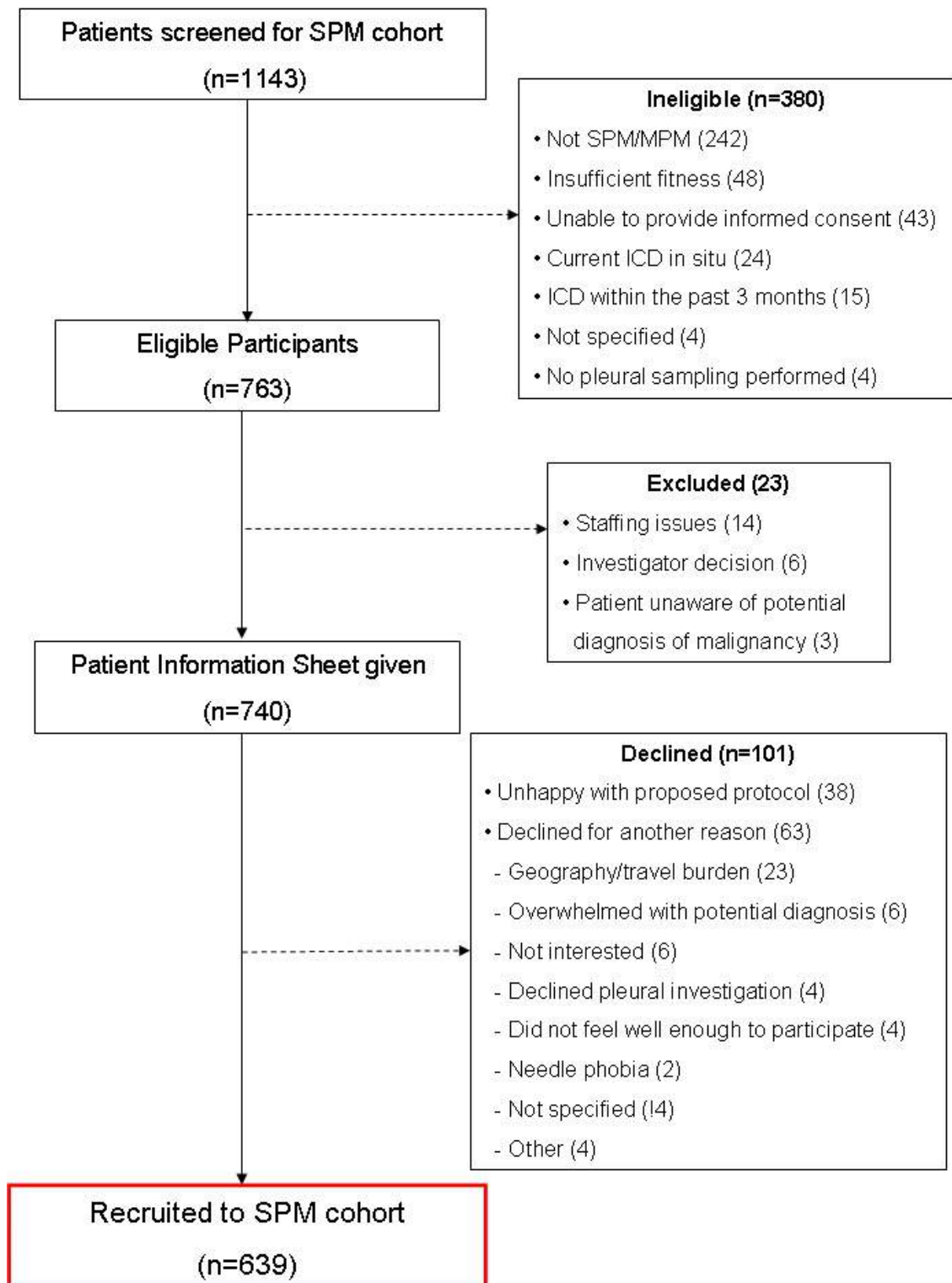


Figure 2.7 Study flowchart summarising recruitment to the Suspected Pleural Malignancy (SPM) cohort of the DIAPHRAGM study

Data cleaning is currently in the final stages of completion by the CRUK Clinical Trials Unit Glasgow, the following results are therefore preliminary. Of the 639 patients recruited to the SPM cohort, mean age was 72 (SD 10) years, 75% (n=478) were male, 70% were current or ex-smokers and 56% (n=361) were asbestos-exposed. 28% (n=179) had a previous or current history of malignancy. 85% (n=540) presented with breathlessness, 27% (n=171) with chest pain and 42% (n=270) as an acute admission.

The preliminary results of final diagnoses of the SPM cohort are summarised in table 2.7. 165/639 (26%) of SPM patients had MPM and 209/639 (33%) had secondary pleural malignancy. 218/639 (34%) had benign pleural disease. Confirmation of final diagnosis is awaited in 47/639 (7%) at the time of writing. Provisional clinical staging data was available in 160/165 (97%) of MPM cases at the time of writing. Stage distribution for these patients was: I (32.5%, n=52), II (10%, n=16), III (38.75%, n=62) and IV (18.75%, n=30).

Table 2.7 Preliminary results of final pleural diagnoses for patients recruited to the SPM cohort of the DIAPHRAGM study. Final diagnosis is awaited in 47/639 (7%).

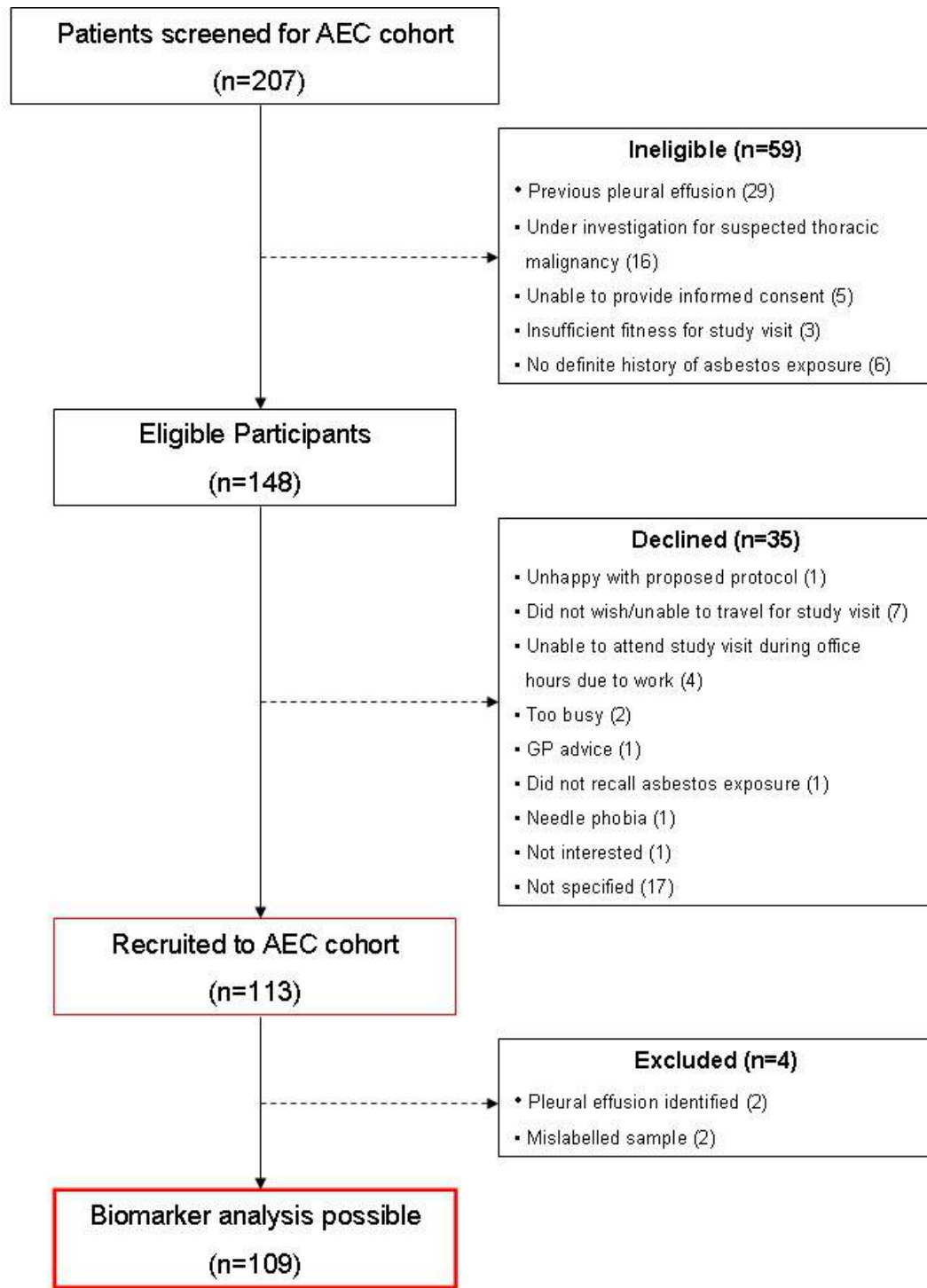
Pleural Malignancy (n=374, 59%)	Benign Disease (n=218, 34%)
<p><i>Mesothelioma (n=165, 44%)</i></p> <p>Epithelioid (n=91, 55.2%)</p> <p>Sarcomatoid (n=20, 12%)</p> <p>Biphasic (n=18, 11%)</p> <p>Desmoplastic (n=2, 1.2%)</p> <p>Lymphohistiocytoid (n=1, 0.6%)</p> <p>Mesothelioma NOS/subtype TBC (n=33, 20%)</p> <p><i>Secondary Malignancies (n=209, 56%)</i></p> <p>Lung Cancer (n=109, 52%)</p> <p>Breast Cancer (n=17, 8%)</p> <p>Gastrointestinal cancer (n=15, 7%)</p> <p>Haematological Cancer (n=15, 7%)</p> <p>Gynaecological cancer (n=9, 4%)</p> <p>Renal (n=9, 4.5%)</p> <p>Other (n=8, 4%)</p> <p>Adenocarcinoma, primary TBC (n=10, 5%)</p> <p>Squamous cell carcinoma, primary TBC (n=4, 2%)</p> <p>Adenosquamous carcinoma, primary TBC (n=1, 0.5%)</p> <p>Unknown primary (n=12, 6%)</p>	<p>BAPE (n=71, 33%)</p> <p>Parapneumonic effusion (n=20, 9%)</p> <p>Chronic empyema (n=7, 3%)</p> <p>Reactive assoc. with Lung Cancer (n=11, 5%)</p> <p>Fibrothorax/Haemothorax (n=9, 4%)</p> <p>Heart failure (n=35, 16%)</p> <p>Tuberculous Pleurisy (n=8, 4%)</p> <p>Pulmonary Thromboembolism (n=4, 2%)</p> <p>Drug-related (n=2, 1%)</p> <p>Post-cardiothoracic surgery (n=4, 2%)</p> <p>Rheumatoid pleurisy/Inflammatory serositis (n=9, 4%)</p> <p>Renal failure (n=3, 1%)</p> <p>Hepatic hydrothorax (n=4, 2%)</p> <p>Other (n=6, 3%)</p> <p>Benign effusion, cause unclear (n=25, 11%)</p>

BAPE; Benign Asbestos-related Pleural Effusion, TBC; to be confirmed

Asbestos-exposed control cohort

113 asbestos-exposed control subjects were recruited (104% of target). 2 patients were withdrawn after study registration due to concern and subsequent confirmation of the presence of pleural effusion at the initial study visit. A further 2 patient's samples were mislabelled and therefore also withdrawn, see Figure 2.8. 15% (n=16) were recruited via the CAA database and 85% (n=93) were recruited from respiratory out-patient clinics.

Mean age was 71 (SD 6) years and 94% (n=102) were male. 37% (n=40) had occupational exposure to asbestos via working in shipyards, reflecting the historic shipbuilding industry along the River Clyde in Glasgow. The remainder were exposed to asbestos through work in the maintenance industry (42%), e.g. electrician, joiner, plumbing, painter and decorator, insulation or heating engineer, boilermaker; construction work (6%); asbestos stripping (2%); the motoring industry (4%) or the merchant navy (3%). 6% (n=6) were exposed to asbestos indirectly via their father or spouse.



AEC; Asbestos-exposed Control

Figure 2.8 Study flowchart summarising recruitment to the Asbestos-exposed Control (AEC) cohort of the DIAPHRAGM study

Cross-sectional MRI sub-study cohort

Patients recruited to the MRI sub-study are described in detail in *Chapter 3: Early Contrast Enhancement*.

2.4.4 Fibulin-3 validation

2.4.4.1 Standard Curve

The standard curve failed on two occasions (see Figure 2.9). On one occasion, the back calculated concentrations were too low (plate 6) and on the other there was a failure across all the whole plate, resulting in no interpretable values (plate 9). In all other occasions, the standard curve met acceptance criteria outlined in section 2.3.11.2.

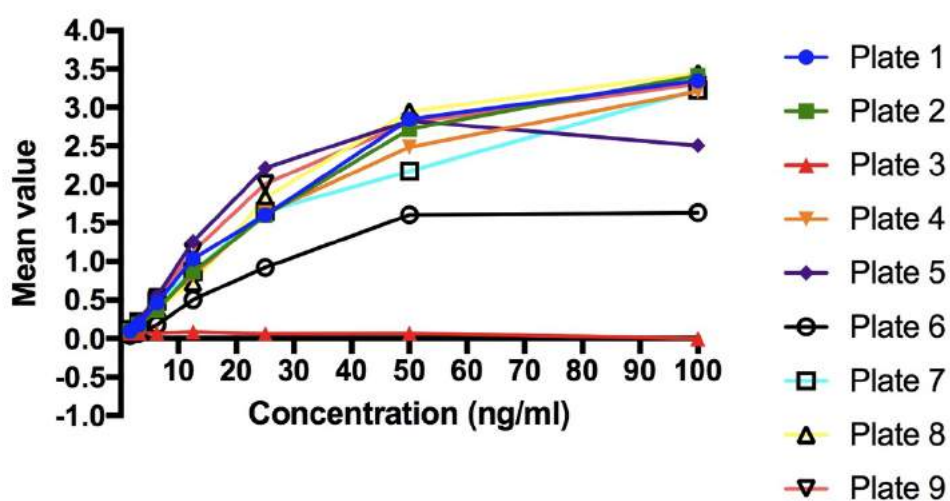


Figure 2.9 Standard curves measuring Fibulin-3 levels across 9 plates

2.4.4.2 Positive Control Samples

The serum-free conditioned medium from all three mesothelioma cell lines HP1, H2595 and H226 all had consistently measurable Fibulin-3 levels, see Table 2.8

Table 2.8 Fibulin-3 levels measured in conditioned medium collected from three different Mesothelioma cell lines

Cell line	Mean Fibulin-3 result (ng/ml)	SD (ng/ml)
HP1		
Undiluted	171.392	10.916
1:1 dilution	166.224	20.046
1:4 dilution	131.918	26.217
H2595		
Undiluted	161.475	45.238
1:1 dilution	136.63	29.712
1:4 dilution	63.042	10.154
H226		
Undiluted	148.744	30.146
1:1 dilution	99.4	1.156
1:4 dilution	45.234	3.057

SD; Standard Deviation

2.4.4.3 Negative Control Samples

The serum-free conditioned medium from the benign mesothelial cell line LP9 and from the Phosphate Buffered Solution had consistently low Fibulin-3 levels, see Table 2.9.

Table 2.9 Fibulin-3 levels measured in conditioned medium collected from benign mesothelial cell line (LP9), Phosphate Buffered Solution (PBS) and distilled water (H₂O)

Cell line	Mean Fibulin-3 result (ng/ml)	SD (ng/ml)
LP9		
Undiluted	4.689	1.226
1:1 dilution	1.78	0.365
1:4 dilution	0.641	0.554
PBS	0.025	0.01
H₂O	0.013	0.008

SD; Standard Deviation

2.5 DISCUSSION

2.5.1 Study Design

DIAPHRAGM was a multi-centre study assessing the diagnostic and prognostic performance of two blood biomarkers, SOMAscan™ and Fibulin-3, recruiting patients with suspected pleural malignancy at time of presentation to secondary care centres. The prospective nature and overall study design was such that blood biomarker draw in the study replicates when these biomarkers would be drawn in clinical practice if they prove to have clinical utility and ensured that blood biomarker sampling and processing was consistent. In addition, body mass index, renal function, concomitant drugs and the effect of diagnostic pleural aspiration were all recorded, allowing the effect of these potential confounders to be established.

Furthermore, patients were recruited from a mixture of district general hospitals, central teaching hospitals and tertiary referral centres, making the results more generalisable to the overall MPM population. Additionally, eligibility criteria were selected to maximise the potential participant population and provide a representative population encountered in normal clinical practice. Asbestos-related pleural plaques were not included as an inclusion criterion since these are absent in up to 25% of MPM cases, (46) and are also common in asbestos-exposed populations without MPM. (47) Patients with lung nodules or other visceral mass lesions were not excluded, assuming that pleural malignancy was suspected. This was because of the high prevalence of lung nodules in the target population (older patients, commonly smokers) and the high false positive rate of CT imaging in this regard.

2.5.2 Challenges of recruiting in a multi-centre study

DIAPHRAGM achieved 109% target recruitment to the SPM cohort and 104% target recruitment to the AEC cohort, but required a study extension period of 12 months. Successful recruitment of the target number of study participants was essential for the study to have valid and reliable outcomes. A multi-centre trial

design, involving tertiary specialist centres in addition to more general secondary care centres, as was the case in this study, increases the likelihood that results are reflective of the general population. Additionally, it allows for a wider population of potential study participants therefore increasing the likelihood that recruitment targets will be achieved more timeously. However, recruiting participants in a multi-centre study can be challenging and investigators often overestimate the pool of eligible participants (a factor sometimes referred to as Lasagna's Law).⁽²⁶⁰⁾ This is highlighted by the frequent finding of under-recruitment in many multi-centre clinical trials. In a study of 114 multicentre RCTs, McDonald *et al* reported that only 31% reached their original recruitment target, 34% revised recruitment targets (86% of which resulted in a lower target) and 53% of trials required a study extension. ⁽²⁶¹⁾ 20% of trials included in this study were in the clinical area of cancer and 53% were in a hospital setting. More recently, in an updated review of multicentre randomised controlled trials, including 73 studies, of which 5% were in the clinical area of cancer and 40% were in a hospital setting, Sully *et al* reported 55% of trials achieved target recruitment, with 47% requiring a study extension. ⁽²⁶²⁾

In the current study, time from site set up initiation to site opening for patient recruitment ranged from 56 days to 364 days (mean 157 (SD 80) days). Site set up was completed in a significantly shorter period of time in WoS centres, which were local to the TMG. The time taken from a site opening for recruitment to their first patient being recruited ranged from 0 days to 208 days (median 31 days). Delays to recruitment commencement are not uncommon in multi-centre trials (reported to occur in up to 41% of trials) and can result from a number of reasons including ethics, central and local trial procedures, such as Research and Development (R&D) approvals, contracts and paperwork completion. ⁽²⁶¹⁾ Many members of the trials team in WoS centres were also members of the central TMG, including the chief investigator, and this may explain the more rapid site set up time in these centres.

Additional challenges in multi-centre studies include competing studies, as many centres will be recruiting to several trials that the same cohort of patients may be eligible for; local staffing issues, such as staff shortages or changes and

differing clinical practices between centres. (261) The DIAPHRAGM study protocol aimed to address the issue of slightly differing clinical practices/pathways between centres by having some flexibility around the patient recruitment time-frame. Some centres will perform a diagnostic pleural aspiration at the initial clinic visit, in contrast other centres, who arrange for the patient to return for a diagnostic pleural aspiration at a later date. The study protocol allowed for patients to be recruited as long as they had sufficient time to consider the patient information sheet, with no requirement for a minimum period of 24 hours for consideration, as is required in many studies. This allowed patient recruitment at the initial clinic visit if required. Additionally, patients could be recruited after initial diagnostic pleural aspiration, which therefore also allowed tertiary centres, who were referred patients from other hospitals for further investigation such as thoracoscopy following an initial non-diagnostic pleural aspiration, to recruit these patients if eligible. The requirement for a follow-up study blood draw to be performed 3 months after diagnosis in patients with MPM did however result in some eligible patients not being recruited at these tertiary centres, as follow-up was planned at the patient's local secondary care hospital. This highlights the importance of close communication with centres who are likely to be a study recruiting centre when constructing a study protocol so that local clinical pathways and practices can be considered and addressed if possible.

2.5.3 Challenges of recruiting a suspected pleural malignancy cohort

Recruitment of a cohort of patients with suspected malignancy, who are often symptomatic with breathlessness or fatigue presents an additional challenge. Accrual to adult cancer trials has been reported to be as low as 5%, depending on the cancer primary and the treatment centre. (263) 639/763 (84%) of patients eligible for the SPM cohort in DIAPHRAGM were enrolled. Reasons for non-participation of eligible patients in the study included lack of interest in the study, feeling too unwell to participate and feeling overwhelmed with information at the clinic visit. The proportion of eligible patients recruited in this study is superior to accrual described by Cooley *et al*, who recruited 230 patients with lung cancer to a cross-sectional quality of life study, which was 63% of all eligible patients. (264) Similar to that described herein, the most

common reasons provided when declining consent in this study included health limitations and lack of interest. Jenkins *et al* studied 240 patients with cancer eligible to participate in an RCT, assessing study participation and reasons for non-participation via a postal questionnaire. They reported a 72% acceptance rate for trial participation with the most common reasons for non-participation principally being associated with concerns regarding the randomisation process or not wanting to be randomised. (263) DIAPHRAGM was not a treatment intervention trial, nor did it require the need for randomisation, which is an additional likely reason for the higher rate of accrual in this study.

LeBlanc *et al* have previously described barriers to patient recruitment to palliative care trials including patient factors, such as frailty, limited life expectancy, competing demands, not being interested in the trial, fatigue and the reminder of impending death. Additional barriers include patient burden when patients are in multiple studies and clinician gatekeeping, where the patients' clinicians assume that clinical research would be too burdensome or upsetting to the patient. (265,266) While these barriers may be more prominent in recruitment of palliative patients, particularly to intervention trials, they undoubtedly also factor in recruiting patients with suspected cancer to studies such as DIAPHRAGM, particularly where initial invitation often coincided with initial presentation with suspected pleural malignancy. Gate-keeping can be a particularly difficult barrier in this context, as was experienced in the DIAPHRAGM study, where some clinicians were either hesitant to discuss a potential diagnosis of pleural malignancy early at presentation, or felt that providing additional study information would be too burdensome for patients at such an uncertain time in their diagnostic journey. The relationship between the clinician and the patient, including the degree of trust, and the communication of study information when first approaching a potential study participant is of paramount importance to the recruitment process. (267) In several of the recruiting centres in DIAPHRAGM, the patient's clinician was also the local principal investigator for the study, with associated advantages of recruiting team having an existing patient-clinician relationship in addition to detailed knowledge of the study. In the earlier lung cancer study, an additional common reason reported for declining to participate was inconvenience. (264) Cox *et al* also describe the burden of trial participation on the patient in terms of time,

travel, interference with other commitments and discomfort from medical procedures as being important barriers to trial participation. (267) This was not observed frequently in the DIAPHRAGM study, perhaps due to the deliberate co-ordination of study procedures with clinical visits, the short duration of study participation (a single visit) and the relatively low medical intervention burden of a single blood draw for the majority of patients. This may have resulted in the higher proportion of eligible patients recruited in our study.

2.5.4 Strategies to improve study recruitment

In a systematic review of 45 randomised controlled trials, Treweek *et al* described six principal categories of intervention adopted for trial recruitment: trial design (e.g. open versus blinded), obtaining consent, approaching participants, financial incentives, training for recruiters and trial co-ordination. (268) Interventions focused on consenting study participants included use of an 'opt-out' approach, where all potential participants are approached as opposed to an 'opt-in' approach, where potential participants have to agree to be approached by the study team before being screened for eligibility. Sygna *et al* similarly described improved recruitment when adopting an opt-out approach in a randomised controlled trial recruiting cancer patients. (269) In the DIAPHRAGM study, the opt-out approaches included on-site screening and approaching all potentially eligible in-patients or patients attending clinic, with patients having the option to decline after a brief introduction to the study by the research team. Telephone or SMS message reminders as a follow-up to written invitation has also been found to improve trial recruitment. (268) In addition, face-to-face eligibility screening was found to increase recruitment, as was adopted in the DIAPHRAGM study for both SPM and AEC cohorts. The systematic review found conflicting results for the effect of additional education for recruiters on study recruitment, but consistent findings regarding little effect on recruitment for centres receiving on-site trial initiation visits versus none. (268) Concordantly, In the DIAPHRAGM study, there was no significant difference in study recruitment between centres who received a face-to-face site initiation visit and training versus those who received site initiation documentation and training via e-mail correspondence only. However, all sites did receive trial newsletters, which included individual feedback on recruitment progress and tips for successful

study recruitment from the trial management group. Personalised site feedback on recruitment has previously been reported to be an effective intervention in reducing time to meet recruitment targets in one randomised controlled trial (RCT), although this was not statistically significant. (270) Additionally, DIAPHRAGM was managed centrally by the CRUK Clinical Trials Unit Glasgow, who co-ordinated site set-up, answered queries from individual recruiting sites, confirmed participant eligibility, produced trial newsletters and provided updates to the CRUK trials website and the Mesothelioma UK newsletter. Sully *et al* reported that trials with CTU input appeared more likely to achieve successful recruitment (65% versus 48% for trials without CTU input, although this did not reach statistical significance). (262)

Strategies adopted in the DIAPHRAGM study to maximise successful recruitment in the WoS centres included having a myself as a dedicated recruitment co-ordinator for these sites and providing clinical teams with a pleural fluid aspiration service to incentivise clinicians to alert the research team of potential participants. Broad and simple eligibility criteria, resulting in 67% of screened patients being eligible, and reminder posters printed at each site also facilitated clinicians' referral to the research team. Furthermore, pre-screening using the electronic Trakcare® system done by myself ensured that potentially eligible participants were not missed by clinical teams. I also regularly visited in-patient respiratory and acute medical receiving wards to identify potential participants.

Similar strategies to improve recruitment have previously been identified as being commonly implemented in numerous multi-centre trials. (261) These strategies were also adopted in the earlier palliative care trial by LeBlanc *et al*, who had broad eligibility criteria, resulting in 79% of screened patients being eligible, and a dedicated recruitment nurse who relieved clinical nurses of the burden of identifying potential participants. (265) Coinciding study recruitment with a clinical visit, i.e. when the patient attended for their initial diagnostic pleural aspiration, was a further strategy adopted to facilitate recruitment. This was adopted to minimise the number of hospital visits, and therefore burden, for patients. Aligning study protocols with standard clinical practice and minimising burden on participants have both been recommended as potential strategies to improve study recruitment. (271)

For the asbestos-exposed control cohort, invitation letters were sent via Clydeside Action on Asbestos (CAA). Invitation via CAA was thought to be a useful source of potential study participants as the members included in their database were likely to be motivated (having independently approached CAA in the first instance) and have a definite history of asbestos exposure. However, recruitment via CAA was not as successful as initially anticipated, with only small numbers responding to the initial invitation letter and subsequently recruited (n=16). Personalised invitation letters, telephone reminders to non-responders and financial incentives included with the trial invitation are all strategies which might have improved recruitment in this context, based on previously reported evidence. (268,272) However, adopting these strategies was not possible in the DIAPHRAGM study, as the CAA member database remained strictly confidential to the study team and CAA were unable to provide staffing resource for telephone reminders. Furthermore, study funding was limited, prohibiting the provision of financial incentive for potential study participants. However, reimbursement for travel costs or provision of transportation to the study centre was provided in order to minimise study participant burden. A significant improvement in the rate of recruitment to the asbestos-exposed control group was demonstrated when a protocol amendment allowed for patients attending respiratory out-patient clinics to be screened for the study. This is likely to be due to a combination of reduced patient burden, with potential participants no longer having to contact the study team independently to enquire about the study; consenting and completing study procedures on the same visit as the patient's clinic attendance and the advantage of the clinician-patient relationship, as discussed previously.

2.5.5 Use of electronic health records for screening

As a member of the clinical team, in addition to being responsible for recruitment in WoS centres, I was able to utilise the electronic health record (EHR) system (Trakcare®) to pre-screen potential participants attending respiratory outpatient clinics. The advantages of having access and utilising EHR to facilitate recruitment to clinical studies are well recognised. (273,274) These include the ability to efficiently pre-screen participants remotely, avoiding

unnecessary attendance at clinics or wards to recruit patients where there may not be any patients who are eligible and potentially reducing the number of potentially eligible participants who are missed by the recruiting team. As utilised in DIAPHRAGM, several previous studies have utilised EHR to identify potentially eligible participants. (275-277) Other trials have utilised EHR with an automated clinical trial alert system to prompt clinicians that their patient may be eligible for a clinical trial if eligibility criteria are met, with the option of subsequently alerting the trials team. This system has previously been reported to increase clinician referral rates and study enrolment. (278) EHR can also be used as source data in clinical studies, as they typically include basic demographic data in addition to detail on co-morbidities and concomitant medications. (274) Clearly care must be taken in confirming accuracy of data identified in EHR with the study participant.

Prior consent is often required for research teams to access clinical records, reducing the utility of using EHR for identifying potential participants in prospective clinical trials. (275) One advantage of the DIAPHRAGM study is that clinical teams were responsible for identifying and recruiting patients, allowing utilisation of EHR. Having inclusion criteria that were easily identifiable on EHR was an additional advantage in this study.

2.5.6 Review of preliminary results

The results reported herein summarises patient recruitment and preliminary demographic data of the study participants prior to completion of the data cleaning process. Biomarker analyses are in progress and these results are not yet available.

Suspected Pleural Malignancy Cohort

The mean age of patients in the SPM cohort was 72 years and 75% were male, this is similar to the age and sex distribution of patients included in the National Lung Cancer Audit pleural mesothelioma report 2016 (median age 75 years and 83.4% male). (279) The majority of patients presented with chest pain and/or breathlessness, which is in keeping with previous reports of presenting symptoms in MPM. (39)

Final diagnoses were available for 93% (n=592) of the SPM cohort at the time of writing. The prevalence of PM in this study was 59%. Of the patients with a final diagnosis of PM, the primary cancer was MPM in 44%, lung in 29%, breast in 5%, gynaecological in 2%, gastrointestinal in 4%, haematological in 4%, renal in 2%. The remaining primaries were either unknown or awaiting confirmation from the local site. The British Thoracic Society (BTS) pleural disease guidelines, summarising 5 different studies incorporating 2040 patients with malignant pleural effusion, report lung and breast cancer to be the most common primary tumour sites in patients with malignant pleural effusion (approximately 37.5% and 17% respectively). (280) Haematological, gastrointestinal, genitourinary, 'other primary' and unknown primary accounted for the remaining 11.5%, 7%, 9%, 8% and 11% of malignant pleural effusions respectively. (280) This distribution of secondary pleural malignancies is similar to that reported in the DIAPHRAGM study. However, the earlier report was based on historical studies (published between 1975 - 1987) and is therefore likely to underestimate the prevalence of MPM, as these studies predate the use of local anaesthetic thoracoscopy and diagnoses were therefore predominantly based on cytological examination of pleural fluid samples. (281) (282) (283) (284,285) Additionally, the increasing incidence of MPM in the UK over the past 30 years (279) and the targeted recruitment of potential MPM patients referred for thoracoscopy after non-diagnostic pleural cytological examination in selected centres is likely to be responsible for the higher prevalence of MPM in our study cohort. Concordant with this is the higher proportion of MPM patients in the more recent multi-centre study of MPE by Clive *et al*, which recruited from centres in the UK, the Netherlands and Australia (21.5%), (14) and that reported by Hallifax *et al* in a study of patients referred to a tertiary centre for LA thoracoscopy (54.5%). (82)

Final staging data was available in 97% of MPM cases at the time of writing of this thesis. 68/160 (42.5%) presented with early stage disease (IMIG stage I/II). This is higher than that reported by the National Lung Cancer Audit pleural mesothelioma report 2016, which reported 17% of patients presenting with stage I/II disease. However, the reporting of stage in MPM has historically been poor, due to staging being relatively complex and only 42% of cases submitted to the audit had stage recorded. (279) Similarly, a recent review of the Western Australia Mesothelioma Registry, incorporating 2024 cases of MPM did not report

on stage distribution at all, (286) and a retrospective review of 337 MPM patients registered in the National Cancer Registry Ireland reported only 45% of patients having stage recorded (n=153), of which 33.4% (n=51) had stage I/II disease. (287) Another retrospective review of 101 patients diagnosed or referred for treatment at a single Dutch institution (Antwerp University Hospital) reported 39% of patients had stage I/II disease (only 2/101 patients did not have stage recorded in this study). (288)

2.5.7 Fibulin-3 Validation

As previously discussed in Chapter 1: Introduction, there was significant variability in the both the reported diagnostic performance of Fibulin-3 (sensitivity varying between 12.7% and 100%) and the reported levels measured in blood (mean levels ranging from 11.51ng/ml to 112.9ng/ml). (151,247,250-253) While varying study design, incorporating variable sampling time-points could be one explanation for this variability, the validity and performance of the Fibulin-3 assay itself must also be considered. Pre-validation testing by the TPL highlighted concerns regarding assay consistency. In addition, the volume of positive control sample provided by the assay manufacturer was insufficient to complete assay validation testing. We therefore needed to source alternative positive controls to use as quality control samples, as described herein. Furthermore, at the time of writing further inconsistencies related to antibody printing on several of the 96-well plates in the FBLN3 kit have been reported by the Translational Pharmacology Laboratory. Exploration and testing of alternative Fibulin-3 assay kits are therefore in progress.

2.6 CONCLUSION

DIAPHRAGM was an adequately-powered, multi-centre study that successfully achieved target recruitment of patients to a suspected pleural malignancy cohort and asbestos-exposed control cohort. It represents the largest prospective biomarker study in MPM to date, recruiting over 700 patients, including over 160 patients with Malignant Pleural Mesothelioma. The prospective nature, study design and Fibulin-3 assay validation will allow the diagnostic performance of Fibulin-3, SomaSCAN™ and Mesothelin in Malignant Pleural Mesothelioma to be clearly defined. At the time of writing, Mesothelin assays are

complete for all baseline samples. SOMALogic[®] have measured 11 of the original 13 proteins included in the original SOMAscan[™] assay in all baseline MPM cases, 83 non-MPM effusion cases and 83 AEC cases. Fibulin-3 assays are complete for approximately half of the baseline samples. Data cleaning is currently in its final stages and analysis of available biomarker results is due to commence shortly.

CHAPTER 3: EARLY CONTRAST ENHANCEMENT

3 Chapter 3: Early Contrast Enhancement (ECE)

3.1 INTRODUCTION

Clinically overt pleural metastases are associated with a median survival of only 3 months in patients with Lung Cancer (14). In patients with macro-nodular pleural tumour this is easy to detect, with sensitivity and specificity exceeding 90% in previous studies using Computed Tomography (CT) (77,289) and Magnetic Resonance Imaging (MRI). (77,99) Simple pleural effusion is, however, detectable in 25% of Lung Cancer patients at presentation, and affects 40% at some time during their journey. (15) This is associated with a significant survival disadvantage, even if the effusion is too small to safely aspirate, or pleural cytology appears reassuring. (15,290) This suggests that occult pleural metastases are present in at least a proportion of these patients. Unfortunately it is difficult to define, using existing techniques, which patients should be directed to thoracoscopic sampling as part of Lung Cancer staging. Subjective cross-sectional imaging, using CT or MRI, is poorly suited to the detection of typically sessile pleural tumours, distributed heterogeneously over a large surface area. This makes it impossible to reliably distinguish between low-volume pleural metastases and a benign reactive effusion (e.g. due to lobar collapse).

Similar challenges are encountered when assessing asbestos-exposed patients with a new pleural effusion, where the principal differential lies between Benign Asbestos-related Pleural Effusion (BAPE) and early-stage Malignant Pleural Mesothelioma (MPM). Misdiagnosis at this stage probably contributes to rates of emergency MPM presentation, via recurrent symptomatic pleural effusion, which exceed 50% in parts of the UK (43,291). This is associated with adverse survival (43,291), and limits opportunity for enrolment in clinical trials, which may ultimately improve MPM outcomes.

These diagnostic difficulties are reflected in the poor diagnostic sensitivity (between 58% - 68%) of CT for detecting pleural malignancy in routine clinical practice. (82,83) As previously discussed, LAT is extremely sensitive, but cannot be performed in all patients and centres, and is still an invasive test. (71) Therefore, a novel, non-invasive method of selecting patients for invasive

sampling is urgently required. This should ideally be objective and sensitive, even in patients with subtle or absent morphologic features of malignancy, as is frequently the case, particularly in early stage MPM.

3.1.1 Tumour Angiogenesis

Tumour angiogenesis describes the formation of new blood vessels, which is necessary for tumour cell population expansion and tumour growth beyond 1 - 2mm in diameter (292) and metastatic spread. (293) Increased microvessel density, a surrogate marker of tumour angiogenesis, has been shown to be associated with poorer patient outcomes in numerous cancers including breast (294,295), prostate (296), lung (297) and MPM. (37,298,299) The timing of tumour angiogenesis varies between tumour type, (300) but can occur early in tumour development in several cancers (301-303), including breast (304), bladder (305) and lung cancer. (306)

3.1.2 Imaging of Angiogenesis

There are several imaging techniques that can be used to assess angiogenesis, including number and spacing of blood vessels, blood volume, blood flow and vascular permeability (307), with resulting potential clinical utility in the non-invasive diagnostic assessment of malignancy and in the assessment of response to anti-angiogenic therapies. These include DCE-MRI, PET, ultrasound, CT and single photon emission computed tomography (SPECT).

Ultrasound

Doppler US is readily accessible and allows assessment of the vascular anatomy and blood flow through tumour, however this technique is limited to assessment of larger vessels rather than intra-tumoural microvessels. The introduction of intravascular microbubble-enhanced doppler US allows assessment of vessels and blood flow down to 50 - 100µm in diameter. (308,309) This technique is however heavily operator-dependent with a limited field of view, does not provide information on vascular permeability and is not currently widely used.

Perfusion CT

Perfusion CT (or Dynamic Contrast Enhanced-CT (DCE-CT)) involves the serial acquisition of the same volume of tissue over time following the administration of intravenous iodinated contrast agent. (310) This imaging technique allows assessment of tissue blood flow, blood volume mean transit time and vascular permeability. (311) Detection of increased or abnormal tissue perfusion can suggest malignancy even prior to the development of gross anatomical abnormality detectable morphologically. Previous studies have demonstrated potential utility in assessment of pulmonary nodules and MPM. (312-314) Perfusion CT has the advantage of widespread availability and there is also a direct linear relationship between iodine concentration and enhancement (measured in Hounsfield Units). (311) However, the multiplicity of protocols using different mathematical models (315) and high radiation burden have limited its widespread use in routine clinical practice to date. (110,316)

PET

^{15}O -labelled tracers can be used in PET imaging. Inhalation of fixed doses of C^{15}O results in binding of C^{15}O to haemoglobin, forming $\text{C}^{15}\text{O-Hb}$, which remains within the vasculature. ^{15}O PET imaging can therefore be used to detect blood flow and vascular volume. (308) However, the tracer has a short half-life and requires patient inhalation. The technique is also limited by high cost, limited availability of equipment and poor anatomic resolution. (309) ^{18}F -Fluciclatide is a novel PET tracer targeting integrins $\alpha_v\beta_3$ and $\alpha_v\beta_5$, currently being examined in imaging research in tumours such as breast cancer. (98) Integrins are a family of cell-extracellular matrix adhesion molecules. Integrin $\alpha_v\beta_3$ in particular is known to play a key role in angiogenesis and expression of $\alpha_v\beta_3$ and $\alpha_v\beta_5$ is increased in activated tumour-associated endothelial cells. (317) (318)

Dynamic contrast-enhanced MRI (DCE-MRI)

MRI allows acquisition of high-fidelity anatomical and biological data in multiple phases of contrast enhancement, without use of ionizing radiation, making it an attractive research imaging tool. DCE-MRI is an MRI technique that can exploit the characteristic feature of high permeability of immature new vessels within

tumour. (319) Due to high vascular permeability, MRI contrast agents (most frequently a low-molecular weight Gadolinium chelate) demonstrate rapid 'wash-in' and 'wash-out' as it passes through tumour vessels on T1-weighted imaging. The differential pattern of 'wash-in' and 'wash-out' can be mathematically fit into compartment models to produce estimates of tissue perfusion and permeability. (319)

DCE-MRI has been widely used in clinical trials to assess early response to anti-angiogenic chemotherapeutic agents. As previously highlighted in Chapter 1, DCE-MRI involves the administration of an intravenous contrast agent, typically of low molecular weight such as gadolinium, followed by rapid image acquisition to allow temporal imaging of signal intensity changes within a volume of (tumour) tissue. Signal intensity changes result from changes in contrast concentration in the extravascular and extracellular space, which depends on tumour perfusion, tumour vascularity, tumour vascular permeability and the fractional volume of the extravascular and extracellular space. (308,309,320) Unlike perfusion CT, where the relationship between enhancement is directly linear to the concentration of iodine contrast within the tissue, signal intensity at T1-weighted DCE-MRI is also dependent on the native T1 relaxation rate of the tissue. (309) Acquisition of DCE-MRI data therefore requires sequences that allow for anatomic localisation of tumour followed by sequences that allow for calculation of the baseline T1 of the tissue before acquiring dynamic data post-contrast. (320) DCE-MRI has previously been used as a diagnostic imaging biomarker in the evaluation of breast mass lesions, being able to differentiate benign from malignant breast masses. (113) Previous studies have demonstrated that assessment of contrast kinetics at DCE-MRI results in improved specificity of differentiation between benign and malignant breast masses over conventional MR imaging with morphological assessment. (112) A systematic review of studies assessing breast lesions using MRI found that DCE-MRI had an overall sensitivity of 82% and specificity of 74% for the detection of breast malignancy. (321) This improved to a sensitivity of 95% and specificity of 86% when morphologic data was combined with perfusion data obtained at DCE-MRI. (321)

DCE-MRI has also been shown to be of diagnostic utility in the assessment of prostate lesions, (116) with differing contrast kinetic parameters allowing

differentiation between benign and malignant prostate lesions. (322,323) Similar to the early contrast enhancement pattern of pleural malignancy reported here, previous authors have demonstrated an initial increase in contrast enhancement followed by a decrease being typical of a malignant prostate lesion. (324) DCE-MRI has also been used as a predictive biomarker of response to anti-angiogenic chemotherapeutic agents such as bevacizumab in a number of cancers, including mesothelioma, (117) lung cancer (325), glioma (326) and breast cancer. (327)

However, as discussed previously, DCE-MRI requires a mass lesion to define an adequate Region of Interest (ROI), and image acquisition is limited to a relatively small number of slices so the entire hemithorax, and therefore pleura, cannot be assessed. This limits its clinical utility in the early detection of MPM, which typically has a sessile, heterogeneous growth pattern and rarely presents as a mass lesion in early stage disease. Giesel *et al* performed DCE-MRI in 19 patients with confirmed MPM and reported different contrast kinetic parameters between tumour tissue and normal tissue, (117) however, 10/19 (53%) of these patients had bulky stage IV disease, which adds little value over morphological assessment.

This chapter describes a novel MR imaging biomarker of pleural malignancy, Early Contrast Enhancement (ECE), which can be applied to patients with pleural effusion and minimal pleural thickening.

3.2 AIM AND OBJECTIVES

The aim of this study was to define a contrast-enhanced MR imaging method to detect pleural malignancy with high diagnostic sensitivity and specificity, exploiting pathognomonic, non-anatomical features of pleural malignancy that would be present in all patients, including those with pleural effusion and minimal pleural thickening.

We hypothesized that MRI methodology targeted to increases in constituent blood vessel density, and therefore tumour angiogenesis, could accurately identify pleural malignancy, even in early stage disease.

Study objectives and outcome measures are presented in Table 3.1.

Table 3.1 Study Objectives and Outcome Measures of the Early Contrast Enhancement Study

STUDY OBJECTIVE	OUTCOME MEASURES
<p>Primary</p> <p>To determine whether perfusion-based, ce-MRI can differentiate pleural malignancy from benign pleural disease with comparable or superior sensitivity and specificity to subjective CT or MRI morphology assessment</p>	<p>Diagnostic classification based on</p> <ul style="list-style-type: none"> • MRI contrast enhancement pattern • CT morphology assessment • MRI morphology assessment <p>Diagnostic assessment including pleural biopsy results</p>
<p>Secondary</p> <p>To determine whether there is a correlation between contrast enhancement pattern at MRI and tumour vascularity</p> <p>To determine the reproducibility of ECE, CT and MRI morphology</p>	<ul style="list-style-type: none"> • Mean Signal Intensity Gradient at ce-MRI • Tumour MVD based on Factor VIII immunostaining in FFPE pleural biopsies <ul style="list-style-type: none"> • Inter-observer agreement (Cohen's Kappa) • Intra-observer agreement for ECE only (Cohen's Kappa)
<p>Exploratory</p> <p>To determine whether there is an association between:</p> <ol style="list-style-type: none"> 1. ce-MRI parameters and Survival 2. Tumour vascularity and Survival 	<ul style="list-style-type: none"> • MSIG at ce-MRI • Overall Survival (months) <ul style="list-style-type: none"> • Tumour MVD (Factor VIII immunostaining in FFPE pleural biopsies) • Overall Survival (months)

ce-MRI; Contrast-enhanced Magnetic Resonance Imaging, CT; Computed Tomography, ECE; Early Contrast Enhancement, FFPE; Formalin-Fixed Paraffin-Embedded, MVD; Micro-vessel Density, MSIG; Mean Signal Intensity Gradient

3.3 METHODS

3.3.1 Ethical Approval

Ethical approval for this study was provided by the West of Scotland Research and Ethics Service (reference 12/WS/0219 and 13/WS/0240). NHS Greater Glasgow and Clyde acted as the study sponsor.

3.3.2 Study Population

Patients included in this chapter were recruited from a pilot study conducted to establish MR imaging acquisition and analysis protocols, and as part of the DIAPHRAGM MRI sub-study (further details of which are included in chapter 2).

Patients presenting with suspected pleural malignancy, as defined by a pleural effusion or pleural-based mass lesion, to the Southern General Hospital (now the Queen Elizabeth University Hospital), Gartnavel General Hospital, Victoria Infirmary and Glasgow Royal Infirmary between January 2013 and October 2016 were invited to participate. Patients were identified at respiratory outpatient clinics and in acute admission units or respiratory inpatient wards. All patients were reviewed by myself or Dr Kevin Blyth (Consultant Respiratory Physician) who reviewed the need for pleural biopsy (either image-guided or thoracoscopically), based on clinical need and patient wishes, and their eligibility for the study. Eligibility criteria were as follows:

Inclusion criteria

- Suspected pleural malignancy requiring investigation by thoracoscopy (medical or surgical) or image-guided pleural biopsy
- Sufficient fitness for pleural biopsy
- Informed written consent

Exclusion criteria

- Pregnancy
- Known allergy to gadolinium contrast
- Significant renal impairment (eGFR <30ml/min)
- Known MRI contraindication (e.g. cardiac pacemaker, metallic foreign body)

All patients underwent comprehensive diagnostic assessment for an unexplained pleural effusion as described in chapter 1. This included routine blood tests, chest radiograph, thoracic ultrasound, pleural fluid analysis and contrast-enhanced CT imaging, followed by LAT, VATS or image-guided pleural biopsy.

3.3.3 Clinical Assessment

Local anaesthetic thoracoscopy

All patient assessments and procedures were performed by myself and Dr Kevin Blyth. Assessment for LAT included a review of appropriateness and fitness for LAT as per BTS guidelines, (71) and a repeat thoracic ultrasound to ensure that the patient had an accessible pleural space lying in a lateral decubitus position, i.e. sufficient pleural fluid volume or if pleural fluid volume was insufficient or absent then the presence of normal lung 'sliding'. Lung sliding on thoracic ultrasound describes the normal appearance of the visceral pleura moving relative to the parietal pleura and chest wall (328) and is an indication that a pneumothorax can be induced at LAT.

Patients were admitted to the Queen Elizabeth University Hospital the evening before or the morning of LAT, with the procedure being performed in the afternoon. Patients were given fasting instructions and pre-medication (20mg oral morphine solution and 1.2mg oral atropine (if the patient was aged <75 years and had no contra-indications on 12-lead electrocardiograph)) was given approximately 1 hour prior to LAT. LAT was performed in a dedicated endoscopy suite (and in a sterile theatre prior to June 2015). The patient was positioned appropriately in bed before being attached to 3-lead cardiac monitoring, blood pressure monitoring and a pulse oximeter. The procedure was performed under

conscious sedation (using intravenous midazolam +/- alfentanil) and strict aseptic technique. A repeat thoracic ultrasound was performed with the patient on the procedure table in every case. After appropriate infiltration of local anaesthetic (1% lidocaine with adrenaline 1:200,000), a pneumothorax was induced using a Boutin needle followed by blunt dissection to the pleural space. A single 7mm port was then inserted and any residual pleural fluid aspirated. A rigid thoracoscope was then inserted via the port to allow thorough inspection of the pleural cavity. Biopsies were taken of any obvious tumour affecting the costal pleura or in the absence of obvious tumour, multiple biopsies of representative costal pleura were taken. Talc poudrage was performed on a case-by-case basis before a 24-French intercostal chest drain was inserted and secured with sutures. Residual pneumothorax was evacuated using thoracic suction before the patient was returned to the ward to convalesce. A post-procedure chest radiograph was taken and the chest drain removed when deemed appropriate (in cases where talc poudrage was not undertaken this was generally when the lung was shown to be re-inflated on the chest radiograph). Following discharge post-LAT, all patients were followed-up at a dedicated specialist pleural clinic.

Diagnostic Protocol

Final diagnoses were based on histology results and MDT consensus where available. In the event of suspected false negative pleural biopsy in patients with suspected MPM, repeat biopsy results were reviewed. A diagnostic review at 12 months was undertaken in all patients, which included review of any interval imaging or repeat biopsy where performed.

3.3.4 Sample Size and Assumptions

An *a priori* sample size calculation was not possible given the novel nature of the primary contrast-enhanced MRI outcome measure. A target sample size of 60 was deemed to be large enough for these methods to be developed and tested. Assuming a 50% incidence of MPM in the study cohort (based on our unit's MPM incidence at LAT), 30 MPM patients would also allow a moderate correlation ($r=0.5$) between the relevant secondary outcome measures to be detected with 80% power at a 5% two-sided level of statistical significance.

3.3.5 Imaging acquisition

3.3.5.1 Contrast enhanced-CT Acquisition

Contrast-enhanced CT imaging was acquired prior to pleural biopsy or other significant pleural intervention (except pleural aspiration) in all patients. CT examinations were performed in the course of routine clinical work-up at one of three Clinical Radiology Departments with expertise in thoracic imaging, using standard techniques and were not protocolised. CT scans were acquired on a variety of machines (GE Medical Systems BrightSpeed, LightSpeed or Optima 660; Toshiba Aquilion). In all patients, multi-slice helical CT images reconstructed with a maximum contiguous slice thickness of 2 mm were acquired at baseline and following administration of intravenous iodinated contrast material, typically 100 ml of 300 mg/ml of Optiray™ (Mallinckrodt Pharmaceuticals, Ireland) according to standard local clinical protocols. In 53/58 (91%) patients, post-contrast imaging acquisition was in the venous phase, between 60 and 70 seconds following contrast injection. In 5/58 (9%) patients, post-contrast imaging acquisition was in the pulmonary arterial phase (bolus-tracked CTPA).

3.3.5.2 Pleural MRI Acquisition

All MRI scans in this thesis were performed by the Glasgow Clinical Research Imaging Facility radiographers and myself under their guidance. Scans were performed at the BHF Glasgow Cardiovascular Imaging Facility between January 2013 and August 2015, and at the Queen Elizabeth University Hospital between August 2015 and October 2016. Scans were performed using a 3-T Siemens Magnetom Verio® (Siemens, Erlangen, Germany) between January 2013 and August 2015, and using a 3-T Siemens Magnetom Prisma® (Siemens, Erlangen, Germany) between August 2015 and October 2016. Full resuscitation equipment, including a defibrillator and emergency drugs were available within close and easily accessible proximity to the patient at all times, as was a fully qualified Advanced Life Support provider (myself). All patients had pleural MRI performed prior to pleural biopsy or other significant pleural intervention (except pleural

aspiration). All study participants were provided with access to study transportation to and from the MR imaging facility.

Patient preparation and positioning

All patients were asked to complete a safety questionnaire before entry into the MR scanning room (see Appendix 12). A plain orbital radiograph was taken if there was any history of previous injury involving metal fragments with potential involvement of the eyes, and reviewed by a consultant radiologist (Dr David Stobo) to exclude retained metal fragments. Patients were asked to remove any metal clothing or accessories, such as watches or belts, and were provided with a patient gown to change in to. A 20 or 22-gauge cannula was inserted into the patient's antecubital fossa, wrist or hand for intravenous contrast administration. Patients were then positioned head first and supine on the MR examination table and a phased array chest coil placed and secured on their chest with straps. They were then supplied with ear plugs and headphones, allowing them to hear instructions during the scan and to listen to music in between instructions, and an emergency buzzer. After describing breathing instructions that would be given throughout the course of the scan acquisition, the patient's bed was moved inside the bore of the magnet. Communication via the headphones and the emergency buzzer were both tested prior to initiating image acquisition.

MR Image Acquisition

Imaging protocols were developed in the first 6 patients, all of whom had non-contrast-enhanced scans and are not included in the final analyses. Initially, images were acquired in three separate axial blocks. This methodology was adapted from cardiovascular magnetic resonance imaging protocols performed pulmonary hypertension studies previously conducted by Dr Blyth. (329)

However, the objective of these prior studies was to assess the right ventricle rather than the entire thorax, which was required in the present study. The three axial blocks acquired in these initial patients needed to be 'stitched' together, which inevitably resulted in the potential for image overlap and/or discontinuity. Additionally, the resulting images were not isotropic and 3-

dimensional (3D) volumetric assessment was therefore not possible, see Figure 3.1.

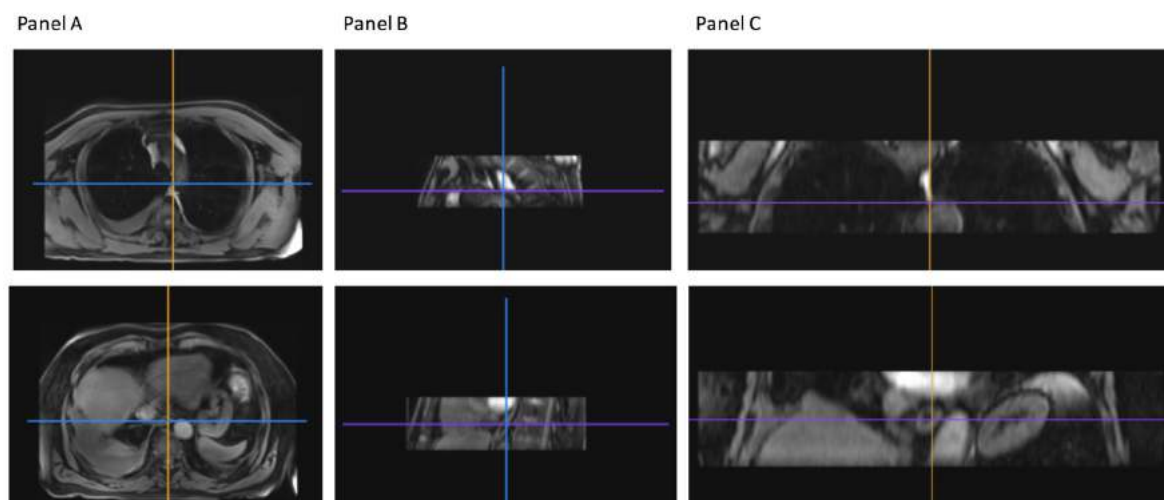


Figure 3.1 Example of a non-contrast enhanced MRI scan, acquired in separate axial blocks (Panel A) and their corresponding sagittal (Panel B) and coronal (Panel C) images, early in the process of developing imaging protocols for the Early Contrast Enhancement study

A new 3D isotropic imaging protocol was therefore developed by Dr Foster and Dr Blyth in the remaining 60 patients (see Figure 3.2). T1-weighted, fat-saturated, 3D spoiled gradient echo sequences (repetition time 2.8 - 3.23ms, echo time 1 - 1.08ms, field of view 400 - 440mm, matrix 224 x 100, flip angle 9° , slice thickness 1.8 - 1.9mm, no inter-slice gap), were acquired during a short breath-hold at end-inspiration. Number of slices acquired ranged between 104 - 144 slices (median 120 (IQR 120 - 128)). Breath-hold duration varied between 16 - 22 seconds, depending on the size of the patient's thorax. If the patient reported difficulty with the breath-hold or initial MR images had evidence of significant breathing artefact, then slice thickness was increased to reduce the breath-hold time. The field of view was adjusted if required to ensure all image acquisitions remained isotropic despite any adjustments in slice thickness. All Images were acquired isotropically in the coronal plane at baseline and at numerous set time points after intravenous gadobutrol contrast (Gadovist (0.1 mmol/kg), Bayer Healthcare Pharmaceuticals, Berlin, Germany) was administered, at an injection rate of 2 ml/second.

In the majority of patients (53/60), images were acquired at baseline, 40 seconds, 80 seconds, 4.5 minutes, 9 minutes and 13.5 minutes after intravenous contrast administration. In one patient, there was incomplete contrast enhancement, possibly due to contrast extravasation and was therefore excluded from further analysis. In 6/60 patients, the 40 second and 80 second post-contrast images were omitted and TrueFISP sequences were performed in the first 120 seconds post-contrast, as described in previous DCE-MRI studies in MPM patients. (117) After review of the contrast enhancement patterns in the first 27 patients, the imaging protocol was altered to include additional images acquired at 3 minutes post-contrast (acquired in 33/60 patients) in order to allow more detailed analysis of contrast enhancement at earlier time points.

Imaging protocols for each patient are summarised in Table 3.2.

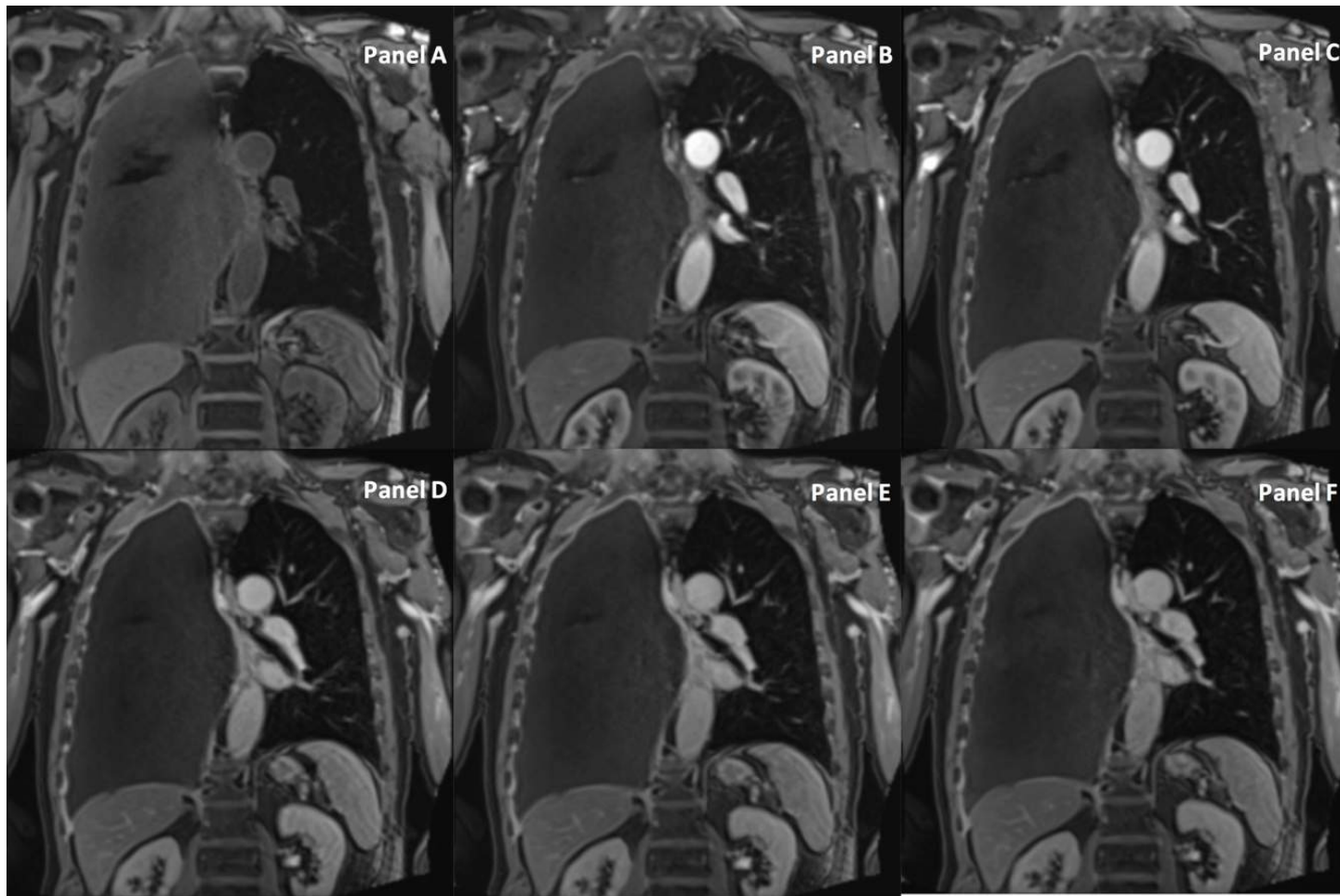


Figure 3.2 Isotropically-acquired, contrast-enhanced MR images acquired over time pre-contrast (Panel A) and 40 seconds (Panel B), 80 seconds (Panel C), 4.5 minutes (Panel D), 9 minutes (Panel E) and 13.5 minutes (Panel F) post-administration of intravenous Gadobutrol

Table 3.2 Magnetic Resonance Imaging (MRI) protocols used in 66 patients with suspected pleural malignancy

Case No.	MRI Scanner	Contrast Agent	Orientation of VIBE acquisition	FOV (mm)	Repetition Time (ms)	Flip Angle (°)	Echo Time (ms)	Matrix	Slice Thickness (mm)	No. of Slices	Baseline	40s post-contrast acquired	80s post-contrast acquired	180s post-contrast acquired	270s post-contrast acquired	540s post-contrast acquired	810s post-contrast acquired
1	3T Verio	None	Axial/Coro	380/450	3.92	9	1.39	320x70	3	36	✓						
2	3T Verio	None	Axial	380	3.92	9	1.39	320x100	3	28	✓						
3	3T Verio	None	Axial/Coro	380	4.31	9	1.33	320x70	1.7	28	✓						
4	3T Verio	None	Axial/Coro /Sagg	420/380/380	4.31	9	1.33	224x100	1.7	28	✓						
5	3T Verio	None	Axial/Coro /Sagg	420/380/380	4.31	9	1.33	224x100	1.7	28	✓						
6	3T Verio	None	Axial	420	4.31	9	1.33	224x100	1.9	28x5	✓						
7	3T Verio	Gadobutrol	Coronal	400	3.21	9	1.08	224x100	1.8	120	✓	✓	✓		✓	✓	✓
8	3T Verio	Gadobutrol	Coronal	400	3.21	9	1.08	224x100	1.9	120	✓	✓	✓		✓	✓	✓
9	3T Verio	Gadobutrol	Coronal	425	3.23	9	1.06	224x100	1.9	128	✓	✓	✓		✓	✓	✓
10	3T Verio	Gadobutrol	Coronal	400	3.06	9	1.07	224x100	1.8	128	✓	✓	✓		✓	✓	✓
11	3T Verio	Gadobutrol	Coronal	400	3.06	9	1.08	224x100	1.8	120	✓				✓	✓	✓
12	3T Verio	Gadobutrol	Coronal	400	3.23	9	1.08	224x100	1.8	128	✓	✓	✓		✓	✓	✓
13	3T Verio	Gadobutrol	Coronal	400	3.23	9	1.08	224x100	1.8	112	✓				✓	✓	✓
14	3T Verio	Gadobutrol	Coronal	400	3.23	9	1.08	224x100	1.8	128	✓				✓	✓	✓
15	3T Verio	Gadobutrol	Coronal	400	3.2	9	1.1	224x100	1.9	128	✓				✓	✓	✓
16	3T Verio	Gadobutrol	Coronal	380	3.23	9	1.04	192x100	2	128	✓				✓	✓	✓
17	3T Verio	Gadobutrol	Coronal	420	3.23	9	1.07	224x100	1.9	120	✓	✓	✓		✓	✓	✓
18	3T Verio	Gadobutrol	Coronal	440	3.23	9	1.05	224x100	1.96	104	✓	✓	✓		✓	✓	✓
19	3T Verio	Gadobutrol	Coronal	400	3.23	9	1.08	224x100	1.8	120	✓	✓	✓		✓	✓	✓
20	3T Verio	Gadobutrol	Coronal	400	3.23	9	1.08	224x100	1.8	144	✓				✓	✓	✓
21	3T Verio	Gadobutrol	Coronal	400	3.23	9	1.08	224x100	1.8	128	✓				✓	✓	✓
22	3T Verio	Gadobutrol	Coronal	400	3.23	9	1.08	224x100	1.8	144	✓	✓	✓		✓	✓	✓

23	3T Verio	Gadobutrol	Coronal	415	3.23	9	1.07	224x100	1.85	128	✓	✓	✓		✓	✓	✓
24	3T Verio	Gadobutrol	Coronal	400	3.23	9	1.08	224x100	1.8	128	✓	✓	✓		✓	✓	✓
25	3T Verio	Gadobutrol	Coronal	385	3.23	9	1.06	224x100	1.94	104	✓	✓	✓		✓	✓	✓
26	3T Verio	Gadobutrol	Coronal	400	3.23	9	1.08	224x100	1.8	120	✓	✓	✓		✓	✓	✓
27	3T Verio	Gadobutrol	Coronal	420	3.23	9	1.07	224x100	1.8	120	✓	✓	✓		✓	✓	✓
28	3T Verio	Gadobutrol	Coronal	437	3.23	9	1.05	224x100	1.95	104	✓	✓	✓		✓	✓	✓
29	3T Verio	Gadobutrol	Coronal	400	3.23	9	1.08	224x100	1.8	120	✓	✓	✓		✓	✓	✓
30	3T Verio	Gadobutrol	Coronal	400	3.23	9	1.08	224x100	1.8	120	✓	✓	✓		✓	✓	✓
31	3T Verio	Gadobutrol	Coronal	400	3.23	9	1.08	224x100	1.8	112	✓	✓	✓		✓	✓	✓
32	3T Verio	Gadobutrol	Coronal	400	3.23	9	1.08	224x100	1.8	120	✓	✓	✓		✓	✓	✓
33	3T Verio	Gadobutrol	Coronal	400	3.23	9	1.08	224x100	1.8	120	✓	✓	✓		✓	✓	✓
34	3T Verio	Gadobutrol	Coronal	400	3.23	9	1.08	224x100	1.8	112	✓	✓	✓	✓	✓	✓	✓
35	3T Verio	Gadobutrol	Coronal	400	3.23	9	1.08	224x100	1.8	120	✓	✓	✓	✓	✓	✓	✓
36	3T Verio	Gadobutrol	Coronal	400	3.23	9	1.08	224x100	1.8	120	✓	✓	✓	✓	✓	✓	✓
37	3T Verio	Gadobutrol	Coronal	400	3.23	9	1.08	224x100	1.8	120	✓	✓	✓	✓	✓	✓	✓
38	3T Prisma	Gadobutrol	Coronal	400	2.83	9	1.03	224x100	1.8	120	✓	✓	✓	✓	✓	✓	✓
39	3T Prisma	Gadobutrol	Coronal	400	2.83	9	1.03	224x100	1.8	120	✓	✓	✓	✓	✓	✓	✓
40	3T Prisma	Gadobutrol	Coronal	400	2.83	9	1.03	224x100	1.8	128	✓	✓	✓	✓	✓	✓	✓
41	3T Prisma	Gadobutrol	Coronal	400	2.83	9	1.03	224x100	1.8	128	✓	✓	✓	✓	✓	✓	✓
42	3T Prisma	Gadobutrol	Coronal	400	2.83	9	1.03	224x100	1.8	120	✓	✓	✓	✓	✓	✓	✓
43	3T Prisma	Gadobutrol	Coronal	400	2.83	9	1.03	224x100	1.8	128	✓	✓	✓	✓	✓	✓	✓
44	3T Prisma	None	Coronal	420	2.83	9	0.99	224x100	2.2	112	✓						
45	3T Prisma	Gadobutrol	Coronal	400	2.83	9	1.03	224x100	1.8	120	✓	✓	✓	✓	✓	✓	✓
46	3T Prisma	Gadobutrol	Coronal	400	2.83	9	1.03	224x100	1.8	112	✓	✓	✓	✓	✓	✓	✓
47	3T Prisma	Gadobutrol	Coronal	400	2.83	9	1.03	224x100	1.8	120	✓	✓	✓	✓	✓	✓	✓
48	3T Prisma	Gadobutrol	Coronal	400	2.83	9	1.03	224x100	1.8	120	✓	✓	✓	✓	✓	✓	✓
49	3T Prisma	Gadobutrol	Coronal	440	2.8	9	1	224x100	2	120	✓	✓	✓	✓	✓	✓	✓

50	3T Prisma	Gadobutrol	Coronal	400	2.8	9	1	224x100	1.8	120	✓	✓	✓	✓	✓	✓	✓
51	3T Prisma	Gadobutrol	Coronal	420	2.8	9	1	224x100	1.9	128	✓	✓	✓	✓	✓	✓	✓
52	3T Prisma	Gadobutrol	Coronal	400	2.8	9	1	224x100	1.8	120	✓	✓	✓	✓	✓	✓	✓
53	3T Prisma	Gadobutrol	Coronal	420	2.8	9	1	224x100	1.9	120	✓	✓	✓	✓	✓	✓	✓
54	3T Prisma	Gadobutrol	Coronal	400	2.8	9	1	224x100	1.8	120	✓	✓	✓	✓	✓	✓	✓
55	3T Prisma	Gadobutrol	Coronal	400	2.8	9	1	224x100	1.8	112	✓	✓	✓	✓	✓	✓	✓
56	3T Prisma	Gadobutrol	Coronal	400	2.8	9	1	224x100	1.8	112	✓	✓	✓	✓	✓	✓	✓
57	3T Prisma	Gadobutrol	Coronal	400	2.8	9	1	224x100	1.8	120	✓	✓	✓	✓	✓	✓	✓
58	3T Prisma	Gadobutrol	Coronal	400	2.8	9	1	224x100	1.8	128	✓	✓	✓	✓	✓	✓	✓
59	3T Prisma	Gadobutrol	Coronal	400	2.8	9	1	224x100	1.8	120	✓	✓	✓	✓	✓	✓	✓
60	3T Prisma	Gadobutrol	Coronal	400	2.8	9	1	224x100	1.8	112	✓	✓	✓	✓	✓	✓	✓
61	3T Prisma	Gadobutrol	Coronal	400	2.8	9	1	224x100	1.8	120	✓	✓	✓	✓	✓	✓	✓
62	3T Prisma	Gadobutrol	Coronal	420	2.8	9	1	224x100	1.9	120	✓	✓	✓	✓	✓	✓	✓
63	3T Prisma	Gadobutrol	Coronal	400	2.8	9	1	224x100	1.8	112	✓	✓	✓	✓	✓	✓	✓
64	3T Prisma	Gadobutrol	Coronal	400	2.8	9	1	224x100	1.8	120	✓	✓	✓	✓	✓	✓	✓
65	3T Prisma	Gadobutrol	Coronal	400	2.8	9	1	224x100	1.8	120	✓	✓	✓	✓	✓	✓	✓
66	3T Prisma	Gadobutrol	Coronal	400	2.8	9	1	224x100	1.8	120	✓	✓	✓	✓	✓	✓	✓

MRI; Magnetic Resonance Imaging, Coro; Coronal, Sagg; Saggital, FOV; Field of View, 3T; 3-Tesla

3.3.6 Imaging Analysis

3.3.6.1 CT Analysis

CT scans were anonymised and analysed in a blinded fashion by two experienced consultant thoracic radiologists (Dr Gordon Cowell (GWC) and Dr David Stobo (DBS), using VuePACS version 11.4 (Carestream Health Inc., Rochester, NY). Each made a subjective diagnosis of pleural malignancy or benignity based on the presence or absence of established morphological features of PM (81). Briefly, this was nodular pleural thickening, pleural thickening >1cm, mediastinal pleural thickening, enhancing pleural lesions, fissural nodularity, pleural mass or infiltration of mediastinal structures, chest wall or diaphragm. A third, independent, thoracic radiologist (Dr Colin Noble (CN)) provided a third opinion to resolve any discordant cases.

3.3.6.2 MRI Analysis: Morphology

MRI scans were anonymised and analysed for morphological features of pleural malignancy in a blinded fashion by the same consultant thoracic radiologists who performed the CT analyses. The presence or absence of established morphological features of PM, (76) including nodular or mediastinal pleural thickening, fissural nodularity, pleural thickening >1cm and chest wall or diaphragmatic invasion, was used to classify patients. Dr Colin Noble again provided a third thoracic radiology opinion, providing a casting classification in discordant cases. All radiologists were blinded to the perfusion MRI and other clinical data.

3.3.6.3 MRI Analysis: Perfusion Data

Perfusion analyses were performed by myself (ST) and Dr Kevin Blyth (KGB) (consultant respiratory physician) using OsiriX for Mac v5.8, 32-bit (Pixmeo, Bernex, Switzerland). I was designated the 'primary' operator and my results were used for diagnostic analyses. KGB was designated the secondary operator, whose results were used to assess inter-observer agreement only. Intra-observer agreement was assessed by the primary operator repeating a random selection of analyses after a 2-month interval. All images were anonymised, assigned a random study number and analysed in batches. Both operators were blinded to

clinical and histological data. Each reviewed the entire MRI exam at each time point. Each defined up to 15 Regions of Interest (ROI), using a track-ball mouse and cursor, on what they felt were representative areas of disease affecting the pleura.

The pleura was defined as the visible structure running parallel with, and medial to, the rib-cage and immediately contiguous with either aerated lung, pleural fluid or air (depending on the presence of a fully expanded lung, pleural effusion or pneumothorax, respectively at the imaged location). Care was taken to constrain the boundaries of the ROI to the parietal pleura, where possible, accepting that in cases where there was no pleural fluid or air separating parietal and visceral pleura this could not be guaranteed. Once the required number of ROI (minimum of 5 in patients with macro-nodular disease and 15 in patients with non-nodular disease) was defined on the 4.5-minute post-contrast scan, these were electronically copied and pasted onto all other scans. Each scan was then visually assessed and each operator was asked to make minor adjustments to the position of each ROI to account for inconsistencies in the patient's breath-hold and chest wall position, where required.

In patients with macro-nodular pleural disease, the positioning of the Pleural ROIs was based entirely on the operator's suspicion of pleural tumour at that site (which in turn was based on the presence of a nodular mass lesion or an area of thickened pleural thickening exceeding 10 mm, see Figure 3.3 for an example. If large mass lesions or areas of contiguous pleural thickening were present, care was taken to ensure that ROIs within a single area were separated by at least 1 slice. Each operator was asked to place up to 15 ROIs on areas of suspected parietal pleural tumour in these case.

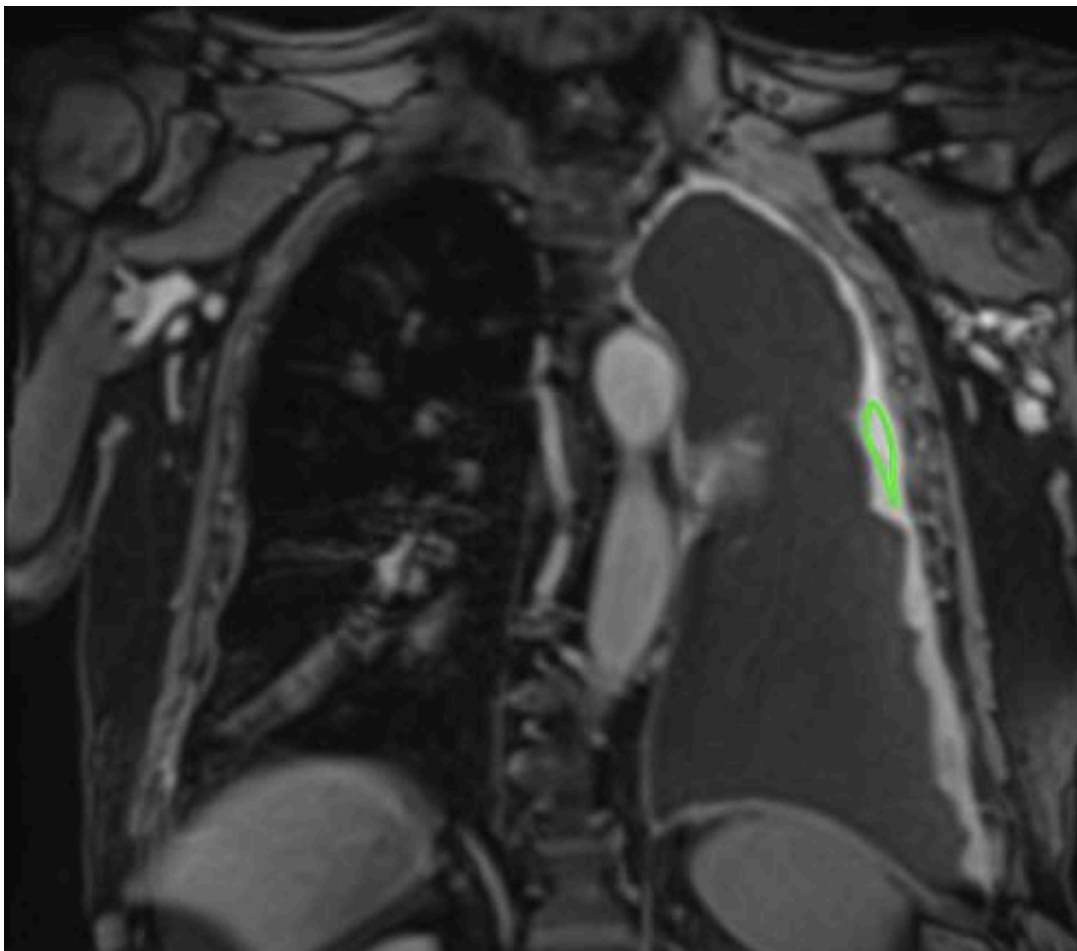


Figure 3.3 Example of ROI placed on macro-nodular pleural disease at contrast-enhanced MRI

In the absence of macro-nodular pleural disease or pleural thickening greater than 10mm, it was not possible to visually select the most suitable location for ROI definition. Therefore, an alternative and consistent method of comprehensively sampling the imaging characteristics of the parietal pleura in these cases was defined. This involved placement of 15 ROIs at anatomically similar locations in each patient. These 15 ROIs were distributed across 3 coronal pleural slices which were defined as follows (also see Figure 3.4):

1. Midpoint slice: slice with the largest continuous length of parietal pleura measured cranio-caudally. 9 ROIs were evenly distributed from cupula to costophrenic recess.
2. Anterior slice: slice half-way from the midpoint slice to the most anterior slice where parietal pleura is identifiable. 3 ROIs were evenly distributed.
3. Posterior slice: slice half-way from the midpoint slice to the most posterior slice where parietal pleura is identifiable. 3 ROIs were evenly distributed.

The ROI sampling methodology was chosen to mirror thoracoscopic sampling, where biopsies are taken of obvious costal pleural tumour where present and in the absence of obvious pleural tumour, random biopsies of representative parietal pleura are taken.

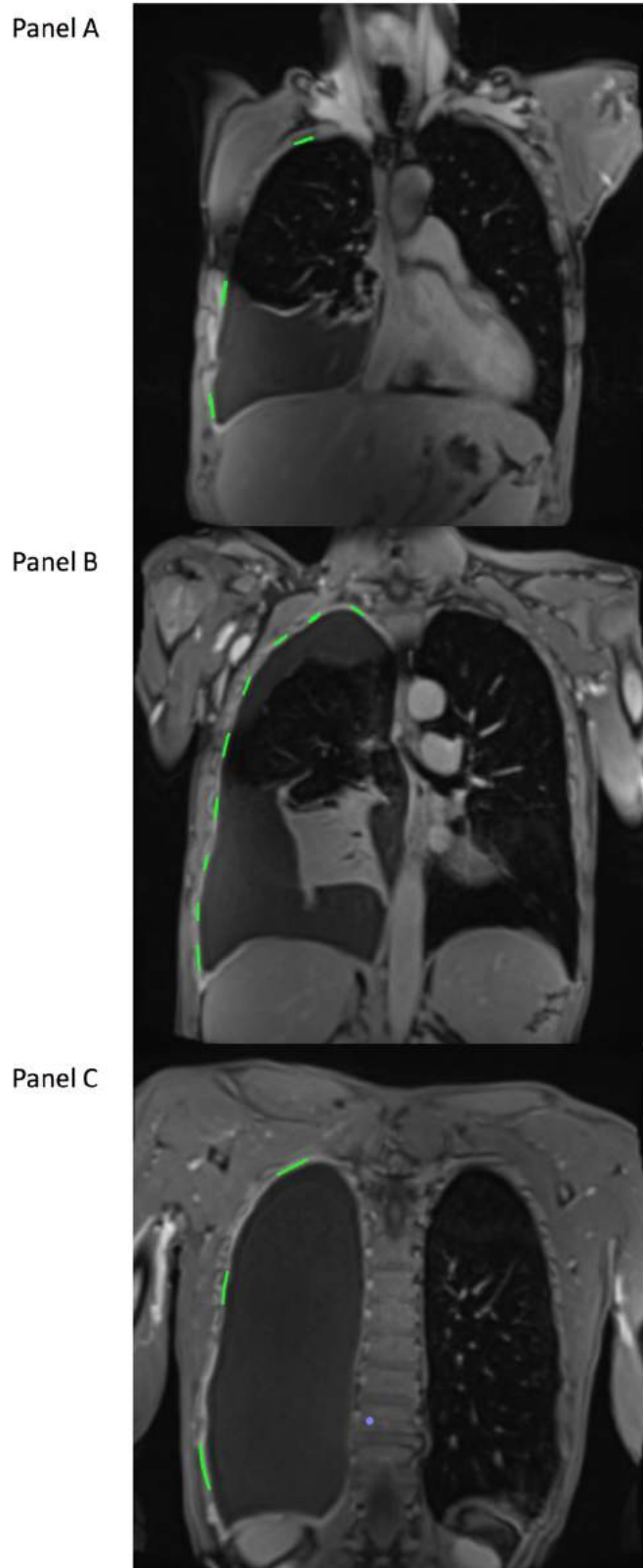


Figure 3.4 Example of ROI placed on representative pleura in the absence of macro-nodular disease at contrast-enhanced MRI

Signal intensity (SI) was measured by the software within each ROI at each time point, allowing ROI SI/time plots to be generated (see Figure 3.5 for examples). A Mean SI/time plot was also generated for each patient, based on the mean SI measured in all ROI at each time point (see Figure 3.6). All signal intensities were corrected for background signal noise using SI measured in a ROI placed in extra-corporeal air (see Figure 3.7). The time point that SI peaked in each ROI and that Mean SI peaked in each patient was recorded. This allowed computation of ROI SI gradient (ROISIG) for each ROI, and Mean SI gradient (MSIG) for each patient. SI gradient was calculated using the formula:

$$(\text{mean or ROI}) \text{ SI gradient} = (\text{peak SI} - \text{baseline SI}) / \text{time to peak SI}$$

MSIG was used to summarize ECE characteristics of each patient. ROISIG was used in a post-hoc analysis to define the characteristics of each ROI.

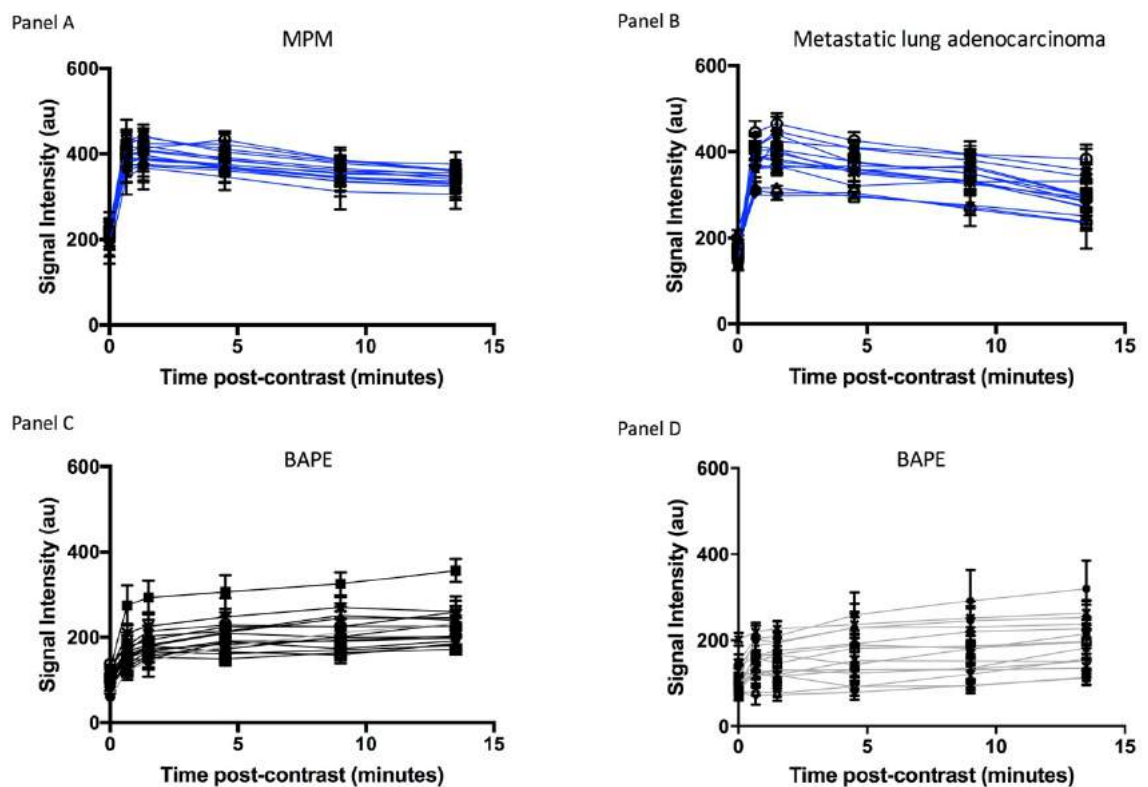


Figure 3.5 Examples of signal intensity (SI)/time curves measured from up to 15 ROI placed on representative pleura at contrast-enhanced MRI

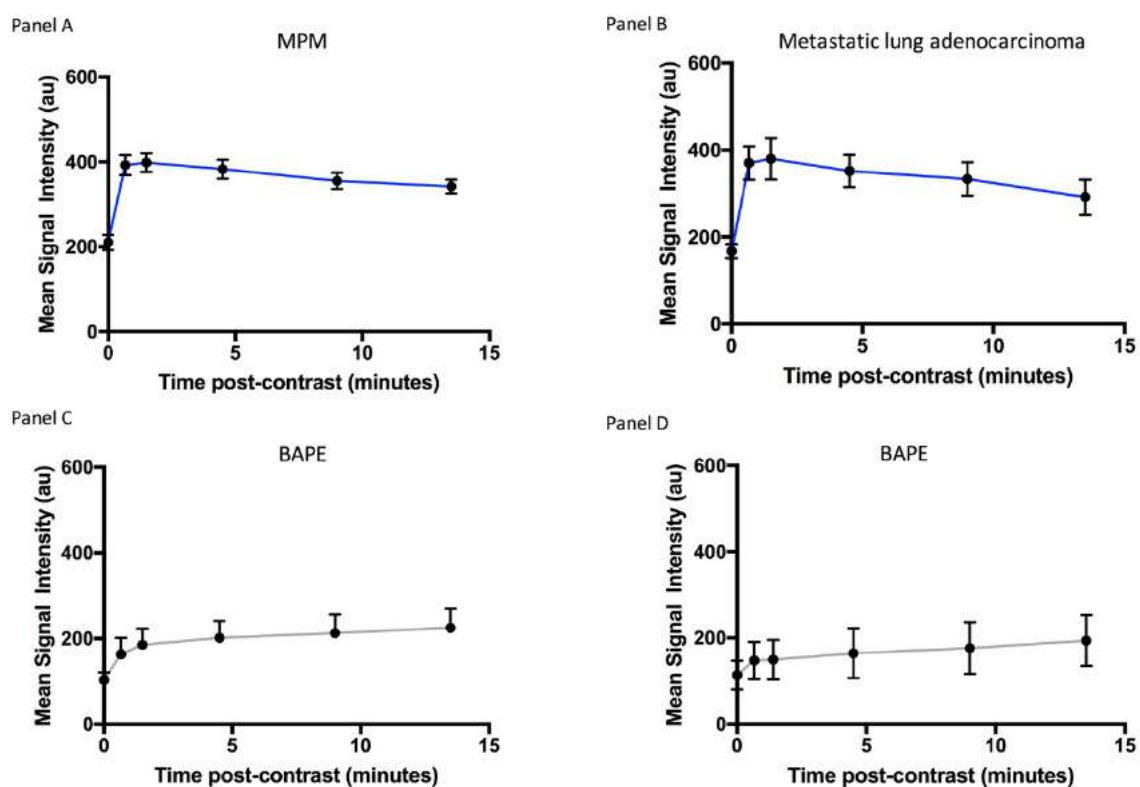


Figure 3.6 Example of mean signal intensity (SI)/time curves summarising ROI SI/time curves for individual patients at contrast-enhanced MRI

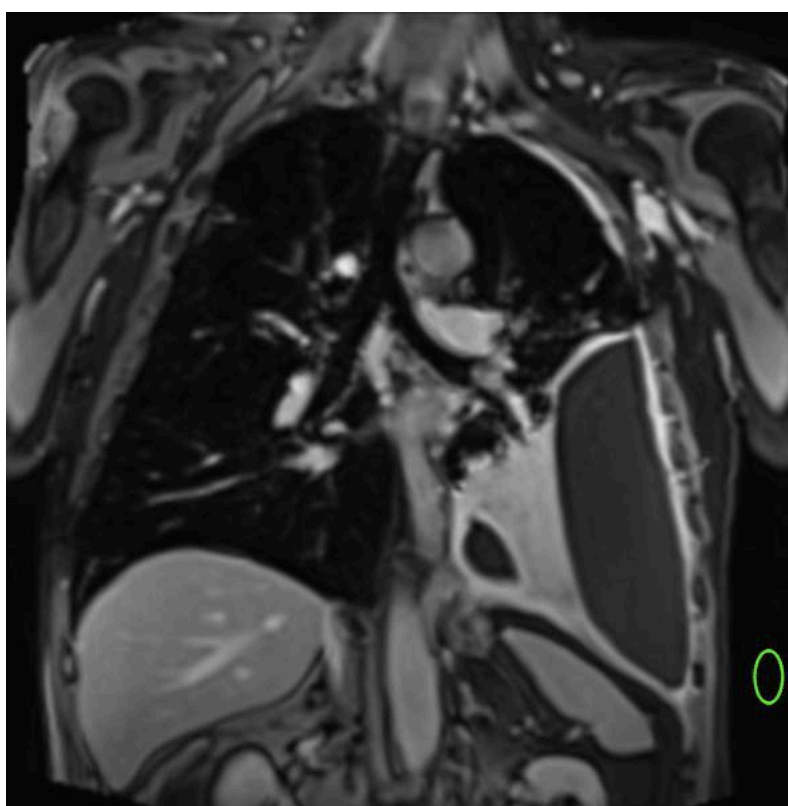


Figure 3.7 Contrast-enhanced, T1-weighted coronal MR image with a ROI placed on extra-corporeal air, used to correct for background signal noise

Early Contrast Enhancement (ECE)

To define a contrast enhancement pattern typical of malignancy the ROI and Mean SI/time curves recorded in the first 6 patients with nodular pleural disease typical of malignancy were reviewed by myself and Dr Blyth, who were blinded to the radiologist's morphological diagnoses. This pattern was termed Early Contrast Enhancement (ECE). The presence or absence of ECE in each patient's ROI SI/time curves was used to classify the patient as malignant or benign respectively. This diagnostic criterion was chosen to mirror interpretation of pleural biopsy results, where all pleural biopsy samples are reviewed by a pathologist and identification of the presence of malignant features in any one pleural biopsy will result in a diagnosis of pleural malignancy, even if all other submitted biopsy samples demonstrate benign features only.

3.3.6.4 Post-hoc Analyses regarding ROI Signal Intensity Gradient (ROISIG)

Evidence of heterogeneous contrast enhancement in some patients with pleural malignancy prompted a post-hoc analysis to assess the contribution of benign (ECE-negative) ROI to the discriminant performance of ECE. We interpreted this as evidence of non-contiguous disease, commonly observed at thoracoscopy. Receiver Operator Characteristic (ROC) curves were plotted based on ROISIG for 1) all ROI in malignant cases relative to patients with benign disease and 2) only ECE-positive ROI in patients with malignancy relative to ROIs in benign cases.

3.3.6.5 Combining MRI morphology with ECE

To assess the diagnostic performance of combined MRI morphology and ECE assessment, a two-step approach was adopted.

1. MRI morphology was examined first. If the patient has morphological features of PM as previously described then the patient was classified as malignant, regardless of their ECE findings
2. If MRI morphology was found to be benign, then ECE results were examined. If ECE was present, then the patient was classified as malignant

3.3.7 Assessment of Tissue Microvessel Density

Paraffin-embedded pleural tissue biopsies obtained at thoracoscopy were examined by a Consultant Lung Pathologist (Dr. Craig Dick) to confirm that the tissue was representative of the histological diagnosis. Sections were cut on a digital microtome (4µm thickness) and stained with CD34 and Factor VIII immunostains (Leica Biosystems, UK, 1:50 and 1:200 dilution, respectively), see Figure 3.8 (Panels A and B respectively). Slides were digitized using Hamamatsu NDP (Hamamatsu, Welwyn Garden City). Microvessel density with lumen in the entire tissue specimen was measured using quantitative image analysis software (Leica Biosystems, U.K.), see Figure 3.8 (Panels C and D respectively), by either a pathologist (Dr. Catherine Humphreys) or a pathology research technician (Ms. Clare Orange).

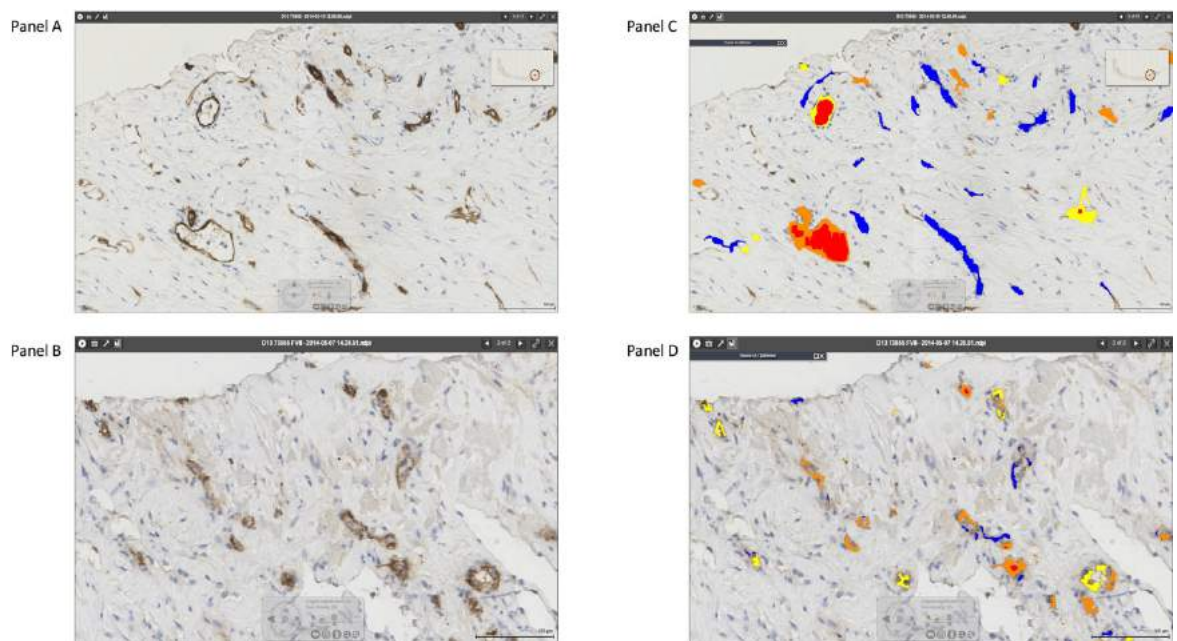


Figure 3.8 Paraffin-embedded representative pleural biopsies stained with CD34 (Panel A) and Factor VIII (Panel B) immunostain (highlighting vessels as brown). Computer software was used to detect the immunostain (Panels C and D) to calculate Microvessel Density (highlighting vessels in different colours depending on vessel size and presence/absence of a vessel lumen)

3.3.8 Statistical Analysis

Data distribution was assessed using histograms and D'Agostino-Pearson normality test. Normally distributed data are described by mean (\pm SD) and non-normally distributed data are described by median (inter-quartile range). 2 x 2 contingency tables were used to calculate the sensitivity, specificity, negative and positive predictive values of ECE, CT morphology and MRI morphology for pleural malignancy. McNemar's test was used to compare the sensitivity and specificity between ECE, CT morphology, MRI morphology and combined MRI morphology-ECE methodologies. Cohen's Kappa statistic was used to assess inter- and intra-observer agreement.

The discriminant performance of ECE was further assessed by plotting ROC curves for 1) only ECE-positive ROI and 2) all ROI in malignant cases, relative to patients with benign disease. MSIG was used to summarize the ECE characteristics of each patient. Any difference between MSIG and MVD in patients with PM relative to those with benign pleural disease was compared using unpaired t-test for normally distributed data and the Mann-Whitney test for non-normally distributed data. MVD was correlated against MSIG using Spearman's rho test. A p value ≤ 0.05 was considered statistically significant in all tests. P values were adjusted to account for false discovery rate with multiple testing using R v3.4.0 (The R Foundation). All other statistical analyses were performed using Graphpad Prism v7 (San Diego, USA) and IBM SPSS Statistics v22.0 (IBM, New York, USA) for Mac.

3.4 RESULTS

3.4.1 Patient Demographics

118 patients were potentially eligible for the study, 66 were recruited to the study and 58 patients underwent contrast-enhanced MRI examination. 31/58 were diagnosed with MPM, all of whom had surplus tissue available and suitable for tissue vascularity measurements (see Figure 3.9).

51/58 (88%) were male and 39/58 (67%) asbestos-exposed. 9/58 (16%) had a history of previous malignancy and 13/58 (22%) had pleural plaque disease. Final

diagnoses are summarised in Table 3.3. 36/58 (62%) had a final diagnosis of PM. 31/36 (86%) were diagnosed with MPM, of whom 65% (n=20) had epithelioid MPM, 16% (n=5) sarcomatoid MPM, 13% (n=4) biphasic MPM and 6% (n=2) had MPM not otherwise specified (NOS). 5/36 (14%) were diagnosed with secondary pleural malignancy, of whom 60% (n=3) had metastatic breast cancer and 40% (n=2) had metastatic lung cancer.

22/58 (38%) of patients had a final diagnosis of benign pleural disease. Benign pleural diagnoses included BAPE (50%, n=11), tuberculous pleurisy (14%, n=3), fibrothorax (9%, n=2), rheumatoid pleurisy (9%, n=2), reactive effusion associated with lung cancer (4.5%, n=1), post-lobectomy effusion (4.5%, n=1), secondary to pulmonary thromboembolism (4.5%, n=1) and drug-related (4.5%, n=1).

Final diagnoses were based on histology from LAT in 46/58 (79%), VATS in 7/58 (12%) and image-guided biopsy in 4/58 (7%). 1/58 (2%) were diagnosed based on radiology, MDT consensus and interval follow-up. All MPM cases were staged at regional MDT as I in 20/31 (64.5%), II in 0/31 (0%), III in 9/31 (29%) and IV in 2/31 (6.5%). Median overall survival for patients with PM was 20 months. Mean follow-up for patients with a benign pleural diagnosis was 20 (9) months.

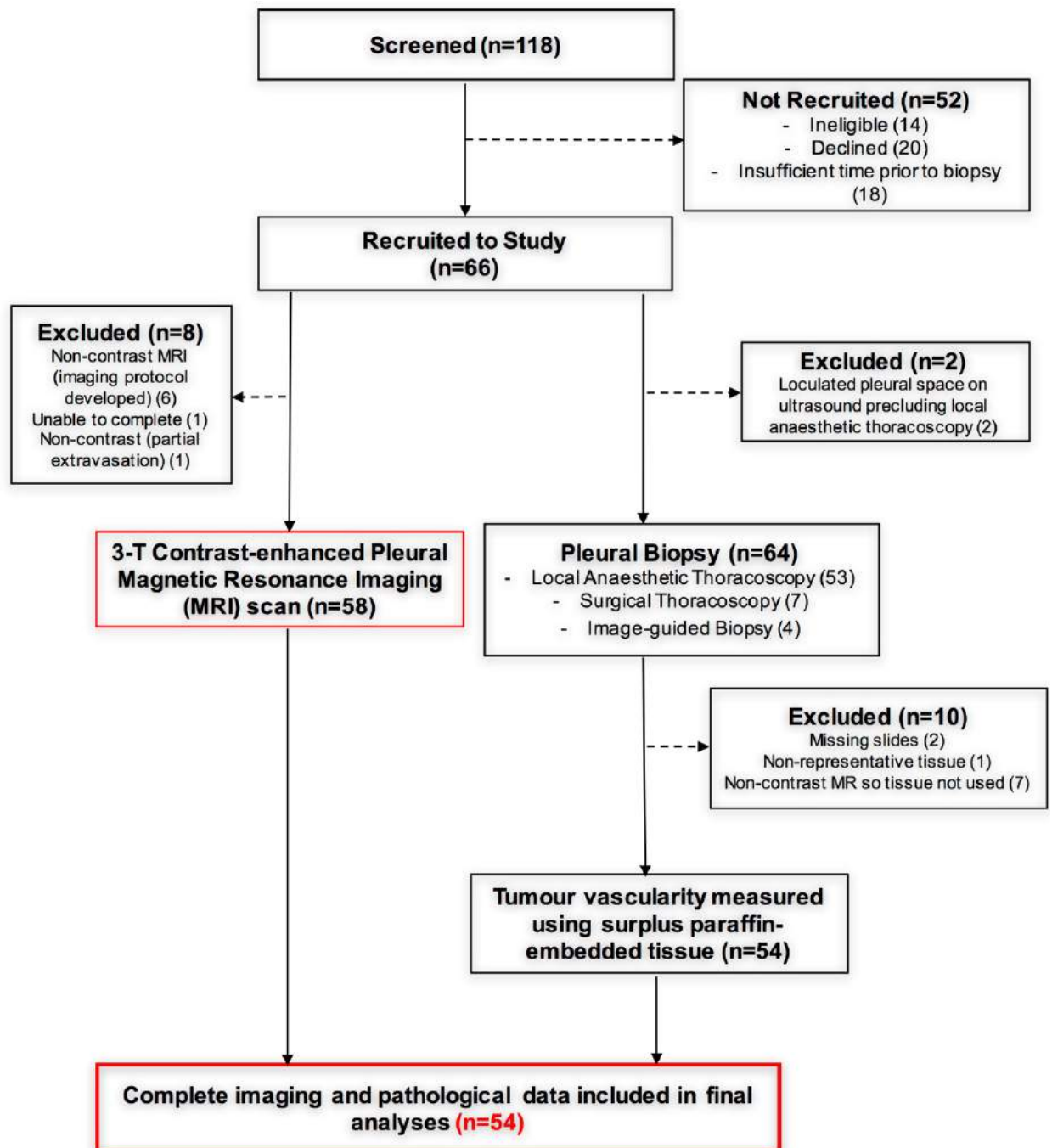


Figure 3.9 Study flowchart of patients recruited to the MRI sub-study in the Early Contrast Enhancement study

Table 3.3. Summary of pleural diagnoses in 58 patients with suspected malignancy recruited to the Early Contrast Enhancement study

Pleural Malignancy (n=36, 62%)	Benign Disease (n=22, 38%)
Mesothelioma (n=31, 86%)	BAPE (n=11, 50%)
Epithelioid (n=20, 65%)	Reactive assoc. with Lung Cancer (n=1, 4.5%)
Sarcomatoid (n=5, 16%)	
Biphasic (n=4, 13%)	Fibrothorax (n=2, 9%)
Mesothelioma NOS (n=2, 6%)	Tuberculous Pleurisy (n=3, 14%,)
Secondary Malignancies (n=5, 14%)	Pulmonary Thromboembolism (n=1, 4.5%)
Lung Cancer (n=2, 40%)	Drug-related (n=1, 4.5%)
Breast Cancer (n=3, 60%)	Post-lobectomy (n=1, 4.5%)
	Rheumatoid pleurisy (n=2, 9%)
BAPE; Benign Asbestos-related Pleural Effusion	

3.4.2 Imaging results

In all patients, MRI was performed prior to pleural biopsy (median 1 (1 - 7) days) and after CT (median 20 (13 - 34) days). All imaging analyses were confined to the 59 patients who had contrast-enhanced MRI scans acquired. 49/58 (84%) patients had pleural thickening <10mm. Median pleural thickness for all patients 5mm (IQR 4 - 7mm)), 47/58 (81%) lacked gross tumour nodules.

3.4.2.1 CT Morphology

Using CT morphology, 24/36 (67%) patients were correctly classified as PM (see Table 3.4). The majority of false negative cases had MPM (11/12 (92%)). All of these patients had early (IMIG Stage I) MPM. The single remaining false negative case had metastatic breast cancer.

15/22 (68%) patients were correctly identified as having benign pleural disease (see Table 3.5). The false positive cases had BAPE (n=2), tuberculous (TB) pleurisy (n=2), haemothorax (n=1), rheumatoid pleurisy (n=1) and reactive effusion secondary to underlying lung cancer (n=1).

3.4.2.2 MRI Morphology

MR morphology correctly classified 28/36 (78%) patients with PM (see Table 3.4). The majority of false negative cases had MPM (7/8 (87.5%)). 86% (n=6) of these cases had early stage (IMIG Stage I) MPM. The single remaining false negative case had metastatic breast cancer.

17/22 (77%) patients were correctly identified as having benign pleural disease (see Table 3.5). The false positive cases had BAPE (n=1), TB pleurisy (n=2), rheumatoid pleurisy (n=1) and reactive effusion secondary to underlying lung cancer (n=1).

3.4.2.3 Early Contrast Enhancement

The mean number of ROI defined was 14 (3) per patient. The average time taken to perform ROI placement and ECE calculations was 14 (3.5) minutes.

An early peak in SI (occurring at or before 4.5 minutes (270 seconds)) was identified in 6/6 mean SI/time curves and 58/62 ROI SI/time curves in the preliminary cohort of 6 patients with obvious nodular pleural disease (see Figure 3.10 (Panels B and C) for examples). This curve shape was defined as being typical of malignancy and termed Early Contrast Enhancement (ECE). The ROI SI/time curves in the remaining patients were then reviewed. ECE was reported to be present, and the patient classified as Malignant, if at least one ROI SI/time curve demonstrated a peak in SI at, or before, 4.5 minutes, see Figure 3.10 (Panels E and F) for examples). If ECE was not identified in any ROI SI/time curve the patient was classified as benign (see Figure 3.10 (Panels G and H) for examples).

ECE was demonstrated in 92% (33/36) of patients with PM (see Table 3.4). All three false negatives had MPM, two were diagnosed with Sarcomatoid MPM (IMIG stage I and IV respectively) and one patient was diagnosed with Mesothelioma NOS (IMIG stage I) at pleural biopsy. Both false negative cases with Sarcomatoid MPM were accurately classified as malignant based on CT and MRI morphology.

Two cases of Epithelioid MPM were initially diagnosed with BAPE at LAT but reclassified as Epithelioid MPM after developing progressive pleural thickening on interval CT follow-up and undergoing repeat pleural biopsies several months later. In both cases, the final diagnosis of malignancy was consistent with the initial positive ECE result. Both of these cases were classified as benign based on MRI morphology and one of the cases was classified as benign based on CT morphology.

ECE was absent in 68% (15/22) patients with benign pleural disease (see Table 3.5). The false positive cases had TB pleurisy (2/7), BAPE (2/7), rheumatoid pleurisy (1/7), PTE (1/7) and eosinophilic pleuritis secondary to drugs (1/7).

3.4.2.4 Combined MRI Morphology and ECE Assessment

Combined MRI morphology and ECE assessment correctly identified 35/36 (97%) patients with PM. The false negative case had MPM. It did however result in an increased number of false positives. There were 10/22 (45%) false positives following combined assessment, which included TB pleurisy (n=2), BAPE (n=3),

rheumatoid pleurisy (n=2), drug-related (n=1), PTE (n=1) and reactive effusion secondary to underlying lung cancer (n=1).

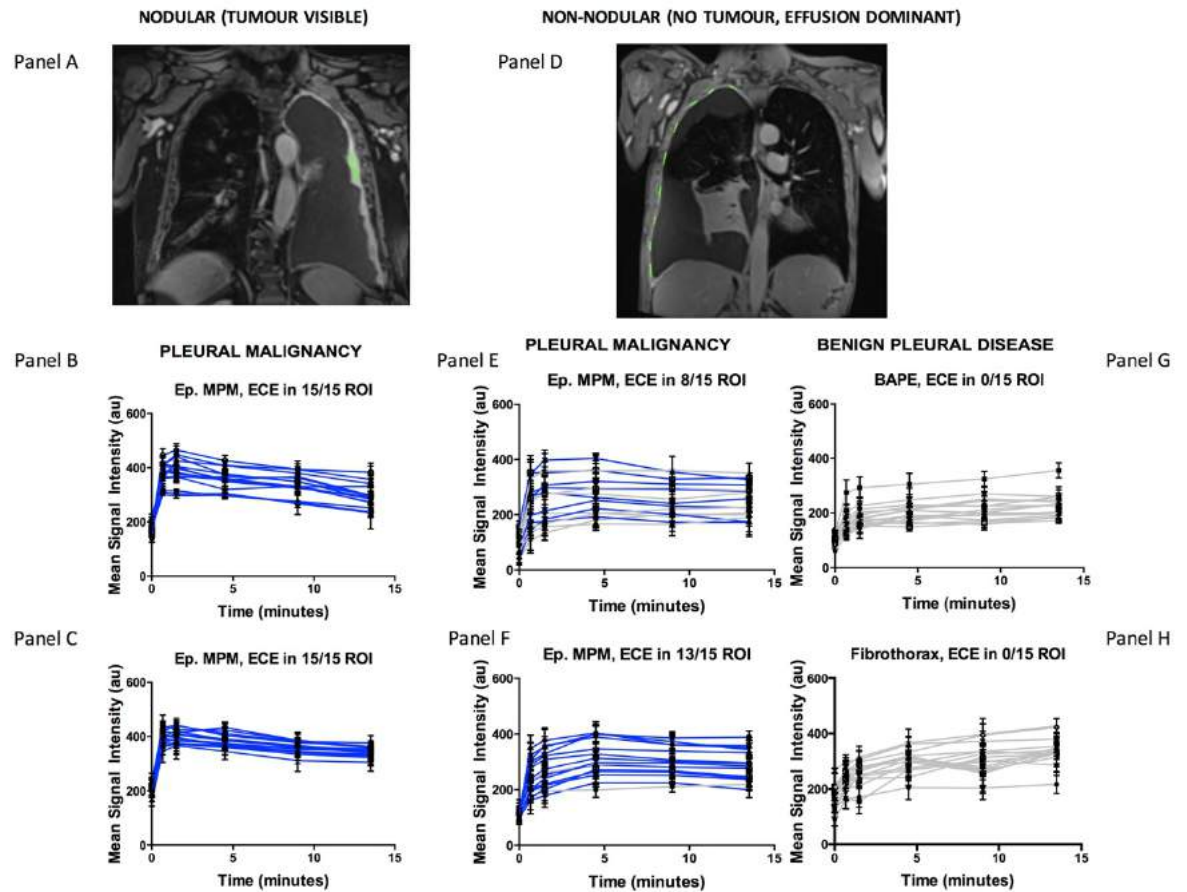


Figure 3.10 Contrast-enhanced, coronal T1-weighted MR images and ROI signal intensity/time curves in patients with obvious macro-nodular disease (Panel A) demonstrating ECE (Panels B - C), in patients with effusion-dominant, low volume pleural disease (Panel D) but at least one ROI demonstrating ECE (Panels E - F) and where no single ROI demonstrated ECE (Panels G - H)

Table 3.4 Demographics, diagnostics and imaging results in 58 patients with suspected pleural malignancy (PM) who underwent contrast-enhanced MRI for ECE assessment, contrast-enhanced CT scanning and pleural biopsy. 36/58 were diagnosed with PM, 23/58 with benign pleural disease. False negative (*) and false positive (†) results are highlighted.

Malignant Cases							
Case No.	Age (yrs)	Sex	Diagnosis	Disease Stage	CT Morphology	MRI Morphology	MRI-ECE
7	64	♂	Epithelioid MPM	I	B*	M	M
9	73	♂	Metastatic lung	IV	M	M	M
11	72	♂	Epithelioid MPM	I	M	M	M
14	81	♂	Sarcomatoid MPM	III	M	M	M
16	85	♂	Epithelioid MPM	I	M	M	M
17	64	♂	Sarcomatoid MPM	I	B*	M	M
19	72	♂	Epithelioid MPM	III	M	B*	M
20	78	♂	Epithelioid MPM	III	M	M	M
21	81	♂	Biphasic MPM	I	M	M	M
23	77	♂	Epithelioid MPM	III	M	M	M
24	66	♂	Epithelioid MPM	III	M	M	M
25	79	♂	Sarcomatoid MPM	I	M	M	B*
28	83	♂	Epithelioid MPM	III	M	M	M
29	76	♀	Metastatic breast	IV	B*	B*	M
30	74	♂	Epithelioid MPM	I	M	M	M

31	70	♀	Metastatic breast	IV	M	M	M
32	80	♂	Sarcomatoid MPM	IV	M	M	M
35	78	♂	Epithelioid MPM	I	M	M	M
37	66	♀	Epithelioid MPM	I	B*	B*	M
39	83	♂	Biphasic MPM	III	M	M	M
41	61	♂	Sarcomatoid MPM	IV	M	M	B*
42	72	♂	Biphasic MPM	III	M	M	M
43	82	♂	Epithelioid MPM	I	B*	M	M
46	76	♂	Mesothelioma	I	B*	B*	B*
47	85	♂	Epithelioid MPM	I	B*	B*	M
48	83	♂	Biphasic MPM	I	M	M	M
49	72	♂	Epithelioid MPM	I	B*	M	M
52	82	♂	Epithelioid MPM	I	M	M	M
54	56	♂	Metastatic lung	IV	M	M	M
55	85	♀	Epithelioid MPM	I	B*	M	M
56	84	♀	Epithelioid MPM	I	B*	B*	M
57	75	♂	Epithelioid MPM	I	B*	B*	M
58	82	♂	Mesothelioma	I	B*	B*	M
61	76	♂	Epithelioid MPM	III	M	M	M
63	63	♂	Metastatic lung	IV	M	M	M
65	67	♂	Epithelioid MPM	I	M	M	M

MRI; Magnetic Resonance Imaging, CT; Computed Tomography, ECE; Early Contrast Enhancement, MPM; Malignant Pleural Mesothelioma, B; Benign, M; Malignant, N/A; Not Appropriate

Table 3.5 Demographics, diagnostics and imaging results in 58 patients with suspected pleural malignancy (PM) who underwent contrast-enhanced MRI for ECE assessment, contrast-enhanced CT scanning and pleural biopsy. 36/58 were diagnosed with PM, 23/58 with benign pleural disease. False negative (*) and false positive (†) results are highlighted.

Benign Cases							
Case No.	Age (yrs)	Sex	Diagnosis	Disease Stage	CT Morphology	MRI Morphology	MRI-ECE
7	82	♂	BAPE	N/A	B	M†	B
9	85	♂	BAPE	N/A	M†	B	B
11	71	♂	Rheumatoid pleurisy	N/A	M†	M†	B
12	80	♂	Haemothorax	N/A	B	B	B
15	64	♂	BAPE	N/A	B	B	B
18	71	♂	BAPE	N/A	B	B	B
22	87	♂	BAPE	N/A	B	B	B
26	51	♂	TB	N/A	M†	M†	M†
27	76	♂	BAPE	N/A	B	B	B
33	79	♂	Haemothorax	N/A	M†	B	B
34	83	♀	PTE	N/A	B	B	M†
36	62	♂	Post-lobectomy change	N/A	B	B	B
38	69	♂	Rheumatoid pleurisy	N/A	B	B	M†
40	81	♂	BAPE	N/A	B	B	M†
45	76	♂	TB	N/A	M†	M†	M†
50	72	♂	BAPE	N/A	B	B	B
51	72	♂	BAPE	N/A	B	B	B

53	79	♂	BAPE	N/A	M†	B	M†
59	33	♀	TB	N/A	B	B	B
60	72	♂	Reactive effusion, underlying lung cancer	N/A	M†	M†	B
62	80	♂	Drug-related	N/A	B	B	M†
65	63	♂	BAPE	N/A	B	B	B

MRI; Magnetic Resonance Imaging, CT; Computed Tomography, ECE; Early Contrast Enhancement, BAPE; Benign Asbestos Pleural Effusion, TB; Tuberculous pleurisy
B; Benign, M; Malignant, N/A; Not Appropriate

3.4.3 Overall Diagnostic Performance

The overall diagnostic performance of CT morphology, MRI morphology, ECE and combined MRI morphology and ECE are summarised in Table 3.6. Contingency tables used to generate this data are summarised in Table 3.7.

CT Morphology

Overall diagnostic performance of CT morphology was: sensitivity 56% (95% CI 37 - 72%), specificity 77% (95% CI 60 - 89%), positive predictive value 68% (95% CI 47 - 84%), negative predictive value 67% (95% CI 50 - 80%).

MRI Morphology

Overall diagnostic performance of MR morphology was sensitivity 68% (95% CI 48 - 83%), specificity 85% (95% CI 69 - 93%), positive predictive value 77% (95% CI 57 - 90%), negative predictive value 78% (95% CI 62 - 88%).

ECE

Overall diagnostic performance of ECE was: sensitivity 83% (95% CI 61 - 94%), specificity 83% (95% CI 68 - 91%), positive predictive value 68% (95% CI 47 - 84%), negative predictive value 92% (78 - 97%).

Combined MRI Morphology and ECE Assessment

Overall diagnostic performance of combined MRI morphology and ECE was: sensitivity 92% (95% CI 67 - 100%), specificity 78% (95% CI 64 - 87%), PPV 55% (95% CI 35 - 73%), NPV 97% (95% CI 86 - 100%).

Table 3.6 The diagnostic performance and reproducibility of CT morphology, MRI morphology and MRI-Early Contrast Enhancement (ECE) assessed in 58 patients with suspected Pleural Malignancy. Agreement was assessed using Cohen's Kappa statistic. Diagnostic performance between groups is compared by McNemar's test, adjusted for multiple comparisons. Statistically significant differences before and after adjustment are highlighted below

	CT Morphology	MRI Morphology	MRI-ECE	Combined MRI Morphology-ECE
Sensitivity	56%	68%	83%*	92%**
(95% CI)	(37 - 72%)	(48 - 83%)	(61 - 94%)	(67 - 100%)
Specificity	77%	85%	83%	78%
(95% CI)	(60 - 89%)	(69 - 93%)	(68 - 91%)	(64 - 87%)
PPV	68%	77%	68%	55%
(95% CI)	(47 - 84%)	(57 - 90%)	(47 - 84%)	(35 - 73%)
NPV	67%	78%	92%	97%
(95% CI)	(50 - 80%)	(62 - 88%)	(78 - 97%)	(86 - 100%)
Inter-observer Agreement	0.65	0.593	0.784	N/R
Intra-observer Agreement	N/R	N/R	0.864	N/R

*Unadjusted p value 0.022 but adjusted p value 0.066 (MRI-ECE vs. CT morphology)

**Unadjusted p value 0.016 but adjusted p value 0.66 (Combined MRI morphology and ECE assessment vs. MRI morphology). For all other comparisons p >0.05
CT; Computed Tomography, MRI; Magnetic Resonance Imaging, CI; Confidence Interval, PPV; Positive Predictive Value, NPV; Negative Predictive Value, N/R; Not Recorded

Table 3.7 2 x 2 Contingency tables describing results of Computed Tomography (CT) Morphology, Magnetic Resonance Imaging (MRI) Morphology, Early Contrast Enhancement (ECE) at MRI and Combined MRI Morphology-ECE assessment in 58/66 patients with suspected pleural malignancy

		Final Pleural Diagnosis	
		Malignant	Benign
CT morphology	Malignant	24	7
	Benign	12	15

		Final Pleural Diagnosis	
		Malignant	Benign
MRI morphology	Malignant	28	5
	Benign	8	17

		Final Pleural Diagnosis	
		Malignant	Benign
MRI ECE	Malignant	33	7
	Benign	3	15

		Final Pleural Diagnosis	
		Malignant	Benign
Combined MRI morphology-ECE	Malignant	35	10
	Benign	1	12

CT; Computed Tomography, MRI; Magnetic Resonance Imaging, ECE; Early Contrast Enhancement

3.4.4 Post-hoc Analyses regarding ROI Signal Intensity Gradient

A ROC curve plotted using only ROISIG data from ECE-positive ROI (n=273) demonstrated optimum sensitivity (90% (95% CI 86 - 94%)) and specificity (86% (95% CI 81 - 89%)) at a threshold of ROISIG >0.43 AU/sec (AUC 0.938, (95% CI 0.918 - 0.957), $p < 0.0001$, see Figure 3.11 (Panel A).

Using all ROISIG data (n=482), regardless of the presence or absence of ECE, a ROISIG >0.29 AU/sec provided optimum, but reduced sensitivity (71% (95% CI 67 - 75%)), specificity (68% (95% CI 63 - 73%)) and discriminatory performance (AUC 0.776 (95% CI 0.744 - 0.808), $p < 0.0001$, see Figure 3.11 (Panel B).

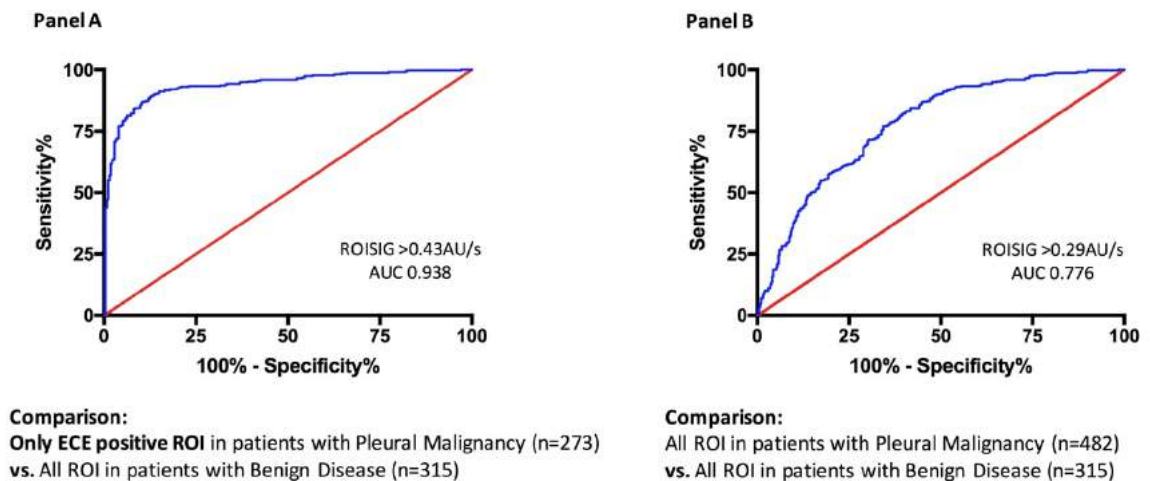


Figure 3.11 Receiver Operating Characteristic (ROC) curves of Region of Interest Signal Intensity Gradient (ROISIG) measured in 58 patients with suspected pleural malignancy (PM) using contrast-enhanced MRI. In Panel A, only ROI demonstrating Early Contrast Enhancement (ECE) in patients with PM are included and in Panel B, all ROI are included, including those who failed to demonstrate ECE, resulting in reduced discriminative performance

3.4.5 Mean Signal Intensity Gradient (MSIG)

Median MSIG was significantly higher in patients with PM (median 0.58 (0.27 - 0.88) AU/s) than those with benign pleural disease (median 0.2 (0.06 - 0.29) AU/s, $p < 0.0001$).

3.4.6 Reproducibility

CT Morphology

There were 10 discordant classifications between the thoracic radiologists using CT morphology (17%), see Table 3.8. Overall inter-observer agreement for CT morphology was $\kappa = 0.650$.

MRI Morphology

There were 11 discordant classifications between the thoracic radiologists using MRI morphology (19%), see Table 3.9. Overall inter-observer agreement for MRI morphology was $\kappa = 0.593$.

Early Contrast Enhancement

19/58 cases were reviewed by KGB for inter-observer agreement. Of the cases reviewed, there were 2 discordant classifications between ST and KGB (11%), see Table 3.10. Overall inter-observer agreement for ECE was $\kappa = 0.784$.

ECE was repeated by ST in 29/58 cases for intra-observer agreement. Of the cases repeated, there were 3 discordant classifications (10%), see Table 3.11. Overall inter-observer agreement for ECE was $\kappa = 0.864$.

Table 3.8 Discordant cases at CT Morphology Assessment by two thoracic radiologists. False negatives (*) and false positives (†) are highlighted

Patient No.	Age (yrs)	Sex	Diagnosis	Disease Stage	Observer 1 GWC	Observer 2 DBS
6	87	♂	BAPE	N/A	M†	B
19	79	♂	Haemothorax	N/A	M†	B
26	76	♂	TB	N/A	M†	B
27	82	♂	Epithelioid MPM	I	B*	M
28	61	♂	Sarcomatoid MPM	IV	M	B*
36	72	♂	BAPE	N/A	B	M†
38	79	♂	BAPE	N/A	B	M†
42	82	♂	Mesothelioma	I	M	B*
51	64	♂	Epithelioid MPM	I	M	B*
54	85	♂	BAPE	N/A	M†	B

CT; Computed Tomography, MPM; Malignant Pleural Mesothelioma, BAPE; Benign Asbestos Pleural Effusion, TB; Tuberculous pleurisy, B; Benign, M; Malignant, N/A; Not Appropriate

Table 3.9 Discordant cases at MRI Morphology Assessment by two thoracic radiologists. False negatives (*) and false positives (†) are highlighted

Patient No.	Age (yrs)	Sex	Diagnosis	Disease Stage	Observer 1 GWC	Observer 2 DBS
4	72	♂	Epithelioid MPM	III	B*	M
6	87	♂	BAPE	N/A	B	M†
19	79	♂	Haemothorax	N/A	M†	B
20	78	♂	Epithelioid MPM	I	B*	M
22	69	♂	Rheumatoid pleurisy	N/A	B	M†
28	61	♂	Sarcomatoid MPM	IV	B*	M
30	85	♂	Epithelioid MPM	I	M	B*
39	84	♀	Epithelioid MPM	I	M	B*
41	75	♂	Epithelioid MPM	I	B*	M
44	33	♀	TB	N/A	B	M†

MRI; Magnetic Resonance Imaging, MPM; Malignant Pleural Mesothelioma

BAPE; Benign Asbestos Pleural Effusion, TB; Tuberculous pleurisy
B; Benign, M; Malignant, N/A; Not Appropriate

Table 3.10 Discordant cases at MRI Early Contrast Enhancement by two respiratory physicians. False negatives (*) and false positives (†) are highlighted

Patient No.	Age (yrs)	Sex	Diagnosis	Disease Stage	Observer 1 ST	Observer 2 KGB
5	78	♂	Epithelioid MPM	III	M	B*
6	87	♂	BAPE	N/A	B	M†

MRI; Magnetic Resonance Imaging, MPM; Malignant Pleural Mesothelioma
 BAPE; Benign Asbestos Pleural Effusion, B; Benign, M; Malignant,
 N/A; Not Appropriate

Table 3.11 Discordant cases at MRI Early Contrast Enhancement at repeated (intra-observer) testing. False negatives (*) and false positives (†) are highlighted

Patient No.	Age (yrs)	Sex	Diagnosis	Disease Stage	Review 1 ST	Review 2 ST
24	81	♂	BAPE	N/A	B	M†
36	72	♂	BAPE	N/A	B	M†
41	75	♂	Epithelioid MPM	I	M	B*

MRI; Magnetic Resonance Imaging, MPM; Malignant Pleural Mesothelioma
 BAPE; Benign Asbestos Pleural Effusion, B; Benign, M; Malignant,
 N/A; Not Appropriate

3.4.7 Tissue Microvessel Density

There was no difference in tissue MVD between patients with PM and those with benign pleural disease using CD34 immunostaining (8.614×10^{-5} (8.393×10^{-5}) vessels/tissue pixel and 7.052×10^{-5} (5.655×10^{-5}) vessels/tissue pixel respectively, $p=0.53$, or using Factor VIII immunostaining (5.882×10^{-5} (4.877×10^{-5}) vessels/tissue pixel and 7.357×10^{-5} (5.349×10^{-5}) vessels/tissue pixel respectively, $p=0.29$.

3.4.8 Relationship between MRI Perfusion Data and Tissue Microvessel Density in patients with MPM

There was a modest but statistically significant positive correlation between MSIG and MVD with lumen using Factor VIII immunostain (r 0.4258, $p=0.02$) in patients with MPM (see Figure 3.12 (Panel A)). There was also a modest but statistically significant negative correlation between MSIG and MVD with lumen measured using CD34 immunostain (r -0.412, $p=0.0365$) in patients with MPM (see Figure 3.12 (Panel B)).

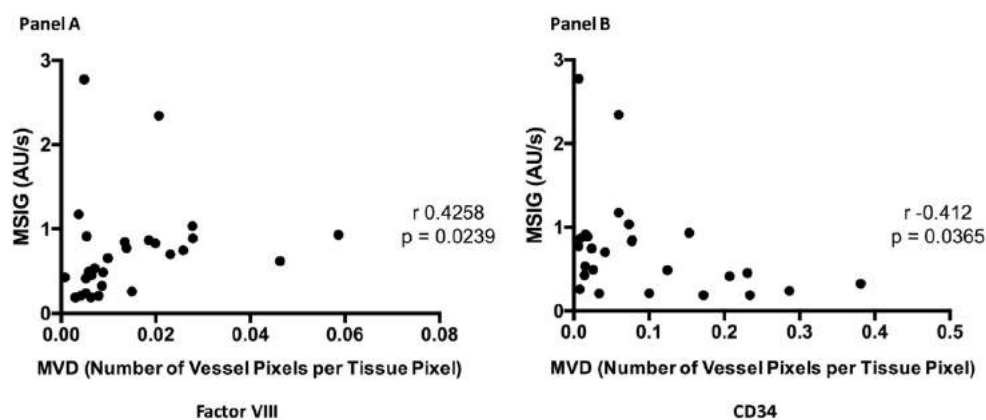


Figure 3.12 Correlation between mean signal intensity gradient (MSIG) and tumour Microvessel Density measured using Factor VIII (Panel A) and CD34 (Panel B) immunostain

3.4.9 Relationship between Tissue MVD and survival in MPM

Median tissue MVD with lumen in patients with MPM was 0.008761 using Factor VIII immunostain. MPM patients with a higher tissue MVD (>0.008761) with lumen had a significantly poorer overall survival in comparison to those with lower tissue MVD with lumen (0.008761) using Factor VIII immunostain (median overall survival 10 months vs. 20 months, HR 2.723 (95% CI 1.093 - 6.784), $p=0.03$), see Figure 3.13 (Panel A).

Median tissue MVD with lumen in patients with MPM using CD34 immunostain was higher (0.05966). In contrast to the above findings using Factor VIII immunostain, MPM patients with a higher tissue MVD (>0.05966) had a trend towards better overall survival than those with a lower tissue MVD, although this was not statistically significant (median overall survival 16 months vs. 10 months respectively, HR 0.484 (95% CI 0.207 - 1.138), $p=0.08$), see Figure 3.13 (Panel B).

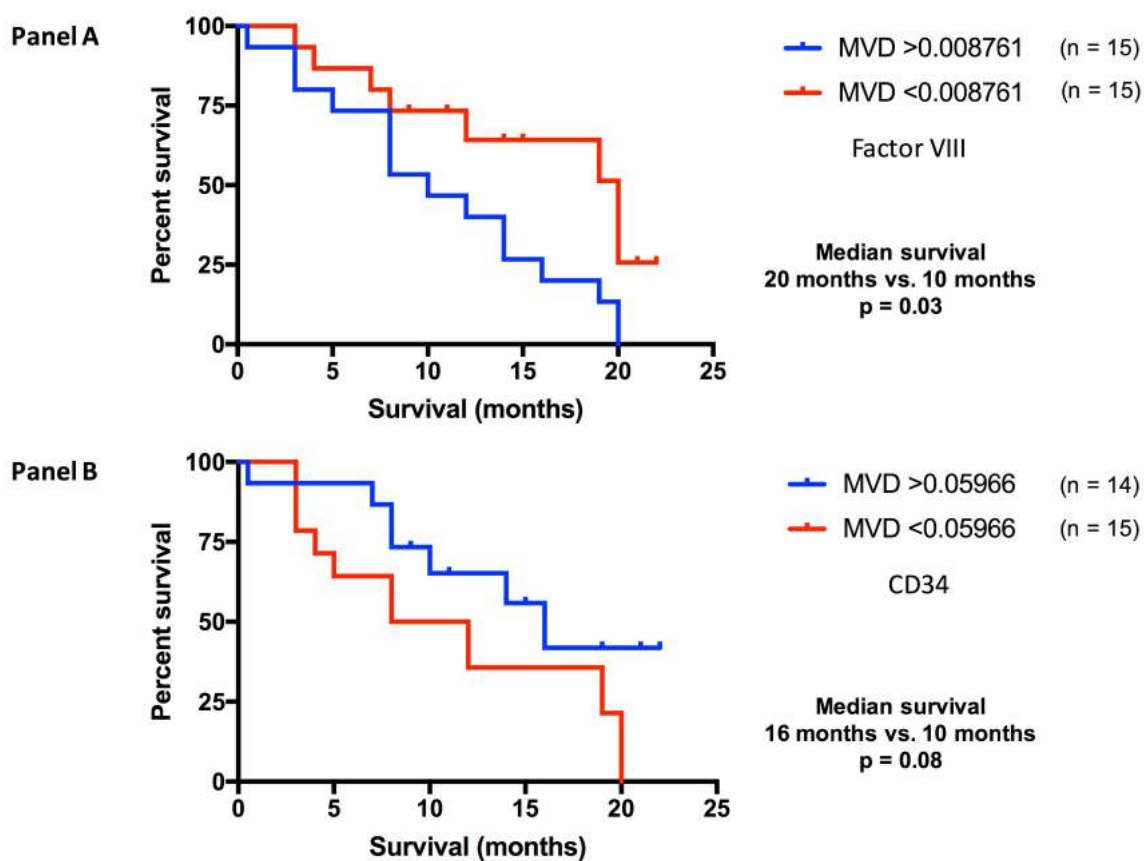


Figure 3.13 Kaplan-Meier curves demonstrating the relationship between tumour Microvessel Density (MVD) and median overall survival using Factor VIII (Panel A) and CD34 (Panel B) immunostain

3.4.10 Relationship between MRI perfusion data and survival in MPM

Median MSIG in patients with MPM was 0.533AU/s. Patients with PM and a high MSIG of $>0.533\text{AU/s}$ had a significantly poorer median overall survival than those with a low MSIG of $<0.533\text{AU/s}$ (median survival 12 months vs. 20 months, HR 1.898 (95% CI 0.8349 - 4.316), $p=0.047$), see Figure 3.14.

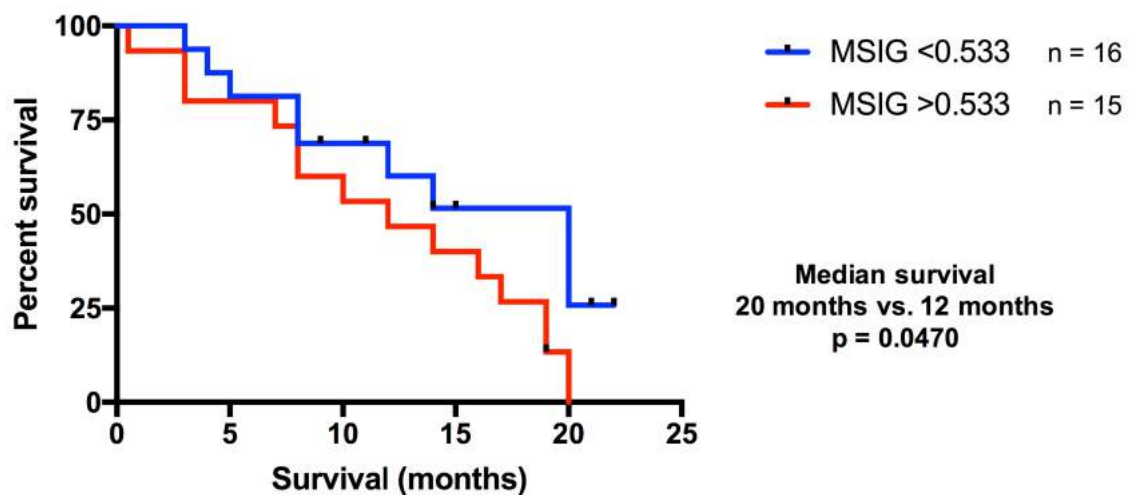


Figure 3.14 Kaplan-Meier curves demonstrating the relationship between patient mean signal intensity gradient (MSIG) and median overall survival

3.5 DISCUSSION

3.5.1 Early Contrast Enhancement

The aim of this study was to develop a novel imaging biomarker of PM, targeted to non-anatomical, perfusion-based changes that occur in malignancy, even at an early stage of disease. We hypothesised that a perfusion-based biomarker could differentiate between PM and benign pleural disease with sufficient diagnostic accuracy to be of routine clinical value.

Early Contrast Enhancement at contrast-enhanced MRI is a novel biomarker of PM, which differentiates PM from benign pleural disease with high diagnostic performance: sensitivity 83% (95% CI 61 - 94%), specificity 82.5% (95% CI 68 - 91%), PPV 68% (95% CI 47 - 84%), NPV 92% (78 - 97%).

ECE was defined as a peak in signal intensity at or before 4.5 minutes (270 seconds) post-intravenous gadolinium contrast administration. ECE was demonstrated in 33/36 (92%) patients with PM in this study. This is later than the 'optimum' pleural image acquisition timing of approximately 60 seconds post-contrast at CT reported by previous authors. (75,330-332) However, this practice is recommended when utilising CT as the imaging technique and is based on differing Hounsfield Units rather than signal intensity at MRI as described here.

Gadolinium is a low molecular weight, extracellular contrast agent with low osmotic activity, which is largely renally-excreted. Following intravenous administration, the diffusion of Gadolinium from the intravascular space into the extravascular extracellular space (EES) dependent on blood perfusion, microvessel permeability, surface area and diameter, water diffusion and tissue oxygenation and metabolism. (309,333,334) As Gadolinium is unable to cross cell membranes, its volume of distribution is essentially the interstitial space. Contrast enhancement gradient in the initial period after intravenous injection (wash in) is therefore dependent on tissue perfusion, maximal contrast enhancement dependent on the total uptake of contrast medium within the interstitial space and contrast washout dependent on vascular permeability. (335,336) Biological characteristics of the interstitial space, including stromal cellularity, fibrosis, collagen content and tumour proliferation will all therefore influence contrast kinetics at Gadolinium-enhanced MRI. (336)

In semi-quantitative DCE-MRI of breast cancer, peak contrast enhancement has been reported to occur in the first 2 - 3 minutes following contrast administration, (113,337) which is earlier than the time point reported for ECE in this study. However, similar to our study, Buckley *et al* performed DCE-MRI in 40 patients with breast cancer, and reported that contrast enhancement at 4 minutes had a modest but statistically significant correlation with MVD measured using Factor VIII immunostain. (338) Additionally, Partridge *et al* examined 'delayed contrast kinetics' at 4.5 minutes and 7.5 minutes post-contrast

administration at DCE-MRI in 280 patients with breast lesions and reported a higher percentage of patients with breast malignancy displaying persistent or plateau contrast enhancement at 4.5 minutes in comparison to the later time point. (339)

One possibility for the slightly later contrast enhancement time point of 4.5 minutes reported herein is the histology of MPM. MPM tumour tissue also contains interspersed regions of non-malignant stroma, which consists of moderately cellular fibrous tissue. Epithelioid MPM commonly produces high amounts of hyaluronic acid and sarcomatoid MPM contains large amounts of collagenous tissue. (340) As highlighted earlier, stromal cellularity and fibrosis also affect contrast kinetics and may be responsible for the 'delayed' contrast enhancement time point demonstrated in this study. Late gadolinium enhancement (>10 minutes post-contrast administration) has been demonstrated in cardiac sarcoid (341,342) and cardiomyopathies (343,344), as a result of myocardial fibrosis and increased EES secondary to collagen deposits. (345)

The pattern of contrast enhancement reported in the current study is consistent with findings reported in a small retrospective study of 10 patients with MPM undergoing MRI assessment prior to surgery. In this study, Patel *et al* demonstrated peak tumour enhancement at 280 seconds post intravenous gadolinium contrast administration. (346) Our findings are also in agreement with those of Falaschi *et al* and Boraschi *et al* who reported pleural hyper-intensity on T1-weighted gadolinium-enhanced MR imaging in patients with PM. (100,347) Although the exact post-contrast timing is not specified in these studies, it is likely to fall within the definition used here for ECE.

3.5.2 ECE - An Imaging Biomarker of Pleural Malignancy

ECE demonstrated higher diagnostic sensitivity (83%) and NPV (92%) than subjective CT morphology without perfusion analysis (56% and 67%, respectively) and MRI morphology (68% and 78%, respectively). After adjustment for multiple comparisons, these differences did not reach statistical significance. Combining MRI morphology with ECE resulted in slightly reduced specificity (78%) and PPV (55%) than with ECE alone (83% and 68%, respectively). ECE was associated with

superior inter-observer agreement (κ 0.784) relative to CT (κ 0.65) and MRI morphology (κ 0.593).

The high diagnostic performance of ECE reported in this current study is consistent with that reported in previous studies of signal intensity-based, contrast-enhanced MRI assessment of suspected PM. Falaschi *et al* reported sensitivity of 100%, specificity of 60%, PPV 70% and NPV 100% in 34 patients, 18/34 (53%) were diagnosed with PM (9/18 with MPM), based on increased signal intensity of pleural lesions at T1-weighted contrast-enhanced MRI. Similarly, Boraschi *et al* reported sensitivity of 100%, specificity 95%, PPV 92% and NPV 100% in a small study of 30 asbestos-exposed patients, 11/30 (37%) of whom were diagnosed with MPM. In this latter study, morphological features of PM were combined with the finding of increased pleural signal intensity to classify patients and authors did not report the diagnostic performance of signal intensity-based assessment alone. Neither author reported the stage distribution of the patients with MPM included in their studies and it is therefore impossible to conclude the added value of signal intensity data to routine morphological assessment, which is often less complex in advanced stage disease, based on the reported findings in these two small studies.

The excellent specificity of 95% reported in the study by Boraschi *et al* is superior to the specificity reported here (specificity 83%). This is likely to be as a result of the benign pleural disease population included in the earlier study. While all patients included in the study had suspected PM, all of the patients with benign disease (n=16) were diagnosed with pleural plaques, which is arguably an easier population to differentiate from PM than the population included in the present study, which included 10 patients (45%) with BAPE and 1 patient with a reactive effusion secondary to underlying lung cancer (Table 3.7). Similar to our findings, Falaschi *et al* reported false positive contrast enhancement results in patients with tuberculous pleurisy. This may reflect neoangiogenesis in active TB pleural lesions, since previous studies demonstrate increased serum vascular endothelial growth factor (VEGF) levels in TB, and evidence of VEGF expression in macrophages surrounding tuberculous lesions. (348,349)

Combining MRI morphology assessment with ECE assessment resulted in increased sensitivity of 92% and NPV of 97% at the cost of reduced specificity (78%) and PPV (55%). Hierholzer *et al* reported improvements in both sensitivity and specificity when combining morphology with signal intensity changes at MRI over morphology assessment alone (sensitivity 100% vs. 96% and specificity 93% vs. 80%). (77)

As discussed in chapter 1, DCE-MRI and DWI-MRI have both previously been used in studies assessing patients with suspected MPM, based on differences in perfusion and tissue cellularity respectively. Both techniques have been reported to have excellent diagnostic sensitivity and specificity comparable and in some studies superior to that of ECE reported here. Giesel *et al* performed DCE-MRI in 19 patients with confirmed MPM and reported different contrast kinetic parameters between tumour tissue and normal tissue, (117) however, 10/19 (53%) of these patients had bulky stage IV disease, which adds little value over morphological assessment. Coolen *et al* performed quantitative analysis of images taken at DWI-MRI in 31 patients with suspected PM, reporting on overall sensitivity of 71% and specificity 100% for PM. When combining this data with contrast enhancement patterns at DCE-MRI, diagnostic performance improved to a sensitivity of 93%, at the cost of a reduced specificity of 94%. (90) In a later study, Coolen *et al* reported on a novel biomarker of PM at DWI-MRI - pleural pointillism. (350) They defined this as the presence of multiple, heterogeneous areas of pleural hyper-intensity at high b value DWI-MRI. The visual-based analysis methodology of pleural pointillism was felt to be simpler than calculating ADC values as was previously used when assessing PM using DWI-MRI. Using this novel imaging biomarker in a study of 100 patients, pleural pointillism differentiated benign from malignant pleural lesions with a sensitivity of 93% and specificity of 79%. (350)

However, as discussed previously, DWI-MRI is limited by image quality due to low signal-to-noise ratio with frequent image distortion. (106) DCE-MRI also has limitations, as it requires a mass lesion to define an adequate ROI, and image acquisition is limited to a finite number of slices so the entire hemithorax, and therefore pleura, cannot be assessed. This limits its clinical utility in the early detection of MPM, which typically has a sessile growth pattern and rarely

presents as a mass lesion in early stage disease. Similarly, quantitative perfusion parameters at DCE-CT have been shown to correlate with tumour MVD. (351-353) Previous studies have reported on the potential utility of perfusion CT in the differentiation of benign from malignant pulmonary nodules. (354) In addition, results from a pilot study assessing DCE-CT in 13 patients with MPM, imaging a 5.5cm axial extent of the thorax, reported correlation of contrast uptake with tumour burden and differential contrast uptake in patients undergoing chemotherapy versus observation alone. (314) However, the role of perfusion CT in the differentiation of PM from benign pleural disease has not been widely studied. A potential advantage of perfusion CT over MRI- ECE, described here, is the greater availability of CT scanners and a quicker acquisition time. However, current perfusion CT methods do not allow complete assessment of the entire pleura, as is reported here using MRI, since perfusion CT is currently limited to defined sections of the thorax. Furthermore, high radiation exposure has so far limited clinical deployment of perfusion CT on a routine basis. (110,316)

PET-CT also offers potential advantages over the MRI methods reported here. In MPM, PET-CT out-performs both CT and MRI in assessment of nodal and distant metastases. (140) In addition, previous studies report elevated maximal standardised uptake values (SUVmax), in PM, relative to benign disease and high sensitivity and specificity (pooled sensitivity of 95% and specificity of 82%) in a meta-analysis (89), However, PET-CT specificity is reduced in TB pleuritis (91), as is reported here for MRI-ECE, and following talc pleurodesis (220,355,356). PET-CT sensitivity is also reduced in early stage MPM, and epithelioid sub-types. (89,92) This significantly limits the utility of PET-CT as an early diagnostic test, particularly in effusion-dominant cases of MPM, which are most commonly of epithelioid origin.

The principal advantage of ECE assessment described herein is its applicability to patients with minor pleural thickening (and therefore early disease stage) and the ability to assess multiple areas of pleura rather than being confined to a limited number of slices. In this study, 49/58 (84%) patients had pleural thickening <10mm and 47/58 (81%) lacked gross tumour nodules. Median pleural thickness for all patients 5mm (IQR 4 - 7mm)) and the minimum pleural thickness was 2.33mm. Of the 58/66 patients who underwent contrast-enhanced MRI and subsequent ECE assessment, 31/58 (53%) had a diagnosis of MPM and the

majority of these patients (64.5% (n=20) had IMIG stage I disease. Despite this, ROI placement and assessment for ECE was possible in all cases and with superior sensitivity and comparable specificity to CT and MRI morphology for PM, and similar diagnostic performance reported by Falaschi *et al* and Boraschi *et al*. Importantly, the patients included in these earlier studies had pleural thickening >10mm, or significant but undefined pleural thickening. (99,100)

In addition, the native T1 of the tissue of interest needs to be known or acquired in order to allow calculation of contrast kinetic parameters such as amplitude, k_{ep} and k_{el} at DCE-MRI. In cardiac MR imaging, the native T1 of the myocardium changes with pathology, for example, there is an increased T1 with myocardial oedema following infarction or with cardiac amyloidosis or lupus and a decrease in T1 in conditions with lipid or iron overload. (357,358) It is therefore possible that the native T1 of pleura may differ between underlying pathologies. Given the significant heterogeneity of disease distribution in MPM, this could therefore result in significant difficulties in accurately calculating contrast kinetic parameters at DCE-MRI. An additional advantage of ECE, as described in this chapter, over DCE-MRI therefore, is that the methodology does not require knowledge of the native T1 of the pleura to allow for ECE assessment.

3.5.3 CT and MRI Morphology in Pleural Malignancy

The presence of morphological features at CT and MRI that were used to classify patients as having PM in this study, including the presence of a pleural rind, nodular pleural thickening, fissural pleural thickening, parietal pleural thickening >1mm and evidence of invasion of the diaphragm or chest wall are consistent with those commonly reported in previous CT and MRI studies assessing patients with PM. (40,76,79,81) These studies have all demonstrated that these features are consistently more commonly visualised in PM than in benign pleural disease.

3.5.3.1 Diagnostic Performance of CT Morphology

The diagnostic performance of CT morphology reported in this study (sensitivity 56%, specificity 77%) is concordant with findings of recently reported studies by Hallifax *et al*, who reported CT sensitivity of 68% in 370 patients referred for LAT, (82) and by Tsim *et al*, who reported CT sensitivity of 58% in 315 patients at

initial presentation with suspected PM. (83) Both of these studies utilised the reporting radiologist's original report, without any study-specific CT reporting. This better replicates clinical practice than the current study, where all CT scans were assessed by expert thoracic specialist radiologists. CT scans that were reported by thoracic radiologists in the previous study by Tsim *et al* demonstrated a higher level of sensitivity (68%). (83) However, the patients included in this study were recruited at the time of presentation, rather than prior to pleural biopsy as in the current study. The current study population could therefore be considered to be a more difficult to diagnose population than the one described in the original study as patients had already undergone initial assessment and pleural cytology examination and still required further assessment with pleural biopsy.

The specificity reported in the current study is similar to numerous previous CT imaging studies, including Metintas *et al* who reported up to 70% sensitivity and 65 - 95% specificity in a retrospective review of 215 patients with benign and malignant pleural disease (81) and Hierholzer *et al*, who reported sensitivity of 93% and specificity of 87% in a retrospective review of 42 patients. (77) However, the sensitivity reported here is lower than that reported in this previous study. One possible explanation is that one of the false negative cases of MPM (patient 17, see Table 3.6) had an arterial-phase CT performed, which is associated with a significantly reduced sensitivity in comparison to venous phase CT. (83) In addition, all CT scans performed in the current study were acquired as part of routine clinical work-up and were therefore performed under local imaging protocols. Many authors recommend delaying image acquisition to 60 seconds post-contrast in order to allow optimum assessment of the pleura. (330,359) It is therefore possible that these earlier studies, which included CT scans acquired as per research protocols, would have utilised more optimum contrast timing than that used in herein.

Similarly, a study by Traill *et al* demonstrated superior sensitivity (84%) and specificity (100%) in comparison to the present study. (360) However, the earlier study included a small number of patients with benign pleural disease (8/40 (20%)) relative to the current study ((22/58 (38%)). The false positive cases in the current study included 2 patients with TB pleurisy who were both noted to

have irregular pleural thickening at CT, resulting in malignant classification. Circumferential and nodular pleural thickening have previously been noted to feature in as many as 30% of cases of pleural TB at CT. (361) While the earlier study by Traill *et al* did include one patient with TB pleurisy, no pleural abnormality was identified on their CT. (360)

The discordance between ‘real-life’ clinical imaging acquisition and reporting and research imaging acquisition and reporting highlights that although CT (and MRI) morphology *can* be highly accurate, these are operator-dependent, subjective processes.

3.5.3.2 Diagnostic Performance of MRI Morphology

The diagnostic performance of MRI morphology demonstrated in this study (sensitivity 68%, specificity 85%, PPV 77%, NPV 78%) is similar to results reported in previous studies of MRI assessment of PM. While MRI is typically reserved for staging, particularly prior to surgical resection, in MPM rather than as a diagnostic tool, (359) previous studies have demonstrated diagnostic performance comparable to CT in the differentiation of PM from benign pleural disease. (77,79,362) Hierholzer *et al* reported high sensitivity of 96% and specificity of 80% for PM in a retrospective review of 42 patients. (77) Similarly, Coolen *et al* reported sensitivity of 81% and specificity of 73% when assessing MRI morphology (and principally the finding of mediastinal pleural thickening) for the detection of PM in a prospective study of 100 patients with suspected MPM. (109)

However, similar to CT morphology assessment, MRI morphology is an operator-dependent, subjective assessment. The diagnostic performance of MRI morphology in routine clinical practice is therefore potentially lower than that reported in previous and this current study.

3.5.4 Reproducibility

The more objective nature of ECE suggests that this novel biomarker could improve consistency in radiological reporting of PM that is frequently responsible for reduced diagnostic performance of more subjective morphological assessment in clinical practice. (83) ECE in this study demonstrated higher inter-

observer agreement ($\kappa = 0.784$) than both CT ($\kappa = 0.65$) and MRI morphology ($\kappa = 0.593$). However, while the presence or absence of ECE is an objective assessment, the ROI placement is clearly a subjective, operator-dependent process. There is therefore the potential for sampling 'error', particularly in patients with a heterogeneous disease process such as MPM. 273/482 (57%) ROI placed in patients with PM did not demonstrate ECE and all of the false negative cases ($n=3$) had a diagnosis of MPM without evidence of macronodular disease (Table 3.6). These false negatives may represent ROI being placed on areas of benign pleural tissue interspersed with pleural tumour. Analysis of individual ROI contrast enhancement behaviour demonstrated superior discriminatory power when confounding ROI exhibiting a benign enhancement pattern (i.e. ROI not demonstrating ECE) in patients with PM were excluded (ROISIG AUC improved from 0.776 (95% CI 0.744 - 0.808) to 0.938, (95% CI 0.918 - 0.957).

3.5.5 The Biological Basis of Early Contrast Enhancement

In patients with MPM, MVD with lumen, measured in pleural tissue stained with pan-endothelial cell marker Factor VIII, positively correlated with MSIG at contrast-enhanced MRI, a surrogate marker for ECE ($r\ 0.426$, $p=0.02$) in this study. A relationship between MSIG and MVD with lumen measured using pan-endothelial cell marker CD34 was also identified, however in contrast to Factor VIII immunostain, this was a negative correlation ($r\ -0.412$, $p=0.037$). No relationship was identified in patients with benign pleural disease. Importantly, our MRI and tissue perfusion measurements were performed prior to any intervention that could have altered the pleural microcirculation, including pleural drainage, pleurodesis or chemotherapy. This suggests that ECE is a perfusion-based biomarker, which is present in patients with PM because of increased MVD within areas of pleural tumour. Similar to the findings in the current study, contrast kinetic parameters at MRI have been reported to correlate with MVD measured in glioma, (363) breast lesions, (338) prostate cancer (364) and mesothelioma. (118) Since ECE was defined based on observations in patients with macro-nodular tumour (MPM in 5/6, secondary PM in 1/6) it is possible that a different definition may perform better in patients with lower volume pleural tumour or in cancers of different types, in which different microvascular or other features predominate. However, the correlation

we observed between tissue MVD and MSIG in MPM ($r=0.4258$, $p=0.02$, $n=28$) appeared preserved, and indeed more powerful, when this analysis was confined to patients without macro-nodules ($r=0.6594$, $p=0.003$, $n=18$).

Tumour angiogenesis is now well-established as a prognostic biomarker in human solid tumours, including breast cancer, (365) prostate cancer (366) and NSCLC.(367) Kumar-Singh *et al* reported significantly increased intra-tumoural MVD in malignant mesothelium relative to non-malignant mesothelium and found that higher intra-tumoural MVD was associated with significantly worse survival outcomes in a study of 25 cases of MPM. They also described heterogeneity in the degree of vascularity both within and between tumour samples. (299) Edwards *et al* also demonstrated worsening survival outcomes associated with increasing MVD in a larger study of 104 cases of MPM. (298) Similar to the findings in these earlier studies, increasing MVD measured using Factor VIII was associated with worsening survival in this current study (Figure 3.13(a)). However, in contrast, intra-tumoural MVD measured using CD34 in this study was not found to be prognostically significant (Figure 3.13(b)) and there was no significant difference in MVD between patients with PM and those with benign pleural disease. One possibility is the individual antibodies used to quantify MVD in this study. Intra-tumoural MVD, measured using pan-endothelial cell markers such as Factor VIII and CD34, is a valid measure of tumour angiogenic activity. (368,369) CD34 and Factor VIII antibodies used in the current study have previously been shown to demonstrate reproducible immunostaining of microvessels in both frozen and paraffin-embedded tissue sections. (369,370) However, while Factor VIII is known to be a highly specific antibody for detecting intratumoural microvessel density, CD34 has been shown to also stain perivascular stromal cells and lymphatic vessels. The reduced specificity of CD34 as an endothelial cell marker may have contributed to the contradictory relationships demonstrated between Factor VIII and CD34 immunostains and the lack of prognostic significance of MVD measured using CD34 in this study.

Kumar *et al* demonstrated a correlation between overall survival and MVD measured using CD105 but not CD34 immunostain in breast cancer. Similarly, Taneka *et al* demonstrated that MVD measured using CD105, but not CD34 in patients with NSCLC. While Edwards *et al* did demonstrate a correlation between

overall survival and MVD measured using CD34 in 104 patients with MPM, they did report positive staining of stromal elements, which had morphological features of myofibroblasts, in 17% of cases and this precluded MVD quantification in 11% of all cases. (298)

Another possibility for the differing result in the current study is the significant heterogeneity previously reported in the distribution of neovascularization within individual MPM tumour samples, (299) which composes the vast majority of our patients with PM (86% (n=31)). This highlights an important difference in methodology between our study, where there was computerised quantification of MVD within an entire section of tumour, and the previously discussed studies where MVD was quantified within selected 'hot-spots' of tumour.

Identification of vascular hot spots at low magnification followed by quantification of MVD within these hot spots at 200x field was first described by Weidner *et al* (365) who initially examined tumour vascularity in breast cancer. An alternative to this method is microvessel quantification using Chalkley counting. Similar to the method described by Weidner *et al*, the Chalkley method involves examining tumour sections at low magnification to identify a vascular hot spot, before an eyepiece graticule containing 25 randomly positioned dots is rotated at higher magnification so that the maximum number of dots are on the vessels within the hot spot. The number of overlying dots are then counted rather than individual microvessels. (368) However, these methods can be subject to significant inter-observer variability and the hot spots are unlikely to be representative of the entire tumour. Computer-aided analysis systems, such as the one described herein, are a valid alternative to manual vessel counting (371-373) and has the advantage of being more objective than manual vessel counting. in addition, it allows counting within entire tumour sections, rather than restriction to vascular hot spots, and allows further information regarding tumour vascularity, such as vessel perimetry, to be defined.

However, none of these described methods allow for 'sampling' of the entire tumour as measurements can only be made within biopsy samples, which may not be representative of the entire disease. This is particularly important in MPM due to its heterogeneous disease distribution. It also highlights another

important potential advantage of using an imaging biomarker to quantify tumour angiogenesis, as it would allow sampling of the entire tumour, while being non-invasive.

Clearly tumour angiogenesis is a dynamic process and therefore the degree of tumour vascularity and intra-tumour MVD will change over time. Assessment of MVD in tumour specimens taken at pleural biopsy therefore only provides a 'snapshot' of tumour angiogenesis as it was at the time of biopsy. Changes in tumour angiogenesis over time cannot be assessed using intra-tumoural MVD unless repeated biopsies are taken. However, signal intensity measurements (in the form of MSIG) at contrast-enhanced MRI in this current study were prognostically significant (median survival 11 months for high MSIG vs. 20 months for low MSIG, $p=0.047$), see Figure 3.14. This highlights its potential as a prognostic biomarker, particularly as it can be repeated serially as it is non-invasive and does not require ionising radiation.

3.5.6 Potential clinical implications

While MRI is becoming increasingly available, the ability to assess patients with suspected MPM with thoracoscopy remains relatively limited to specialist centres. If validated in larger studies, ECE may improve the accuracy of pleural imaging in cases of suspected MPM. This may allow pathway rationalization, directing patients appropriately to specialist centres and early invasive sampling, including early thoracoscopy when MPM appears likely. The results of our ROISIG post-hoc analyses suggest that benign (ECE-negative) ROI in patients with PM negatively contribute to discriminant performance. This is consistent with a hypothesis that these data originate from areas of interspersed benign disease in patients with discontinuous malignant pleural lesions, which are commonly observed at thoracoscopy. Measurement of SI and assessing ECE behaviour across the entire pleura using a volumetric approach could be developed in future studies. Theoretically, this would allow the pleura to be treated as a 'single ROI'. Pleural SIG, being a continuous variable like ROISIG, could then be applied at different thresholds depending on the clinical context. For example, a lower threshold (maximizing sensitivity) in a pleural staging population vs. a higher threshold (maximizing specificity) for screening of asbestos-exposed persons for early MPM. MRI's ability to acquire data without

use of radiation would be significant additional advantage in a screening setting. However, the performance of ECE in lower prevalence populations is likely to be inferior to that described here, and this would require further detailed study. Additionally, MSIG calculated at ECE assessment may provide important prognostic information. The significant correlation between intra-tumoural MVD as a marker of tumour angiogenesis and MSIG at contrast-enhanced MRI highlights its potential as a future predictive biomarker of response to anti-angiogenic chemotherapeutic agents. This would however require significant further study to assess its performance in this regard.

3.5.7 Limitations of this study

The principal limitation is the relatively small sample size, reflected in relatively wide confidence intervals around some measures of diagnostic performance. Nevertheless, we have assessed ECE in large number of individual ROI (n=814) using a technique which appears reproducible.

A second limitation, as discussed earlier, is that although ECE is objectively defined, the user-defined ROI from which SI is measured are not. Our pre-defined strategy for ROI definition was devised to minimize variation. In nodular cases with visible tumour, ROI definition mirrored thoracoscopic tissue sampling, i.e. sampling of all malignant-looking disease if available, and if not sampling of multiple, evenly distributed areas of pleura. The method chosen for non-nodular, effusion-dominant, cases was designed to be consistent, with ROIs defined on similar positions of similar slices by different operators. Although we demonstrated moderate ECE reproducibility, which exceeded that for MRI/CT morphology, this element of the method is a source of potential disagreement. Measuring SI and assessing ECE behaviour of the entire pleura, using a volumetric approach, could theoretically overcome this, but would require significant further development.

An additional limitation is that we did not perform perfusion CT assessment for comparison with ECE, as all CT imaging in this study was performed as part of routine clinical work-up. However, as previously discussed, perfusion CT has not yet been widely studied in PM and is not routinely used in the assessment of patients with suspected PM in most centres at present.

Another limitation is the duration of follow-up of patients diagnosed with benign pleural disease. Median follow-up for patients with benign pleural disease was 20 (8 - 27) months. The prevalence of MPM reported here may therefore be an underestimate of the true MPM rate since it is routine practice to follow-up patients with BAPE for a minimum of 2 years, because of the potential false negative pleural biopsy rate of up to 12% reported in previous case series. (45) However, all cases of BAPE underwent clinical follow-up at a specialist pleural clinic, with re-biopsy if there was any evidence of progressive disease. Furthermore, it remains unclear whether MPM during this 2-year follow-up period represents a genuine false negative biopsy at original assessment or a new diagnosis of MPM.

The final limitation of the methods described is the time taken to perform ECE analysis. Although not excessive it is slower than subjective morphology assessment. Evolution of the technique, including increased computer automation should allow reduction in the time required in the future.

3.6 CONCLUSION

In this chapter, the methods for acquisition and measurement of a novel, and largely objective MRI biomarker of pleural malignancy - Early Contrast Enhancement (ECE) have been described. CT remains an important imaging tool in the assessment of suspected PM, however in clinical practice it is limited in its sensitivity for detection of early stage MPM and its specificity for differentiating reactive effusion from pleural metastatic disease in lung cancer, particularly when pleural thickening is minimal.

Within the limitations of this study, ECE appears to be a sensitive, specific and reproducible, perfusion- based biomarker of PM. The methodology used to define ECE is applicable to patients with minimal pleural thickening, making this technique useful in patients with pleural effusion predominant, low volume metastatic pleural disease and early stage MPM.

CHAPTER 4: VOLUMETRIC ASSESSMENT OF MALIGNANT PLEURAL MESOTHELIOMA

4 Chapter 4: Volumetric Assessment of Malignant Pleural Mesothelioma

4.1 INTRODUCTION

Accurate staging in cancer practice is of vital importance for patient management and clinical research as it provides information regarding patient prognosis and suitability for radical treatment measures and clinical trials. It also allows researchers to group patients appropriately in order to accurately compare treatment outcomes and allows clinicians to monitor disease and therapeutic response. In addition, accurate cancer staging and stage groupings allow international comparisons regarding timing of patient presentation, treatment rates and overall cancer survival rates to be made.

4.1.1 Staging of Malignant Pleural Mesothelioma

Well-established staging systems exist for most cancers, including lung cancer, often based on large international datasets. One of the most widely used cancer staging systems is the 'TNM' system proposed by the American Joint Committee on Cancer (AJCC) and the International Union for Cancer Control (UICC). The TNM staging system is based on the extent of the primary tumour (T), the degree of lymph node involvement (N) and the presence or absence of metastasis (M), with patients being grouped into stage grouping based on their individual T, N and M. (374) However, staging in MPM is difficult due to its unusual, non-spherical growth pattern, proximity to intercostal muscle and vessels and the limitations of current imaging techniques in accurately quantifying disease extent, particularly of the primary tumour (T).

The first mesothelioma staging system was proposed by Butchart *et al* in 1976, (375) based on 29 patients undergoing pleuro-pneumectomy: Stage I - tumour confined to ipsilateral pleura, lung and pericardium; stage II - tumour invading chest wall or mediastinum, disease involving contralateral pleura or lymph nodes within the chest; stage III - tumour infiltrating through the diaphragm with peritoneal involvement or lymph node involvement outside the chest; stage IV - distant blood-borne metastases. Similarly, Sugarbaker *et al* proposed a mesothelioma staging system based on 55 patients undergoing pleuro-

pneumonectomy, which predominantly differentiated patients based on surgical resectability and lymph node involvement. (376)

Subsequently, the International Mesothelioma Interest Group (IMIG) proposed a TNM-based staging system for MPM, (121) which was adopted by the American Joint Committee on Cancer (AJCC) and Union for International Cancer Control (UICC) in the 7th edition of their staging manuals. (377) This staging system was largely derived from evidence from small scale retrospective, surgical data. T staging was based on survival differences reported by Boutin *et al* based on the presence or absence of visceral pleural involvement (378) (T1a versus T1b); surgical resectability (T2 and T3 disease resectable by extra-pleural pneumonectomy +/- resection of focal chest wall disease versus unresectable T4 disease). N descriptors were based on nodal staging for non-small cell lung cancer (NSCLC). M descriptors were identical to that used in early (5th) editions of lung cancer staging (M0 - no distant metastatic disease, M1 - metastatic disease outside of the ipsilateral hemithorax). (121)

However, the IMIG proposed mesothelioma staging system had several limitations. The International Association for the Study of Lung Cancer (IASLC) in collaboration with IMIG reviewed the staging system against a large, retrospective database comprising 3101 patients from 15 international centres. Review of the staging in 1056 patients in whom both clinical and pathologic staging data was available, demonstrated significant rates of upstaging of patients thought clinically to have early (stage I/II) disease following pathological assessment. (125) Differentiation between some of the T-descriptors is only feasible at surgery or thoracoscopy, e.g. T1a (disease limited to parietal pleura only) versus T1b (disease involving visceral pleura), and much more difficult to perform on imaging assessment alone. A lack of significant survival difference between T1a and T1b stages, even at pathological staging, has subsequently been demonstrated. (126)

In addition, the nodal staging system for MPM is identical to that for NSCLC, despite the fact that the lymphatic drainage of the pleura is different to that of the lung. (122,379)

Abdel Rahman *et al* retrospectively reviewed lymph node involvement in 53 MPM patients undergoing EPP and systematic lymph node dissection or sampling. 18/53 (34%) had evidence of lymph node involvement, of these 7/18 (39%) had mediastinal lymph node metastases without any evidence of hilar lymph node involvement. 7 patients included in this study did not have evidence of lung parenchymal involvement, and none of these patients had evidence of hilar nodal involvement. The authors therefore raise the possibility that nodal spread in MPM is different from that in lung cancer, spreading initially to mediastinal nodes, with hilar nodal involvement only occurring via invasion of the lung parenchyma. (124) This perhaps explains the lack of significant survival difference between cN1 versus cN2 disease (median overall survival 16.9 months vs. 17.4 months respectively, HR 1.06, $p=0.78$) on review of the large IASLC mesothelioma database. (127)

As a result, updates to the IMIG/7th edition TNM mesothelioma staging system have recently been proposed, including collapsing the previous T1a and T1b descriptors into a single T1 stage. (126) N-descriptors have also been updated, more accurately reflecting the drainage pattern of the pleura, (122,124,379) with N1 disease now including any ipsilateral, intra-thoracic nodal involvement and N2 disease now including ipsilateral supraclavicular, or contralateral nodal involvement. (127)

4.1.2 Imaging Modalities for the Staging of MPM

4.1.2.1 CT in the Staging of MPM

CT remains the most commonly used imaging modality for the detection and staging of MPM. Subtle invasion through chest wall or diaphragm may be missed utilising CT however, and this is therefore typically better assessed at MRI. (130) In addition, while distant metastases, including pulmonary metastases can usually be readily identified on CT, (132) the sensitivity and specificity of CT for detecting nodal metastases is poor, at 56% and 39% respectively (95% confidence intervals not reported). (130) Review of the IASLC database also demonstrated an underestimation of nodal involvement at clinical staging (22%, 226/1029 clinically staged as having nodal metastatic disease versus 38% (321/851) following pathological staging). (127) Of note, only 56% of clinically staged

patients were reported to have had PET imaging, further highlighting the limitations of CT for nodal staging. Additional staging investigations such as PET-CT and MRI are therefore often applied when patients are being considered for radical treatment such as surgical resection.

4.1.2.2 PET-CT in the Staging of MPM

Plathow *et al* assessed the accuracy of CT, PET-CT and MRI for the selection of patients with potentially-operable disease by acquiring all scans prior to surgery in 54 patients (52 of whom subsequently underwent surgery). They concluded that PET-CT offered the highest diagnostic accuracy, for example in stage III disease, diagnostic accuracy rates for CT, MRI and PET-CT were 75% (sensitivity 75%, specificity 100%), 90% (sensitivity 91%, specificity 100%) and 100% (sensitivity 100%, specificity 100%), respectively, largely due to the superior performance of PET-CT in detecting nodal and distant metastases. (140) Integrated PET-CT has been shown to have better sensitivity than conventional CT for the detection of nodal metastases and extra-thoracic metastases. (139,141,142) However, the limitations of integrated PET-CT should also be appreciated in MPM. Poor spatial resolution translates into relatively poor sensitivity for extra-pleural invasion. One previous study reported a sensitivity of only 67% (at 93% specificity) for the detection of local invasive T4 disease (141) and MRI offers superior performance in this regard. Therefore, PET-CT has important limitations but some utility in the staging of patients who are being considered for radical therapies and/or trials, particularly in the detection of nodal and extra-thoracic disease.

4.1.2.3 MRI in the Staging of MPM

MRI is superior to CT in detecting invasion of chest wall, diaphragm and bony structures, which was best visualised on T1-weighted images, and important for both detection and staging of MPM. (79,144) Stewart *et al* performed contrast-enhanced 1.5-Tesla MRI scans on 69 patients with apparently resectable MPM following contrast-enhanced CT scanning. MRI detected the presence of unresectable disease in 17/69 (22%) of these patients not previously demonstrated on CT. This included mediastinal involvement, diaphragmatic invasion, chest wall infiltration and contralateral pleural disease. (145) Currently

MRI is not routinely used for diagnostic assessment of MPM but has clinical utility in MPM staging and assessment of the presence of infiltrative disease that would preclude surgical resection.

4.1.3 Volumetric Assessment of MPM

Primary tumour volume has been previously demonstrated to be of prognostic significance (see Table 4.1). Pass *et al* first reported shorter median overall survival associated with higher pre-operative tumour volume measured using free-hand manual delineation of tumour at contrast-enhanced CT in patients with MPM undergoing cytoreductive surgery. (134) Similarly, Gill *et al* demonstrated poorer survival in epithelioid MPM with higher primary tumour volume estimated at CT in patients undergoing extrapleural pneumonectomy. (135) More recently, increased primary tumour burden estimated using maximal pleural thickness at CT has been demonstrated to be associated with worsening survival and increased nodal involvement in MPM. (126)

Tumour volume assessment at ^{18}F -FDG PET-CT, utilising SUV-based thresholding to define the volume of interest, has previously been studied as a prognostic biomarker (380) and as predictor of response to surgery and systemic treatment. A higher metabolic tumour volume was reported to be associated with tumour recurrence after extrapleural pneumonectomy or stable or progressive disease following chemotherapy. (381)

While promising, many of these earlier studies assessing primary tumour burden in MPM have been limited by significant inter-observer variability and the laborious or complex nature of manual tumour delineation/segmentation. (382) Delineation of tumour from surrounding structures such as the mediastinum, atelectatic lung and intercostal muscle can be challenging, particularly as neighbouring structures are often of similar HU to pleura, as previously demonstrated by Chen *et al*. (383) MRI has superior sensitivity and inter-observer reproducibility than CT at assessing early chest wall and diaphragmatic involvement in MPM due to its excellent contrast and spatial resolution. (132,384) This makes MRI a potentially more attractive imaging modality in the assessment of primary tumour volume, as it would allow more accurate assessment of tumour extent and delineation from adjacent structures such as

intercostal muscle and diaphragm. In addition, biologic parameters such as signal intensity can be measured and potentially exploited for volumetric assessment at MRI. Plathow *et al* have previously performed tumour volume measurements at MRI in order to assess response to systemic treatment in patients with MPM by combining 2D segmented volumes generated semi-automatically using HASTE sequences. (385)

Table 4.1. Summary of results of previous studies assessing the prognostic significance of imaging-derived tumour volume in patients with Malignant Pleural Mesothelioma

Study	Number of patients	Imaging modality	Median tumour volume (cm ³)	Inter-observer variability	Definition of high tumour volume (cm ³)	Median o.s. (low tumour volume)	Median o.s. (high tumour volume)	Statistical significance
Pass <i>et al</i> (130)	47	CT	100	NR	≥100	22 months	11 months	0.03
Liu <i>et al</i> (382)	30	CT	473	ICC 0.993	>618.49	21.5 months	10.2 months	0.07
Gill <i>et al</i> (131)	88	CT	319	NR	>500	24.4 months	12 months	<0.001
Gill/Rusch <i>et al</i> (132, 133)	129	CT	NR	Spearman Correlation 0.822	Divided into Tertiles: (1) 91.2; (2) 245.35; (3) 511.35	(1) 37 months; (2) 18months	(3) 8 months	<0.0001

o.s.; overall survival, NR; not recorded, ICC; intraclass correlation co-efficient

4.2 AIM AND OBJECTIVES

The aim of this study was to develop methods for the acquisition and measurement of tumour volume, in patients with MPM, at contrast-enhanced MRI. We hypothesised that primary tumour volume measured at contrast-enhanced MRI would correlate with overall disease stage and/or subsequent survival.

Study objectives and outcome measures are summarised in Table 4.2.

Table 4.2. Research Objectives and Outcome Measures for the MRI Volumetry study

Research Objectives	Outcome Measures
<p>Primary</p> <p>To determine a method for MPM primary tumour volumetry based on contrast-enhanced MRI that is:</p> <ul style="list-style-type: none"> a) accurate b) reproducible c) practical 	<p>Outcome of a scoring matrix for different methodologies comprised of:</p> <ul style="list-style-type: none"> a) Accuracy in measurement of an MRI phantom volume b) Accurate coverage of pleural tumour in patients, based on subjective visual assessment c) Intra-observer agreement by intra-class correlation co-efficient d) Time taken to complete volume analysis
<p>Secondary</p> <ul style="list-style-type: none"> 1. To determine the correlation between primary tumour volume and clinical T-stage 2. To determine the relationship between primary tumour volume and subsequent survival 	<ul style="list-style-type: none"> 1. Primary Tumour Volume at MRI and Clinical T-stage based on regional Mesothelioma MDT staging 2. Primary Tumour Volume at MRI and Median Overall Survival

4.3 METHODS

4.3.1 Ethical Approval

Ethical approval for this study was provided by the West of Scotland Research and Ethics Service (reference 12/WS/0219 and 13/WS/0240). NHS Greater Glasgow and Clyde acted as the study sponsor.

4.3.2 Study Population

Patients recruited in this chapter were recruited from a pilot study conducted to establish MR imaging acquisition and analysis protocols, and as part of the DIAPHRAGM MRI sub-study (further details of which are included in chapter 2).

Patients presenting with suspected pleural malignancy, as defined by a pleural effusion or pleural-based mass lesion, to the Southern General Hospital (now the Queen Elizabeth University Hospital), Gartnavel General Hospital, Victoria Infirmary and Glasgow Royal Infirmary between January 2013 and October 2016 were invited to participate. Patients were identified at respiratory outpatient clinics and in acute admission units or respiratory inpatient wards. All patients were reviewed by myself or Dr Kevin Blyth (Consultant Respiratory Physician) who reviewed the need for pleural biopsy (either image-guided or thoracoscopically), based on clinical need and patient wishes, and their eligibility for the DIAPHRAGM MRI sub-study.

Eligibility criteria for the DIAPHRAGM MRI sub-study are described in Chapter 3, section 3.3.2 (page 149 - 150). Only patients with complete contrast-enhanced MRI examinations and a final diagnosis of MPM were included in this volumetry study.

4.3.3 Pleural Diagnostics and Staging

All patients included in this chapter had pleural histology pursued by the following methods: LAT, VATS or image-guided pleural biopsy. All cases were

discussed at the West of Scotland Mesothelioma MDT, where pathological diagnosis and staging based on imaging, and where available, thoracoscopic findings, were confirmed. All patients were followed-up in the pleural clinic.

4.3.4 MR Image Acquisition

MRI acquisition methodology is described in detail in Chapter 3, section 5.2. Briefly, MRI scans were acquired using 3-T Siemens Magnetom Verio® (Siemens, Erlangen, Germany) between January 2013 and August 2015, and using a 3-T Siemens Magnetom Prisma® (Siemens, Erlangen, Germany) between August 2015 and October 2016.

T1-weighted, fat-saturated, 3D spoiled gradient echo sequences were acquired during a short breath-hold at end-inspiration (repetition time 2.8 - 3.23ms, echo time 1 - 1.08ms, field of view 400 - 440mm, matrix 224 x 100, flip angle 9°, slice thickness 1.8 - 1.9mm, no inter-slice gap). Number of slices acquired ranged between 104 - 144 slices (median 120 (IQR 120 - 128)). Images were acquired at baseline pre-contrast and at 40 seconds, 80 seconds, 4.5 minutes, 9 minutes and 13.5 minutes after intravenous gadobutrol contrast (Gadovist (0.1 mmol/kg), Bayer Healthcare Pharmaceuticals, Berlin, Germany) was administered, at an injection rate of 2 ml/second. All images were acquired in the coronal plane but were isotropic allowing tumour volume to be assessed in 3D.

4.3.5 MRI Phantom

An MRI phantom was developed in conjunction with the Department of Clinical Physics and Bioengineering, NHS Greater Glasgow and Clyde. It is composed of a Polymethyl methacrylate (PMMA) outer casing with a central solid cylinder of PMMA. A precise volume of water (1360cm³) was added, creating a shallow pool of fluid between the solid central cylinder of PMMA and the outer casing, broadly similar to the thin pleural space in humans, see Figure 4.1. The phantom was scanned multiple times, removing the phantom and then replacing it into the MRI scanner each time, using a 3-T Siemens Magnetom Prisma® (Siemens, Erlangen, Germany) scanner.

An acceptable error around the MRI-measured phantom volume was defined as a measured volume $< \pm 5\%$ of the true volume.

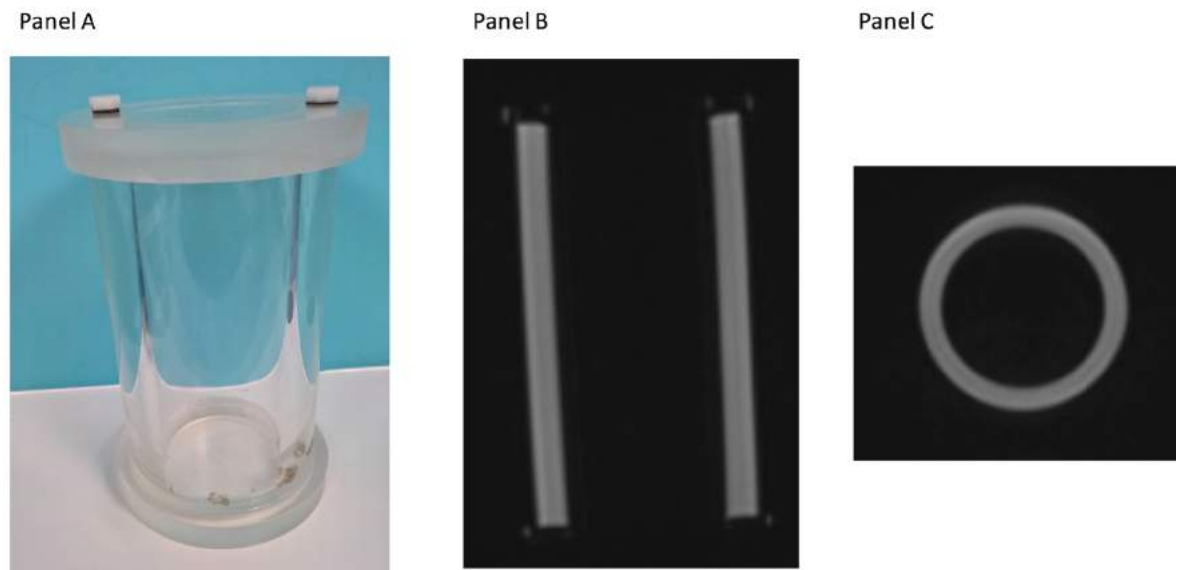


Figure 4.1 MRI phantom. Panel A is a photograph of the MRI phantom containing a precise volume of fluid sitting in between the solid central PMMA cylinder and the outer casing. Panels B and C demonstrate MRI phantom imaged at T1-weighted MRI in coronal (Panel B) and axial (Panel C) planes, where the thin layer of fluid (light grey) can be seen between the two layers of PMMA

4.3.6 Image Analysis

All images were anonymised and analysed in a blinded fashion by ST in batches. All pre- and post-contrast MR images were assessed for the time point at which maximum contrast enhancement and signal intensity separation between pleura and adjacent structures (intercostal muscle, pleural fluid and lung) occurred (see Figure 4.2). In the majority of patients (80% (n=25)), this occurred at 4.5 minutes post intravenous contrast administration and this time point was therefore used for all further image analyses.

Initial analysis methodology involved manual delineation of the pleura in every image slice using OsiriX for Mac (Pixmeo, Geneva, Switzerland), see Figure 4.3 for an example. This methodology was discontinued due to the unacceptable amount of time taken to complete each analysis (approximately 65 minutes). Subsequently, a method using the 'MIALite' plug-in for OsiriX was trialled, which

utilised threshold-based segmentation of the pleura (see Figure 4.4 for an example). However, segmentation could only be ‘seeded’ from a circular ROI, and while a ‘blocking’ circular ROI could also be applied to limit segmentation to pleura, due to the circular nature of the ROI tool, there was significant inclusion of adjacent non-pleural structures or significant exclusion of pleura. This method was also felt to be too time-consuming to be applicable to future clinical practice (approximately 45 minutes per analysis). Finally, analysis using Myrian[®] software v2.0 (Intrasense[®], Montpellier, France) was trialled, using four different analysis methodologies, all of which utilised semi-automated, threshold-based segmentation. MRI phantom volume was also defined using all four methodologies.

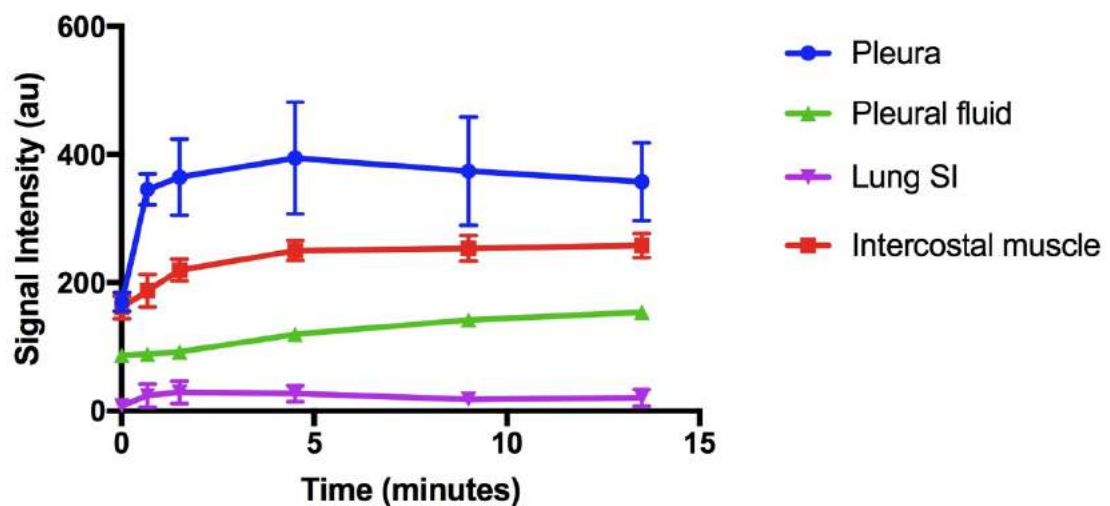


Figure 4.2 Example of mean signal Intensity/time curves for ROI placed on pleura and adjacent structures in a patient with MPM. Peak contrast enhancement and separation of curves at 4.5 minutes post-contrast administration

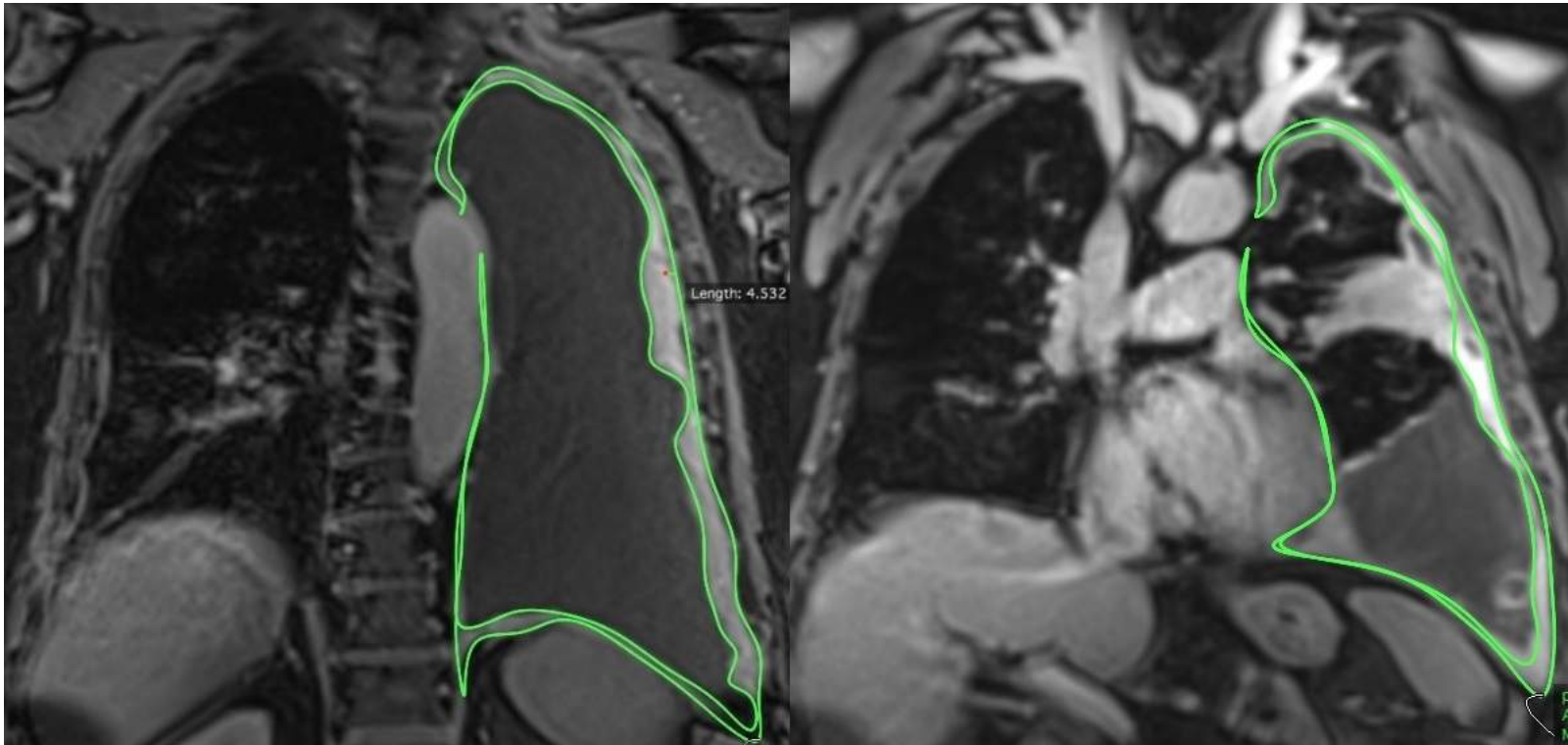
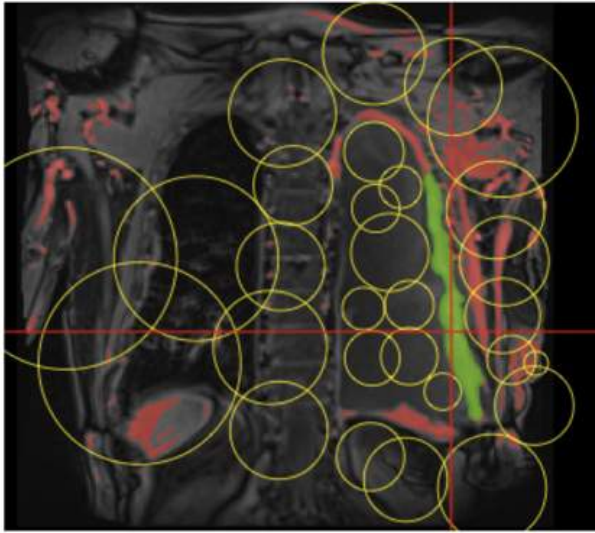
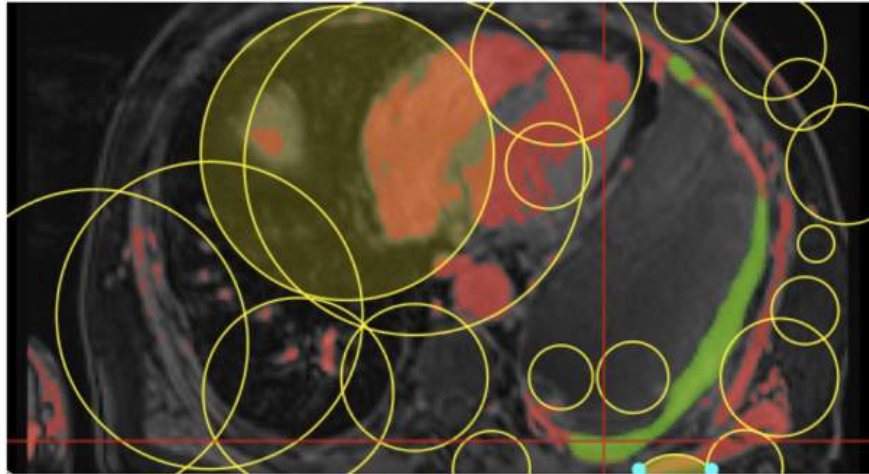


Figure 4.3 Manual delineation of pleural volume at contrast-enhanced MRI using OsiriX software

Panel A



Panel B



Panel C

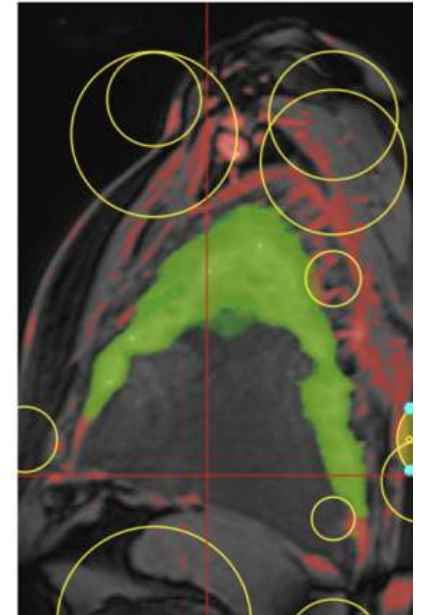


Figure 4.4 Semi-automated volume segmentation in a patient with MPM at contrast-enhanced MRI, in coronal (Panel A), axial (Panel B) and sagittal (Panel C) planes, using the MIAlite plugin for OsiriX. Areas of similar signal intensity to the 'seeding circles' (not shown) are highlighted in red. The yellow 'blocking circles' are placed to prevent seeding in to adjacent structures. The final segmented volume is highlighted in green.

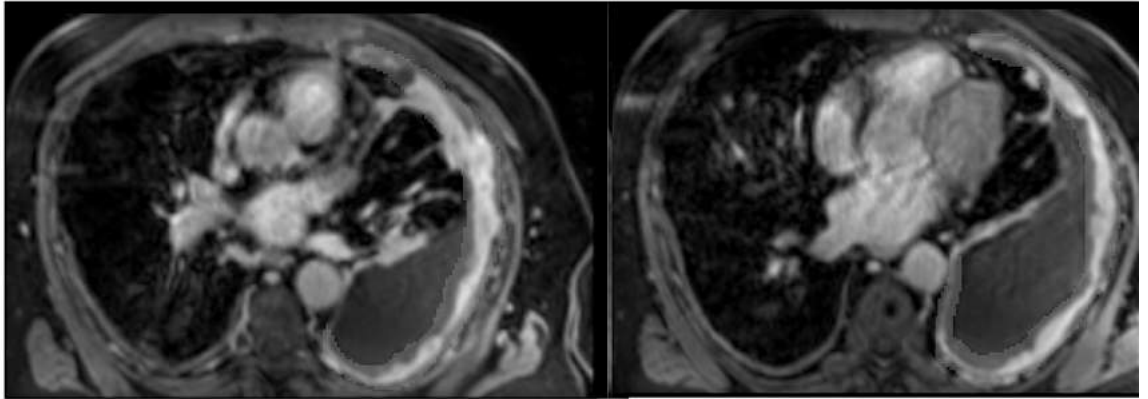
4.3.7 Segmentation using Myrian®

Axial images were used for initial volumetric measurements due to familiarity with axial images from routine clinical practice and perceived easier delineation of anatomical structures, particularly at the extreme ends of the image series, and ease of free-hand ROI drawing. Once these measurements were complete, coronal and sagittal images were also reviewed for completeness.

4.3.7.1 Use of a contour mask to constrain region growing

For all four analysis methodologies subsequently described, a free-hand region of interest (ROI) 'contour mask' was defined prior to signal intensity threshold-based segmentation to improve precision of the final segmented volume of interest. Creation of the contour mask allowed me to largely constrain subsequent signal intensity-based region growing to the pleura. Initially, image brightness was optimised for visualisation of the pleura before the ROI contour mask was defined, based on visual analysis and manual delineation of the pleura every 8 - 10 slices. Care was taken to delineate pleura from adjacent structures. The ROI contour mask was then extended through the entire image series semi-automatically to create a complete contour mask (See Figure 4.5). Small adjustments to the semi-automated contour mask were then made if required. The ability to draw a free-hand contour mask with Myrian® software overcame the limitation of being restricted to blocking circles with the MIAlite plugin for OsiriX.

Panel A



Panel B

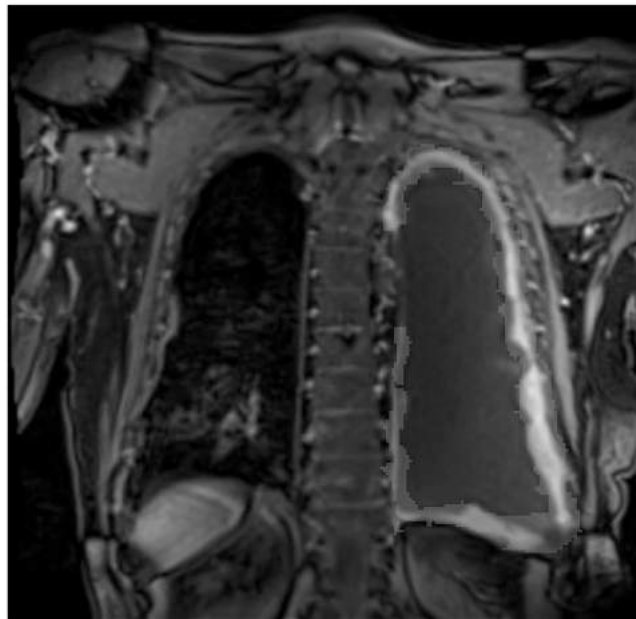


Figure 4.5 Contour mask (grey) of pleural volume in axial (Panel A) and coronal (Panel B) planes, created semi-automatically using Myrian[®] software

4.3.7.2 Segmentation based on signal intensity thresholds

After creation of a contour mask, a semi-automated region-growing step followed, based on signal intensity threshold parameters. Four different signal intensity threshold parameters were defined, as described in the following sections. A semi-objective scoring matrix was used to define the optimum set of parameters to assess tumour volume.

4.3.7.3 Segmentation Method 1

The signal intensity threshold parameters for region growing in method 1 was defined from the median SI range from the 28/31 patients included in the volumetry study who were ECE positive, excluding SI data from ROI where ECE was negative (219/492 ROI excluded) (as described in Chapter 3). This SI range was $\pm 81\text{AU}$.

Exclusion of ECE negative ROI to calculate the SI range was done due to the potential that these ROI were placed on interspersed areas of benign pleura in patients with MPM.

The '3D wand' tool available within Myrian[®] software was then used to measure signal intensity in up to 3 ROI manually placed on the pleura. Region-constraining signal intensity threshold parameters were based on the SI measured by the 3D wand $\pm 163\text{AU}$. Segmentation of everything within the contour mask that had signal intensity within this SI threshold range was then performed automatically resulting in a segmented volume, see Figure 4.6.

4.3.7.4 Segmentation Method 2

The signal intensity threshold parameters for region growing in method 2 was defined using the signal intensity measured from all ROI (n=492) in MPM patients who were ECE positive (28/31). The median SI range for these patients was calculated as $\pm 99\text{AU}$. This SI range was tested as it was felt to be representative pleural sampling in an MPM population.

ECE negative ROI were not excluded as in method 1 so that a wide distribution of pleural ROI per patient remained included for the final median SI range calculation.

The 3D wand tool was used as described in method 1, measuring SI in up to 3 ROI manually placed on pleura. The signal intensity threshold parameter was defined as the SI measured by the 3D wand $\pm 99\text{AU}$.

Identical to method 1, subsequent region growing included all structures included within the contour mask with a signal intensity falling within this SI threshold parameter was performed automatically, see Figure 4.7.

4.3.7.5 Segmentation Method 3

The signal intensity threshold parameters for region growing in method 3 was based on the individual signal intensity range for each patient (31/31). Signal intensity was measured in 15 ROI for each patient, evenly distributed throughout the pleura as described in Chapter 3, section 3.3.6.3, page 162. The difference between the maximum measured SI and the minimum measured SI in these 15 ROI was used as the SI threshold range. Each patient therefore had an individual signal intensity threshold parameter, based on what was felt to be representative pleural sampling.

The 3D wand tool was then used to measure signal intensity in up to 3 ROI manually placed on the pleura as described for Segmentation Methods 1 and 2. Segmentation SI threshold parameters were based on the SI measured by the 3D wand \pm the SI range for that individual patient. Segmentation of everything within the contour mask that had signal intensity within this SI threshold was then performed automatically, resulting in a segmented volume, see Figure 4.8.

4.3.7.6 Segmentation Method 4

The SI threshold parameters used for segmentation in method 4 was based on the mean SI ± 2 standard deviations (SD) measured in pleural ROI for each individual patient (31/31 patients included in the volumetry study). For patients with non-nodular pleural disease (20/31), the mean SI ± 2 SD was based on SI measured in 15 ROI. For patients with nodular pleural disease (11/31), the mean

SI \pm 2 SD was based on SI measured in up to 15 ROI placed on nodular pleura plus an additional 6 ROI placed on areas of non-nodular pleura.

The ROI SI range in non-nodular patients was normally distributed and \pm 2 SD therefore represented individualised 95% confidence intervals for SI threshold parameters. For the nodular patients, the ROI SI range was not normally distributed. \pm 2 SD therefore did not represent a 95% confidence interval for SI distribution in these patients. However, it was felt to be important to include additional SI measured from ROI placed on areas of non-nodular pleura to ensure inclusion of representative pleura in the final volume of interest.

The '3D wand' seeding step was not required for this method. Segmentation of all structures within the contour mask with a signal intensity falling within the segmentation SI threshold parameters were automatically segmented, (see Figure 4.9).

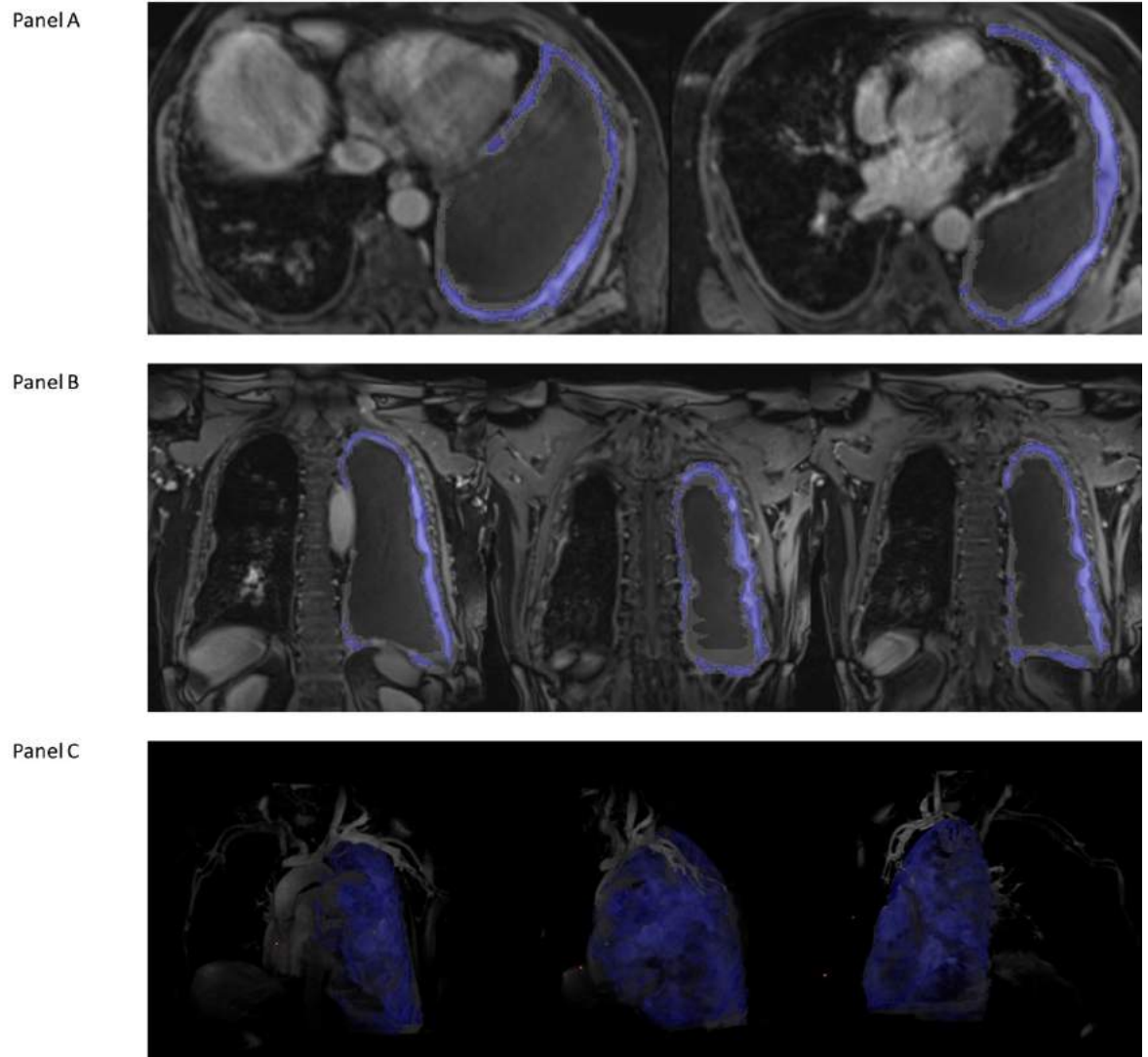
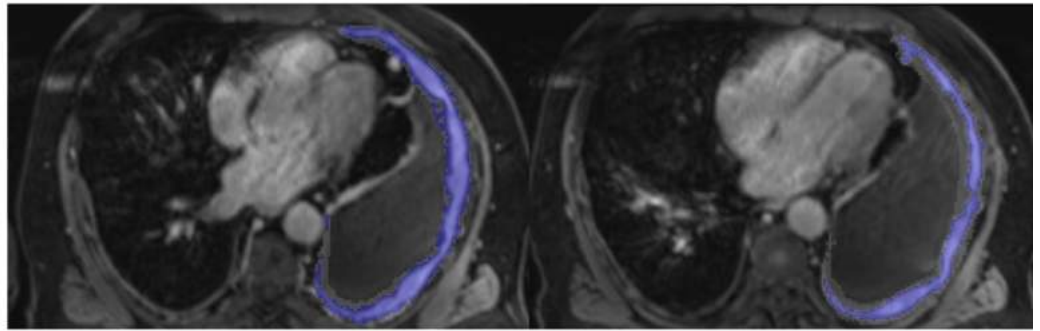
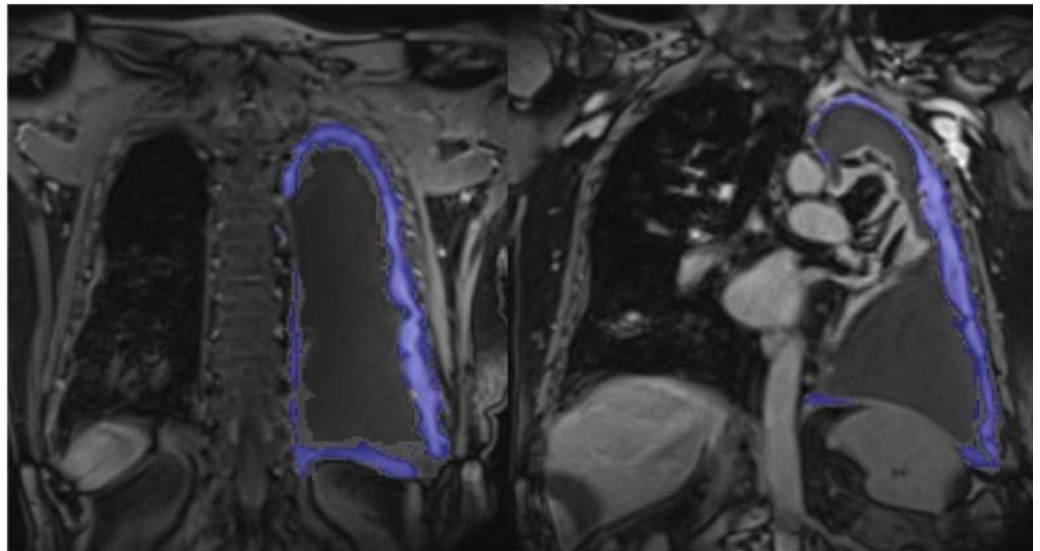


Figure 4.6 Semi-automated, threshold-based segmentation of pleural volume at contrast-enhanced MRI using Methodology 1 (SI of pleural ROI \pm 81AU). The segmented volume is highlighted in blue (Panels A (axial plane) and B (coronal plane)). Panel C is a 2D image of the completed volumetric study from anterior, left lateral and posterior positions.

Panel A



Panel B



Panel C



Figure 4.7 Semi-automated, threshold-based segmentation of pleural volume at contrast-enhanced MRI using Methodology 2 (SI of pleural ROI \pm 99AU). The segmented volume is highlighted in blue (Panels A (axial plane) and B (coronal plane)). Panel C is a 2D image of the completed volumetric study from anterior, and left lateral positions.

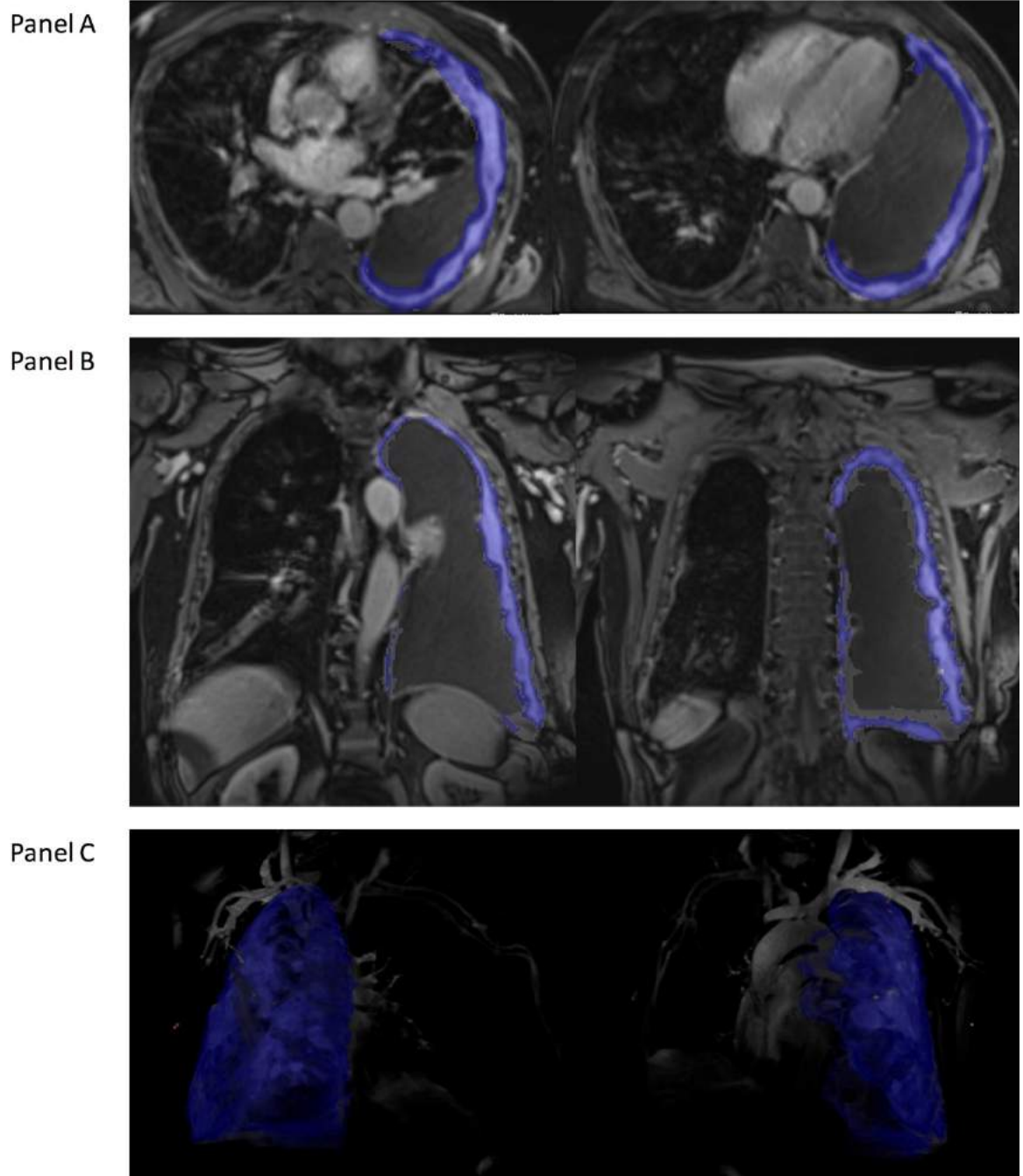
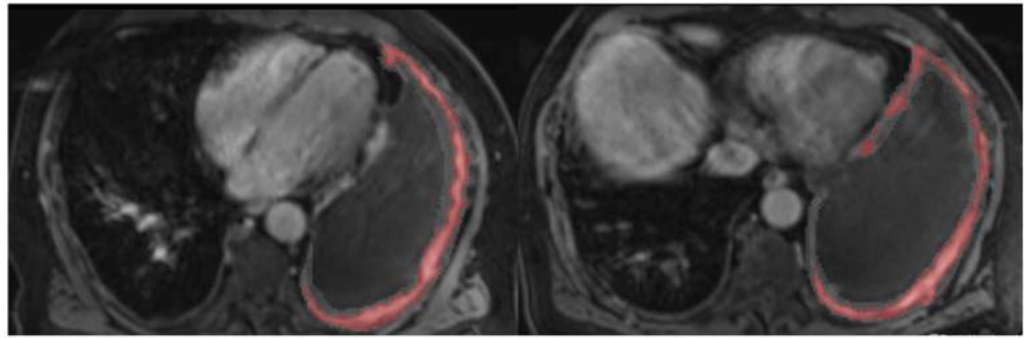
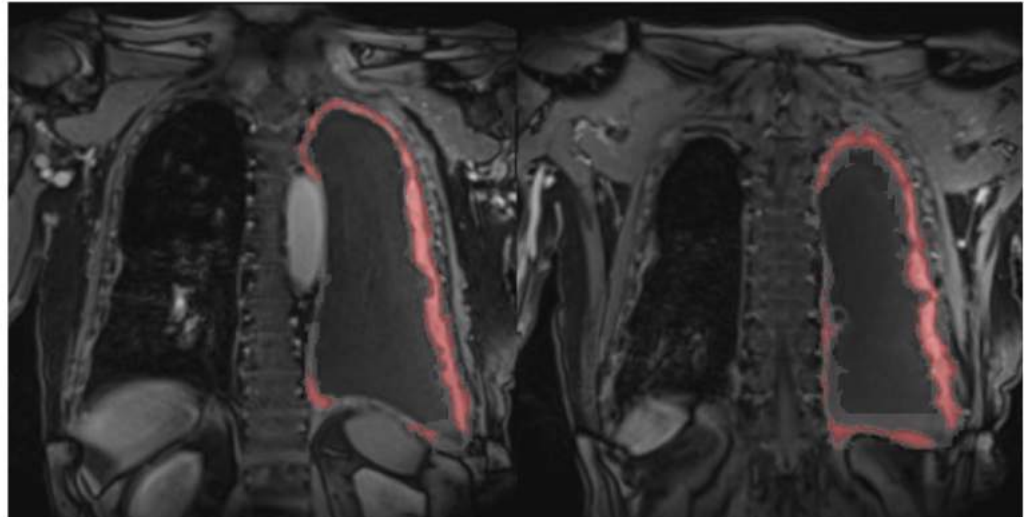


Figure 4.8 Semi-automated, threshold-based segmentation of pleural volume at contrast-enhanced MRI using Methodology 3 (SI of pleural ROI \pm signal intensity range for individual patient). The segmented volume is highlighted in blue (Panels A (axial plane) and B (coronal plane)). Panel C is a 2D image of the completed volumetric study from anterior and left lateral positions.

Panel A



Panel B



Panel C

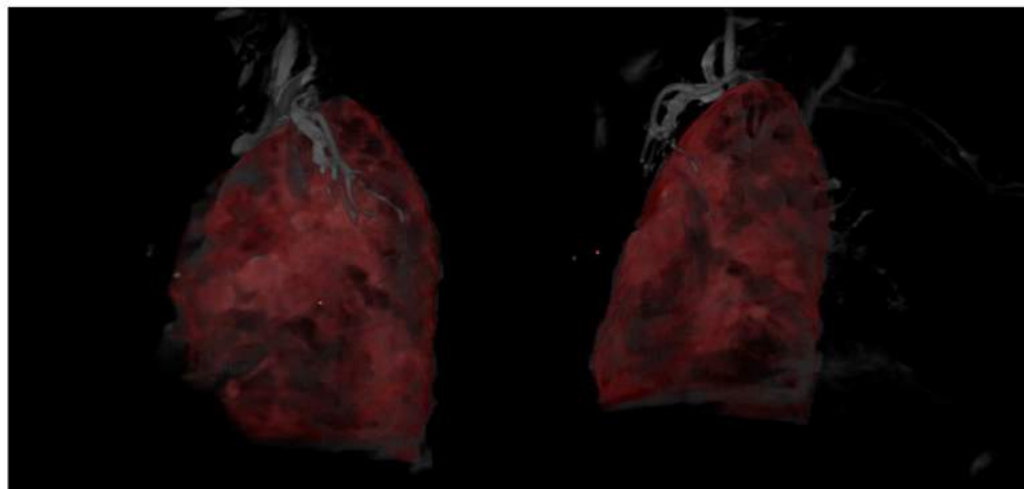


Figure 4.9 Semi-automated, threshold-based segmentation of pleural volume at contrast-enhanced MRI using Methodology 4 (mean signal intensity \pm 2SD for the individual patient). The segmented volume is highlighted in red (Panels A (axial plane) and B (coronal plane). Panel C is a 2D image of the completed volumetric study from anterior and left lateral positions.

4.3.8 Reproducibility

Volume was measured in each of the 3 repeated MRI phantom scan series to estimate variance between measurements. Pleural volumes for 15/31 randomly selected cases were re-measured by ST, after a lapsed time period of approximately 3 months in order to assess intra-observer agreement for all 4 segmentation methodologies.

4.3.9 Defining Optimum Segmentation Methodology

Optimum methodology was defined using a scoring matrix. Points for each method were awarded based on their performance across a number of factors. Points were awarded (minimum of 1 point for the methodology with the poorest performance up to a maximum of 4 points for the methodology with the best performance) for each of the following variables:

- Accuracy of measured MRI phantom volume - points awarded in decreasing order based on the error of the estimated volume around the MRI phantom true volume, e.g. 4 points were awarded to the methodology resulting in the estimated volume with the smallest error around in the MRI phantom and 1 point awarded to the methodology resulting in the largest error around the phantom.
- Subjective visual assessment that the final segmented volume encompasses the majority of visible disease without excessive inclusion of adjacent structures - points awarded in decreasing order from best subjective visual assessment (4 points) to worst subjective visual assessment (1 point).
- Time taken to complete segmentation - points awarded in decreasing order from shortest to longest time to complete volume measurements.
- Reproducibility (based on intra-observer agreement) - points awarded in decreasing order from highest intra-observer Intraclass Correlation Coefficient (ICC) to lowest intra-observer ICC.

The methodology with the highest Optimum Methods Score based on the above parameters was defined as the optimum methodology and was used for all subsequent analyses.

4.3.10 Inter-observer agreement

In order to assess inter-observer agreement, pleural volumes for 15/31 randomly selected cases were also measured by an experienced thoracic radiologist (GC), using the optimum methodology only. GC was blinded to all image analysis results and patient outcomes.

4.3.11 Statistical Analysis

Data distribution was assessed using histograms and D'Agostino-Pearson normality test. Normally distributed data are described by mean (\pm SD) and non-normally distributed data are described by median (inter-quartile range).

Intraclass correlation co-efficient (ICC) was used to assess intra-observer and inter-observer agreement. The relationship between pleural volumetry and clinical T-stage was examined Spearman's rho test and Jonckheere's trend test. Difference in mean MRI tumour volume between patients with T1/T2 disease versus T3/T4 disease was compared using unpaired Student's t-test. Survival analyses were performed using Cox proportional hazards regression and Kaplan-Meier methodology. Patient groups (high volume versus low volume) were dichotomised around increasing intervals of 100cm^3 to determine the volume that resulted in the widest separation of the survival curves. A backwards stepwise Cox proportional hazards regression model was used to determine whether tumour volume (as a categorical variable - high versus low tumour volume) was an independent predictor of survival. The co-variables used in this analysis were Eastern Cooperative Oncology Group (ECOG) performance status (PS), patient age, sex, white cell count (WCC), serum albumin and haemoglobin. Age was treated as a continuous variable and the remaining co-variables were treated as categorical variables. These co-variables were selected as they had previously been identified as being of prognostic significance in MPM. (386,387) Co-variables were tested to exclude multi-collinearity before being included in multivariate analysis.

A p value ≤ 0.05 was considered statistically significant in all tests. All other statistical analyses were performed using Graphpad Prism v7 (San Diego, USA) and IBM SPSS Statistics v22.0 (IBM, New York, USA) for Mac.

4.4 RESULTS

4.4.1 Patient Population

31 patients were included (Figure 4.10), all patients had pleural MRI performed prior to thoracoscopy or image-guided biopsy (median 1 (1 - 13) days) and prior to any significant pleural intervention other than diagnostic pleural aspiration. Mean patient age was 76 (7) years, 28/31 (90%) were male, 27/31 (87%) had a history of asbestos exposure and median overall survival was 14 months.

21/31 (68%) had epithelioid subtype, 4/31 (13%) biphasic subtype, 5/31 (16%) sarcomatoid subtype and 1/31 (3%) had mesothelioma *NOS*. 20/31 (65%) had IMIG/TNM7 stage I disease, 0/31 stage II disease, 9/31 (29%) stage III disease and 2/31 (6%) stage IV disease. 5/31 (16%) had evidence of nodal and/or distant metastatic disease. 6/31 (19%) patients completed four cycles of Platinum/Pemetrexed combination chemotherapy.

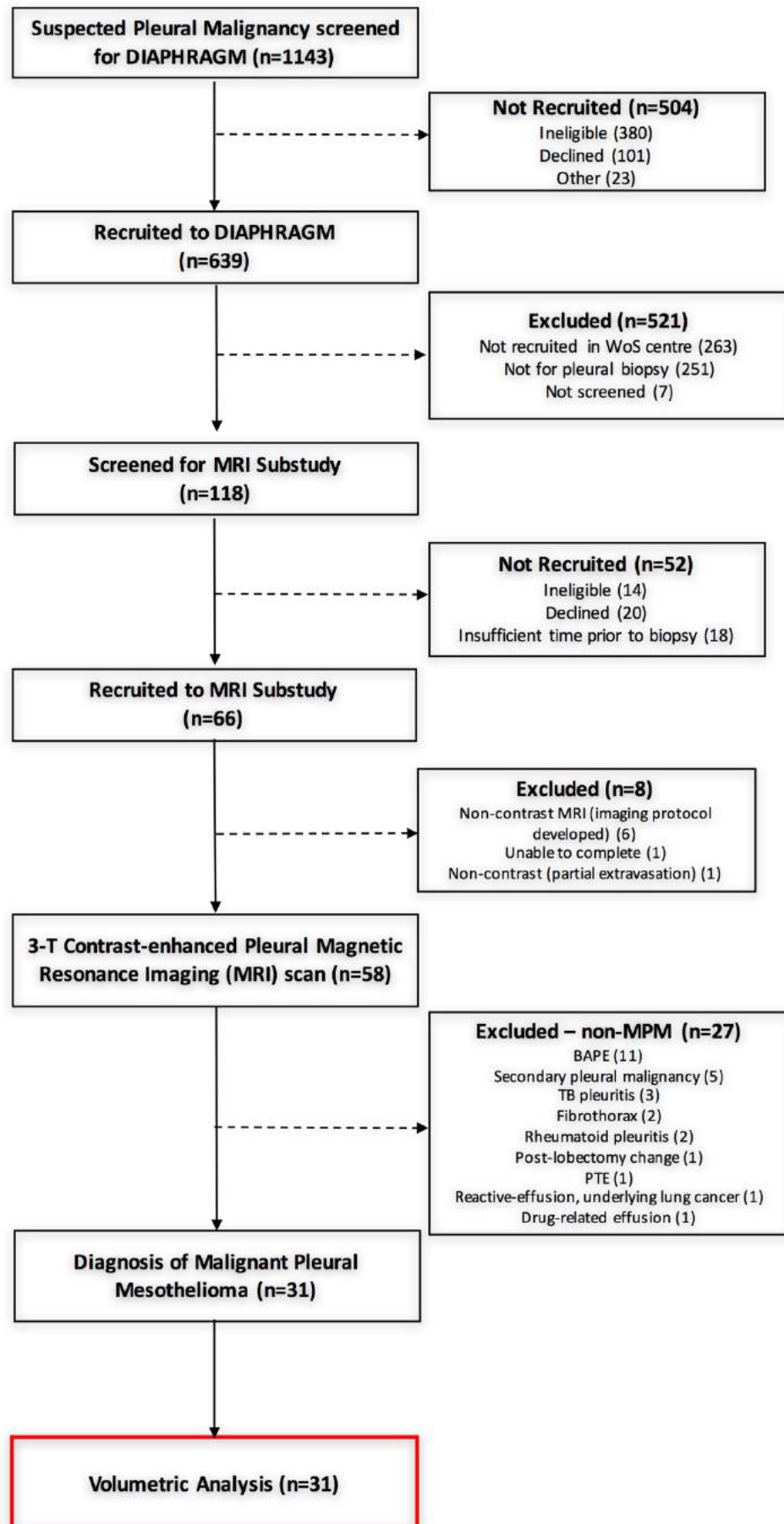


Figure 4.10 MRI Volumetry study flowchart

4.4.2 MRI Volume Analyses

4.4.2.1 MRI Phantom

MRI phantom volume using analysis methodology 1 was 1301cm^3 (-59cm^3 , 4.3% error); using methodology 2 was 1311cm^3 (-49cm^3 , 3.6% error); using methodology 3 was 875cm^3 (-485cm^3 , 35.7% error) and using methodology 4 was 1553cm^3 ($+193\text{cm}^3$, 14.2% error).

4.4.2.2 Patient Volumetry

Measured pleural volume for each patient using each analysis methodology is detailed in Table 4.3. Intra-class correlation coefficient for each of the four methodologies is summarised in Table 4.4. Inter-item correlation matrix for each of the four methodologies is summarised in Table 4.5. Intraclass correlation coefficient between the four methodologies was 0.745 (95% CI 0.616 - 0.851).

Methods one and two had similar analysis times, requiring approximately 14 minutes to complete the contour mask and then a further 1 - 2 minutes to select up the pleural ROI for threshold-based segmentation (i.e. a total analysis time of approximately 16 minutes).

Methods three and four required the additional step of measuring SI within up to 15 ROI to establish threshold criteria prior to segmentation, which took approximately 11 minutes. Method three required selection of a pleural ROI seed-point for segmentation, resulting in a total analysis time of approximately 28 minutes. As method four does not require the user to select a pleural seed-point ROI to perform segmentation, completion of volume analysis using method 4 took approximately 27 minutes.

Table 4.3

Pleural tumour volumes for 31 patients with Malignant Pleural Mesothelioma measured at contrast-enhanced Magnetic Resonance Imaging using four different semi-automated segmentation methodologies

Patient	Method 1 Volume (cm3)	Method 2 Volume (cm3)	Method 3 Volume (cm3)	Method 4 Volume (cm3)
1	380	444	469	234
2	213	259	194	430
3	212	265	215	269
4	499	614	576	304
5	270	453	379	247
6	241	375	445	394
7	367	336	341	436
8	450	185	220	235
9	313	317	320	236
10	128	229	321	149
11	106	281	213	312
12	156	363	270	445
13	337	380	330	155
14	164	223	315	225
15	219	339	699	358
16	134	222	562	316
17	373	461	309	383
18	98	113	125	133
19	109	214	258	185
20	455	654	419	338
21	228	457	544	341
22	313	591	618	595
23	352	346	384	420
24	211	280	259	255
25	501	488	628	472
26	269	317	401	252
27	135	349	336	370
28	272	292	261	354
29	505	517	542	454
30	442	560	284	351
31	471	556	690	342

Table 4.4

Intra-observer agreement of four different methodologies tested in the volumetric assessment of 15/31 patients with Malignant Pleural Mesothelioma

	Intraclass Correlation Co-efficient	95% Confidence Interval
ST (1) vs. ST (2) Method 1	0.869	0.654 - 0.954
ST (1) vs. ST (2) Method 2	0.875	0.665 - 0.953
ST (1) vs. ST (2) Method 3	0.849	0.551 - 0.949
ST (1) vs. ST (2) Method 4	0.941	0.825 - 0.980

Table 4.5

Inter-item Correlation Matrix between four different methodologies tested in the volumetric assessment of 31 patients with Malignant Pleural Mesothelioma

	Method 1	Method 2	Method 3	Method 4
Method 1	1	0.893	0.726	0.694
Method 2	0.893	1	0.8	0.762
Method 3	0.726	0.8	1	0.683
Method 4	0.694	0.762	0.683	1

4.4.3 Methodology Ranking

Methodology ranking is summarised in Table 4.6. As analysis time was identical for methods one, two and three, these methods were all awarded the same number of points. Based on total scoring, Methodology 2 was defined as the optimum methodology for volumetric assessment of the pleura. Volumetry results using analysis methodology 2 are therefore used for the remainder of analyses included in this chapter.

Table 4.6

Scoring matrix to define optimum methodology between four different methodologies in the volumetric assessment of patients with Malignant Pleural Mesothelioma. Scoring is in descending order of best performance to worst performance for four different variables: (1) Error around volume measurements of an MRI Phantom; (2) Subjective visual assessment of inclusion of pleural without excessive inclusion of adjacent structures; (3) Analysis time; (4) Intra-observer intra-class correlation co-efficient

Method	Accuracy: Phantom Error		Accuracy: Visual		Analysis Time		Intra-observer agreement		Total Score
	Result	Score	Result	Score	Result	Score	Result	Score	
1	-4.3%	3	NA	2	16 min	4	0.869	2	11
2	-3.6%	4	NA	4	16 min	4	0.875	3	<u>15</u>
3	-16.6%	2	NA	3	28 min	2	0.849	1	8
4	-35.7%	1	NA	1	27 min	3	0.941	4	9

4.4.4 Reproducibility

The standard deviation around measurement of phantom volume at repeat scanning was $\pm 18\text{cm}^3$ ($\pm 1.4\%$). Regarding measurements of patient tumour volume, ICC for initial and repeated analysis by ST for intra-observer reproducibility was 0.875 (95% CI 0.665 - 0.953). ICC between ST and GC for inter-observer reproducibility was 0.962 (95% CI 0.893 - 0.987). In 87% (13/15) of cases, the absolute difference in volume between the 2 readers was $\leq 100\text{cm}^3$. Bland-Altman analysis demonstrated a bias of 6.896, see Figure 4.11.

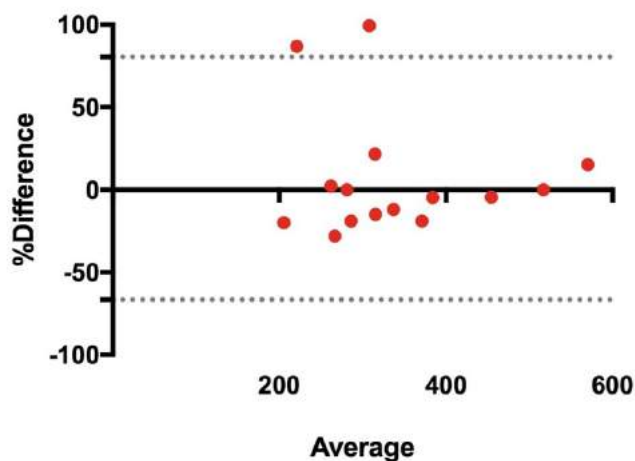


Figure 4.11 Bland-Altman analysis comparing volume measurements performed by ST and GC

4.4.5 Relationship between primary tumour volume and clinical T-stage

Mean MRI primary tumour volumes for T1 (n=20), T2 (n=1), T3 (n=9) and T4 (n=1) were 365.5cm^3 , 349cm^3 , 395.8cm^3 and 259cm^3 respectively, see Figure 4.12. There was no significant difference in MRI primary tumour volume between patients with clinical T1 or T2 disease (tumour volume 364.7cm^3) and those with T3 or T4 disease (tumour volume 382.1cm^3), $p=0.75$. There was no significant correlation between measured primary tumour volume and clinical T-stage (Spearman's $\rho = 0.02$, $p=0.897$, Jonckheere's trend test $p=0.935$).

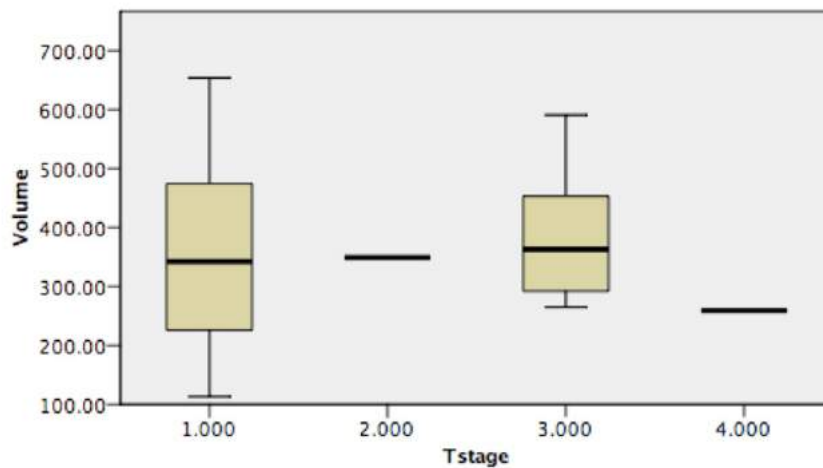


Figure 4.12 Relationship between clinical T-stage and measured pleural tumour volume at contrast-enhanced MRI

4.4.6 Relationship between disease volume and survival

Median survival for all patients was 14 months. Median primary tumour volume was 346cm^3 (IQR $265 - 461$). There was a statistically significant reduction in median overall survival in patients with higher tumour volume, dichotomised around 200cm^3 and 300cm^3 . The widest separation in survival curves occurred when patient groups were dichotomised around 300cm^3 . Patients with a high tumour volume ($\geq 300\text{cm}^3$) had a significantly poorer median overall survival (8.5 months versus 20 months, HR 3.14 (95% CI 1.33 - 7.4), $p=0.0088$, see Figure 4.13 (Panel A)). This remained true when confining the analysis to 21/31 patients with epithelioid disease (median OS 9 months versus 25 months, HR 3.84 (95% CI 1.27 - 11.56), $p=0.017$, see Figure 4.13 (Panel B)) and in 18/31 patients with epithelioid disease with no nodal or distant metastatic involvement (median OS 8.5 months versus 25 months, HR 4.2 (95% CI 1.2 - 15.1), $p=0.027$, see Figure 4.13 (Panel C)). In all patients, increasing tumour volume, by tertile ($\leq 250\text{cm}^3$, $250 - 400\text{cm}^3$, $\geq 400\text{cm}^3$), was associated with decreasing median OS, see Figure 13(d); logrank for trend $p=0.023$).

Haemoglobin and primary tumour volume were the only variables with statistical significance in the univariate Cox model (HR 2.035 (95% CI 1.154 - 3.589) for Hb $<14\text{g/dl}$, $p=0.014$, and HR 2.273 (95% CI 1.162 - 4.446) for primary tumour volume $\geq 300\text{cm}^3$, $p=0.016$), see Table 4.7. Both haemoglobin and primary tumour volume retained statistical significance in the multivariate Cox model, see Table 4.8.

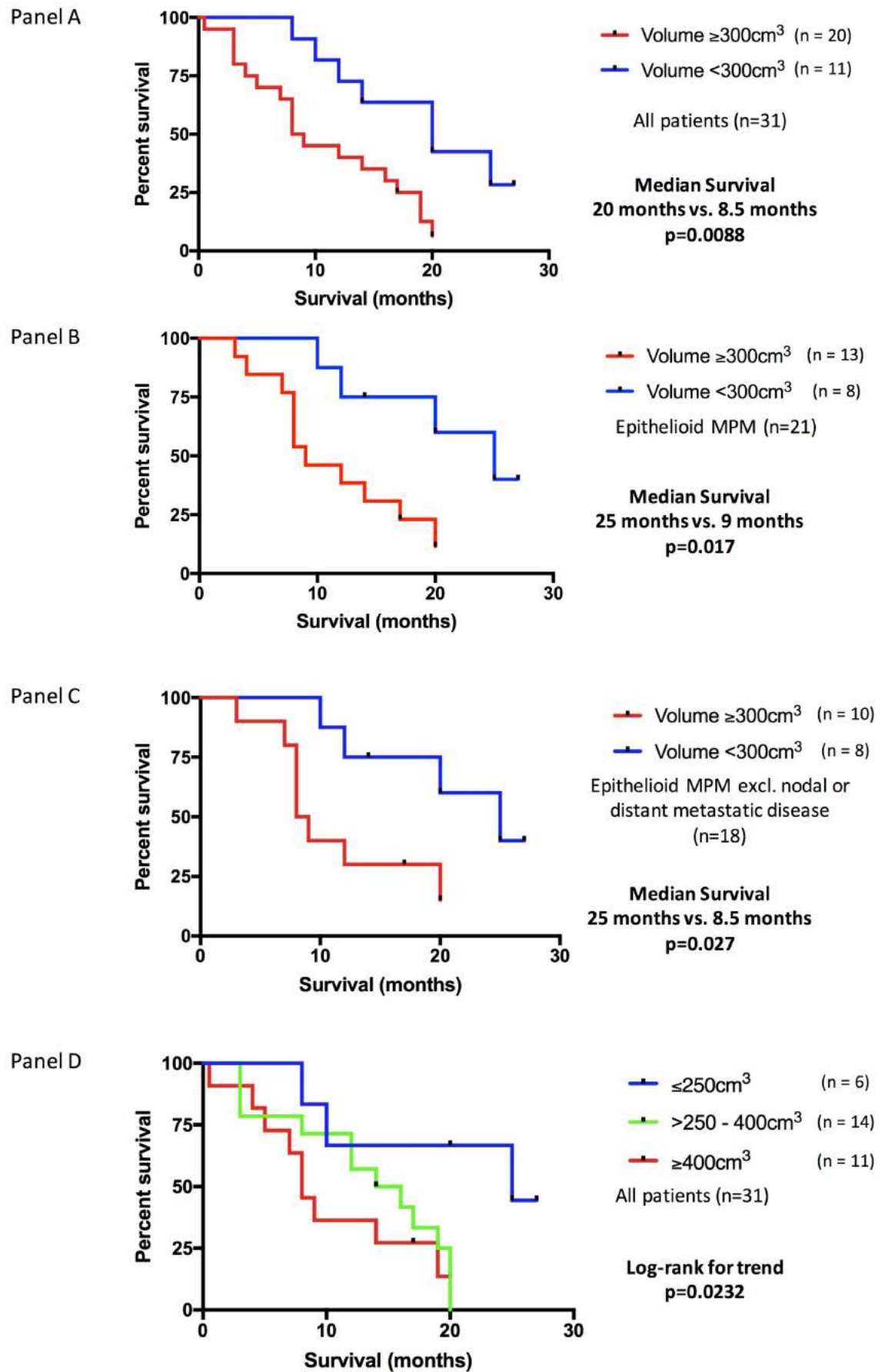


Figure 4.13 Kaplan-Meier curves demonstrating median overall survival based on MRI-estimated tumour volume in patients with MPM

Table 4.7

Prognostic factors for 31 patients with Malignant Pleural Mesothelioma (MPM) analysed in a univariate Cox proportional hazards model

Variable	n	Hazard ratio	95% Confidence Intervals	p value
<i>Sex</i>				
Female	3			
Male	28	4.044	0.952 - 17.188	0.058
<i>Age</i>	31	1.006	0.950 - 1.065	0.829
<i>ECOG Performance Status</i>				
0/1	24			
2/3	7	1.943	0.966 - 3.911	0.063
<i>Haemoglobin</i>				
≥14g/dl	17			
<14g/dl	14	2.035	1.154 - 3.589	0.014
<i>White Cell Count</i>				
<8.2 x10 ⁹ /l	15			
≥8.2 x 10 ⁹ /l	16	0.668	0.380 - 1.174	0.161
<i>Serum albumin</i>				
≥35g/l	17			
<35g/l	14	1.678	0.946 - 2.975	0.077
<i>Histological Subtype</i>				
Epithelioid	21			
Biphasic	4	2.128	0.510 - 8.879	0.3
Not specified	1	1.367	0.497 - 3.756	0.545
Sarcomatoid	5	0.886	0.257 - 3.057	0.847
<i>Disease Stage</i>				
I/II	20			
III/IV	11	1.511	0.854 - 2.673	0.156
<i>Tumour Volume</i>				
<300cm ³	11			
≥300cm ³	20	2.273	1.162 - 4.446	0.016

Table 4.8

Prognostic factors for 31 patients with Malignant Pleural Mesothelioma (MPM) analysed in a backwards stepwise multivariate Cox proportional hazards model

<i>Variable</i>	<i>Hazard Ratio</i>	<i>95% Confidence Interval</i>	<i>p value</i>
Haemoglobin	2.515	1.384 - 4.569	0.002
Tumour volume	2.114	1.046 - 4.270	0.037

4.5 DISCUSSION

This chapter reports on novel methodology for semi-automated assessment of primary tumour volume in patients with MPM, utilising contrast-enhanced MRI and a semi-automated, signal intensity threshold-based segmentation methodology. Myrian® software (Intrasense®, Montpellier, France) was used for volume segmentation. This software has previously been used for MRI-based, semi-automated volumetric assessment of organ volumes in infants undergoing post mortem examination following sudden unexpected death. (388) In this previous study, T2-weighted True FISP sequences and T1-weighted volumetric interpolated breath-hold examination (VIBE) sequences were acquired at 1.5T MRI. Similar to the methods described herein, images were acquired iso-volumetrically to allow image reconstruction and to facilitate organ delineation and contours of organs were outlined semi-automatically. Agreement between MRI volumes and actual organ volume at post-mortem varied depending on the organ under assessment; the authors reported good agreement for brain, liver and lungs in this study. (388) Frauenfelder *et al* also used Myrian® software to examine voxel-based tumour volumes in 30 patients with MPM undergoing CT as a potential alternative to modified RECIST for assessment of response to systemic therapy. (389) They reported a high intra-class correlation coefficient of 0.99 between three independent readers, with superior agreement in comparison to assessment by modified RECIST criteria.

The optimum methodology in our study was defined using an objective scoring matrix, which integrated the accuracy of MRI phantom volume measurements, the time taken to complete the analysis, subjective best visual assessment and reproducibility. Sargent *et al* reported criteria which should be considered when using a novel imaging methodology as an outcome measure in cancer clinical trials. This included accuracy, variance, reproducibility, availability of the imaging technology and a standardised interpretation protocol. (390) In our study, using the optimum methodology, the time taken to complete volume assessment was approximately 16 minutes per study, the standard deviation around the MRI phantom measurement was $\pm 1.4\%$, accuracy was within 5% and

there was good inter-observer reproducibility (ICC 0.964 (95% CI 0.898 - 0.987)). MRI as an imaging technology is becoming more widely available and is accessible in most centres. In addition, the method described involves a standardised signal intensity threshold range for all patients, eliminating one potential source of variability between measurements. The inter-observer agreement in this study was excellent (ICC 0.964). Our reproducibility is similar to the earlier study reported by Frauenfelder *et al* (389) and that reported by Rusch *et al* in a multi-centre study of CT volumetry in MPM. Although Rusch *et al* did not report intraclass correlation co-efficients in this study, they reported good correlation (Spearman's rho = 0.822) between readers and an absolute difference in CT volume of $\leq 200\text{cm}^3$ in 80% of cases, (138) similar to that reported in our study (absolute difference in MRI volume of $\leq 100\text{cm}^3$ in 87% of cases). However, only 129/164 cases were included for examination by both reference radiologists and despite good correlation of CT volume estimates overall, there were discrepancies in volume estimates of $>60\text{cm}^3$ in 35 cases and $>170\text{cm}^3$ in 16 cases between readers. Of the 16 cases with major differences in volume estimate, 8/16 (50%) were as a result of limited distinction between tumour and adjacent tissues, including cases with moderate or large volume loculated effusion. (137) The superior contrast resolution of contrast-enhanced MRI and therefore better delineation of pleural tumour to adjacent tissues and pleural fluid, as discussed herein, is a potential advantage of MRI in this regard. Other reported reasons for discrepancy between volume measurements in the earlier study included data entry errors, perception errors, resulting from difference in the perception of the location of the tumour between readers and user error in software tool knowledge. (137)

A possible source of error in volume measurements in our study was the potential for unintentional exclusion of disease at the extreme apex and costophrenic recess or unintentional inclusion of adjacent structures, such as intercostal muscle. Our use of isotropic image acquisition should however limit this, as it allows for volumetric assessment in axial, coronal and sagittal planes, taking advantage of precise three-dimensional reconstruction of images and potentially limiting partial volume effect at the extreme apex or costophrenic recess. In addition, the MRI acquisition parameters in our study included a 1.8 - 1.9mm slice thickness with no inter-slice gap, which is lower than that

previously in previous CT volumetry studies by Liu *et al* (5 - 7.5mm slice thickness, inter-slice gap thickness not reported) (391) and Gill *et al* (5mm slice thickness with a 5mm inter-slice gap). (135) Previous studies have demonstrated that increasing slice thickness can result in an under-estimation of true volume in CT volumetric assessment of the liver. (392)

In addition, our use of signal intensity thresholds and the contrast timing of 4.5 minutes was with the intention of exploiting differing biologic properties of pleural tumour from its surrounding structures, thus limiting their inclusion into the segmented volume. The ability to utilise differences in signal intensity to differentiate MPM tumour from surrounding structures based on their biologic properties is an additional advantage of the MRI methodology used here over previously described CT-derived methods, where this has been reported to be a significant challenge to overcome. (137)

4.5.1 Prognostic significance of tumour volume

Patients with a higher primary tumour volume ($\geq 300\text{cm}^3$) had significantly poorer survival in the current study. This remained true when confining the analysis to patients with epithelioid disease only, an important consideration as histological subtype has previously been demonstrated to be of prognostic significance, (387) with non-epithelioid histology consistently being associated with poorer overall survival. (393) Furthermore, worsening median O.S. with high tumour volume was demonstrated when excluding patients with epithelioid MPM with prognostically important extra-pleural disease, i.e. those with nodal or distant metastases. The separation in survival curves was in fact wider, with a median O.S. difference of 16.5 months when non-epithelioid and metastatic disease was excluded versus a median O.S. difference of 11.5 months when all patients were included.

Tumour volume was dichotomised around 300cm^3 as this cut-off resulted in the widest separation in survival curves between low and high tumour volumes. This was similar to the methodology of two previous MPM volumetry studies by Gill *et al* and Liu *et al*, who examined survival curves dichotomised around tumour volume at increasing increments, finally dichotomising around the tumour volume that provided the widest separation in survival curves (500cm^3 and

618.49cm³ respectively), rather than around the median tumour volume. On multi-variate analysis, tumour volume and haemoglobin were both independent predictors of survival in the patients with MPM in this study. Tumour volume, haemoglobin, age, sex, histological subtype, WCC, serum albumin and ECOG PS were all included in the multi-variate analysis despite not all variables being statistically significant on univariate analysis due to previous evidence that they are of prognostic significance in larger cohort and population-based studies. (386,387,393)

Our results are in concordance with those of several preceding studies, which utilised CT as the primary imaging modality for assessing primary tumour volume. Pass *et al* initially identified the prognostic significance of CT-derived tumour volume in 47 patients with MPM undergoing cytoreductive surgery +/- post-operative photodynamic therapy. (134) Patients with a higher pre-operative tumour volume ($\geq 100\text{cm}^3$) had a significantly poorer median overall survival than those with a lower tumour volume ($< 100\text{cm}^3$) - 11 months versus 22 months respectively, $p=0.03$. However, this cohort included patients undergoing two different operations- pleurectomy/decortication (P/D) and extrapleural pneumonectomy (EPP), which have subsequently been shown to be associated themselves with different subsequent survival. (394) In this study, patients undergoing EPP had a significantly higher pre-operative tumour volume than those undergoing P/D (418cm^3 versus 88cm^3 respectively, $p < 0.0001$) and the potential independent adverse prognostic impact of EPP itself (395) may confound the volumetric differences observed. Additionally, there was a high rate of nodal involvement in this study (68%). This is important as nodal involvement itself is associated with poorer overall survival in MPM. (127) It is therefore an additional important potential confounding variable here, particularly as higher tumour volumes were also associated with increased rates of nodal involvement in this study. This study was further limited by the laborious method of deriving tumour volume, which required manual delineation of the pleura in each CT slice, and the time taken to complete volume measurements was not reported. Furthermore, the authors did not include assessment of inter-observer variability of these subjectively-defined measurements.

Liu *et al* performed semi-automated primary tumour volume measurements using contrast-enhanced CT in 30 patients with MPM prior to chemotherapy +/- EPP and post-operative hemi-thoracic radiation. (391) Their method for segmenting pleural tumour from surrounding structures involved initially separating the chest wall and ribs from the lung and pleura using an interpolation technique. The authors unfortunately do not detail the steps or time taken to perform this technique. Once this step is complete, sequential thresholding was used to exclude lung, liver and spleen. The user then manually corrected any obvious segmentation error. Using this method, the authors reported good inter-observer agreement (concordance correlation coefficient 0.993 (95% CI 0.988 - 0.998) but did not report on time to assess each scan. Concordant with our findings, patients with a higher baseline primary tumour volume ($>618.49\text{cm}^3$) had a trend towards poorer median overall survival (10.2 months versus 21.5 months for patients with baseline tumour volume $<618.49\text{cm}^3$, $p=0.07$). This tumour volume was chosen to dichotomise patients as it yielded the greatest statistical difference in survival between groups. There was no significant survival difference when patients were dichotomized around the median tumour volume (473cm^3) and neither histological subtype nor nodal involvement were not taken into consideration in this earlier study. Importantly, approximately 50% of patients included had prior talc pleurodesis, a likely significant confounder when assessing pleural tumour volume.

Gill *et al* also reported similar findings to those described herein, again reporting poorer survival with high CT-derived primary tumour volume with 88 patients with epithelioid MPM undergoing EPP. (135) The volume segmentation method described in this earlier study involved automated software exclusion of pleural effusion, atelectatic lung, chest wall and adjacent solid organs followed by manual addition of identified areas of discontinuous and/or extrapleural tumour. The basis for software exclusion of adjacent structures, e.g. whether this was based on differing shape or spatial location of structures or differing Hounsfield Units, was not detailed and analysis time and inter-observer variability using this method were not reported. Median tumour volume was 319cm^3 . The authors reported a significant reduction in median overall survival associated with a higher tumour volume ($>500\text{cm}^3$, median overall survival 12 months versus 24.4 months, $p < 0.0001$). Similar to the present study, patients

were dichotomised at intervals of 100cm^3 to determine the optimum tumour volume cut-off yielding the greatest difference in survival between groups. Tumour volume remained an independent predictor of patient survival in multivariate analysis (HR 2.02, 95% CI 1.18 - 3.47, $p=0.01$).

Although we found the prognostic impact of increasing primary tumour volume to be statistically significant, due to small patient numbers ($n=31$) there was a wide 95% confidence interval around our hazard ratio (HR 2.73 (95% CI 1.162 - 4.446). Nonetheless, tumour volume was a statistically significant prognostic variable on univariate analysis ($p=0.016$) and retained statistical significance on multivariate analysis (HR 2.114 (95% CI 1.046 - 4.270), $p=0.037$).

Similar to our study, Plathow *et al* assessed tumour volume in patients with MPM using MRI. (385) Tumour volume was measured using a semi-automated region-growing technique and shape-based interpolation rather than a signal intensity threshold-based method of segmentation as described herein. Volume estimations in this earlier study were used as a method to assess response to chemotherapy and the authors did not report on the relationship between tumour volume and overall survival. In addition, only a single reader measured tumour volume and the authors therefore did not report on the reproducibility of their method. While the authors report that their volume segmentation methodology had previously been demonstrated to be accurate regarding correlation between measured and true tumour volume, the previous study that they referenced examined volume measurements in intra-pulmonary nodules (396), which, being spherical and surrounded by lung are much simpler structures to volume than primary pleural tumour.

PET-CT is an additional imaging modality that could be used for volumetric segmentation, exploiting increased ^{18}F FDG uptake by pleural tumour in comparison to adjacent lung, intercostal muscle and pleural fluid to potentially improving accuracy of semi-automated segmentation in comparison to CT alone. Nowak *et al* assessed tumour volume utilising ^{18}F FDG-PET in patients with MPM. (380) Tumour volume was measured using a 3-dimensional threshold-based growing algorithm from multiple ROI placed on pleural tumour. The threshold was based on mean FDG activity in the ROI in comparison to neighbouring pixels and the maximum normal background activity in the liver. Total Glycolytic

Volume (TGV) was calculated using total ROI volume and metabolic activity and was an independent predictor of prognosis on multivariate analysis. (380) However, 31% (n=28) of the patients in this study had prior pleurodesis, a potentially significant confounder given the well-documented intense metabolic activity associated with pleurodesis at PET-CT. (355,356) Furthermore, ^{18}F FDG-PET in isolation is limited by poor spatial resolution, particularly in comparison to MRI used in the present study, and while all the patients in this study additionally underwent CT examination, the PET scans were not integrated with CT images and the radiologists computing TGV were in fact blinded to CT analyses. (380)

Similarly, Lee *et al* used integrated PET-CT to measure pleural volume and metabolic activity (computing metabolic tumour volume (MTV) and total lesion glycolysis (TLG) parameters) in a small retrospective study of 13 patients with MPM undergoing extrapleural pneumonectomy +/- cisplatin/pemetrexed chemotherapy. They delineated an automated contour ROI, with thresholding based on mean SUV of the liver + 2SD. Patients with a high MTV and TLG and a significantly shorter time to tumour progression. However, this methodology for defining tumour volume is limited by the decision to use SUV of the liver to define the threshold for segmentation rather than that of the volume of interest, as is described in our methodology. Pleural lesions with intense FDG uptake may therefore be excluded, likewise, pleural tumour with low metabolic activity, e.g. early stage epithelioid tumours. Additionally, the authors did not report on the reproducibility of their method.

Kitajima *et al* recently used PET-CT and gradient-based segmentation (397) in a retrospective review of 201 patients with MPM. They reported that a high TLG $\geq 525\text{g}$ (calculated from $\text{MTV} \times \text{SUV}_{\text{mean}}$, where SUV_{mean} is the mean SUV of the tumour) was an independent predictor of poor survival at multivariate analysis. (398) However, the authors did not report on the reproducibility of their TLG measurements in this study. Gradient-based segmentation requires additional image processing steps to improve image resolution and signal-to-noise ratio prior to image analysis, which introduces another potential source of variability between scans. (397)

4.5.2 Tumour volume and disease stage

In this study, there was no significant correlation between clinical T-stage and primary tumour volume measured at MRI ($r=0.02$, $p=0.897$). This is perhaps not surprising as current T-staging describes the surfaces involved, the degree of extra-pleural invasion and potential resectability rather than tumour dimension measurements as is common in other tumours. (126) Our findings are concordant with that of Armato *et al*, who reported no significant difference in CT-derived tumour volume between patients with T1 or T2 disease and those with T3 or T4 disease. (399)

Conversely, Rush *et al* did report a correlation between CT-derived volume and pathologic T-stage in their multi-centre study, with increasing tumour volume being associated with increasing pathologic T-stage. (138) Importantly, there was considerable upstaging of clinical disease stage at the time of surgery in this study (62.8% clinical stage III/IV versus 86.9% pathologic stage III/IV disease). This again highlights the limitations of current clinical staging modalities and discrepancy between clinical and pathologic staging could be responsible for the contrasting findings between our study and this earlier study.

In our study, increasing tumour volume, when grouping patients into tertiles ($\leq 250\text{cm}^3$, $250 - 400\text{cm}^3$, $\geq 400\text{cm}^3$) was associated with a trend towards worsening median O.S. (not reached, 12 months and 8.5 months respectively), highlighting the potential role of imaging-based primary tumour volume as an alternative to clinical T-staging based on the extent of pleural surface involvement and extra-pleural invasion, as is currently the case. Rusch *et al* divided patients into quartiles based on CT-derived primary tumour volume, separation of Kaplan-Meier survival curves was demonstrated between all quartiles with the exception of quartile 2 and 3 (median O.S. 37 months, 18 months, 18 months and 8 months for quartile 1, 2, 3 and 4 respectively). (138) The author's therefore report that the best correlation between tumour volume and overall survival is demonstrated with three groups of volume measurements, similar to the analysis performed in our study.

In an earlier study, Kircheva *et al* reported that pathologic tumour volume, measured following extended pleurectomy/decortication, was a better predictor

of survival than T-stage (at multivariate analysis, tumour volume increasing per ml HR 1.001, $p=0.021$; T2 versus T1 HR 5.622, $p=0.028$; T3 versus T1 HR 4.55, $p=0.047$; T4 versus T1 HR 5.156, $p=0.033$). (400) This perhaps reflects that tumour burden is more accurately represented by tumour volume than current clinical T-stage.

Tumour thickness measurements is an alternative method for estimating disease burden. Nowak *et al* describe 3 single linear measurements at maximal tumour thickness from either chest wall or mediastinum, using axial CT images of patients with MPM. (126) Pleural tumour thickness measurements correlated with clinical T-stage and using the sum of the 3 measurements, increased tumour thickness was associated with poorer survival (median O.S. 13.2 months for the highest quartile group ($>50.0\text{mm}$) versus 23.4 months for the lowest quartile group ($<16.0\text{mm}$)), in addition to being associated with metastatic nodal involvement. (126) However, this method of tumour thickness measurement is likely to be subject to considerable inter-observer variability. In an earlier study by Armato *et al*, linear tumour thickness measurements perpendicular to either chest wall or mediastinum, were performed by six observers. Across all tumour thickness measurements, the 95% CI for inter-observer tumour thickness measurement differences was - 16.8 to 20.1%. The 95% CI were wider for measurements perpendicular to mediastinum, measurements of a fusiform mass or convex rind and with lower tumour thickness measurements (95% CI -25.6 to 34.5% for tumour thickness measurements $<5\text{mm}$ versus -6.8 to 7.3% for tumour thickness measurements $>20\text{mm}$). (401) In addition, using linear measurements obtained at a single image plane as opposed to 3D measurements as is performed in our study, is perhaps an over-simplification of the disease burden of this complex tumour.

4.5.3 Implementation and Future Testing

To be used in future clinical practice, the optimum methodology for examining tumour volume in this study requires the following steps:

1. Create a contour mask using free-hand ROI delineation of the pleura every 8 - 10 slices before automated propagation of the contour mask using Myrian® software

2. Make manual adjustments to the contour mask if required
3. Input signal intensity threshold parameters as $\pm 99\text{AU}$
4. Select up to three ROI on pleural tumour using the Myrian® 3D wand tool, following which the software will segment a volume based on the ROI signal intensity \pm threshold parameter of 99AU

This optimum methodology is practically simple, semi-automated using computer-based volume software, and appears to have excellent reproducibility. This method is therefore worth testing further in larger, multi-centre studies.

The signal intensity threshold parameter is based on results from the previous study described in *Chapter 3: Early Contrast Enhancement*. In this study, ROI were placed on pleura, distributed evenly cranio-caudally across three evenly spaced slices in an attempt to include sufficient representative pleural sampling. The threshold parameter ($\pm 99\text{AU}$) was the median SI range of all patients with MPM included in this study, excluding 3/31 patients who had ECE negative results. These patients were excluded as it was hypothesised that the ROI sampled in these patients represented false negative sampling of benign pleural interspersed between pleural tumour.

Our ECE analyses were performed in a relatively small group ($n=58$), with 31/58 having MPM, and have not yet been validated in a different population. Therefore, validation of our segmentation SI threshold parameters in another population with a repeat study where ROI signal intensity measurements and ECE assessment is performed prior to volumetric assessment would be preferable. If resulting SI threshold parameters were similar to our findings of $\pm 99\text{AU}$ then it could perhaps be hypothesised that this threshold parameter is reasonably representative of the range in signal intensity in the majority of patients with MPM. If this hypothesis is true then centres elsewhere implementing this methodology would not need to repeat SI measurements in their own population, simply using $\pm 99\text{AU}$ as the threshold range, which would be more time efficient.

4.5.4 Possible Clinical Implications

High tumour volume was an independent predictor of poor survival in this study, suggesting that this method of tumour burden assessment could serve as an additional prognostic biomarker in patients with MPM. If the prognostic significance and reproducibility of volume measurements is reproduced in larger, multi-centre study, pleural tumour volume could be considered as an alternative to current, often difficult, clinical T-staging. The role of tumour volume versus tumour invasion and resectability, as is currently described in staging T descriptors, would require further assessment in a staging context.

In addition, there is a potential role for the inclusion of tumour volume in prognostic models in MPM. Previously described prognostic models in MPM include the European Organisation for Research and Treatment of Cancer (EORTC) prognostic index, (402) the Cancer and Leukaemia Group B (CALGB) prognostic scoring system (403) and more recently, the prognostic model described by Brims *et al.* (386) The EORTC prognostic index comprises white cell count, ECOG performance status, histological subtype, patient sex and probable or possible histological diagnosis. (402) The CALGB model includes performance status, patient age, platelet count, the presence or absence of chest pain as a presenting symptom and lactate dehydrogenase level. (403) The Brims model included histological subtype, weight loss, performance status, haemoglobin and serum albumin. (386) In our study, only haemoglobin and tumour volume were statistically significant prognostic variable on univariate or multivariate Cox proportional hazards analysis. The small patient population is likely to be a significant contributing factor to the contrasting results here to that of previous studies. However, more recently, Kidd *et al* reported that routinely available clinical data are of fundamentally limited use, with clinical prediction models only improving survival prediction by 22% than would be expected by chance. (404) This highlights the limitations of prognostic markers that do not directly describe tumour extent and/or biology. Volumetric assessment of tumour burden may improve the performance of future prognostic models, as may additional emerging predictors such as tumour genomics.

An additional potential future role of volumetry in MPM would be in response assessment following systemic therapy. Currently, modified RECIST (Response

Evaluation Criteria in Solid Tumours) criteria are used for response assessment. (405,406) Modified RECIST was developed to address the deficiencies of uni-dimensional measurements employed in WHO and RECIST criteria for response assessment in a complex tumour such as MPM with its rind-like growth pattern. (407) Modified RECIST criteria incorporates the sum of six measurements of tumour thickness. Measurements are taken perpendicular to the chest wall or mediastinum in two positions at three separate levels on axial images. (405) Partial response and stable disease based on modified RECIST criteria have been shown to be predictive of better survival outcomes in MPM. (408) However, this method of response assessment is limited by inter-observer variability and bias associated with user selection of the sites at which tumour thickness is measured. (401,409) Results from earlier studies suggest that primary tumour volumetry may be a better method of response assessment than modified RECIST, particularly in terms of reproducibility. (383,389) A semi- or fully-automated tool to measure 'volumetric RECIST', such as that described by Chen *et al* in a recent study of computer-assisted CT volumetric assessment of MPM patients, (383) would therefore be a major clinical advance.

4.5.5 Study Limitations

The principal limitation of this study is the use of a small study population (n=31) recruited from a single centre. The relationships reported between tumour volume and survival must therefore be interpreted in the context of wide confidence intervals around hazard ratios. Nevertheless, the method appears to have excellent inter-observer reproducibility and tumour volume remained a statistically significant prognostic variable on multivariate analysis. In addition, our finding that increased tumour volume is associated with poorer median overall survival is consistent with results from previous studies.

Another limitation of this study is the method of deriving the signal intensity threshold subsequently used for segmentation. The threshold used in the final methodology was derived from mean SI measurements from patients with MPM as described in *Chapter 3: Early Contrast Enhancement*, which has not been externally validated.

Additionally, our MRI volumetric measurements were not correlated with post-operative pathological volume, as conducted in the study by Armato *et al.* In this study, CT-based volume measurements modestly correlated ($r = 0.66$) with pathologic tumour volume following extended pleurectomy/decortication in 28 patients with MPM. (399) None of the patients included in our study underwent surgical resection, as this treatment modality is currently not recommended in the U.K. for MPM. (143) We did validate our volume measurements with an MRI phantom, demonstrating little variance in our measurements and good accuracy. However, the MRI phantom in this study was a considerably more basic structure to volume in comparison to pleural tumour.

The final limitation of this study is the relatively lengthy time required to complete volume measurements using the described methodology (approximately 16 minutes). The analysis time is significantly increased (to a total analysis time of approximately 30 minutes) if signal intensity measurements and ECE assessment are completed first. However, if our signal intensity threshold parameter is validated in future study, this additional step would not be required. Although the time taken to complete volume measurements is longer than the time it would normally take a radiologist to clinically stage a patient with MPM, it could still be completed within a time that is still likely to be feasible in clinical practice. Future technological advances will likely allow further automation of the methodology, shortening the time taken to complete volumetric assessment.

4.6 CONCLUSION

In this chapter, novel MRI methodology for the volumetric assessment of primary MPM tumour volume has been described. The methodology appears accurate based on validation against an MRI phantom volume, and reproducible within a patient population. High tumour volume was an independent predictor of poor survival and patients can potentially be grouped into volume tertiles associated with different survival outcomes. Volumetric assessment of MPM is a promising future prognostic biomarker in MPM, with potential utility in the staging of this challenging tumour.

CHAPTER 5: CONCLUSIONS

5 Chapter 5: Conclusions

Malignant Pleural Mesothelioma is a complicated tumour, which can be challenging to diagnose. As a result, patients with suspected MPM often undergo a prolonged pathway from initial presentation to diagnosis. This results in patients being subjected to diagnostic uncertainty, multiple invasive procedures, frequent admissions due to breathlessness associated with recurrent pleural effusion and potential delays in the commencement of systemic treatment or clinical trial entry. Legal requirement for reporting suspected MPM to the procurator fiscal/coroner's office and requirement for a post-mortem in the event of a histological diagnosis not being confirmed in life, due to MPM being classed as an industrial disease, is an additional source of anxiety and burden for family members. Furthermore, difficulties associated with staging and the sub-optimal performance of prognostic models in MPM also results in a degree of clinician uncertainty regarding individual patient's prognostication, making discussions surrounding the patient's life expectancy and appropriateness of certain treatment options more challenging. The work in this thesis was undertaken to examine several blood and novel imaging biomarkers of MPM and their potential clinical utility in the diagnostic and prognostic assessment of patients with MPM in a real-world situation.

5.1 Blood biomarkers in Malignant Pleural Mesothelioma

A reliable diagnostic blood biomarker that offers high diagnostic sensitivity and specificity would be a major clinical advancement for MPM, directing appropriate patients to specialist centres for diagnostic work-up, including access to local anaesthetic thoracoscopy and specialist mesothelioma MDTs earlier in their patient journey. Unfortunately, despite promising early results for several potential blood biomarkers, including SOMAscan™, Fibulin-3, osteopontin, HMGB1 and mesothelin, no blood biomarker as shown reliably sufficient diagnostic performance to enter routine clinical practice. (143)

Prior studies have been limited by their retrospective design, use of selected MPM cohorts (frequently utilising historical archived samples from surgical centres where patients have often undergone prior pleural biopsy, pleurodesis or systemic therapy), inappropriate controls, inconsistent assay methods and cut-

off points and inconsistent sampling protocols, which often do not correlate with when these biomarkers would be used in clinical practice. Such methodological shortcomings and lack of external validation have limited interpretation of the true clinical utility of these biomarkers. (410)

5.1.1 The DIAPHRAGM study

DIAPHRAGM was a study that was rigorously designed to address many of the methodological limitations of these earlier studies. Firstly, DIAPHRAGM was a prospective study, recruiting patients from district general hospitals, larger academic centres and tertiary referral centres. Additionally, multiple centres across the UK and Ireland, all with a varying prevalence of MPM, were involved with recruitment. This means that biomarker results are likely to be relevant to the general MPM population in the UK. Secondly, patients were recruited to DIAPHRAGM at presentation with suspected MPM and the eligibility criteria were deliberately broad. The inclusion criteria did not include the requirement for history or evidence of asbestos exposure, such as pleural plaques, as these are absent in up to 25% of MPM cases. (46) Furthermore, patients with lung nodules or other visceral mass lesions were not excluded, assuming the investigator suspected new pleural malignancy. This was because of the high prevalence of lung nodules in the target population (older patients, commonly smokers) and the high false-positive rate of CT imaging in this regard. (411) The suspected pleural malignancy cohort in DIAPHRAGM is therefore reflective of an undifferentiated, real-world population. Our study cohort includes a generalised population of MPM, of typical histological subtype distribution, with varying stage distribution, which will allow interpretation of blood biomarker results in the context of both subtype and stage. In addition, the non-mesothelioma cohort includes a population of non-MPM pleural malignancy and benign pleural disease, with a significant proportion of these patients having BAPE, a population that often poses a real and significant challenge to differentiate from MPM. This ensures that our findings will be interpretable in the context of realistic differential diagnoses presenting to the clinicians with possible pleural malignancy or MPM. Furthermore, the timing of the blood biomarker sampling in this study (at initial presentation) replicates when these biomarkers would normally be taken (and of greatest diagnostic utility) in normal clinical practice.

In addition, the DIAPHRAGM protocol included a diagnostic review at 12 months of all cases where the baseline diagnosis was either benign or uncertain. Given that MPM can be difficult to diagnosis, even following pleural biopsy, and false negative histological sampling and requirement for repeated biopsy is not uncommon, this diagnostic review allowed for repeat biopsy results to be examined, ensuring that final classification of patients' diagnoses was robust. The difficulty lay in the consideration of which of these patients were considered to have MPM at baseline (i.e. at time of biomarker sampling) with a false negative pleural biopsy versus having an evolving diagnosis of MPM during study follow-up. However, all recruiting centres had access to advanced pleural diagnostics, including medical or surgical thoracoscopy and a specialist mesothelioma MDT. Additionally, all MPM cases were discussed at a local cancer MDT and at least 50% of sites had confirmed that their MPM cases had been discussed at a regional specialist mesothelioma MDT at the time of writing. Finally, unlike previous studies, biomarker sampling and storage in this study were all performed according to a single protocol at all centres. Additional potential confounders such as renal function, body mass index and concomitant medications were all recorded. Importantly, all patients were recruited and had biomarker sampling prior to pleurodesis, intercostal chest drain insertion or pleural biopsy. The temporal relationship between biomarker draw and pleural aspiration was also recorded and we will therefore be able to assess the effect, if any, this has on biomarker levels. DIAPHRAGM is the largest, prospective multi-centre diagnostic biomarker study in the MPM literature to date. Due to the robust study design and successful recruitment of target study participants and MPM cases, DIAPHRAGM will determine the true clinical utility of SOMAscan™, Fibulin-3 and mesothelin in the diagnosis of MPM with precision around diagnostic performance estimates.

5.2 Imaging biomarkers in Malignant Pleural Mesothelioma

Imaging plays a major role in the assessment of patients with suspected MPM, in both diagnostic and staging contexts. Chest radiography and thoracic ultrasound are typically first line investigations. However, further imaging is required for the assessment of suspected MPM. Contrast-enhanced CT imaging is the recommended initial cross-sectional imaging modality for the examination of

patients with suspected MPM. (143) CT can readily identify several features of pleural malignancy, such as pleural enhancement or pleural nodularity, however, radiological interpretation can be difficult, particularly in early stage MPM, where pleural thickening is often minimal or absent. Similarly, PET-CT, while useful in staging of MPM, in particular the identification of nodal and extra-thoracic disease, its use in the diagnostic assessment is limited by its availability, low sensitivity in early stage, epithelioid disease, and false positive FDG uptake in TB pleuritis, inflammatory disorders and prior talc pleurodesis. (143) MRI is an imaging modality that is becoming increasingly available in most centres in the UK. Its principal clinical utility in MPM at present is in the assessment of chest wall invasion or infiltration of the diaphragm, particularly when considering surgical resectability. (140) Previous studies have considered the diagnostic utility of MRI in the detection of pleural malignancy, particularly when combining anatomical with biologic data, such as dynamic contrast enhancement, with promising results. However, the clinical utility of these techniques have been limited by the requirement of bulky pleural tumour for their application, making it unsuitable for early diagnostics.

5.2.1 Early Contrast Enhancement at MRI

In chapter 2 of this thesis, a novel MRI biomarker of pleural malignancy was developed and its diagnostic performance and underlying biologic relevance were examined. I hypothesised that MRI examination targeted to increased microvessel density in malignant pleural tumour could accurately identify patients with pleural malignancy, including those patients with early stage MPM or minimal pleural thickening.

Firstly, I demonstrated that whole MRI series of the entire thorax could be acquired in a single breath-hold, thereby minimising image distortion from breathing artefact, even in patients with large volume pleural effusion, with multiple acquisitions being possible over time post-contrast. Secondly, I demonstrated that pleural signal intensity could be measured, even in the absence of significant pleural thickening (84% of patients included had pleural thickening <10mm and median pleural thickness of all patients included in the study was 5mm). Thirdly, I demonstrated that Early Contrast Enhancement was a feature of pleural malignancy, with high sensitivity (83% (95% CI 61 - 94%)),

specificity (83% (95% CI 68 - 91%)) and NPV (92% (95% CI 78 - 97%)) for the differentiation of malignant from benign pleural disease. Furthermore, I demonstrated that the sensitivity and NPV of ECE could be further improved by combining MRI morphology findings with the functional data provided by ECE (sensitivity 92% (95% CI 67 - 100%), NPV 97% (95% CI 86 - 100%)). Pleural signal intensity measurements and subsequent classification of patients as malignant or benign based on ECE were reproducible (inter-observer agreement κ 0.784) and offered superior inter-observer agreement than subjective morphology assessment using CT (κ 0.65) or MRI (κ 0.593). Additionally, I demonstrated that MSIG (used to summarise ECE characteristics of each patient) correlated with tumour MVD in patients with PM (Spearman's ρ = 0.43, p =0.02), suggesting that early contrast enhancement in PM is at least partially a result of increased blood vessel density in pleural tumour, as a consequence of neoangiogenesis, which is known to occur early in tumourigenesis. Finally, I demonstrated that higher MSIG and tumour MVD were both associated with poorer median overall survival in patients with MPM, supporting my conclusion that ECE is a perfusion-based imaging biomarker.

5.3 Staging of Malignant Pleural Mesothelioma

Accurate staging of any cancer is important in order to provide patients with accurate individual prognostic information, select appropriate patients for different treatment approaches and to assess the survival benefit of emerging therapies in clinical trials. Clinical staging of MPM has proved challenging due its unusual rind-like growth pattern and attempts at developing clinical staging systems thus far have been limited by high inter-observer variability, (412) frequent up-staging at surgical staging (125) and variable prognostic accuracy in a real-world population. Volumetric assessment of MPM as a potential alternative to current staging systems has been garnering increasing interest in recent times. Several studies have demonstrated the prognostic significance of high tumour volume estimated using a number of imaging modalities and measurement techniques. These methods have been variably limited by analysis time and reproducibility. The optimum imaging modality and method of tumour volume assessment has yet to be adequately defined.

5.3.1 Volumetric Assessment of Malignant Pleural Mesothelioma

In chapter 4, novel methodology for the volumetric assessment of patients with MPM was examined and the prognostic significance of tumour volume measurements using this methodology in patients with MPM was assessed. I hypothesised that tumour volume could be accurately and reproducibly assessed in patients with MPM using contrast-enhanced MRI.

Firstly, I defined the best time point post-contrast to perform volumetric assessment in MPM patients by examining signal intensity/time curves of ROI placed on pleura and adjacent structures. I then attempted different methods for volume estimation. I excluded manual delineation of pleural contours using OsiriX as an acceptable method due to excessive time. Following this, I tried and subsequently excluded the use of the MIAlite plugin for OsiriX as an acceptable method due to excessive time and inclusion of inappropriate structures in the segmented volume due to the circular nature of the blocking and seeding circles. Finally, I used Myrian software, which allowed propagation of a free-hand ROI contour mask to constrain subsequent semi-automated, signal intensity threshold-based volume segmentation. I examined four different segmentation methodologies, each with different signal intensity threshold parameters. Each methodology was assessed and ranked in order of: accuracy with an MRI phantom, subjective visual assessment of the final segmented volume, time to complete volume measurements and reproducibility based on intra-observer agreement. The optimum methodology was defined as the method scoring highest based on a scoring matrix of the above variables. The optimum methodology had high accuracy (<5% error in MRI phantom measurement), good intra-observer reproducibility (ICC 0.875) and acceptable analysis time (16 minutes). Secondly, I examined the reproducibility of the optimum method, demonstrating small variance around repeated measurements of the MRI phantom (+/- 1.4%) and excellent inter-observer reproducibility (ICC 0.962). Thirdly, I demonstrated that tumour volume at MRI did not correlate with clinical T-stage in patients with MPM (Spearman's $\rho = 0.02$, $p=0.897$, Jonckheere's trend test $p=0.935$) This perhaps reflects the fact that current clinical staging systems in MPM principally describe invasion and surgical resectability rather than tumour bulk, in contrast to most other cancer staging

systems. Finally, I demonstrated that higher tumour volume ($\geq 300\text{cm}^3$) at MRI was associated with significantly poorer survival (HR 2.273, $p=0.016$) and that tumour volume retained prognostic significance in a backwards stepwise multivariate Cox proportional hazards model (HR 2.114, $p=0.037$), concordant with previous volumetry papers in the MPM literature.

5.4 Future Work

Biomarker validation in a clinical population such as MPM is challenging. Any biomarker discovery studies require external validation in an appropriate population before entering routine clinical practice. Such validation studies have thus far been limited in MPM, reflected in the large number of potential biomarkers that have shown promise in translational studies but not entered clinical practice. In the course of completing DIAPHRAGM, a large, well-phenotyped bioresource, which includes plasma, serum, DNA and, in a proportion, pleural fluid, has been developed. This will provide an invaluable resource for future biomarker validation (and discovery) studies, as all patients and samples included in the bioresource have undergone the rigorous diagnostic and sampling protocols that have been discussed herein.

The reproducibility and simplicity of signal intensity measurements and ECE classification described herein would allow for additional centres to reproduce this technique. This is essential so that our results can be validated in a larger, multi-centre study and further understanding of the complex nature of MPM and its distribution within the pleural space can be gained. The potential implications of ECE entering clinical practice in the diagnostic assessment of patients with suspected MPM include pathway rationalisation, directing patients appropriately to specialist centres and early invasive sampling where MPM appears likely. Additionally, the lack of ionising radiation required for MRI acquisition and the ability of ECE assessment to be performed in cases with minimal pleural thickening means that it has the potential to be utilised in the future for screening of asbestos-exposed individuals for early MPM. *Meso-ORIGINS* is a study which aims to examine genomic, transcriptomic and immunologic events in the development of MPM by performing sequential pleural biopsies in patients with BAPE over a period of two years. The proposed

surveillance programme includes circulating biomarker sampling in addition to repeated imaging surveillance in these patients. The proposed imaging surveillance will further explore the clinical utility and biologic basis of MRI Early Contrast Enhancement. The *Meso-ORIGINS feasibility study*, which will assess the feasibility of recruiting sufficient numbers of patients to the proposed study, has recently been funded by the June Hancock Mesothelioma Research Fund and will commence recruitment shortly.

Although I examined the accuracy of MRI volumetric measurements using an MRI phantom, the accuracy of MRI measurements should also be examined using pathologic volume following surgical resection. MARS 2: a feasibility study comparing extended pleurectomy decortication versus no pleurectomy decortication in patients with MPM (NCT02040272) is currently open for recruitment, and patients are being recruited via the West of Scotland Mesothelioma MDT. Validating our MRI volume measurements in this population with resected pathologic volume is therefore possible.

In addition, the MRI acquisition and volume segmentation methodology described herein is being replicated and progressed in the *pre-EDIT* study (NCT03319186). This study, which has commenced recruitment, is a randomised feasibility trial of pleural elastance-directed treatment of patients with symptomatic malignant pleural effusion. The study protocol incorporates assessment of pleural cavity volume pre- and post- large volume pleural aspiration, in order to validate pleural elastance measurements (Δ intra-pleural pressure (cmH₂O)/ Δ volume of fluid removed (L)).

Appendix 1 Site Feasibility Questionnaire

DIAPHRAGM	Site Confirmation of Interest	
DIAPHRAGM: Diagnostic and Prognostic biomarkers in the Rational Assessment of Mesothelioma		
Site Name:		
Site Address:		
Principal Investigator:		
Approx number of mesothelioma patients reviewed per year:		
Approx number of patients you would recruit to trial per year:		
Does your site have access to the following:		
Medical thoracoscopy	Yes <input type="checkbox"/> No <input type="checkbox"/>	
	If Yes: on-site <input type="checkbox"/> onward referral <input type="checkbox"/>	
Surgical thoracoscopy	Yes <input type="checkbox"/> No <input type="checkbox"/>	
	If Yes: on-site <input type="checkbox"/> onward referral <input type="checkbox"/>	
Mesothelioma MDT	Yes <input type="checkbox"/> No <input type="checkbox"/>	
	If Yes: on-site <input type="checkbox"/> onward referral <input type="checkbox"/>	
Do you have sufficient resource to participate in the trial?		
Please provide details for the main contact at your site:		
If different from above - Please provide contact details for person completing the SSI and regulatory paperwork at your site:		

Appendix 2 Suspected Pleural Malignancy Cohort Patient Information Sheet

THIS STUDY HAS BEEN REVIEWED AND APPROVED BY A RECOGNISED RESEARCH ETHICS COMMITTEE

(Form to be on hospital headed paper)

INFORMATION SHEET FOR PATIENTS/ VOLUNTEERS IN CLINICAL RESEARCH PROJECT

Title of Project:

DIAPHRAGM: Diagnostic and prognostic biomarkers in the rational assessment of mesothelioma

Invitation Paragraph

We would like to invite you to take part in a research study. Before you decide you need to understand why the research is being done and what it would involve for you. Please take time to read the following information carefully. Talk to others about the study if you wish. Ask us if there is anything that is not clear or if you would like more information.

What is the purpose of the study?

This study is being carried out to test the value of a blood test (or biomarker) in determining the cause of a pleural effusion (a collection of fluid around the lung) or a pleural mass (an area of thickening of the lining of the lung). As your doctor will have explained there are numerous causes for this problem and these can be difficult to diagnose, often requiring multiple tests. Many of the causes of a pleural effusion or pleural thickening are benign, however, our specific goal in this study is to assess whether this blood test can be used to diagnose a rare cancer called Malignant Pleural Mesothelioma (MPM), which can present with a pleural effusion or mass.

Although we are asking you to take part this does not mean you have Mesothelioma, in fact the vast majority of people who take part will not have this.

Why have I been invited to take part?

You have been invited to take part in this study because you have a pleural effusion (a collection of fluid around the lung) or a pleural mass (as above). **This does not mean that you have Mesothelioma** but your medical team have decided you need further investigation, including sampling of the pleural effusion to send for analysis and/or biopsies of the lining of the lung (pleura).

Do I have to take part?

No, it is up to you to decide whether or not to take part. We will describe the study and go through this information sheet, which we will then give to you to keep. If you decide to take part, you will be asked to sign a consent form to show you have agreed to take part. If you decide to take part, you are free to withdraw at any time, without giving a reason. This would not affect the standard of care you receive or your future treatment.

What will happen to me if I decide to take part?

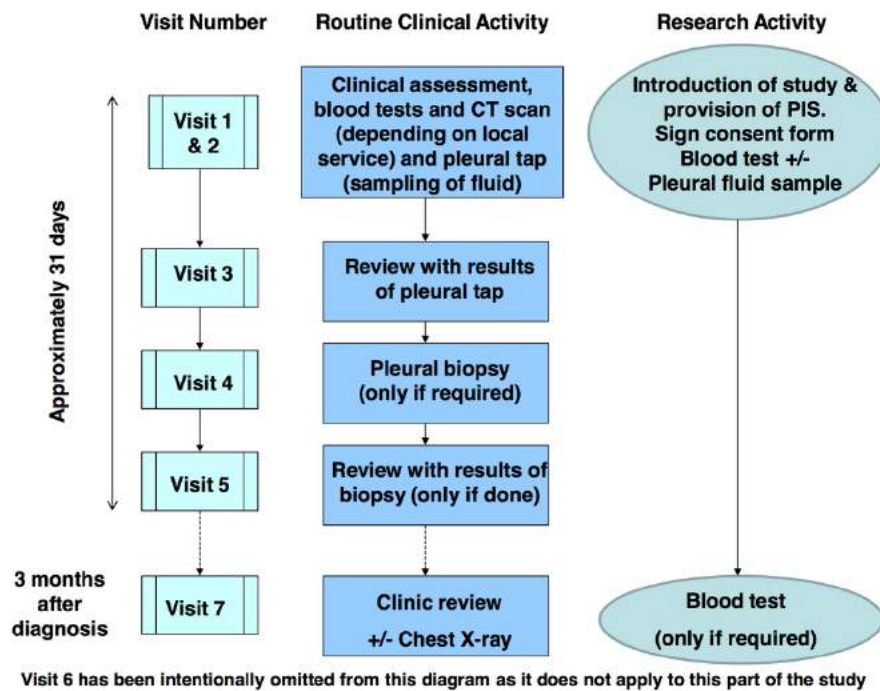
The study involves taking a single extra blood sample, 18 mL in total (4 teaspoonfuls) when you come to the hospital to get a sample of pleural fluid taken, or when you return to clinic for your results. The blood you donate will be split into two samples. One will be sent to a research

laboratory to be analysed in a completely anonymised fashion. This sample will remain there until it is used up or you withdraw your consent. The second sample will be stored locally. This sample will serve as a 'back-up' sample in case samples are damaged or lost during transport to the research laboratory. If not required for this study, it will either be discarded or it will remain in secure storage and may be used for ethically approved research in the future. All samples will be stored securely and confidentially using a study number that will be assigned to you, rather than your name or other information that could identify you. If a diagnosis other than MPM is made from this pleural fluid sample, then no more study tests will be required

If a diagnosis of MPM is made, we would like to take 1 further blood sample (approximately 3 months after diagnosis) when you attend for your usual visit to the clinic. Wherever possible, this will take place when you attend for your usual visit to the clinic. If this is not possible, a single study visit will be arranged with you. As you will be aware, taking blood samples may cause minor discomfort or bruising at the site from which the blood is taken. The following flow chart demonstrates how these blood tests will fit in with your routine clinical visits. If you are currently in hospital because of symptoms caused by your pleural effusion, your first study 'visit' (involving completion of a consent form and a blood test) can be undertaken during your hospital stay.

If you are a patient in a **West of Scotland hospital**, a small sample (approximately 20ml) of pleural fluid will be retained when we take a sample of pleural fluid as part of your routine clinical tests. This sample of fluid will be labelled in a completely anonymised fashion and stored in a secure freezer. The fluid may be used in a subsequent part of the DIAPHRAGM study, depending on the outcome of your initial tests. If this is the case, you will be made fully aware of this by the study team, otherwise this pleural fluid sample will be destroyed and discarded.

Please note that it is only the circle shapes in this diagram that indicate research/study activities



How will my blood sample be used?

In general, blood samples are used for medical research in order to better understand a disease, including how it starts and develops. In this study, scientists will analyse your blood to see if the measurements we are testing are unique to Mesothelioma. It is not clear at present whether these tests have any value in detecting mesothelioma. Therefore, the results of your blood test will not affect you, nor will you be informed of the results. You will, however, receive a summary of the results of the study once it has been completed.

If you do not want your blood to be used for medical research, then when you come to hospital or clinic and are asked for your consent to donate blood you can say no. If you do decide to take part, you can change your mind at any time. If, however, you change your mind after your procedure, some of your blood may have already been used for research. If it is being stored, the blood you donate will be kept in the secure local laboratory/tissue bank until it is all used or your consent is withdrawn.

What are the possible benefits of taking part?

There is no benefit to you but this study may help us define better, quicker and less invasive ways of detecting Mesothelioma.

What are the potential risks in taking part?

As mentioned above, blood taking can cause some minor discomfort or bruising at the site from which the blood is taken. The person taking your blood will be fully competent at doing this safely.

What if something goes wrong?

If you have a concern about any aspect of this study, you should ask to speak with the research doctor/nurse who will do their best to answer your questions.

If taking part in this research study harms you, there are no special compensation arrangements. If you are harmed due to someone's negligence, then you may have grounds for a legal action but you may have to pay your legal costs. Regardless of this, if you wish to complain, or have any concerns about any aspect of the way you have been approached or treated during the course of this study, the normal National Health Service complaints mechanism is available to you.

If you have private medical insurance, you may wish to check with your company before agreeing to take part in the study to ensure that participation in the study will not affect your insurance cover.

Will my taking part in the study be kept confidential?

You can be assured that any data collected during the course of this study and any of the results published will not identify you personally. Your medical records will only be available to the research doctors, your hospital consultant, responsible individuals from the Cancer Research UK Clinical Trials Unit (Glasgow), trial sponsors and regulatory authorities.

We will inform your general practitioner (GP) of your participation in this study.

We would like to use your NHS number to follow-up on your health.

Who is organising and funding the research?

The research is being carried out by Dr. Kevin Blyth from the Department of Respiratory Medicine at the Queen Elizabeth University Hospital, Glasgow.

The study is being coordinated by the Cancer Research UK Clinical Trials Unit, based at the Beatson West of Scotland Cancer Centre in Glasgow and is Sponsored by NHS Greater Glasgow & Clyde. The costs of running and organising this study have been met by a grant from the Chief Scientist Office of the Scottish Government. None of the doctors or other staff conducting the research are being paid for recruiting patients into the study.

Who has reviewed the study?

This study was reviewed by a number of medical specialists during its development. All research in the NHS is also looked at by an independent group of people, called a Research Ethics

Committee, to protect your interests. The West of Scotland Research Ethics Committee 1 has reviewed and approved this study to confirm that the 'rights and protection of patients' health have been considered. In addition, the study has been reviewed by the Research and Development Department of your local hospital.

Contact for further information

If you have further questions about your illness or clinical studies, please discuss them with your doctor.

If you would like independent advice or further information you may also find it useful to contact British Lung Foundation, website: www.blf.org.uk, telephone 03000 030 555 and address: British Lung Foundation, 73-75 Goswell Road, London, EC1V 7ER

If during the course of the study you have any questions regarding your participation or would like further study specific information before making your decision please contact:

Doctor:

Name

Insert Local Contact Details

Telephone Number

Insert Local Contact Details

Doctor/Research Nurse:

Name

Insert Local Contact Details

Telephone Number

Insert Local Contact Details

If you find the wording difficult to understand or would like us to explain things to you once more, please feel free to ask your doctor, or nurse.

Thank you for taking the time to read this information sheet. If you wish to take part you will be given a copy of this information sheet and a signed consent form to keep.

Appendix 3 DIAPHRAGM invitation letter to Clydeside Action on Asbestos members

< to be printed on Clydeside Action on Asbestos headed paper >

Dear

CAA has been asked if we would contact our members who have been diagnosed with pleural plaques, pleural thickening or asbestosis to help with research that is being conducted by the Southern General Hospital.

I have enclosed a letter that I have received from Dr Blyth and Dr Tsim, who are chest specialists based at the Southern General hospital. Dr Blyth is conducting research that aims to better understand a particular asbestos related condition called mesothelioma. Please be assured that we are only writing to you because you **do not** have mesothelioma; rather it is because you have been diagnosed with a different asbestos-related condition that you may be suitable for this study. With this type of medical research, the study team need to compare a group of people with mesothelioma with a group who do not have mesothelioma in order to gain a better understanding of this illness. This study is trying to determine whether there are useful differences in blood test measurements in those with mesothelioma in comparison to people with other asbestos-related conditions. This may lead to better diagnostic tests for mesothelioma in the future.

Should you wish to take part in this study please contact Dr Tsim at the Clinical Research Facility on 0141 232 9533, indicating you are interested in participating in this research (the DIAPHRAGM study). You should also be aware that CAA will not be able to answer any questions relating to the study.

With Kind Regards

Yours Sincerely

Clydeside Action on Asbestos

Appendix 4 Asbestos-exposed Control Cohort Patient Information Sheet

THIS STUDY HAS BEEN REVIEWED AND APPROVED BY A RECOGNISED RESEARCH ETHICS COMMITTEE

INFORMATION SHEET FOR PATIENTS/ VOLUNTEERS IN CLINICAL RESEARCH PROJECT

Title of Project:

DIAPHRAGM: Diagnostic and prognostic biomarkers in the rational assessment of mesothelioma

Invitation Paragraph

We would like to invite you to take part in a research study. Before you decide you need to understand why the research is being done and what it would involve for you. Please take time to read the following information carefully. Talk to others about the study if you wish. Ask us if there is anything that is not clear or if you would like more information.

What is the purpose of the study?

This study is being carried out to find new ways of diagnosing and predicting survival of a cancer of the lining of the lung called Malignant Pleural Mesothelioma (MPM) using a simple blood test known as a biomarker. **Although we are asking you to take part this does not mean you have this condition.** MPM is an uncommon cancer, often related to previous contact or exposure to asbestos. It can be extremely difficult to diagnose. We aim to find simpler initial diagnostic tests in the form of a blood sample to predict who is more likely to have MPM and would therefore benefit from early referral to a specialist centre.

Why have I been invited to take part?

You have been invited to take part in this study because you have had previous exposure to asbestos. In this study we need to ensure that the biomarker we are measuring is specific to Mesothelioma and is not simply related to previous asbestos exposure. We believe you would be a suitable 'control' subject for this study (i.e. a person who does **not** have Mesothelioma but who has been exposed to Asbestos)

Do I have to take part?

No, it is up to you to decide whether or not to take part. If you do you will be asked to sign a consent form to show you have agreed to do so. You are free to withdraw at any time, without giving a reason.

What will happen to me if I decide to take part?

If you wish to take part in the study, please phone the **Glasgow Clinical Research Facility (CRF)** on **0141 232 9533**, quoting the study name **DIAPHRAGM**. A clinical research nurse will then arrange a suitable time for you to attend a single visit to the Clinical Research Facility at the Queen Elizabeth University Hospital. The nurse will also arrange for a taxi to take you to and from the CRF on the day of your appointment (if you require transport). During your visit to the CRF, you will be asked to sign a consent form, your medical history and details of your previous exposure to asbestos will be recorded and a blood sample (18 mL or 4 teaspoonfuls) for biomarkers will be taken. We can arrange for a taxi to take you to and from this visit, free of charge, and it should take no longer than 30 minutes. As you will be aware, taking blood samples may cause some minor discomfort or bruising at the site from which the blood is taken.

How will my blood sample be used?

In general, blood samples are used for medical research in order to better understand a disease, including how it starts and develops. In this study, scientists will analyse your blood to see if the biomarkers we are measuring are unique to Mesothelioma. It is not clear at present whether these tests have any value in detecting mesothelioma. Therefore, the results of your blood test will not affect you, nor will you be informed of the results. You will, however, receive a summary of the results of the study once it has been completed. The blood you donate will be split into two samples. One will be sent to a research laboratory in America to be analysed in an anonymised fashion. The sample will remain there until it is all used or you withdraw your consent. The second sample will be stored locally. This sample will serve as a 'back-up' sample in case the sample is damaged or lost during transport to America. If not required for this study, it will remain in secure storage and may be used for ethically approved research in the future. All samples will be stored securely and confidentially using a study number that will be assigned to you, rather than your name or other information that could identify you. The blood you donate will be kept in the secure local tissue bank indefinitely until it is all used or your consent is withdrawn.

What are the possible benefits of taking part?

There is no direct benefit to you but it is hoped that by taking part in this research, you will be providing valuable information regarding Mesothelioma. In particular, this study may help us define better, quicker and less invasive ways of detecting Mesothelioma.

What are the potential risks in taking part?

As mentioned above, taking blood can cause some minor discomfort or bruising at the site from which the blood is taken. The person taking your blood will be fully competent at doing this safely.

What if something goes wrong?

If you have a concern about any aspect of this study, you should ask to speak with the research doctor/nurse who will do their best to answer your questions. If taking part in this research study harms you, there are no special compensation arrangements. If you are harmed due to someone's negligence, then you may have grounds for a legal action but you may have to pay your legal costs. Regardless of this, if you wish to complain, or have any concerns about any aspect of the way you have been approached or treated during the course of this study, the normal National Health Service complaints mechanism should be available to you.

If you have private medical insurance, you may wish to check with your company before agreeing to take part in the study to ensure that participation in the study will not affect your insurance cover.

Will my taking part in the study be kept confidential?

You can be assured that any data collected during the course of this study and any of the results published will not identify you personally. Your medical records will only be available to the research doctors, your hospital consultant, responsible individuals from the Cancer Research UK Clinical Trials Unit (Glasgow), trial sponsors and regulatory authorities.

With your permission, we will inform your general practitioner (GP) of your participation in this study.

With your permission, the Cancer Research UK Clinical Trials Unit (Glasgow) who are coordinating the study will collect your name or initials, date of birth and NHS number or Community Health

Index (CHI) number. This information will be stored securely on a password protected database and will be kept strictly confidential, with access provided only to authorised personnel.

Your consent for participation in this study also includes your consent to allow the use of the data in your medical/clinical record to be used for the purposes of Cancer Research. Your consent also includes allowing these data to be linked to data coming from other sources such as cancer registries and medical clinical records. All data (personal, clinical, economic and data coming from research on biological material) collected on your behalf will be treated in compliance with the European and UK applicable laws to ensure your confidentiality is maintained.

Who is organising and funding the research?

The research is being carried out by Dr. Kevin Blyth & Dr. Selina Tsim from the Department of Respiratory Medicine at the Queen Elizabeth University Hospital, Glasgow. The study is being coordinated by the Cancer Research UK Clinical Trials Unit, based at the Beatson West of Scotland Cancer Centre in Glasgow and is sponsored by NHS Greater Glasgow & Clyde. The costs of running and organising this study have been met by a grant from the Chief Scientist Office of the Scottish Government. None of the doctors or other staff conducting the research are being paid for recruiting patients into the study.

Who has reviewed the study?

This study was reviewed by a number of medical specialists during its development. All research in the NHS is also looked at by an independent group of people, called a Research Ethics Committee, to protect your interests. The West of Scotland Research Ethics Committee 1 has reviewed and approved this study to confirm that the 'rights and protection of patients' health have been considered. In addition, the study has been reviewed by the NHS GG&C Research and Development Department.

Contact for further information

If you have further questions about your illness or clinical studies, please discuss them with your doctor. If you would like independent advice or further information you may also find it useful to contact The National Asbestos Helpline, website: [http:// www.nationalasbestos.co.uk](http://www.nationalasbestos.co.uk), Freephone. 0808 163 3706 and address: Innospec Park, Ellesmere Port, Cheshire, CH65 4EY

If during the course of the study you have any questions regarding your participation or would like further study specific information before making your decision please contact Dr. Selina Tsim on the following number quoting the study name DIAPHRAGM:

Study Name	DIAPHRAGM
Telephone Number	0754 0230 911

If you find the wording difficult to understand or would like us to explain things to you once more, please feel free to ask your doctor, or nurse.

Thank you for taking the time to read this information sheet. If you wish to take part you will be given a copy of this information sheet and a signed consent form to keep.

Appendix 5 MRI Substudy Patient Information Sheet

THIS STUDY HAS BEEN REVIEWED AND APPROVED BY A RECOGNISED RESEARCH ETHICS COMMITTEE

INFORMATION SHEET FOR PATIENTS/ VOLUNTEERS IN CLINICAL RESEARCH PROJECT

Title of Project:

DIAPHRAGM: Diagnostic and prognostic biomarkers in the rational assessment of mesothelioma

We are grateful to you for agreeing to take part in the DIAPHRAGM research study. We would appreciate it if you would consider participating in an additional part of this study, which is described below. Participation in this additional research is voluntary and you can continue to participate in the main study if you decide not to volunteer for this component

Invitation Paragraph

We would like to invite you to take part in a research sub-study. Before you decide you need to understand why the research is being done and what it would involve for you. Please take time to read the following information carefully. Talk to others about the study if you wish. Ask us if there is anything that is not clear or if you would like more information.

What is the purpose of the study?

This sub-study is being carried to help us understand the biological basis of the biomarker levels we have already measured in your blood. We plan to use Magnetic Resonance Imaging (MRI) to accurately measure the amount of pleural thickening, including any visible tumour, which might be present. We will then look for any relationship between biomarker levels in pleural fluid and blood and these measurements.

Why have I been invited to take part?

You have been invited to take part in this additional sub-study because your medical team have decided that it would be sensible for you to have biopsy samples taken from the lining of your lung. **This does not mean that you have Mesothelioma**

Do I have to take part?

No, it is up to you to decide whether or not to take part. Taking part in the sub-study is voluntary, and is entirely separate from taking part in the main study. We will describe the study and go through this information sheet, which we will then give to you to keep. If you decide to take part, you will be asked to sign a consent form to show you have agreed to take part. If you decide to take part, you are free to withdraw at any time, without giving a reason. This would not affect the standard of care you receive or your future treatment.

What will happen to me if I decide to take part?

If you agree to take part in the sub-study, any tests or treatment your doctor recommends for you will not be affected by taking part in this sub-study. Before your admission for biopsy, we will arrange a suitable time for you to have a single visit for MRI scanning. The pleural fluid sample you consented to be retained when you consented to the main study will also be retrieved for use in this part of the research.

What does the MRI scan involve?

The MRI scan will be performed at the Research MRI Scanner at the Queen Elizabeth University Hospital, Glasgow. We can arrange a taxi to take you, free of charge, to and from your MRI scan and the scan should take no more than an hour.

On arrival at the MRI department a radiographer will go through a safety checklist and make sure that all magnetic objects (e.g. jewellery and bankcards) have been removed. Following this you will be asked to complete and sign a safety questionnaire. Once you have changed into a hospital gown, you will be asked to lie flat on an electric bed that will move you into the scanner. The scanner is basically long and tunnel shaped. You are gently slid into the centre of the tunnel on a moving bed and the scan pictures are taken. Some people find it a little enclosing, but you can come out at any time. If you are claustrophobic please tell staff.

When you are in the scanner you will need to wear a pair of headphones, allowing you to listen to music of your choice (you are welcome to bring your own CD) and allowing us to communicate with you. The headphones are also necessary because of the loud knocking noise that occurs when the pictures are being taken. You will be given an emergency buzzer and can very quickly be taken out of the scanner should you feel uncomfortable or if it is felt necessary. During the scan you will be asked to hold your breath at times to improve the quality of the pictures. A doctor will be in the control room throughout this procedure.

What are the possible risks or disadvantages of taking part?**MRI:**

The MRI scanner is very safe as long as you have no metal implants in your body. Staff who are experienced in MRI scans will be present during your MRI scan and you will be asked a series of safety questions to ensure you have no metal implants/fragment in your body. If you do have a metal implant/fragment an MRI scan may not be safe and you would not be eligible for this additional study.

During the MRI scan a dye (contrast agent) will be injected into a vein in your arm. This makes any abnormal tissue appear brighter on the scan and easier to measure. The dye is called Gadolinium and is generally harmless and will be washed out of your system by your kidneys. There are however some potential side effects, although these are uncommon and generally mild. The most frequent side effects are headache, nausea, a sensation of heat, cold and/or pain at the injection site.. A very rare side effect is an allergic reaction to the dye therefore please inform the doctor if you have a history of allergies.

The dye can affect the kidneys if the kidneys are not working properly. Your doctor, using the blood test taken, will check how your kidneys are working before the scan. Your doctor will ask you if you have had problems with seizures in the past to make sure that you are able to have the dye.

Thoracoscopy/Image guided biopsy:

This is an essential part of your routine care and allows samples of the lining of your lung to be taken (pleural biopsy). It is a safe procedure and will be performed during a short admission to hospital. It will be discussed with you in great detail beforehand and you will be given separate written information regarding it.

How will my blood and pleural fluid sample be used?

In general, blood and pleural fluid samples are used for medical research in order to better understand a disease, including how it starts and develops. In this study, scientists will analyse your blood and pleural fluid to see if the biomarkers we are measuring are truly unique to

Mesothelioma. It is not clear at present whether these tests have any value in detecting Mesothelioma. Therefore, the results of your blood test will not affect you, nor will you be informed of the results. You will, however, receive a summary of the results of the study once it has been completed. The blood and pleural fluid you donate will be split into two samples. One will be sent to a research laboratory to be analysed in an anonymised fashion. The sample will remain there until it is all used or you withdraw your consent. The second sample will be stored locally. This sample will serve as a 'back-up' sample in case samples are damaged or lost during transport to the research labs. If not required for this study, it will either be discarded or it will remain in secure storage and may be used for ethically approved research in the future. All samples will be stored securely and confidentially using a study number that will be assigned to you, rather than your name or other information that could identify you. These samples will remain there until they are all used or you withdraw your consent. Results of tests will only be used for research and education. The blood and pleural fluid you donate will be kept in a secure local tissue bank until it is all used or your consent is withdrawn.

If you do not want your blood or pleural fluid to be used for medical research, then when you come to hospital or clinic and are asked for your consent to donate blood or pleural fluid you can say no. If you do decide to take part, you can change your mind at any time. If, however, you change your mind after your procedure, some of your blood or pleural fluid may have already been used for research.

What if something goes wrong?

If you have a concern about any aspect of this study, you should ask to speak with the research doctor/nurse who will do their best to answer your questions.

If taking part in this research study harms you, there are no special compensation arrangements. If you are harmed due to someone's negligence, then you may have grounds for a legal action but you may have to pay your legal costs. Regardless of this, if you wish to complain, or have any concerns about any aspect of the way you have been approached or treated during the course of this study, the normal National Health Service complaints mechanism is available to you.

If you have private medical insurance, you may wish to check with your company before agreeing to take part in the study to ensure that participation in the study will not affect your insurance cover.

Will my taking part in the study be kept confidential?

You can be assured that any data collected during the course of this study and any of the results published will not identify you personally. Your medical records will only be available to the research doctors, your hospital consultant, responsible individuals from the Cancer Research UK Clinical Trials Unit (Glasgow), trial sponsors and regulatory authorities.

We will inform your general practitioner (GP) of your participation in this study.

We would like to use your NHS number to follow-up on your health.

Who is organising and funding the research?

The research is being carried out by Dr. Kevin Blyth/Dr. Selina Tsim from the Department of Respiratory Medicine at the Queen Elizabeth University Hospital, Glasgow.

The sub-study is being coordinated by the Cancer Research UK Clinical Trials Unit, based at the Beatson West of Scotland Cancer Centre in Glasgow and is Sponsored by NHS Greater Glasgow &

Clyde. The costs of running and organising this sub-study have been met by a grant from the Chief Scientist Office.

None of the doctors or other staff conducting the research are being paid for recruiting patients into the study.

Who has reviewed the sub-study?

This study was reviewed by a number of medical specialists during its development. All research in the NHS is also looked at by an independent group of people, called a Research Ethics Committee, to protect your interests. The West of Scotland Research Ethics Committee 1 has reviewed and approved this study to confirm that the 'rights and protection of patients' health have been considered. In addition, the study has been reviewed by the NHS GG&C Research and Development Department.

Contact for further information

If you have further questions about your illness or clinical studies, please discuss them with your doctor.

If you would like independent advice or further information you may also find it useful to contact The National Asbestos Helpline.

Alternatively you can contact British Lung Foundation, website: www.blf.org.uk, telephone 03000 030 555 and address: British Lung Foundation, 73-75 Goswell Road, London, EC1V 7ER

If during the course of the sub-study you have any questions regarding your participation or would like further study specific information before making your decision please contact:

Doctor:

Name	Dr Selina Tsim
Telephone Number	0754 0230 911


If you find the wording difficult to understand or would like us to explain things to you once more, please feel free to ask your doctor, or nurse.

Thank you for taking the time to read this information sheet. If you wish to take part you will be given a copy of this information sheet and a signed consent form to keep.

Appendix 6 Baseline Information Case Report Form

Page 1/8

Baseline Form - PRTT/3

 CANCER RESEARCH UK Clinical Trials Unit, Glasgow		BASELINE INFORMATION FORM Suspected Pleural Malignancy Group <i>(This form should be completed during the course of Visits 1-5 as described in the Schedule of Assessments)</i>	
L148 - DIAPHRAGM: Diagnostic and Prognostic biomarkers in the Rational Assessment of Mesothelioma			
PATIENT INITIALS: (forename) _____ (surname) _____		DATE of BIRTH: DD / MON / YYYY	
INVESTIGATOR:		REGISTRATION DATE: DD / MON / YYYY	
SITE:		PATIENT TRIAL IDENTIFIER:	
GENDER: Male / Female (please circle)			

PATIENT DEMOGRAPHICS	
Ethnic origin: 1 = White 2 = Asian(Indian/Bangladeshi/Pakistani etc) 3 = South East Asian(Chinese/Japanese/Korean)	4 = Afro/Caribbean 5 = Other, specify: _____ <input type="checkbox"/>
Postcode: _____	

MODE OF PRESENTATION	
Date of Initial Presentation:	Date: DD / MON / YYYY
Mode of Presentation:	1 = Out-Patient Referral 2 = Emergency admission to medicine/respiratory medicine 3 = In-patient referral to medicine/respiratory medicine 4 = Other, specify: _____ <input type="checkbox"/>

SMOKING HISTORY	
Smoking History:	1 = Current smoker 2 = Non-smoker 3 = Ex- smoker <input type="checkbox"/>
If smoker/ex-smoker: When did you start smoking?	Date: DD / MON / YYYY How many per day on average? _____
If ex- smoker: When did you stop?	Date: DD / MON / YYYY

Version 5.0, 25th September 2015

Please return completed form to: Clinical Trial Coordinator – DIAPHRAGM Study, CRUK Clinical Trials Unit, Level 0, The Beatson West of Scotland Cancer Centre, 1053 Great Western Road, Glasgow, G12 0YN

PHYSICAL CHARACTERISTICS	
Weight: _____ kg	Date: DD / MON / YYYY
Height: _____ cm	Date: DD / MON / YYYY

SYMPTOMS (please record all symptoms reported as part of current illness)	
Symptom	Please tick to indicate if patient has or has not had any of these symptoms
Chest pain	Yes <input type="checkbox"/> No <input type="checkbox"/> Not Known <input type="checkbox"/>
Shortness of Breath	Yes <input type="checkbox"/> No <input type="checkbox"/> Not Known <input type="checkbox"/>
Weight loss	Yes <input type="checkbox"/> No <input type="checkbox"/> Not Known <input type="checkbox"/>
Cough	Yes <input type="checkbox"/> No <input type="checkbox"/> Not Known <input type="checkbox"/>
MRC Dyspnea Score (0-5): _____	Date: DD / MON / YYYY
ECOG Performance Status Score (0-4): _____	Date: DD / MON / YYYY
Please specify below any other current symptom. If NO other current symptoms please tick <input type="checkbox"/>	
Other current symptom, specify: _____	
Other current symptom, specify: _____	
Other current symptom, specify: _____	
Other current symptom, specify: _____	

PRESENTING PLEURAL ABNORMALITY		
How did the patient present: (please tick all that apply)		
	Pleural Mass	Pleural Effusion
Left Sided	<input type="checkbox"/>	<input type="checkbox"/>
Right Sided	<input type="checkbox"/>	<input type="checkbox"/>

PAST MEDICAL HISTORY		
	Please tick to indicate if patient has or does not have any of these conditions	Please tick to indicate if condition is ONGOING at present
RESPIRATORY – please specify below any history of respiratory events – if none please tick <input type="checkbox"/>		
Chronic Obstructive Pulmonary Disease	Yes <input type="checkbox"/> No <input type="checkbox"/>	Yes <input type="checkbox"/> No <input type="checkbox"/>
Asthma	Yes <input type="checkbox"/> No <input type="checkbox"/>	Yes <input type="checkbox"/> No <input type="checkbox"/>
Pulmonary Fibrosis	Yes <input type="checkbox"/> No <input type="checkbox"/>	Yes <input type="checkbox"/> No <input type="checkbox"/>
Other specify:	Yes <input type="checkbox"/> No <input type="checkbox"/>	Yes <input type="checkbox"/> No <input type="checkbox"/>
Other, specify:	Yes <input type="checkbox"/> No <input type="checkbox"/>	Yes <input type="checkbox"/> No <input type="checkbox"/>
CARDIOVASCULAR– please specify below any history of cardiovascular events – if none please tick <input type="checkbox"/>		
Ischaemic Heart Disease	Yes <input type="checkbox"/> No <input type="checkbox"/>	Yes <input type="checkbox"/> No <input type="checkbox"/>
LV Systolic Dysfunction	Yes <input type="checkbox"/> No <input type="checkbox"/>	Yes <input type="checkbox"/> No <input type="checkbox"/>
CVA or TIA	Yes <input type="checkbox"/> No <input type="checkbox"/>	Yes <input type="checkbox"/> No <input type="checkbox"/>
Hypertension	Yes <input type="checkbox"/> No <input type="checkbox"/>	Yes <input type="checkbox"/> No <input type="checkbox"/>
Other, specify:	Yes <input type="checkbox"/> No <input type="checkbox"/>	Yes <input type="checkbox"/> No <input type="checkbox"/>
Other, specify:	Yes <input type="checkbox"/> No <input type="checkbox"/>	Yes <input type="checkbox"/> No <input type="checkbox"/>
CANCER – please specify below any history of cancer – if none please tick <input type="checkbox"/>		
	Yes <input type="checkbox"/> No <input type="checkbox"/>	Yes <input type="checkbox"/> No <input type="checkbox"/>
	Yes <input type="checkbox"/> No <input type="checkbox"/>	Yes <input type="checkbox"/> No <input type="checkbox"/>
OTHER PAST MEDICAL HISTORY – please specify below any other past medical history – if none please tick <input type="checkbox"/>		
Chronic Renal Failure	Yes <input type="checkbox"/> No <input type="checkbox"/>	Yes <input type="checkbox"/> No <input type="checkbox"/> If yes, please provide most recent eGFR result: _____mls/min DD/MON/YYYY
Diabetes Mellitus	Yes <input type="checkbox"/> No <input type="checkbox"/>	Yes <input type="checkbox"/> No <input type="checkbox"/>
Other, specify:	Yes <input type="checkbox"/> No <input type="checkbox"/>	Yes <input type="checkbox"/> No <input type="checkbox"/>
Other, specify:	Yes <input type="checkbox"/> No <input type="checkbox"/>	Yes <input type="checkbox"/> No <input type="checkbox"/>
Other, specify:	Yes <input type="checkbox"/> No <input type="checkbox"/>	Yes <input type="checkbox"/> No <input type="checkbox"/>

PLEURAL IMAGING PERFORMED <i>(please record first investigations performed)</i>		
INVESTIGATION	DATE	Tick if investigation not performed
Chest X-Ray	DD / MON / YYYY	<input type="checkbox"/>
CT Chest	DD / MON / YYYY	<input type="checkbox"/>
Chest Ultrasound Performed by radiology <input type="checkbox"/> Performed by respiratory <input type="checkbox"/>	DD / MON / YYYY	<input type="checkbox"/>
MRI Chest	DD / MON / YYYY	<input type="checkbox"/>
Other Investigation (specify type of investigation, date). If no other investigations, please tick <input type="checkbox"/>		
	DD / MON / YYYY	
	DD / MON / YYYY	

PLEURAL SAMPLING			
Has a diagnostic pleural aspiration been taken?	1 = Yes 2 = No	<input type="checkbox"/>	if yes please give date taken DD / MON / YYYY
Intention:	1 = Diagnostic 2 = Diagnostic/Therapeutic	<input type="checkbox"/>	
Please list all other investigations performed:			if yes please give date(s), including repeat investigations where these were performed.
Abram's pleural biopsy	1 = Yes 2 = No	<input type="checkbox"/>	DD/MON/YYYY DD/MON/YYYY
CT-guided biopsy	1 = Yes 2 = No	<input type="checkbox"/>	DD/MON/YYYY DD/MON/YYYY
US-guided biopsy	1 = Yes 2 = No	<input type="checkbox"/>	DD/MON/YYYY DD/MON/YYYY
Medical Thoracoscopy	1 = Yes 2 = No	<input type="checkbox"/>	DD/MON/YYYY DD/MON/YYYY
Surgical Thoracoscopy	1 = Yes 2 = No	<input type="checkbox"/>	DD/MON/YYYY DD/MON/YYYY
Other biopsy – please specify _____	1 = Yes 2 = No	<input type="checkbox"/>	DD/MON/YYYY DD/MON/YYYY

HAEMATOLOGY RESULTS (taken at baseline)	
Date:	DD/MON/YYYY
Haemoglobin (g/l)	
WBC ($\times 10^9/l$)	
Platelets ($\times 10^9/l$)	
Lymphocytes ($\times 10^9/l$)	
Neutrophils ($\times 10^9/l$)	

BIOCHEMISTRY RESULTS <i>(taken at baseline)</i>	
Date:	DD / MON / YYYY
Laboratory Code*	
Sodium (mmol/L)	
Potassium (mmol/L)	
Urea (mmol/L)	
Creatinine (µmol/L)	
C reactive protein (mg/L)	
Albumin (g/L)	

*= laboratory code issued at site set up. If another laboratory is used please request a laboratory code and ensure a copy of the reference ranges for the laboratory are sent to CRUK Clinical Trials Unit, Glasgow.

PLEURAL CHEMISTRY RESULTS <i>(please tick if not done <input type="checkbox"/>)</i>					
Date:	DD / MON / YYYY	DD / MON / YYYY	DD / MON / YYYY	DD / MON / YYYY	DD / MON / YYYY
Fluid total protein (g/l)					
Serum total protein (g/l)					
Fluid LDH (U/L)					
Serum LDH (U/L)					
Fluid glucose (mmol/l)					

PLEURAL CULTURE RESULT

(please tick if not done ☐)

1. Microscopy

Date of report: DD / MON / YYYY

Select one of the following:

No organisms ☐

AAFB seen ☐

Other organism seen ☐
Specify _____

2. Final Culture

Date of report: DD / MON / YYYY

Select one of the following:

Negative ☐

Positive ☐

If positive

AAFB ☐

Other ☐

Specify _____

PLEURAL CYTOLOGY RESULTS

(please tick if not done ☐)

Date of report: DD / MON / YYYY

1 = Normal mesothelial cells
2 = Suspicious of mesothelioma
3 = Diagnostic of mesothelioma
4 = Diagnostic of other malignancy
Specify _____

5 = Lymphocytic or predominantly lymphocytes
6 = Blood or predominantly blood
7 = Neutrophilic or predominantly neutrophilic
8 = Acellular

☐

PLEURAL HISTOLOGY RESULTS

(please tick if not done ☐)

Date: DD / MON / YYYY

1 = Epithelioid Mesothelioma
2 = Sarcomatoid Mesothelioma
3 = Biphasic Mesothelioma
4 = Mesothelioma NOS
5 = Other malignancy,
Specify _____

6 = Suspicious of Mesothelioma
7 = Benign Fibrinous Pleurisy
8 = Granulomatous Inflammation
9 = Other, please specify _____

☐

Version 5.0, 25th September 2015

Please return completed form to: Clinical Trial Coordinator – DIAPHRAGM Study, CRUK Clinical Trials Unit, Level 0,
The Beatson West of Scotland Cancer Centre, 1053 Great Western Road, Glasgow, G12 0YN

FINAL DIAGNOSIS			
Final Diagnosis: Has the patient been diagnosed with Mesothelioma? 1 = Yes 2 = No (If "No" AND the diagnosis is NOT a cytological or histological diagnosis of another cancer, the Diagnostic Review at 12 months Form must be completed.) Date of Diagnosis: DD / MON / YYYY	<input type="checkbox"/>	If yes, please provide mesothelioma stage (IMIG): Stage I <input type="checkbox"/> Stage II <input type="checkbox"/> Stage Ia <input type="checkbox"/> Stage III <input type="checkbox"/> Stage Ib <input type="checkbox"/> Stage IV <input type="checkbox"/> T stage (1a,1b,2,3,4): _____ N stage (X,0,1,2,3): _____ M stage (X,0,1): _____	
If yes, please indicate type of diagnosis: (If yes, the Follow Up Form must be completed (visit 6 only applies to West of Scotland, MRI sub study, visit 7 applies to all participants) 1 = Radiological 2 = Cytological 3 = Histological 4 = Other, specify: _____	<input type="checkbox"/>	If No, please indicate non-mesothelioma diagnosis: 1 = Other malignancy, specify: _____ 2 = Para-pneumonic effusion 3 = Benign asbestos pleural effusion 4 = Tuberculosis pleurisy 5 = Pulmonary embolism 6 = Rheumatoid pleural effusion 7 = Other, specify: _____	<input type="checkbox"/>


SAMPLING FOR TRANSLATIONAL RESEARCH	
Has the first translational blood Test (visit 2 or 3) been taken for this patient?	1= Yes 2= No, patient refused consent 3= No, not taken other reason. Please specify: _____ <input type="checkbox"/>
Date blood sample taken:	DD / MON / YYYY
Was this sample pre or post pleural aspiration:	1= pre 2= post <input type="checkbox"/>
ASBESTOS EXPOSURE QUESTIONNAIRE	
Has the Asbestos Exposure Questionnaire been completed for this patient?	1= Yes 2= No, patient refused consent 3= No, other reason. Please specify: _____ <input type="checkbox"/>

DATE: DD / MON / YYYY INVESTIGATOR'S SIGNATURE: _____

Appendix 7 MPM Follow-up Visit Case Report Form

Page 1/4

Follow Up Form – FUP/

 <p>CANCER RESEARCH UK Clinical Trials Unit, Glasgow</p>	<h3 style="text-align: center;">FOLLOW UP VISITS FORM</h3> <h4 style="text-align: center;">Suspected Pleural Malignancy Group</h4> <p style="text-align: center;"><i>(To be completed at approximately Visit 6 (1 month post MPM diagnosis, West of Scotland MRI sub-study patients only) and Visit 7 (3 months post MPM diagnosis) This form should capture any new diagnostic or clinical data which has become available since Visit 5 and Completion of Baseline Information Form)</i></p>	
L148 - DIAPHRAGM: Diagnostic and Prognostic biomarkers in the Rational Assessment of Mesothelioma		
PATIENT INITIALS: (forename) _____ (surname) _____	DATE of BIRTH: DD / MON / YYYY	
INVESTIGATOR:	REGISTRATION DATE: DD / MON / YYYY	
SITE:	PATIENT TRIAL IDENTIFIER:	

Please tick one box to confirm the review period covered by this form			
Visit 6 (West of Scotland MRI sub-study patients only)	<input type="checkbox"/>	Visit 7 (confirmed MPM Patients Only)	<input type="checkbox"/>

CURRENT STATUS	
Date last known alive or date of death: DD / MON / YYYY	
Patient's status at above date:	1 = Alive <input type="checkbox"/> 2 = Dead
If dead, cause of death:	1 = Mesothelioma 2 = Malignant Disease (non-mesothelioma), please specify below:- 3 = Toxicity of treatment, please specify below:- 4 = Inter-current disease, please specify below:- 5 = Associated chronic disease, please specify below:- 6 = Other, please specify below:- <div style="border-bottom: 1px solid black; height: 15px; margin-top: 5px;"></div> 7 = Unknown <input type="checkbox"/>
Reliable evidence for cause of death:	1 = Autopsy 2 = Histological 3 = Clinical 4 = Microbiological 5 = Death certificate 6 = No reliable evidence 7 = Other, please specify below:- <div style="border-bottom: 1px solid black; height: 15px; margin-top: 5px;"></div> <input type="checkbox"/>

Version 2 Final 12th March 2015

Please return completed form to: Clinical Trial Coordinator – DIAPHRAGM Study, CRUK Clinical Trials Unit, Level 0,
The Beatson West of Scotland Cancer Centre, 1053 Great Western Road, Glasgow, G12 0YN

PHYSICAL CHARACTERISTICS			
Weight:	_____ Kg	Date: DD / MON / YYYY	Please tick box if date is the same as previous
ECOG Performance Status Score (0-4):	_____	Date: DD / MON / YYYY	<input type="checkbox"/>
MRC Dyspnoea Score (0-5):	_____	Date: DD / MON / YYYY	<input type="checkbox"/>

RELEVANT IMAGING INVESTIGATIONS SINCE LAST STUDY VISIT						
Investigation	DATE or Tick if investigation not performed	RESULT – please tick one				
		No change in extent of pleural opacification since last CXR	Increased extent of pleural opacification since last CXR	Decreased extent of pleural opacification since last CXR	Normal	
Chest X-Ray please refer to the chest x-ray closest in time to the repeat biomarker blood draw (at visit 7)	DD / MON / YYYY	<input type="checkbox"/>	<input type="checkbox"/>	<input type="checkbox"/>	<input type="checkbox"/>	<input type="checkbox"/>
CT Scan of Chest	DD / MON / YYYY	<input type="checkbox"/>				
MRI Chest	DD / MON / YYYY	<input type="checkbox"/>				
Chest Ultrasound	DD / MON / YYYY	<input type="checkbox"/>				
Other, specify: _____	DD / MON / YYYY	<input type="checkbox"/>				
Other, specify: _____	DD / MON / YYYY	<input type="checkbox"/>				

DIAGNOSTIC SAMPLING METHODS USED			
Have any further pleural aspiration been taken since last protocol scheduled visit?	1 = Yes 2 = No	<input type="checkbox"/>	DD/MON/YYYY DD/MON/YYYY
Intention:	1 = Diagnostic 2 = Diagnostic/Therapeutic	<input type="checkbox"/>	
Please list all other investigations performed since last scheduled visit:			If yes please give date(s), including repeat investigations where these were performed
Abram's pleural biopsy	1 = Yes 2 = No	<input type="checkbox"/>	DD/MON/YYYY DD/MON/YYYY
CT-guided biopsy	1 = Yes 2 = No	<input type="checkbox"/>	DD/MON/YYYY DD/MON/YYYY
US-guided biopsy	1 = Yes 2 = No	<input type="checkbox"/>	DD/MON/YYYY DD/MON/YYYY
Medical Thoracoscopy	1 = Yes 2 = No	<input type="checkbox"/>	DD/MON/YYYY DD/MON/YYYY
Surgical Thoracoscopy	1 = Yes 2 = No	<input type="checkbox"/>	DD/MON/YYYY DD/MON/YYYY
Other biopsy – please specify _____	1 = Yes 2 = No	<input type="checkbox"/>	DD/MON/YYYY DD/MON/YYYY

ANTI CANCER TREATMENT	
Has the patient started any anti-cancer treatment in the period covered by this form?	<p>1 = No</p> <p>2 = Yes, for confirmed progression</p> <p>3 = Yes, other reason, please specify below: _____</p> <p style="text-align: right;"><input type="checkbox"/></p>
If yes, then type of anti-cancer treatment: (please put the option number in the box at the side)	<p>1 = Chemotherapy or chemotherapy combination, please specify all drugs and number of cycles given: _____</p> <p>2 = Palliative Radiotherapy, please specify dose and number of fractions: _____</p> <p>3 = Radical Radiotherapy, please specify total dose and number of fractions: _____</p> <p>4 = Surgical Treatment, please specify nature of surgery performed: _____</p> <p>5 = Clinical Trial, please specify: _____</p> <p>6 = Combination of above treatments, please specify: _____</p> <p>7 = Other, please specify: _____</p> <p style="text-align: right;"><input type="checkbox"/></p>
	Date treatment started
	DD / MON / YYYY

SAMPLING FOR TRANSLATIONAL RESEARCH	
Have the scheduled repeat translational blood samples been taken at this visit?	<p>1 = Yes</p> <p>2 = No, patient refused consent</p> <p>3 = No, not taken other reason. Please specify: _____</p> <p style="text-align: right;"><input type="checkbox"/></p>
Date blood sample taken:	DD / MON / YYYY

DATE: DD / MON / YYYY INVESTIGATOR'S SIGNATURE: _____


Version 2 Final 12th March 2015

Please return completed form to: Clinical Trial Coordinator – DIAPHRAGM Study, CR-UK Clinical Trials Unit, Level 0,
The Beatson West of Scotland Cancer Centre, 1053 Great Western Road, Glasgow, G12 0YN

Appendix 8 MPM Long-term Follow-up Case Report Form

Page 1/3

Long Term Follow Up Form – FUP/

 <p>CANCER RESEARCH UK Clinical Trials Unit, Glasgow</p>	<h2 style="text-align: center;">LONG TERM FOLLOW UP FORM</h2> <p style="text-align: center;"><i>For Mesothelioma Patients only</i> (To be completed at 2 monthly intervals from the Date of Final Diagnosis. First form is due 2 months after Visit 7)</p>	
<h3 style="text-align: center;">L148 - DIAPHRAGM: Diagnostic and Prognostic biomarkers in the Rational Assessment of Mesothelioma</h3>		
PATIENT INITIALS: (forename) _____ (surname) _____	DATE of BIRTH: <u>DD</u> / <u>MON</u> / <u>YYYY</u>	
INVESTIGATOR:	REGISTRATION DATE: <u>DD</u> / <u>MON</u> / <u>YYYY</u>	
SITE:	PATIENT TRIAL IDENTIFIER:	

Tick to indicate the follow-up period covered by this form (tick one only):-			
2 months after visit 7	<input type="checkbox"/>	14 months after visit 7	<input type="checkbox"/>
4 months after visit 7	<input type="checkbox"/>	16 months after visit 7	<input type="checkbox"/>
6 months after visit 7	<input type="checkbox"/>	18 months after visit 7	<input type="checkbox"/>
8 months after visit 7	<input type="checkbox"/>	20 months after visit 7	<input type="checkbox"/>
10 months after visit 7	<input type="checkbox"/>	22 months after visit 7	<input type="checkbox"/>
12 months after visit 7	<input type="checkbox"/>	24 months after visit 7	<input type="checkbox"/>

CURRENT STATUS	
Date last known alive or date of death:	<u>DD</u> / <u>MON</u> / <u>YYYY</u>
Patient's status at above date:	1 = Alive 2 = Dead <input type="checkbox"/>
If dead, cause of death:	1 = Mesothelioma 2 = Malignant disease (non-mesothelioma), please specify below:- 3 = Toxicity of treatment, please specify below:- 4 = Inter-current disease, please specify below:- 5 = Associated chronic disease, please specify below:- 6 = Other, please specify below:- 7 = Unknown <input type="checkbox"/>
Reliable evidence for cause of death:	1 = Autopsy 2 = Histological 3 = Clinical 4 = Microbiological 5 = Death certificate 6 = No reliable evidence 7 = Other, please specify below:- <input type="checkbox"/>

Version 1.1 12th June 2015

Please return completed form to: Clinical Trial Coordinator – DIAPHRAGM Study, CR-UK Clinical Trials Unit, Level 0,
The Beatson West of Scotland Cancer Centre, 1053 Great Western Road, Glasgow, G12 0YN

ANTI CANCER TREATMENT

Has the patient started any anti-cancer treatment in the period covered by this form?

- 1 = No
 2 = Yes, for confirmed progression
 3 = Yes, other reason, please specify below:

☐

If yes, then type of anti-cancer treatment:

(please put the option number in the box at the side)

1 = Chemotherapy or chemotherapy combination, please specify all drugs and number of cycles given:

Drug _____ No of Cycles _____

Drug _____ No of Cycles _____

Drug _____ No of Cycles _____

2 = Palliative Radiotherapy, please specify dose and number of fractions:

Dose No of fractions

3 = Radical Radiotherapy, please specify total dose and number of fractions:

Dose No of fractions

☐

4 = Surgical Treatment, please specify nature of surgery performed:

5 = Clinical Trial, please specify:

6 = Combination of above treatments, please specify:

7 = Other, please specify:

Date treatment started:

DD / MON / YYYY

PLEURAL INTERVENTIONS	
Has the patient had any pleural interventions in the period covered by this form?	1 = No 2 = Yes, for recurrent symptomatic pleural effusion 3 = Yes, other reason, please specify below: _____
If yes, then type of pleural intervention? (please tick all that apply)	<div style="display: flex; justify-content: space-between;"> <div> Therapeutic Pleural Aspiration Intercostal Drainage Poundrage Pleurodesis Slurry Pleurodesis IPC Insertion Medical Thoracoscopy Other, please specify below: _____ </div> <div style="display: flex; flex-direction: column; align-items: flex-end;"> <input type="checkbox"/> <input type="checkbox"/> <input type="checkbox"/> <input type="checkbox"/> <input type="checkbox"/> <input type="checkbox"/> <input type="checkbox"/> </div> </div>
Date of pleural intervention:	DD / MON / YYYY

DATE: DD / MON / YYYY


INVESTIGATOR'S SIGNATURE: _____

Appendix 9 Diagnostic Review Case Report Form

Page 1/3

DIAPHRAGM (L148)

Diagnostic Review – DR/

 <p>CANCER RESEARCH UK Clinical Trials Unit, Glasgow</p>	DIAGNOSTIC REVIEW <i>(To be completed as soon as any new pleural diagnosis is available, or if date and cause of death is available. If no new diagnosis made, to be completed at 12 months following Final Diagnosis. Applicable for all patients except those with a cytological or histological diagnosis of malignancy including Mesothelioma)</i>	
	L148 - DIAPHRAGM: Diagnostic and Prognostic biomarkers in the Rational Assessment of Mesothelioma	
PATIENT INITIALS: (forename) _____ (surname) _____		DATE of BIRTH: <u>DD</u> / <u>MON</u> / <u>YYYY</u>
INVESTIGATOR:		REGISTRATION DATE: <u>DD</u> / <u>MON</u> / <u>YYYY</u>
SITE:		PATIENT TRIAL IDENTIFIER:

CURRENT STATUS			
Date last known alive or date of death:			<u>DD</u> / <u>MON</u> / <u>YYYY</u>
Patient's status at above date:	1 = Alive 2 = Dead		<input type="checkbox"/>
If dead, cause of death:	1 = Mesothelioma 2 = Malignant disease (non-mesothelioma), please specify below:- 3 = Toxicity of treatment, please specify below:- 4 = Inter-current disease, please specify below:- 5 = Associated chronic disease, please specify below:- 6 = Other, please specify below:- <hr/> 7 = Unknown		<input type="checkbox"/>
Reliable evidence for cause of death:	1 = Autopsy 2 = Histological 3 = Clinical 4 = Microbiological 5 = Death certificate 6 = No reliable evidence 7 = Other, please specify below:- <hr/>		<input type="checkbox"/>

PATIENT DIAGNOSIS			
Has there been any new Pleural Diagnosis made since the Date of Final Diagnosis	1 = Yes 2 = No	If yes, please continue with the remainder of the form. If no, ignore pages 2 & 3, sign and date.	<input type="checkbox"/>

Version 2.0, 20May2016

Please return completed form to: Clinical Trial Coordinator – DIAPHRAGM Study, CRUK Clinical Trials Unit, Level 0,
The Beatson West of Scotland Cancer Centre, 1053 Great Western Road, Glasgow, G12 0YN

RELEVANT IMAGING INVESTIGATIONS SINCE LAST STUDY VISIT						
Investigation	DATE	or Tick if investigation not performed	RESULT – please tick one			
			No change in extent of of pleural opacification since last CXR	Increased extent of pleural opacification since last CXR	Decreased extent of pleural opacification since last CXR	Normal
Chest X-Ray	DD / MON / YYYY	<input type="checkbox"/>	<input type="checkbox"/>	<input type="checkbox"/>	<input type="checkbox"/>	<input type="checkbox"/>
CT Scan of Chest	DD / MON / YYYY	<input type="checkbox"/>				
MRI Chest	DD / MON / YYYY	<input type="checkbox"/>				
Chest Ultrasound	DD / MON / YYYY	<input type="checkbox"/>				
Other, specify: _____	DD / MON / YYYY	<input type="checkbox"/>				
Other, specify: _____	DD / MON / YYYY	<input type="checkbox"/>				

DIAGNOSTIC SAMPLING METHODS USED			
Have any further pleural aspiration been taken since last protocol scheduled visit?	1 = Yes 2 = No	<input type="checkbox"/>	DD/MON/YYYY DD/MON/YYYY
Intention:	1 = Diagnostic 2 = Diagnostic/Therapeutic	<input type="checkbox"/>	
Please list all other investigations performed since last scheduled visit:		If yes please give date(s), including repeat investigations where these were performed	
Abram's pleural biopsy	1 = Yes 2 = No	<input type="checkbox"/>	DD/MON/YYYY DD/MON/YYYY
CT-guided biopsy	1 = Yes 2 = No	<input type="checkbox"/>	DD/MON/YYYY DD/MON/YYYY
US-guided biopsy	1 = Yes 2 = No	<input type="checkbox"/>	DD/MON/YYYY DD/MON/YYYY
Medical Thoracoscopy	1 = Yes 2 = No	<input type="checkbox"/>	DD/MON/YYYY DD/MON/YYYY
Surgical Thoracoscopy	1 = Yes 2 = No	<input type="checkbox"/>	DD/MON/YYYY DD/MON/YYYY
Other (please specify) _____	1 = Yes 2 = No	<input type="checkbox"/>	DD/MON/YYYY DD/MON/YYYY

UPDATED FINAL DIAGNOSIS <i>(tick if not done or reported on previous form ☐)</i>			
Final Diagnosis: Has the patient been diagnosed with Mesothelioma? 1 = Yes 2 = No (If "No" AND the diagnosis is NOT a cytological or histological diagnosis of another cancer, the Diagnostic Review at 12 months Form must be completed.) Date of Diagnosis: DD / MON / YYYY	<input type="checkbox"/>	If yes, please provide mesothelioma stage (IMIG): Stage I <input type="checkbox"/> Stage II <input type="checkbox"/> Stage Ia <input type="checkbox"/> Stage III <input type="checkbox"/> Stage Ib <input type="checkbox"/> Stage IV <input type="checkbox"/> T stage (1a,1b,2,3,4): _____ N stage (X,0,1,2,3): _____ M stage (X,0,1): _____	
If yes, please indicate type of diagnosis: (if yes, the Follow Up Form must be completed (visit 6 only applies to West of Scotland, MRI sub study, visit 7 applies to all participants) 1 = Radiological 2 = Cytological 3 = Histological 4 = Other, specify: _____	<input type="checkbox"/>	If No, please indicate non-mesothelioma diagnosis: 1 = Other malignancy, specify: _____ 2 = Para-pneumonic effusion 3 = Benign asbestos pleural effusion 4 = Tuberculosis pleurisy 5 = Pulmonary embolism 6 = Rheumatoid pleural effusion 7 = Other, specify: _____	<input type="checkbox"/>


DATE: DD / MON / YYYY **INVESTIGATOR'S SIGNATURE:** _____

Appendix 10 Asbestos-exposed Control Case Report Form

Page 1 of 5

L148 DIAPHRAGM Study

AECF/5

 CANCER RESEARCH UK Clinical Trials Unit, Glasgow		ASBESTOS EXPOSED CONTROLS FORM (to be completed for participants in the Asbestos Exposed Control Group)	
DIAPHRAGM: Diagnostic and Prognostic biomarkers in the Rational Assessment of Mesothelioma			
PATIENT INITIALS: (f) _____ (s) _____		DATE of BIRTH: DD / MON / YYYY	
INVESTIGATOR:		REGISTRATION DATE: DD / MON / YYYY	
SITE: CRF, Glasgow		PATIENT TRIAL IDENTIFIER:	
DATE OF COMPLETION OF FORM:		DD / MON / YYYY	

PATIENT DEMOGRAPHICS	
Ethnic origin:	1 = White 2 = Asian (Indian /Bangladeshi/Pakistani) 3 = South East Asian (Chinese/Japanese/Korean) 4 = Afro/Caribbean 5 = Other, specify: <input type="checkbox"/> _____

PERSONAL INFORMATION	
Postcode: _____	
Height: _____ cm	Weight: _____ kg
MRC Dyspnoea Score (1-5): <input type="checkbox"/>	1 = Not troubled by breathlessness except of strenuous exercise 2 = Short of breath when hurrying or walking up a slight hill 3 = Walks slower than contemporaries on level ground because of breathlessness, or has to stop for breath when walking at own pace 4 = Stops for breath after walking about 100m or after a few minutes on level ground 5 = Too breathless to leave the house, or breathless when dressing or undressing

Version 2, 2nd December 2014

Please return completed form to: Clinical Trial Coordinator – DIAPHRAGM Study
 CRUK Clinical Trials Unit, Level 0,
 The Beatson West of Scotland Cancer Centre, 1053 Great Western Road, Glasgow, G12 0YN

SMOKING HISTORY	
Smoking History:	1 = Current smoker <input type="checkbox"/> 2 = Non-smoker 3 = Ex-smoker
If Smoker/Ex-Smoker:	When did you start smoking? DD / MON / YYYY How many per day on average? _____
If Ex-Smoker:	When did you stop? DD / MON / YYYY

CURRENT SYMPTOMS	
Symptom	Please tick to indicate if patient has or has not had any of these symptoms
Shortness of Breath within last 6 months	Yes <input type="checkbox"/> No <input type="checkbox"/> Not Known <input type="checkbox"/>
Chest pain within last 6 months	Yes <input type="checkbox"/> No <input type="checkbox"/> Not Known <input type="checkbox"/>
Weight loss within last 6 months	Yes <input type="checkbox"/> No <input type="checkbox"/> Not Known <input type="checkbox"/>
Please specify below any other current symptom. If NO other current symptoms please tick <input type="checkbox"/>	
Other current symptom, specify:	
Other current symptom, specify:	
Other current symptom, specify:	
Other current symptom, specify:	

PAST MEDICAL HISTORY		
	Please tick to indicate if patient has or has not had any of these events	Please tick to indicate if event is ONGOING at present
RESPIRATORY – please specify below any history of respiratory events - if none please tick <input type="checkbox"/>		
Chronic Obstructive Pulmonary Disease	Yes <input type="checkbox"/> No <input type="checkbox"/>	Yes <input type="checkbox"/> No <input type="checkbox"/>
Asthma	Yes <input type="checkbox"/> No <input type="checkbox"/>	Yes <input type="checkbox"/> No <input type="checkbox"/>
Pulmonary Fibrosis	Yes <input type="checkbox"/> No <input type="checkbox"/>	Yes <input type="checkbox"/> No <input type="checkbox"/>
Other specify:	Yes <input type="checkbox"/> No <input type="checkbox"/>	Yes <input type="checkbox"/> No <input type="checkbox"/>
Other, specify:	Yes <input type="checkbox"/> No <input type="checkbox"/>	Yes <input type="checkbox"/> No <input type="checkbox"/>
CARDIOVASCULAR – please specify below any history of cardiovascular events - if none please tick <input type="checkbox"/>		
Ischaemic Heart Disease	Yes <input type="checkbox"/> No <input type="checkbox"/>	Yes <input type="checkbox"/> No <input type="checkbox"/>
LV Systolic Dysfunction	Yes <input type="checkbox"/> No <input type="checkbox"/>	Yes <input type="checkbox"/> No <input type="checkbox"/>
CVA or TIA	Yes <input type="checkbox"/> No <input type="checkbox"/>	Yes <input type="checkbox"/> No <input type="checkbox"/>
Hypertension	Yes <input type="checkbox"/> No <input type="checkbox"/>	Yes <input type="checkbox"/> No <input type="checkbox"/>
Other, specify:	Yes <input type="checkbox"/> No <input type="checkbox"/>	Yes <input type="checkbox"/> No <input type="checkbox"/>
Other, specify:	Yes <input type="checkbox"/> No <input type="checkbox"/>	Yes <input type="checkbox"/> No <input type="checkbox"/>
CANCER – please specify below any history of cancer - if none please tick <input type="checkbox"/>		
	Yes <input type="checkbox"/> No <input type="checkbox"/>	Yes <input type="checkbox"/> No <input type="checkbox"/>
	Yes <input type="checkbox"/> No <input type="checkbox"/>	Yes <input type="checkbox"/> No <input type="checkbox"/>
OTHER PAST MEDICAL HISTORY – please specify below any other past medical history - if none please tick <input type="checkbox"/>		
Chronic Renal Failure	Yes <input type="checkbox"/> No <input type="checkbox"/>	Yes <input type="checkbox"/> No <input type="checkbox"/> If yes, please provide most recent eGFR result: _____mls/min DD/MON/YYYY
Diabetes Mellitus	Yes <input type="checkbox"/> No <input type="checkbox"/>	Yes <input type="checkbox"/> No <input type="checkbox"/>
Other, specify:	Yes <input type="checkbox"/> No <input type="checkbox"/>	Yes <input type="checkbox"/> No <input type="checkbox"/>
Other, specify:	Yes <input type="checkbox"/> No <input type="checkbox"/>	Yes <input type="checkbox"/> No <input type="checkbox"/>
Other, specify:	Yes <input type="checkbox"/> No <input type="checkbox"/>	Yes <input type="checkbox"/> No <input type="checkbox"/>

Version 2, 2nd December 2014

Please return completed form to: Clinical Trial Coordinator – DIAPHRAGM Study
CRUK Clinical Trials Unit, Level 0,
The Beatson West of Scotland Cancer Centre, 1053 Great Western Road, Glasgow, G12 0YN

RADIOGRAPHIC EVIDENCE OF ASBESTOS EXPOSURE (Please use most recent report available from clinical portal) NB. Pleural effusion or Mesothelioma is an exclusion criteria								
INVESTIGATION	DATE or	Tick if investigation not performed	RESULT – please tick all that apply					
			Normal	Pleural Plaques	Pulmonary Fibrosis	Diffuse Pleural Thickening	Other Abnormality, specify	Imaging performed, result not available *
Chest X-Ray	DD / MON / YYYY	<input type="checkbox"/>	<input type="checkbox"/>	<input type="checkbox"/>	<input type="checkbox"/>	<input type="checkbox"/>	<input type="checkbox"/>	<input type="checkbox"/>
			Where applicable, please specify _____					
CT Chest	DD / MON / YYYY	<input type="checkbox"/>	<input type="checkbox"/>	<input type="checkbox"/>	<input type="checkbox"/>	<input type="checkbox"/>	<input type="checkbox"/>	<input type="checkbox"/>
			Where applicable, please specify _____					
Other Investigation (specify type of investigation, date and result). If no other investigations, please tick <input type="checkbox"/>								
	DD / MON / YYYY	<input type="checkbox"/>	<input type="checkbox"/>	<input type="checkbox"/>	<input type="checkbox"/>	<input type="checkbox"/>	<input type="checkbox"/>	<input type="checkbox"/>
			Where applicable, please specify _____					
	DD / MON / YYYY	<input type="checkbox"/>	<input type="checkbox"/>	<input type="checkbox"/>	<input type="checkbox"/>	<input type="checkbox"/>	<input type="checkbox"/>	<input type="checkbox"/>
			Where applicable, please specify _____					
	DD / MON / YYYY	<input type="checkbox"/>	<input type="checkbox"/>	<input type="checkbox"/>	<input type="checkbox"/>	<input type="checkbox"/>	<input type="checkbox"/>	<input type="checkbox"/>
			Where applicable, please specify _____					

* Where possible, please specify the diagnosis previously given to the patient

SAMPLING FOR TRANSLATIONAL RESEARCH

Have the scheduled translational blood samples been taken for this patient at this visit?

- 1= Yes
2= No, patient refused consent
3= No, not taken other reason Please specify:

☐

Date blood sample taken:

DD / MON / YYYY

ASBESTOS EXPOSURE QUESTIONNAIRE

Has the Asbestos Exposure Questionnaire been completed for this patient?

- 1= Yes
2= No, patient refused consent
3= No, other reason. Please specify:

☐

DATE: DD / MON / YYYY

INVESTIGATOR'S SIGNATURE: _____

Version 2, 2nd December 2014


Please return completed form to: Clinical Trial Coordinator – DIAPHRAGM Study
CRUK Clinical Trials Unit, Level 0,
The Beatson West of Scotland Cancer Centre, 1053 Great Western Road, Glasgow, G12 0YN

Appendix 11 Asbestos Exposure Questionnaire

Page 1 of 2

L148 DIAPHRAGM Study

AEQ/4

 CANCER RESEARCH UK Clinical Trials Unit, Glasgow		ASBESTOS EXPOSURE QUESTIONNAIRE (to be completed for all patients on study)							
DIAPHRAGM: Diagnostic and Prognostic biomarkers in the Rational Assessment of Mesothelioma									
PATIENT INITIALS: (f) _____ (s) _____					DATE of BIRTH: DD / MON / YYYY				
INVESTIGATOR:					REGISTRATION DATE: DD / MON / YYYY				
SITE:					PATIENT TRIAL IDENTIFIER:				
DATE OF COMPLETION OF QUESTIONNAIRE: DD / MON / YYYY									
Employment History									
No known asbestos exposure <input type="checkbox"/>									
Industry / Occupation e.g. joiner, shipyard worker	Period of Employment			No. of Hours per day	Days per week	Airway protection?	Job Type <small>Please refer to codes below</small>	Job Code <small>Please refer to Page 2</small>	Indirect Exposure Details <small>e.g. via husband, via father</small>
	Start Year	No. of Years	No. of Months						
1.	YYYY			_____	_____	Yes <input type="checkbox"/> No <input type="checkbox"/>			
2.	YYYY			_____	_____	Yes <input type="checkbox"/> No <input type="checkbox"/>			
3.	YYYY			_____	_____	Yes <input type="checkbox"/> No <input type="checkbox"/>			
4.	YYYY			_____	_____	Yes <input type="checkbox"/> No <input type="checkbox"/>			
5.	YYYY			_____	_____	Yes <input type="checkbox"/> No <input type="checkbox"/>			

JOB TYPE: M = Manufacturing asbestos products S = Asbestos Stripping/Removal O = Something else I = Indirect exposure

Version 2, 7th Jan 2015

Please return completed form to: Clinical Trial Coordinator – DIAPHRAGM Study
 CRUK Clinical Trials Unit, Level 0, The Beatson West of Scotland Cancer Centre, 1053 Great Western Road, Glasgow, G12 0YN

Job Codes (Taken from Appendix 5 of the HSE Asbestos Survey)

CODE LIST M

Textile manufacture	42 Other exposed worker
01 Raw material store	
02 Raw material & finished product transport	Asbestos board and paper manufacture
03 Disintegrating/heating/opening/fibrising	43 Raw material store
04 Hopper feeding	44 Raw material transport
05 Carding	45 Disintegrating/opening/fibrising
06 Weaving	46 Mixing/beating
07 Spinning	47 Handling wet mixture
08 Doubling/twisting	48 Drying
09 Braiding	49 Handling dry mixture
10 Warping	50 Cutting/machining
11 Detritus handling	51 Store/transport/packing/dispatching products
12 Inspecting	52 Supervising
13 Supervising	53 Detritus handling
14 Finished product store & dispatch	54 Inspecting
15 Other exposed workers	55 Other exposed workers
95 'Fortex' process	
Asbestos cement mixture board and pipe manufacture	Garment manufacture
16 Supervising	56 Cloth store
17 Raw material store	57 Cutting out
18 Raw material transport	58 Stitching
19 Disintegrating	59 Transport of materials
20 Mixing/beating	60 Storing/packing/dispatching
21 Wet board or pipe manufacture	61 Inspecting
22 Wet board or pipe handling	62 Supervising
23 Drying	63 Other exposed workers
24 Dry board handling	Manufacture of dry mixes for insulation & plastering
25 Machining or cutting	70 Raw material stores
26 Sanding	71 Raw material handling/bag tipping/weighting/mixing
27 Inspecting	72 Packaging
28 Finished product store/packing/dispatch/transport	73 Stores and dispatch
29 Detritus handling wet	74 Other exposed workers
30 Detritus handling dry	
31 Other exposed worker	Maintenance workers all manufacturing sectors
Manufacture of asbestos/rubber/resin bitumen mixtures	75 Supervising
32 Raw material store	76 Fault finder/machine fitter/installation engineer/plant engineer
33 Transporting raw materials	77 Labour to plant engineers etc
34 Disintegrating	78 Carpenters/joiners
35 Handling raw fibre (bag tipping/weighting/mixing)	79 Electrician
36 Pressing/moulding	80 Plumber
37 Cutting/finishing/machining	81 Other building trade craftsmen eg painter
38 Transporting finished product	82 Labourer to building trade craftsman
39 Finished product storage/packing/dispatching	83 Ventilation plant servicing
40 Inspecting	84 Factory cleaning
41 Supervising	

CODE LIST S

Asbestos stripping/removal	65 Stripping/encapsulating
64 Supervising	69 Other exposed workers (eg sampler, cleaner, scaffolder)



CODE LIST O

Ship building, repair, & breaking	97 Asbestos board cutting/fitting
85 Asbestos storeman	98 Asbestos roofing construction and maintenance
86 Lagging	99 Demolition
87 Boilermakers and installers	104 Other building trade craftsmen eg painter (81)*
88 Carpenters/joiners	105 Labourer to building trade craftsman (82)
89 Plumber	106 Plumber (80)
90 Engine fitter	107 Carpenters/joiners (78)
91 Other exposed workers	
92 Asbestos stripping	Miscellaneous processes
93 Cleaner	101 Use of asbestos string/rope/felt (65)
94 Shipbreaking	102 Fitting clutch and brake pads (37)
Building & construction	108 Machining/cutting asbestos/resin board (50)
96 Heating engineer	109 Other exposed workers (69)

Version 2, 7th Jan 2015

Please return completed form to: Clinical Trial Coordinator – DIAPHRAGM Study
CRUK Clinical Trials Unit, Level 0, The Beatson West of Scotland Cancer Centre,
1053 Great Western Road, Glasgow, G12 0YN

Appendix 12 MRI Safety Questionnaire

	Clinical Research Imaging Facility MRI Safety Checklist - <i>PATIENTS</i>	
---	---	---

Patient Name:	Date of Birth:	Date of Scan:
Address:	Investigator:	Study ID:
CHI:	Weight:	Height:

Have you ever:		
Had a cardiac pacemaker?	YES	NO
Had any surgery to your heart?	YES	NO
• If yes, give details.....		
Had any surgery on your head, brain or eyes?	YES	NO
• If yes, give details.....		
Had any surgery involving the use of metal implants, plates, or clips?	YES	NO
• If yes, give details.....		
Had any surgery involving the use of electronic, mechanical or magnetic implants?	YES	NO
• If yes, give details.....		
Had any other surgery?	YES	NO
• If yes, give details.....		
Had metal fragments in your eyes or any other part of the body?	YES	NO
Do you:		
Have any kidney problems, kidney failure or ever had dialysis?	YES	NO
Have asthma, eczema, hayfever or any known allergies?	YES	NO
Have metal dentures/dental plate, hearing aid or wig?	YES	NO
Wear a false limb, calliper or brace?	YES	NO
Have any tattoos, permanent makeup or body piercing?	YES	NO
Wear any type of skin patch?	YES	NO
Ladies:	YES	NO
Could you be pregnant?		
• LMP date:		
Are you breast feeding?	YES	NO
Have you been sterilised or have an IUD fitted?	YES	NO
Before entry into the examination room all metallic objects must be removed: Metal tools, scissors, keys, watches, pagers, credit cards, coins, hair clips, hearing aid etc. Have all objects been removed? <div style="border: 1px solid black; width: 80px; height: 40px; display: inline-block; vertical-align: middle;"></div>		

I confirm that the answers to the above safety questions are correct and I will accept a contrast agent injection if required.

Signature of patient _____ Date / /

Signature of Authorised Scanning Staff Member	
---	--

Refer to supervising doctor that a patient is safe to image if:

- An implant or operation is not included in safety literature

The **supervising doctor** should sign here if they now consider the scan to be completely safe.

MRI Drug and Contrast Administration Record

eGFR _____

Date of eGFR _____

If eGFR <59ml/min consult Supervising Doctor

Contrast Details

Contrast Label:

Expiry Checked By:

Contrast Type:

Total Contrast Injected:

Total Saline Injected:

Signature of Person Administering Contrast:

Images Checked for Contrast

☐

Drug reaction/ extravasation details:

Post Processing

PACS

Sent - Checked

CRIS

Yes/No

WHITE FOLDER

Yes/No

BHF

Sent - Checked

CRF

Yes/No

Daily Activity

Yes/No

DVD No

Sent/Checked

Upload..... (Please note method i.e. SFTP/Web Upload)

References

1. Røe OD. Malignant pleural mesothelioma: history, controversy and future of a manmade epidemic. 2016 Sep 19;:1-17.
2. Yalcin NG, Choong CKC, Eizenberg N. Anatomy and pathophysiology of the pleura and pleural space. *Thorac Surg Clin*. Elsevier; 2013 Feb;23(1):1-10-v.
3. Charalampidis C, Youroukou A, Lazaridis G, Baka S, Mpoukovinas I, Karavasilis V, et al. Pleura space anatomy. *J Thorac Dis*. 2015 Feb;7(Suppl 1):S27-32.
4. Miserocchi G. Physiology and pathophysiology of pleural fluid turnover. *European Respiratory Journal*. 1997 Jan 1;10(1):219-25.
5. Zocchi L. Physiology and pathophysiology of pleural fluid turnover. *Eur Respir J*. 2002 Dec 1;20(6):1545-58.
6. Romero-Candeira S, Hernández L, Romero-Brufao S, Orts D, Fernández C, Martín C. Is it meaningful to use biochemical parameters to discriminate between transudative and exudative pleural effusions? *Chest*. 2002 Nov;122(5):1524-9.
7. Light RW, Macgregor MI, Luchsinger PC, Ball WC. Pleural effusions: the diagnostic separation of transudates and exudates. *Ann Intern Med*. American College of Physicians; 1972 Oct;77(4):507-13.
8. Sahn SA. The pathophysiology of pleural effusions. *Annu Rev Med*. Annual Reviews 4139 El Camino Way, P.O. Box 10139, Palo Alto, CA 94303-0139, USA; 1990;41(1):7-13.
9. Stathopoulos GT, Kalomenidis I. Malignant pleural effusion: tumor-host interactions unleashed. *Am J Respir Crit Care Med*. 2012 Sep 15;186(6):487-92.
10. Meyer PC. Metastatic carcinoma of the pleura. *Thorax*. BMJ Group; 1966 Sep;21(5):437-43.
11. Sahn SA. Pleural diseases related to metastatic malignancies. *European Respiratory Journal*. 1997 Aug 1;10(8):1907-13.
12. Porcel JM, Esquerda A, Vives M, Bielsa S. Etiology of pleural effusions: analysis of more than 3,000 consecutive thoracenteses. *Arch Bronconeumol*. 2014 May;50(5):161-5.
13. Psallidas I, Kalomenidis I, Porcel JM, Robinson BW, Stathopoulos GT. Malignant pleural effusion: from bench to bedside. *Eur Respir Rev*. European Respiratory Society; 2016 Jun;25(140):189-98.
14. Clive AO, Kahan BC, Hooper CE, Bhatnagar R, Morley AJ, Zahan-Evans N, et al. Predicting survival in malignant pleural effusion: development and validation of the LENT prognostic score. *Thorax*.

BMJ Publishing Group Ltd and British Thoracic Society; 2014 Dec;69(12):1098-104.

15. Porcel JM, Gasol A, Bielsa S, Civit C, Light RW, Salud A. Clinical features and survival of lung cancer patients with pleural effusions. *Respirology*. 2015 May;20(4):654-9.
16. HSE. Mesothelioma in Great Britain. 2016 Jun 27;:1-8.
17. Hodgson JT, Darnton A. The quantitative risks of mesothelioma and lung cancer in relation to asbestos exposure. *Ann Occup Hyg*. Oxford University Press; 2000 Dec;44(8):565-601.
18. Yates DH, Corrin B, Stidolph PN, Browne K. Malignant mesothelioma in south east England: clinicopathological experience of 272 cases. *Thorax*. BMJ Group; 1997 Jun;52(6):507-12.
19. Carbone M, Kratzke RA, Testa JR. The pathogenesis of mesothelioma. *Seminars in Oncology*. 2002 Feb;29(1):2-17.
20. Rake C, Gilham C, Hatch J, Darnton A, Hodgson J, Peto J. Occupational, domestic and environmental mesothelioma risks in the British population: a case-control study. *Br J Cancer*. Nature Publishing Group; 2009 Apr 7;100(7):1175-83.
21. Bourdès V, Boffetta P, Pisani P. Environmental exposure to asbestos and risk of pleural mesothelioma: review and meta-analysis. *Eur J Epidemiol*. 2000 May;16(5):411-7.
22. WAGNER JC, SLEGGs CA, MARCHAND P. Diffuse pleural mesothelioma and asbestos exposure in the North Western Cape Province. *Br J Ind Med*. BMJ Group; 1960 Oct;17(4):260-71.
23. Stephens RJ, Whiting C, Cowan K, Committee2 JLAMPSPS. Research priorities in mesothelioma: A James Lind Alliance Priority Setting Partnership. *Lung Cancer*. Elsevier Ireland Ltd; 2015 Aug 1;89(2):175-80.
24. Riaz SP, Coupland VH, Lüchtenborg M, Peake MD, Møller H. Mesothelioma incidence projections in South East England. *Eur Respir J*. 2012 Sep 30;40(4):965-8.
25. Hodgson JT, McElvenny DM, Darnton AJ, Price MJ, Peto J. The expected burden of mesothelioma mortality in Great Britain from 2002 to 2050. *Br J Cancer*. 2005 Jan 25;:1-7.
26. PhD ALFM, LSHTM TKJMMSM. The Global Spread of Asbestos. *Annals of Global Health*. Elsevier Inc; 2014 Jul 8;80(4):257-62.
27. louise. REPORTING DEATHS TO THE PROCURATOR FISCAL Information and Guidance for Medical Practitioners Produced by Crown Office and Procurator Fiscal Service 2015. 2015 Nov 5;:1-16.
28. Goodman JE, Nascarella MA, Valberg PA. Ionizing radiation: a risk

- factor for mesothelioma. *Cancer Causes Control*. Springer Netherlands; 2009 Oct;20(8):1237-54.
29. Vilchez RA, Butel JS. Emergent Human Pathogen Simian Virus 40 and Its Role in Cancer. *Clinical Microbiology Reviews*. 2004 Jul 16;17(3):495-508.
 30. Robinson BWS, Musk AW, Lake RA. Malignant mesothelioma. *Lancet*. Elsevier; 2005 Aug;366(9483):397-408.
 31. Miserocchi G, Sancini G, Mantegazza F, Chiappino G. Translocation pathways for inhaled asbestos fibers. *Environ Health*. 2nd ed. 2008 Jan 24;7(1):701-8.
 32. Yang H, Testa JR, Carbone M. Mesothelioma Epidemiology, Carcinogenesis, and Pathogenesis. *Curr Treat Options in Oncol*. 2008 Aug 15;9(2-3):147-57.
 33. Yang H, Bocchetta M, Kroczyńska B, Elmishad AG, Chen Y, Liu Z, et al. TNF-alpha inhibits asbestos-induced cytotoxicity via a NF-kappaB-dependent pathway, a possible mechanism for asbestos-induced oncogenesis. *Proc Natl Acad Sci USA*. 2006 Jul 5;103(27):10397-402.
 34. Philip M, Rowley DA, Schreiber H. Inflammation as a tumor promoter in cancer induction. *Semin Cancer Biol*. 2004 Dec;14(6):433-9.
 35. Rascoe PA, Cao X, Daniel JC, Miller SD, Smythe WR. Receptor tyrosine kinase and phosphoinositide-3 kinase signaling in malignant mesothelioma. *J Thorac Cardiovasc Surg*. 2005 Aug;130(2):393-400.
 36. Zucali PA, Ceresoli GL, De Vincenzo F, Simonelli M, Lorenzi E, Gianoncelli L, et al. Advances in the biology of malignant pleural mesothelioma. *Cancer Treatment Reviews*. Elsevier Ltd; 2011 Nov 1;37(7):543-58.
 37. Ohta Y, Shridhar V, Bright RK, Kalemkerian GP, Du W, Carbone M, et al. VEGF and VEGF type C play an important role in angiogenesis and lymphangiogenesis in human malignant mesothelioma tumours. *Br J Cancer*. Nature Publishing Group; 1999 Sep;81(1):54-61.
 38. Liu Z, Klominek J. Chemotaxis and chemokinesis of malignant mesothelioma cells to multiple growth factors. *Anticancer Res*. 2004 May;24(3a):1625-30.
 39. Adams VI, Unni KK, Muhm JR, Jett JR, Ilstrup DM, Bernatz PE. Diffuse malignant mesothelioma of pleura. Diagnosis and survival in 92 cases. *Cancer*. 1986 Oct 1;58(7):1540-51.
 40. Seely JM, Nguyen ET, Churg AM, Müller NL. Malignant pleural mesothelioma: computed tomography and correlation with histology. *Eur J Radiol*. 2009 Jun;70(3):485-91.
 41. Sahin AA, Cöplü L, Selçuk ZT, Eryilmaz M, Emri S, Akhan O, et al. Malignant pleural mesothelioma caused by environmental exposure to

- asbestos or erionite in rural Turkey: CT findings in 84 patients. *AJR American journal of roentgenology*. American Public Health Association; 1993 Sep;161(3):533-7.
42. Tsim S, Dick C, Roberts F, Gronski M, Stobo D, Noble C, et al. 76 Early experience of a regional mesothelioma MDT in the West of Scotland. *Lung Cancer*. *Lung Cancer*; 2014;Supplement 1(83):S28-9.
 43. National Lung Cancer Audit Report2014Mesothelioma. 2014 Sep 9;:1-27.
 44. Hooper C, Lee YCG, Maskell N, BTS Pleural Guideline Group. Investigation of a unilateral pleural effusion in adults: British Thoracic Society Pleural Disease Guideline 2010. Vol. 65 Suppl 2, *Thorax*. BMJ Publishing Group Ltd and British Thoracic Society; 2010. pp. ii4-17.
 45. Davies HE, Nicholson JE, Rahman NM, Wilkinson EM, Davies RJO, Lee YCG. Outcome of patients with nonspecific pleuritis/fibrosis on thoracoscopic pleural biopsies. *Eur J Cardiothorac Surg*. Oxford University Press; 2010 Oct;38(4):472-7.
 46. Pairon J-C, Laurent F, Rinaldo M, Clin B, Andujar P, Ameille J, et al. Pleural plaques and the risk of pleural mesothelioma. *J Natl Cancer Inst*. Oxford University Press; 2013 Feb 20;105(4):293-301.
 47. Paris C, Thierry S, Brochard P, Letourneux M, Schorle E, Stoufflet A, et al. Pleural plaques and asbestosis: dose- and time-response relationships based on HRCT data. *Eur Respir J*. European Respiratory Society; 2009 Jul;34(1):72-9.
 48. Salonen O, Kivisaari L, Standertskjöld-Nordenstam CG, Somer K, Mattson K, Tammilehto L. Computed tomography of pleural lesions with special reference to the mediastinal pleura. *Acta Radiol Diagn (Stockh)*. 1986 Sep;27(5):527-31.
 49. Villena V, López-Encuentra A, García-Luján R, Echave-Sustaeta J, Martínez CJA. Clinical implications of appearance of pleural fluid at thoracentesis. *Chest*. 2004 Jan;125(1):156-9.
 50. Light RW, Erozan YS, Ball WC. Cells in pleural fluid. Their value in differential diagnosis. *Arch Intern Med*. American Medical Association; 1973 Dec;132(6):854-60.
 51. Walters J, Maskell NA. Biopsy techniques for the diagnosis of mesothelioma. *Recent Results Cancer Res*. Berlin, Heidelberg: Springer Berlin Heidelberg; 2011;189(Chapter 4):45-55.
 52. Segal A, Sterrett GF, Frost FA, Shilkin KB, Olsen NJ, William Musk A, et al. A diagnosis of malignant pleural mesothelioma can be made by effusion cytology: results of a 20 year audit. *Pathology*. 2013 Jan;45(1):44-8.
 53. Paintal A, Raparia K, Zakowski MF, Nayar R. The diagnosis of

- malignant mesothelioma in effusion cytology: a reappraisal and results of a multi-institution survey. *Cancer Cytopathol.* 2013 Dec;121(12):703-7.
54. Husain AN, Colby T, Ordonez N, Krausz T, Attanoos R. ... Group. Guidelines for pathologic diagnosis of malignant mesothelioma: 2012 update of the consensus statement from the International Mesothelioma *Arch Pathol Lab Med*; 2013.
 55. Churg A, Colby TV, Cagle P, Corson J, GIBBS AR, Gilks B, et al. The separation of benign and malignant mesothelial proliferations. *Am J Surg Pathol.* 2000 Sep;24(9):1183-200.
 56. Rakha EA, Patil S, Abdulla K, Abdulkader M, Chaudry Z, Soomro IN. The sensitivity of cytologic evaluation of pleural fluid in the diagnosis of malignant mesothelioma. *Diagn Cytopathol.* 2010 Nov 19;38(12):874-9.
 57. Henderson DW, Reid G, Kao SC, van Zandwijk N, Klebe S. Challenges and controversies in the diagnosis of mesothelioma: Part 1. Cytology-only diagnosis, biopsies, immunohistochemistry, discrimination between mesothelioma and reactive mesothelial hyperplasia, and biomarkers. *J Clin Pathol.* 2013 Sep 24;66(10):847-53.
 58. Garcia LW, Ducatman BS, Wang HH. The value of multiple fluid specimens in the cytological diagnosis of malignancy. *Mod Pathol.* 1994 Aug;7(6):665-8.
 59. Chung C-L, Chen Y-C, Chang S-C. Effect of repeated thoracenteses on fluid characteristics, cytokines, and fibrinolytic activity in malignant pleural effusion. *Chest.* 2003 Apr;123(4):1188-95.
 60. Lee C, Bayman N, Swindell R, Faivre-Finn C. Prophylactic radiotherapy to intervention sites in mesothelioma: a systematic review and survey of UK practice. *Lung Cancer.* Elsevier; 2009 Nov;66(2):150-6.
 61. Attanoos RL, GIBBS AR. The comparative accuracy of different pleural biopsy techniques in the diagnosis of malignant mesothelioma. *Histopathology.* 2008 Sep;53(3):340-4.
 62. Boutin C, Dumortier P, Rey F, Viallat JR, de Vuyst P. Black spots concentrate oncogenic asbestos fibers in the parietal pleura. Thoracoscopic and mineralogic study. *Am J Respir Crit Care Med.* American Public Health Association; 1996 Jan;153(1):444-9.
 63. Heilo A, Stenwig AE, Solheim OP. Malignant pleural mesothelioma: US-guided histologic core-needle biopsy. *Radiology.* Radiological Society of North America; 1999 Jun;211(3):657-9.
 64. Maskell NA, Gleeson FV, Davies R. Standard pleural biopsy versus CT-guided cutting-needle biopsy for diagnosis of malignant disease in pleural effusions: a randomised controlled trial. *The Lancet.* 2003 Apr;361(9366):1326-30.

65. Beckett P, Edwards J, Fennell D, Hubbard R, Woolhouse I, Peake MD. Demographics, management and survival of patients with malignant pleural mesothelioma in the National Lung Cancer Audit in England and Wales. *Lung Cancer*. Elsevier Ireland Ltd; 2015 Jun 1;88(3):344-8.
66. Harris RJ, Kavuru MS, Mehta AC, Medendorp SV, Wiedemann HP, Kirby TJ, et al. The impact of thoracoscopy on the management of pleural disease. *Chest*. 1995 Mar;107(3):845-52.
67. Grossebnier MW, Arifi AA, Goddard M, Ritchie AJ. Mesothelioma--VATS biopsy and lung mobilization improves diagnosis and palliation. *European Journal of Cardio-Thoracic Surgery*. 1999 Dec;16(6):619-23.
68. Loddenkemper R. Thoracoscopy - state of the art. *European Respiratory Journal*. 1998 Jan 1;11(1):213-21.
69. Boutin C, Rey F. Thoracoscopy in pleural malignant mesothelioma: a prospective study of 188 consecutive patients. Part 1: Diagnosis. *Cancer*. 1993 Jul 15;72(2):389-93.
70. Medford ARL, Agrawal S, Free CM, Bennett JA. A local anaesthetic video-assisted thoracoscopy service: Prospective performance analysis in a UK tertiary respiratory centre. *Lung Cancer*. 2009 Dec;66(3):355-8.
71. Rahman NM, Ali NJ, Brown G, Chapman SJ. Local anaesthetic thoracoscopy: British Thoracic Society pleural disease guideline 2010. *Thorax*. 2010.
72. Galateau-Salle F, Churg A, Roggli V, Travis WD. The 2015 World Health Organization Classification of Tumors of the Pleura: Advances since the 2004 Classification. *Journal of Thoracic Oncology*. Elsevier; 2016 Feb 1;11(2):142-54.
73. Klebe S, Brownlee NA, Mahar A, Burchette JL, Sporn TA, Vollmer RT, et al. Sarcomatoid mesothelioma: a clinical-pathologic correlation of 326 cases. *Mod Pathol*. Nature Publishing Group; 2010 Mar;23(3):470-9.
74. Wu D, Hiroshima K, Matsumoto S, Nabeshima K, Yusa T, Ozaki D, et al. Diagnostic usefulness of p16/CDKN2A FISH in distinguishing between sarcomatoid mesothelioma and fibrous pleuritis. *Am J Clin Pathol*. The Oxford University Press; 2013 Jan;139(1):39-46.
75. Raj V, Kirke R, Bankart MJ, Entwisle JJ. Multidetector CT imaging of pleura: comparison of two contrast infusion protocols. *Br J Radiol*. The British Institute of Radiology. 36 Portland Place, London, W1B 1AT; 2011 Sep;84(1005):796-9.
76. Leung AN, Müller NL, Miller RR. CT in differential diagnosis of diffuse pleural disease. *AJR American journal of roentgenology*. American Public Health Association; 1990 Mar;154(3):487-92.
77. Hierholzer J, Luo L, Bittner RC, Stroszczyński C, Schröder R-J,

- Schoenfeld N, et al. MRI and CT in the Differential Diagnosis of Pleural Disease. *Chest*. American College of Chest Physicians; 2000 Sep 1;118(3):604-9.
78. Kawashima A, Libshitz HI. Malignant pleural mesothelioma: CT manifestations in 50 cases. *AJR American journal of roentgenology*. American Public Health Association; 1990 Nov;155(5):965-9.
 79. Knuuttila A, Kivisaari L, Kivisaari A, Palomäki M, Tervahartiala P, Mattson K. Evaluation of pleural disease using MR and CT. *Acta Radiologica*. Munksgaard International Publishers; 2001 Sep 1;42(5):502-7.
 80. Malignant Pleural Mesothelioma Caused by Environmental Exposure to Asbestos in the Southeast of Turkey: CT Findings in 117 Patients. *Respiration*. Karger Publishers; 2000 Dec 15;67(6):615-22.
 81. Metintas M, Ucgun I, Elbek O, Erginel S, Metintas S, Kolsuz M, et al. Computed tomography features in malignant pleural mesothelioma and other commonly seen pleural diseases. *Eur J Radiol*. 2002 Jan;41(1):1-9.
 82. Hallifax RJ, Haris M, Corcoran JP, Leyakathalikhan S, Brown E, Srikantharaja D, et al. Role of CT in assessing pleural malignancy prior to thoracoscopy. *Thorax*. BMJ Publishing Group Ltd and British Thoracic Society; 2015 Feb;70(2):192-3.
 83. Tsim S, Stobo DB, Alexander L, Kelly C, Blyth KG. The diagnostic performance of routinely acquired and reported computed tomography imaging in patients presenting with suspected pleural malignancy. *Lung Cancer*. Elsevier; 2017 Jan;103:38-43.
 84. Blyth KG, Murphy DJ. Progress and challenges in Mesothelioma: From bench to bedside. *Respir Med*. 2018 Jan;134:31-41.
 85. Yildirim H, Metintas M, Entok E, Ak G, Ak I, Dundar E, et al. Clinical value of fluorodeoxyglucose-positron emission tomography/computed tomography in differentiation of malignant mesothelioma from asbestos-related benign pleural disease: an observational pilot study. *J Thorac Oncol*. 2009 Dec;4(12):1480-4.
 86. Bénard F, Sterman D, Smith RJ, Kaiser LR, ALBELDA SM, Alavi A. Metabolic Imaging of Malignant Pleural Mesothelioma With Fluorodeoxyglucose Positron Emission Tomography. *Chest*. American College of Chest Physicians; 1998 Sep 1;114(3):713-22.
 87. Abe Y, Tamura K, Sakata I, Ishida J, Ozeki Y, Tamura A, et al. Clinical implications of 18F-fluorodeoxyglucose positron emission tomography/computed tomography at delayed phase for diagnosis and prognosis of malignant pleural mesothelioma. *Oncol Rep*. Spandidos Publications; 2012 Feb;27(2):333-8.
 88. Adams MC, Turkington TG, Wilson JM, Wong TZ. A systematic review of the factors affecting accuracy of SUV measurements. *AJR American*

journal of roentgenology. American Roentgen Ray Society; 2010 Aug;195(2):310-20.

89. Treglia G, Sadeghi R, Annunziata S, Lococo F, Cafarotti S, Bertagna F, et al. Diagnostic accuracy of 18F-FDG-PET and PET/CT in the differential diagnosis between malignant and benign pleural lesions: a systematic review and meta-analysis. *Acad Radiol*. Elsevier; 2014 Jan;21(1):11-20.
90. Coolen J, De Keyzer F, Nafteux P, De Wever W, Doms C, Vansteenkiste J, et al. Malignant pleural disease: diagnosis by using diffusion-weighted and dynamic contrast-enhanced MR imaging--initial experience. *Radiology*. Radiological Society of North America, Inc; 2012 Jun;263(3):884-92.
91. Elboga U, Yılmaz M, Uyar M, Zeki Çelen Y, Bakır K, Dikensoy Ö. The role of FDG PET-CT in differential diagnosis of pleural pathologies. *Revista Española de Medicina Nuclear e Imagen Molecular (English Edition)*. 2012 Jul;31(4):187-91.
92. Porcel JM, Hernández P, Martínez-Alonso M, Bielsa S, Salud A. Accuracy of fluorodeoxyglucose-PET imaging for differentiating benign from malignant pleural effusions: a meta-analysis. *Chest*. 2015 Feb;147(2):502-12.
93. De Fonseka D, Underwood W, Staddon L, Rahman N, Edey A, Rogers C, et al. Randomised controlled trial to compare the diagnostic yield of positron emission tomography CT (PET-CT) TARGETed pleural biopsy versus CT-guided pleural biopsy in suspected pleural malignancy (TARGET trial). *BMJ Open Respir Res*. Archives of Disease in childhood; 2018 Feb 1;5(1):e000270.
94. Mavi A, Basu S, Cermik TF, Urhan M, Bathaii M, Thiruvengatasamy D, et al. Potential of dual time point FDG-PET imaging in differentiating malignant from benign pleural disease. *Mol Imaging Biol*. Springer-Verlag; 2009 Sep;11(5):369-78.
95. Yamamoto Y, Kameyama R, Togami T, Kimura N, Ishikawa S, Yamamoto Y, et al. Dual time point FDG PET for evaluation of malignant pleural mesothelioma. *Nucl Med Commun*. 2009 Jan;30(1):25-9.
96. Xu Z, Li X-F, Zou H, Sun X, Shen B. 18F-Fluoromisonidazole in tumor hypoxia imaging. *Oncotarget*. Impact Journals; 2017 Nov 7;8(55):94969-79.
97. Cheng G. Non-Small-Cell Lung Cancer PET Imaging Beyond F18 Fluorodeoxyglucose. *PET Clin*. 2018 Jan;13(1):73-81.
98. Sharma R, Kallur KG, Ryu JS, Parameswaran RV, Lindman H, Avril N, et al. Multicenter Reproducibility of 18F-Fluciclatide PET Imaging in Subjects with Solid Tumors. *J Nucl Med*. Society of Nuclear Medicine; 2015 Dec;56(12):1855-61.

99. Boraschi P, Neri S, Braccini G, Gigoni R, Leoncini B, Perri G. Magnetic resonance appearance of asbestos-related benign and malignant pleural diseases. *Scand J Work Environ Health*. 1999 Feb;25(1):18-23.
100. Falaschi F, Battolla L, Mascalchi M, Cioni R, Zampa V, Lencioni R, et al. Usefulness of MR signal intensity in distinguishing benign from malignant pleural disease. *AJR American journal of roentgenology*. American Public Health Association; 1996 Apr;166(4):963-8.
101. Bammer R. Basic principles of diffusion-weighted imaging. *Eur J Radiol*. 2003 Mar;45(3):169-84.
102. Le Bihan D. Apparent diffusion coefficient and beyond: what diffusion MR imaging can tell us about tissue structure. *Radiology*. Radiological Society of North America, Inc; 2013 Aug;268(2):318-22.
103. Beauchamp NJ, Ulug AM, Passe TJ, van Zijl PC. MR diffusion imaging in stroke: review and controversies. *Radiographics*. 1998 Sep;18(5):1269-83-discussion1283-5.
104. Cova M, Squillaci E, Stacul F, Manenti G, Gava S, Simonetti G, et al. Diffusion-weighted MRI in the evaluation of renal lesions: preliminary results. *Br J Radiol*. 2004 Oct;77(922):851-7.
105. Issa B. In vivo measurement of the apparent diffusion coefficient in normal and malignant prostatic tissues using echo-planar imaging. *J Magn Reson Imaging*. 2002 Aug;16(2):196-200.
106. Gill RR, Umeoka S, Mamata H, Tilleman TR, Stanwell P, Woodhams R, et al. Diffusion-Weighted MRI of Malignant Pleural Mesothelioma: Preliminary Assessment of Apparent Diffusion Coefficient in Histologic Subtypes. *American Journal of Roentgenology*. American Roentgen Ray Society; 2012 Nov 23;195(2):W125-30.
107. Gill RR, Umeoka S, Mamata H, Tilleman TR, Stanwell P, Woodhams R, et al. Diffusion-Weighted MRI of Malignant Pleural Mesothelioma: Preliminary Assessment of Apparent Diffusion Coefficient in Histologic Subtypes. *American Journal of Roentgenology*. 2010 Aug;195(2):W125-30.
108. Revelli M, Chiesa F, Del Prato A, Tagliafico A, Rosenberg I, Canessa PA, et al. Role of respiratory-triggered diffusion-weighted MRI in the assessment of pleural disease. *Br J Radiol*. 2016 Aug;89(1064):20160289-7.
109. Coolen J, De Keyzer F, Nafteux P, De Wever W, Doms C, Vansteenkiste J, et al. Malignant Pleural Mesothelioma: Visual Assessment by Using Pleural Pointillism at Diffusion-weighted MR Imaging. *Radiology*. 2015 Feb;274(2):576-84.
110. Yamamuro M, Gerbaudo VH, Gill RR, Jacobson FL, Sugarbaker DJ, Hatabu H. Morphologic and functional imaging of malignant pleural mesothelioma. *Eur J Radiol*. 2007 Dec;64(3):356-66.

111. Kuhl CK, Mielcareck P, Klaschik S, Leutner C, Wardelmann E, Gieseke J, et al. Dynamic breast MR imaging: are signal intensity time course data useful for differential diagnosis of enhancing lesions? *Radiology*. Radiological Society of North America; 1999 Apr;211(1):101-10.
112. Mussurakis S, Buckley DL, Drew PJ, Fox JN, Carleton PJ, Turnbull LW, et al. Dynamic MR imaging of the breast combined with analysis of contrast agent kinetics in the differentiation of primary breast tumours. *Clin Radiol*. 1997 Jul;52(7):516-26.
113. Khouli El RH, Macura KJ, Kamel IR, Jacobs MA, Bluemke DA. 3-T dynamic contrast-enhanced MRI of the breast: pharmacokinetic parameters versus conventional kinetic curve analysis. *AJR American journal of roentgenology*. American Roentgen Ray Society; 2011 Dec;197(6):1498-505.
114. Wang B, Gao ZQ, Yan X. Correlative study of angiogenesis and dynamic contrast-enhanced magnetic resonance imaging features of hepatocellular carcinoma. *Acta Radiol*. 2005 Jul;46(4):353-8.
115. Padhani AR, Gapinski CJ, Macvicar DA, Parker GJ, Suckling J, Revell PB, et al. Dynamic contrast enhanced MRI of prostate cancer: correlation with morphology and tumour stage, histological grade and PSA. *Clin Radiol*. Elsevier; 2000 Feb;55(2):99-109.
116. Tan CH, Paul Hobbs B, Wei W, Kundra V. Dynamic contrast-enhanced MRI for the detection of prostate cancer: meta-analysis. *AJR American journal of roentgenology*. American Roentgen Ray Society; 2015 Apr;204(4):W439-48.
117. Giesel FL, Bischoff H, Tengg-Koblighk von H, Weber M-A, Zechmann CM, Kauczor H-U, et al. Dynamic Contrast-Enhanced MRI of Malignant Pleural Mesothelioma: A Feasibility Study of Noninvasive Assessment, Therapeutic Follow-up, and Possible Predictor of Improved Outcome. *Chest*. American College of Chest Physicians; 2006 Jun 1;129(6):1570-6.
118. Giesel FL, Choyke PL, Mehndiratta A, Zechmann CM, Tengg-Koblighk von H, Kayser K, et al. Pharmacokinetic analysis of malignant pleural mesothelioma-initial results of tumor microcirculation and its correlation to microvessel density (CD-34). *Acad Radiol*. Elsevier; 2008 May;15(5):563-70.
119. Hylton N. Dynamic contrast-enhanced magnetic resonance imaging as an imaging biomarker. *J Clin Oncol*. American Society of Clinical Oncology; 2006 Jul 10;24(20):3293-8.
120. Evelhoch JL. Key factors in the acquisition of contrast kinetic data for oncology. *J Magn Reson Imaging*. 1999 Sep;10(3):254-9.
121. Rusch VW. A proposed new international TNM staging system for malignant pleural mesothelioma. From the International Mesothelioma Interest Group. *Chest*. 1995 Oct;108(4):1122-8.

122. Okiemy G, Foucault C, Avisse C, Hidden G, Riquet M. Lymphatic drainage of the diaphragmatic pleura to the peritracheobronchial lymph nodes. *Surg Radiol Anat*. Springer-Verlag; 2003 Apr;25(1):32-5.
123. Bilgi Z, Colson YL. Lymphatic drainage of the pleura and its effect on tumor metastasis and spread. *Türk Toraks Derneği Plevra Bülteni*. 2009.
124. Abdel Rahman ARM, Gaafar RM, Baki HA, Hosieny El HM, Aboulkasem F, Farahat EG, et al. Prevalence and pattern of lymph node metastasis in malignant pleural mesothelioma. *Ann Thorac Surg*. Elsevier; 2008 Aug;86(2):391-5.
125. Rusch VW, Giroux D, Kennedy C, Ruffini E, Cangir AK, Rice D, et al. Initial Analysis of the International Association For the Study of Lung Cancer Mesothelioma Database. *Journal of Thoracic Oncology*. Elsevier; 2012 Nov 1;7(11):1631-9.
126. Nowak AK, Chansky K, Rice DC, Pass HI, Kindler HL, Shemanski L, et al. The IASLC Mesothelioma Staging Project: Proposals for Revisions of the T Descriptors in the Forthcoming Eighth Edition of the TNM Classification for Pleural Mesothelioma. *J Thorac Oncol*. 2016 Dec;11(12):2089-99.
127. Rice D, Chansky K, Nowak A, Pass H, Kindler H, Shemanski L, et al. The IASLC Mesothelioma Staging Project: Proposals for Revisions of the N Descriptors in the Forthcoming Eighth Edition of the TNM Classification for Pleural Mesothelioma. *J Thorac Oncol*. 2016 Dec;11(12):2100-11.
128. Rusch VW, Chansky K, Kindler HL, Nowak AK, Pass HI, Rice DC, et al. The IASLC Mesothelioma Staging Project: Proposals for the M Descriptors and for Revision of the TNM Stage Groupings in the Forthcoming (Eighth) Edition of the TNM Classification for Mesothelioma. *J Thorac Oncol*. 2016 Dec;11(12):2112-9.
129. Rusch VW, Godwin JD, Shuman WP. The role of computed tomography scanning in the initial assessment and the follow-up of malignant pleural mesothelioma. *J Thorac Cardiovasc Surg*. 1988 Jul;96(1):171-7.
130. Heelan RT, Rusch VW, Begg CB, Panicek DM, Caravelli JF, Eisen C. Staging of malignant pleural mesothelioma: comparison of CT and MR imaging. *AJR American journal of roentgenology*. American Public Health Association; 2013 Jan 19;172(4):1039-47.
131. Patz EF, Shaffer K, Piwnica-Worms DR, Jochelson M, Sarin M, Sugarbaker DJ, et al. Malignant pleural mesothelioma: value of CT and MR imaging in predicting resectability. *AJR American journal of roentgenology*. American Public Health Association; 1992 Nov;159(5):961-6.
132. Wang ZJ, Reddy GP, Gotway MB, Higgins CB, Jablons DM, Ramaswamy M, et al. Malignant pleural mesothelioma: evaluation with CT, MR

- imaging, and PET. Radiographics. Radiological Society of North America; 2004 Jan;24(1):105-19.
133. Wilcox BE, Subramaniam RM, Peller PJ, Aughenbaugh GL, Nichols Iii FC, Aubry MC, et al. Utility of integrated computed tomography-positron emission tomography for selection of operable malignant pleural mesothelioma. Clin Lung Cancer. Elsevier; 2009 Jul;10(4):244-8.
 134. Pass HI, Temeck BK, Kranda K, Steinberg SM, Feuerstein IR. Preoperative tumor volume is associated with outcome in malignant pleural mesothelioma. J Thorac Cardiovasc Surg. 1998 Feb;115(2):310-7-discussion317-8.
 135. Gill RR, Richards WG, Yeap BY, Matsuoka S, Wolf AS, Gerbaudo VH, et al. Epithelial malignant pleural mesothelioma after extrapleural pneumonectomy: stratification of survival with CT-derived tumor volume. AJR American journal of roentgenology. American Roentgen Ray Society; 2012 Feb;198(2):359-63.
 136. Chaisaowong K, Jager P, in SVOI, 2007. Computer-assisted Diagnosis for Early Stage Pleural Mesothelioma--Towards Automated Detection and Quantitative Assessment of Pleural Thickenings from pdfssemanticsscholarorg
 - .
 137. Gill RR, Naidich DP, Mitchell A, Ginsberg M, Erasmus J, Armato SG, et al. North American Multicenter Volumetric CT Study for Clinical Staging of Malignant Pleural Mesothelioma: Feasibility and Logistics of Setting Up a Quantitative Imaging Study. J Thorac Oncol. 2016 Aug;11(8):1335-44.
 138. Rusch VW, Gill R, Mitchell A, Naidich D, Rice DC, Pass HI, et al. A Multicenter Study of Volumetric Computed Tomography for Staging Malignant Pleural Mesothelioma. Ann Thorac Surg. 2016 Sep 2.
 139. Sørensen JB, Ravn J, Loft A, Brenøe J, Berthelsen AK, Nordic Mesothelioma Group. Preoperative staging of mesothelioma by 18F-fluoro-2-deoxy-D-glucose positron emission tomography/computed tomography fused imaging and mediastinoscopy compared to pathological findings after extrapleural pneumonectomy. Eur J Cardiothorac Surg. Oxford University Press; 2008 Nov;34(5):1090-6.
 140. Plathow C, Staab A, Schmaehl A, Aschoff P, Zuna I, Pfannenberger C, et al. Computed Tomography, Positron Emission Tomography, Positron Emission Tomography/Computed Tomography, and Magnetic Resonance Imaging for Staging of Limited Pleural Mesothelioma. Invest Radiol. 2008 Oct;43(10):737-44.
 141. Erasmus JJ, Truong MT, Smythe WR, Munden RF, Marom EM, Rice DC, et al. Integrated computed tomography-positron emission tomography in patients with potentially resectable malignant pleural mesothelioma: Staging implications. J Thorac Cardiovasc Surg.

Elsevier; 2005 Jun;129(6):1364-70.

142. Flores RM, Akhurst T, Gonen M, Larson SM, Rusch VW. Positron emission tomography defines metastatic disease but not locoregional disease in patients with malignant pleural mesothelioma. *J Thorac Cardiovasc Surg.* 2003 Jul;126(1):11-6.
143. Woolhouse I, Bishop L, Darlison L, De Fonseka D, Edey A, Edwards J, et al. British Thoracic Society Guideline for the investigation and management of malignant pleural mesothelioma. *Thorax.* BMJ Publishing Group Ltd; 2018 Mar;73(Suppl 1):i1-i30.
144. Knuuttila A, Halme M, Kivisaari L, Kivisaari A, Salo J, Mattson K. The clinical importance of magnetic resonance imaging versus computed tomography in malignant pleural mesothelioma. *Lung Cancer.* 1998 Dec;22(3):215-25.
145. Stewart D, Waller D, Edwards J, Jeyapalan K, Entwisle J. Is there a role for pre-operative contrast-enhanced magnetic resonance imaging for radical surgery in malignant pleural mesothelioma? *Eur J Cardiothorac Surg.* 2003 Dec;24(6):1019-24.
146. de Gramont A, Watson S, Ellis LM, Rodón J, Tabernero J, de Gramont A, et al. Pragmatic issues in biomarker evaluation for targeted therapies in cancer. *Nat Rev Clin Oncol.* Nature Publishing Group; 2015 Apr;12(4):197-212.
147. Mayeux R. Biomarkers: potential uses and limitations. *NeuroRx.* Springer-Verlag; 2004 Apr;1(2):182-8.
148. Chang K, Pai LH, Batra JK, Pastan I, Willingham MC. Characterization of the antigen (CAK1) recognized by monoclonal antibody K1 present on ovarian cancers and normal mesothelium. *Cancer Res.* 1992 Jan 1;52(1):181-6.
149. Chang K, Pai LH, Pass H, Pogrebniak HW, Tsao MS, Pastan I, et al. Monoclonal antibody K1 reacts with epithelial mesothelioma but not with lung adenocarcinoma. *Am J Surg Pathol.* 1992 Mar;16(3):259-68.
150. Creaney J, Yeoman D, Demelker Y, Segal A, Musk AW, Skates SJ, et al. Comparison of osteopontin, megakaryocyte potentiating factor, and mesothelin proteins as markers in the serum of patients with malignant mesothelioma. *J Thorac Oncol.* 2008 Aug;3(8):851-7.
151. Creaney J, Dick IM, Meniawy TM, Leong SL, Leon JS, Demelker Y, et al. Comparison of fibulin-3 and mesothelin as markers in malignant mesothelioma. *Thorax.* BMJ Publishing Group Ltd and British Thoracic Society; 2014 Oct;69(10):895-902.
152. Hollevoet K, Reitsma JB, Creaney J, Grigoriu BD, Robinson BW, Scherpereel A, et al. Serum mesothelin for diagnosing malignant pleural mesothelioma: an individual patient data meta-analysis. *J Clin Oncol.* American Society of Clinical Oncology; 2012 May 1;30(13):1541-9.

153. Hollevoet K, Nackaerts K, Thimpont J, Germonpré P, Bosquée L, De Vuyst P, et al. Diagnostic performance of soluble mesothelin and megakaryocyte potentiating factor in mesothelioma. *Am J Respir Crit Care Med*. American Thoracic Society; 2010 Mar 15;181(6):620-5.
154. Pass HI, Lott D, Lonardo F, Harbut M, Liu Z, Tang N, et al. Asbestos exposure, pleural mesothelioma, and serum osteopontin levels. *N Engl J Med*. Massachusetts Medical Society; 2005 Oct 13;353(15):1564-73.
155. Scaffidi P, Misteli T, Bianchi ME. Release of chromatin protein HMGB1 by necrotic cells triggers inflammation. *Nature*. 2002 Jul 11;418(6894):191-5.
156. Lotze MT, Tracey KJ. High-mobility group box 1 protein (HMGB1): nuclear weapon in the immune arsenal. *Nat Rev Immunol*. Nature Publishing Group; 2005 Apr;5(4):331-42.
157. Qi F, Okimoto G, Jube S, Napolitano A, Pass HI, Laczko R, et al. Continuous exposure to chrysotile asbestos can cause transformation of human mesothelial cells via HMGB1 and TNF- α signaling. *Am J Pathol*. Elsevier; 2013 Nov;183(5):1654-66.
158. Napolitano A, Antoine DJ, Pellegrini L, Baumann F, Pagano I, Pastorino S, et al. HMGB1 and Its Hyperacetylated Isoform are Sensitive and Specific Serum Biomarkers to Detect Asbestos Exposure and to Identify Mesothelioma Patients. *Clin Cancer Res*. American Association for Cancer Research; 2016 Jan 5.
159. Tabata C, Shibata E, Tabata R, Kanemura S, Mikami K, Nogi Y, et al. Serum HMGB1 as a prognostic marker for malignant pleural mesothelioma. *BMC Cancer*. BioMed Central; 2013;13(1):205.
160. Gold L, Ayers D, Bertino J, Bock C, Bock A, Brody EN, et al. Aptamer-based multiplexed proteomic technology for biomarker discovery. Gelain F, editor. *PLoS ONE*. Public Library of Science; 2010;5(12):e15004.
161. Gold L, Walker JJ, Wilcox SK, Williams S. Advances in human proteomics at high scale with the SOMAscan proteomics platform. *New BIOTECHNOLOGY*. Elsevier B.V; 2012 Jun 15;29(5):543-9.
162. Brody EN, Gold L. Aptamers as therapeutic and diagnostic agents. *Reviews in Molecular Biotechnology*. 2000 Mar;74(1):5-13.
163. Ostroff RM, Mehan MR, Stewart A, Ayers D, Brody EN, Williams SA, et al. Early detection of malignant pleural mesothelioma in asbestos-exposed individuals with a noninvasive proteomics-based surveillance tool. Behrens T, editor. *PLoS ONE*. Public Library of Science; 2012;7(10):e46091.
164. Horie R, Watanabe T. CD30: expression and function in health and disease. *Semin Immunol*. Academic Press; 1998 Dec;10(6):457-70.

165. Romagnani S, Del Prete G, Maggi E, Chilosi M, Caligaris-Cappio F, Pizzolo G. CD30 and type 2 T helper (Th2) responses. *J Leukoc Biol. Society for Leukocyte Biology*; 1995 May;57(5):726-30.
166. Caligaris-Cappio F, Bertero MT, Converso M, Stacchini A, Vinante F, Romagnani S, et al. Circulating levels of soluble CD30, a marker of cells producing Th2-type cytokines, are increased in patients with systemic lupus erythematosus and correlate with disease activity. *Clin Exp Rheumatol*. 1995 May;13(3):339-43.
167. Horie R, Aizawa S, Nagai M, Ito K, Higashihara M, Ishida T, et al. A novel domain in the CD30 cytoplasmic tail mediates NFkappaB activation. *Int Immunol*. 1998 Feb;10(2):203-10.
168. Pizzolo G, Vinante F, Chilosi M, Dallenbach F, Josimovic-Alasevic O, Diamantstein T, et al. Serum levels of soluble CD30 molecule (Ki-1 antigen) in Hodgkin's disease: relationship with disease activity and clinical stage. *Br J Haematol*. 1990 Jun;75(2):282-4.
169. Nadali G, Vinante F, Stein H, Todeschini G, Tecchio C, Morosato L, et al. Serum levels of the soluble form of CD30 molecule as a tumor marker in CD30+ anaplastic large-cell lymphoma. *Journal of Clinical Oncology*. 1995 Jun;13(6):1355-60.
170. Garcia-Prats MD, Ballestin C, Sotelo T, Lopez-Encuentra A, Mayordomo JI. A comparative evaluation of immunohistochemical markers for the differential diagnosis of malignant pleural tumours. *Histopathology*. 1998 May;32(5):462-72.
171. Novak H, Muller A, Harrer N, Gunther C, Carballido JM, Woisetschlager M. CCL23 Expression Is Induced by IL-4 in a STAT6-Dependent Fashion. *The Journal of Immunology*. 2007 Mar 19;178(7):4335-41.
172. Son K-N, Hwang J, Kwon BS, Kim J. Human CC chemokine CCL23 enhances expression of matrix metalloproteinase-2 and invasion of vascular endothelial cells. *Biochem Biophys Res Commun*. 2006 Feb 10;340(2):498-504.
173. Hwang J, Son K-N, Kim CW, Ko J, Na DS, Kwon BS, et al. Human CC chemokine CCL23, a ligand for CCR1, induces endothelial cell migration and promotes angiogenesis. *Cytokine*. 2005 Jun 7;30(5):254-63.
174. Yanaba K, Yoshizaki A, Muroi E, Ogawa F, Asano Y, Kadono T, et al. Serum CCL23 levels are increased in patients with systemic sclerosis. *Arch Dermatol Res*. 2010 Sep 8;303(1):29-34.
175. Dhavan R, Tsai LH. A decade of CDK5. *Nat Rev Mol Cell Biol. Nature Publishing Group*; 2001 Oct;2(10):749-59.
176. Utreras E, Futatsugi A, Rudrabhatla P, Keller J, Iadarola MJ, Pant HC, et al. Tumor necrosis factor-alpha regulates cyclin-dependent kinase 5 activity during pain signaling through transcriptional activation of

- p35. Journal of Biological Chemistry. American Society for Biochemistry and Molecular Biology; 2009 Jan 23;284(4):2275-84.
177. Ansel KM, Ngo VN, Hyman PL, Luther SA, Förster R, Sedgwick JD, et al. A chemokine-driven positive feedback loop organizes lymphoid follicles. *Nature*. Nature Publishing Group; 2000 Jul 20;406(6793):309-14.
 178. Hayden MS, West AP, Ghosh S. NF- κ B and the immune response. *Oncogene*. 2006 Oct 30;25(51):6758-80.
 179. Sun S-C. Non-canonical NF- κ B signaling pathway. Nature Publishing Group. Nature Publishing Group; 2010 Dec 21;21(1):71-85.
 180. Panse J, Friedrichs K, Marx A, Hildebrandt Y, Luetkens T, Bartels K, et al. Chemokine CXCL13 is overexpressed in the tumour tissue and in the peripheral blood of breast cancer patients. *Br J Cancer*. 2008 Sep 16;99(6):930-8.
 181. Fosbrink M, Niculescu F, Rus H. The role of C5b-9 terminal complement complex in activation of the cell cycle and transcription. *Immunol Res*. 2005;31(1):37-46.
 182. Rutkowski MJ, Sughrue ME, Kane AJ, Mills SA, Parsa AT. Cancer and the Complement Cascade. *Molecular Cancer Research*. 2010 Nov 23;8(11):1453-65.
 183. Vlaicu SI, Tegla CA, Cudrici CD, Danoff J, Madani H, Sugarman A, et al. Role of C5b-9 complement complex and response gene to complement-32 (RGC-32) in cancer. *Immunol Res*. 2012 Dec 18;56(1):109-21.
 184. Gancz D, Lusthaus M, Fishelson Z. A role for the NF- κ B pathway in cell protection from complement-dependent cytotoxicity. *The Journal of Immunology*; 2012.
 185. Chen J, Yang W-J, Sun H-J, Yang X, Wu Y-Z. C5b-9 Staining Correlates With Clinical and Tumor Stage in Gastric Adenocarcinoma. *Appl Immunohistochem Mol Morphol*. 2016 Aug;24(7):470-5.
 186. Niculescu F, Rus HG, Retegan M, Vlaicu R. Persistent complement activation on tumor cells in breast cancer. *AJPA. American Society for Investigative Pathology*; 1992 May;140(5):1039-43.
 187. Kilpatrick DC, Chalmers JD. Human L-ficolin (ficolin-2) and its clinical significance. *J Biomed Biotechnol*. Hindawi Publishing Corporation; 2012;2012(33):138797-10.
 188. Matsushita M, Fujita T. Ficolins and the lectin complement pathway. *Immunol Rev*. 2001 Apr;180:78-85.
 189. Renkonen R, Paavonen T, Nortamo P, Gahmberg CG. Expression of endothelial adhesion molecules in vivo. Increased endothelial ICAM-2 expression in lymphoid malignancies. *AJPA. American Society for*

Investigative Pathology; 1992 Apr;140(4):763-7.

190. Yoon KJ, Phelps DA, Bush RA, Remack JS, Billups CA, Khoury JD. ICAM-2 expression mediates a membrane-actin link, confers a nonmetastatic phenotype and reflects favorable tumor stage or histology in neuroblastoma. Cordes N, editor. PLoS ONE. Public Library of Science; 2008;3(11):e3629.
191. Perez OD, Kinoshita S, Hitoshi Y, Payan DG, Kitamura T, Nolan GP, et al. Activation of the PKB/AKT pathway by ICAM-2. Immunity. 2002 Jan;16(1):51-65.
192. Yoon KJ, Miller AL, Kreitzburg KM. The role of ICAM-2 in neuroblastoma. Oncoscience. 2015;2(11):915-6.
193. Muramatsu T, Kadomatsu K. Midkine: an emerging target of drug development for treatment of multiple diseases. Br J Pharmacol. 2014 Feb;171(4):811-3.
194. Jones DR. Measuring midkine: the utility of midkine as a biomarker in cancer and other diseases. Br J Pharmacol. 2014 Jun;171(12):2925-39.
195. Zhao Z-Q, Yang S, Lu H-S. Expression of midkine and vascular endothelial growth factor in gastric cancer and the association of high levels with poor prognosis and survival. Mol Med Rep. Spandidos Publications; 2012 Feb;5(2):415-9.
196. Zhu W-W, Guo J-J, Guo L, Jia H-L, Zhu M, Zhang J-B, et al. Evaluation of midkine as a diagnostic serum biomarker in hepatocellular carcinoma. Clin Cancer Res. Clinical Cancer Research; 2013 Jul 15;19(14):3944-54.
197. Ikematsu S, Yano A, Aridome K, Kikuchi M, Kumai H, Nagano H, et al. Serum midkine levels are increased in patients with various types of carcinomas. Br J Cancer. Nature Publishing Group; 2000 Sep;83(6):701-6.
198. Ibusuki M, Fujimori H, Yamamoto Y, Ota K, Ueda M, Shinriki S, et al. Midkine in plasma as a novel breast cancer marker. Cancer Science. Blackwell Publishing Asia; 2009 Sep;100(9):1735-9.
199. Ikematsu S, Nakagawara A, Nakamura Y, Sakuma S, Wakai K, Muramatsu T, et al. Correlation of elevated level of blood midkine with poor prognostic factors of human neuroblastomas. Br J Cancer. Nature Publishing Group; 2003 May 19;88(10):1522-6.
200. Lv M, Mou Y, Wang P, Chen Y, Wang T, Hou Y. Diagnostic and predictive role of cell-free midkine in malignant pleural effusions. J Cancer Res Clin Oncol. 2012 Dec 5;139(4):543-9.
201. Cine N, Baykal AT, Sunnetci D, Canturk Z, Serhatli M, Savli H. Identification of ApoA1, HPX and POTE genes by omic analysis in breast cancer. Oncol Rep. Spandidos Publications; 2014

Sep;32(3):1078-86.

202. Grundy SM, Vega GL. Role of Apolipoprotein Levels in Clinical Practice. *Arch Intern Med. American Medical Association*; 1990 Aug 1;150(8):1579-82.
203. Zamanian-Daryoush M, Lindner D, Tallant TC, Wang Z, Buffa J, Klipfell E, et al. The cardioprotective protein apolipoprotein A1 promotes potent anti-tumorigenic effects. *J Biol Chem. American Society for Biochemistry and Molecular Biology*; 2013 Jul 19;288(29):21237-52.
204. Borgquist S, Butt T, Almgren P, Shiffman D, Stocks T, Orho-Melander M, et al. Apolipoproteins, lipids and risk of cancer. *Int J Cancer*. 2016 Feb 8;138(11):2648-56.
205. Wang X-P, Li X-H, Zhang L, Lin J-H, Huang H, Kang T, et al. High level of serum apolipoprotein A-I is a favorable prognostic factor for overall survival in esophageal squamous cell carcinoma. *BMC Cancer. BioMed Central*; 2016;16(1):516.
206. Cheng T, Dai X, Zhou D-L, Lv Y, Miao L-Y. Correlation of apolipoprotein A-I kinetics with survival and response to first-line platinum-based chemotherapy in advanced non-small cell lung cancer. *Med Oncol. Springer US*; 2015;32(1):407.
207. Pankov R. Fibronectin at a glance. *Journal of Cell Science*. 2002 Oct 15;115(20):3861-3.
208. Wang K, Seo BR, Fischbach C, Gourdon D. Fibronectin Mechanobiology Regulates Tumorigenesis. *Cellular and Molecular Bioengineering. Springer US*; 2016 Sep 6;9(1):1-11.
209. Kinnula VL, Linnala A, Viitala E, Linnainmaa K, Virtanen I. Tenascin and fibronectin expression in human mesothelial cells and pleural mesothelioma cell-line cells. *Am J Respir Cell Mol Biol. American Thoracic Society New York, NY*; 1998 Sep;19(3):445-52.
210. Siri A, Carnemolla B, Raffanti S, Castellani P, Balzano E, Zardi L. Fibronectin concentrations in pleural effusions of patients with malignant and non-malignant diseases. *Cancer Letters. Elsevier*; 1984 Feb;22(1):1-9.
211. Emri S, Ustündağ Y, Budak T, Karakoca Y, Ozdemir O. Assessment of the value of fibronectin as a tumour marker in malignant pleural mesothelioma. *Monaldi Arch Chest Dis*. 1997 Aug;52(4):335-8.
212. Broudy VC. Stem cell factor and hematopoiesis. *Blood. American Society of Hematology*; 1997 Aug 15;90(4):1345-64.
213. Yee NS, Paek I, Besmer P. Role of kit-ligand in proliferation and suppression of apoptosis in mast cells: basis for radiosensitivity of white spotting and steel mutant mice. *J Exp Med. The Rockefeller University Press*; 1994 Jun 1;179(6):1777-87.

214. Pérez-Losada J, Sánchez-Martín M, Pérez-Caro M, Pérez-Mancera PA, Sánchez-García I. The radioresistance biological function of the SCF/kit signaling pathway is mediated by the zinc-finger transcription factor Slug. *Oncogene*. 2003 Jul 3;22(27):4205-11.
215. Catalano A, Rodilossi S, Rippo MR, Caprari P, Procopio A. Induction of Stem Cell Factor/c-Kit/Slug Signal Transduction in Multidrug-resistant Malignant Mesothelioma Cells. *Journal of Biological Chemistry*. 2004 Oct 29;279(45):46706-14.
216. Chao J, Tillman DM, Wang MY, Margolius HS, Chao L. Identification of a new tissue-kallikrein-binding protein. *Biochem J*. Portland Press Ltd; 1986 Oct 15;239(2):325-31.
217. Miao RQ. Kallistatin is a new inhibitor of angiogenesis and tumor growth. *Blood*. 2002 Jul 5;100(9):3245-52.
218. Li P, Guo Y, Bledsoe G, Yang Z, Chao L, Chao J. Kallistatin induces breast cancer cell apoptosis and autophagy by modulating Wnt signaling and microRNA synthesis. *Experimental Cell Research*. Elsevier; 2016 Jan 15;340(2):305-14.
219. Huang KF, Huang XP, Xiao GQ, Yang HY, Lin JS, Diao Y. Kallistatin, a novel anti-angiogenesis agent, inhibits angiogenesis via inhibition of the NF- κ B signaling pathway. *Biomedicine et Pharmacotherapy*. Elsevier Masson SAS; 2014 May 1;68(4):455-61.
220. Genofre EH, Vargas FS, Acencio MMP, Antonangelo L, Teixeira LR, Marchi E. Talc pleurodesis: Evidence of systemic Inflammatory response to small size talc particles. *Respir Med*. Elsevier Ltd; 2009 Jan 1;103(1):91-7.
221. Ukale V, Agrenius V, Widström O, Hassan A, Hillerdal G. Inflammatory parameters after pleurodesis in recurrent malignant pleural effusions and their predictive value. *Respir Med*. 2004 Dec;98(12):1166-72.
222. Pinato DJ, Mauri FA, Ramakrishnan R, Wahab L, Lloyd T, Sharma R. Inflammation-Based Prognostic Indices in Malignant Pleural Mesothelioma. *Journal of Thoracic Oncology*. 2012 Mar;7(3):587-94.
223. Kao SCH, Pavlakis N, Harvie R, Vardy JL, Boyer MJ, van Zandwijk N, et al. High blood neutrophil-to-lymphocyte ratio is an indicator of poor prognosis in malignant mesothelioma patients undergoing systemic therapy. *Clin Cancer Res*. American Association for Cancer Research; 2010 Dec 1;16(23):5805-13.
224. Lecka-Czernik B, Lumpkin CK, Goldstein S. An overexpressed gene transcript in senescent and quiescent human fibroblasts encoding a novel protein in the epidermal growth factor-like repeat family stimulates DNA synthesis. *Mol Cell Biol*. American Society for Microbiology (ASM); 1995 Jan;15(1):120-8.
225. Zhang Y, Marmorstein LY. Focus on molecules: Fibulin-3 (EFEMP1). *Experimental Eye Research*. 2010 Mar;90(3):374-5.

226. Djokic J, Fagotto-Kaufmann C, Bartels R, Nelea V, Reinhardt DP. Fibulin-3, -4, and -5 Are Highly Susceptible to Proteolysis, Interact with Cells and Heparin, and Form Multimers. *Journal of Biological Chemistry*. 2013 Aug 2;288(31):22821-35.
227. Giltay R, Timpl R, Kostka G. Sequence, recombinant expression and tissue localization of two novel extracellular matrix proteins, fibulin-3 and fibulin-4. *Matrix Biology*. 1999 Oct;18(5):469-80.
228. Obaya AJ, Rua S, Moncada-Pazos A, Cal S. The dual role of fibulins in tumorigenesis. *Cancer Letters*. Elsevier Ireland Ltd; 2012 Dec 28;325(2):132-8.
229. de Vega S, Iwamoto T, Yamada Y. Fibulins: Multiple roles in matrix structures and tissue functions. *Cell Mol Life Sci*. Birkhäuser-Verlag; 2009 Feb 5;66(11-12):1890-902.
230. Papke CL, Yanagisawa H. Fibulin-4 and fibulin-5 in elastogenesis and beyond: Insights from mouse and human studies. *Matrix Biology*. International Society of Matrix Biology; 2014 Jul 1;37(C):142-9.
231. McLaughlin PJ, Bakall B, Choi J, Liu Z, Sasaki T, Davis EC, et al. Lack of fibulin-3 causes early aging and herniation, but not macular degeneration in mice. *Human Molecular Genetics*. 2007 Sep 12;16(24):3059-70.
232. Seeliger H, Camaj P, Ischenko I, Kleespies A, De Toni EN, Thieme SE, et al. EFEMP1 Expression Promotes In vivo Tumor Growth in Human Pancreatic Adenocarcinoma. *Molecular Cancer Research*. 2009 Feb 1;7(2):189-98.
233. Sadr-Nabavi A, Ramser J, Volkmann J, Naehrig J, Wiesmann F, Betz B, et al. Decreased expression of angiogenesis antagonist EFEMP1 in sporadic breast cancer is caused by aberrant promoter methylation and points to an impact of EFEMP1 as molecular biomarker. *Int J Cancer*. 2009 Apr 1;124(7):1727-35.
234. Tian H, Liu J, Chen J, Gatza ML, Blobe GC. Fibulin-3 is a novel TGF- β pathway inhibitor in the breast cancer microenvironment. *Oncogene*. 2015 Mar 30;34(45):5635-47.
235. TONG J, JIAO N, WANG Y, ZHANG Y, HAN F. Downregulation of fibulin-3 gene by promoter methylation in colorectal cancer predicts adverse prognosis. *neo*. 2011;58(5):441-8.
236. Rui W, You-Wei Z, Long-Bang C. Aberrant promoter methylation of FBLN-3 gene and clinicopathological significance in non-small cell lung carcinoma. *Lung Cancer*. Elsevier Ireland Ltd; 2010 Aug 1;69(2):239-44.
237. Yue W, Dacic S, Sun Q, Landreneau R, Guo M, Zhou W, et al. Frequent inactivation of RAMP2, EFEMP1 and Dutt1 in lung cancer by promoter hypermethylation. *Clin Cancer Res*. Clinical Cancer Research; 2007 Aug 1;13(15 Pt 1):4336-44.

238. Hwang C-F, Chien C-Y, Huang S-C, Yin Y-F, Huang C-C, Fang F-M, et al. Fibulin-3 is associated with tumour progression and a poor prognosis in nasopharyngeal carcinomas and inhibits cell migration and invasion via suppressed AKT activity. *J Pathol.* 2010 Oct 6;222(4):367-79.
239. Nomoto S, Kanda M, Okamura Y, Nishikawa Y, Qiyong L, Fujii T, et al. Epidermal Growth Factor-Containing Fibulin-Like Extracellular Matrix Protein 1, EFEMP1, a Novel Tumor-Suppressor Gene Detected in Hepatocellular Carcinoma Using Double Combination Array Analysis. *Ann Surg Oncol.* Springer-Verlag; 2009 Nov 7;17(3):923-32.
240. Nandhu MS, Hu B, Cole SE, Erdreich-Epstein A, Rodriguez-Gil DJ, Viapiano MS. Novel Paracrine Modulation of Notch-DLL4 Signaling by Fibulin-3 Promotes Angiogenesis in High-Grade Gliomas. *Cancer Res.* 2014 Sep 30;74(19):5435-48.
241. Hu B, Thirtamara-Rajamani KK, Sim H, Viapiano MS. Fibulin-3 Is Uniquely Upregulated in Malignant Gliomas and Promotes Tumor Cell Motility and Invasion. *Molecular Cancer Research.* 2009 Nov 17;7(11):1756-70.
242. En-lin S, Sheng-guo C, Hua-qiao W. The expression of EFEMP1 in cervical carcinoma and its relationship with prognosis. *Gynecologic Oncology.* Elsevier Inc; 2010 Jun 1;117(3):417-22.
243. Albig AR. Fibulins 3 and 5 Antagonize Tumor Angiogenesis In vivo. *Cancer Res.* 2006 Mar 1;66(5):2621-9.
244. Kim EJ, Lee SY, Woo MK, Choi SI, Kim TR, Kim M-J, et al. Fibulin-3 promoter methylation alters the invasive behavior of non-small cell lung cancer cell lines via MMP-7 and MMP-2 regulation. *Int J Oncol.* Spandidos Publications; 2012 Feb;40(2):402-8.
245. Camaj P, Seeliger H, Ischenko I, Krebs S, Blum H, De Toni EN, et al. EFEMP1 binds the EGF receptor and activates MAPK and Akt pathways in pancreatic carcinoma cells. *Biological Chemistry.* 2009 Oct 29;390(12):1-10.
246. Davidson B, Zhang Z, Kleinberg L, Li M, Flørenes VA, Wang T-L, et al. Gene expression signatures differentiate ovarian/peritoneal serous carcinoma from diffuse malignant peritoneal mesothelioma. *Clin Cancer Res.* American Association for Cancer Research; 2006 Oct 15;12(20 Pt 1):5944-50.
247. Pass HI, Levin SM, Harbut MR, Melamed J, Chiriboga L, Donington J, et al. Fibulin-3 as a blood and effusion biomarker for pleural mesothelioma. *N Engl J Med.* Massachusetts Medical Society; 2012 Oct 11;367(15):1417-27.
248. Schwarz Y, Star A. Role of talc modulation on cytokine activation in cancer patients undergoing pleurodesis. *Pulm Med.* Hindawi Publishing Corporation; 2012;2012(2):806183-6.

249. Corradi M, Goldoni M, Alinovi R, Tiseo M, Ampollini L, Bonini S, et al. YKL-40 and mesothelin in the blood of patients with malignant mesothelioma, lung cancer and asbestosis. *Anticancer Res.* 2013 Dec;33(12):5517-24.
250. Agha MA, El-Habashy MM, El-Shazly RA. Role of fibulin-3 in the diagnosis of malignant mesothelioma. *Egyptian Journal of Chest Diseases and Tuberculosis.* 2014 Jan;63(1):99-105.
251. Demir M, Kaya H, Taylan M, Ekinci A, Yılmaz S, Teke F, et al. Evaluation of New Biomarkers in the Prediction of Malignant Mesothelioma in Subjects with Environmental Asbestos Exposure. *Lung.* Springer US; 2016 Mar 31;194(3):409-17.
252. Kaya H, Demir M, Taylan M, Sezgi C, Tanrikulu AC, Yilmaz S, et al. Fibulin-3 as a Diagnostic Biomarker in Patients with Malignant Mesothelioma. *Asian Pacific Journal of Cancer Prevention.* 2015 Mar 9;16(4):1403-7.
253. Kirschner MB, Pulford E, Hoda MA, Rozsas A, Griggs K, Cheng YY, et al. Fibulin-3 levels in malignant pleural mesothelioma are associated with prognosis but not diagnosis. *Br J Cancer.* 2015 Sep 15;113(6):963-9.
254. Creaney J, Dick IM, Meniawy TM, Leong SL, Leon JS, Demelker Y, et al. Comparison of fibulin-3 and mesothelin as markers in malignant mesothelioma. *Thorax.* BMJ Publishing Group Ltd and British Thoracic Society; 2014 Oct;69(10):895-902.
255. Hooper CE, Lyburn ID, Searle J, Darby M, Hall T, Hall D, et al. The South West Area Mesothelioma and Pemetrexed trial: a multicentre prospective observational study evaluating novel markers of chemotherapy response and prognostication. *Br J Cancer.* Nature Publishing Group; 2015 Mar 10;112(7):1175-82.
256. Moore HM, Kelly AB, Jewell SD, McShane LM, Clark DP, Greenspan R, et al. Biospecimen reporting for improved study quality (BRISQ). Vol. 119, *Cancer cytopathology.* John Wiley & Sons, Inc; 2011. pp. 92-101.
257. Pass HI, Vogelzang N, Carbone M. *Malignant Mesothelioma.* Pass HI, Vogelzang NJ, Carbone M, editors. New York: Springer Science & Business Media; 2006. 1 p.
258. *Mesothelioma Mortality by Geographical Area.* 2018 Mar 13;:1-22.
259. HSE. *The Asbestos Survey.* 2016 Sep 5;:1-150.
260. Thoma A, Farrokhyar F, McKnight L, Bhandari M. Practical tips for surgical research: how to optimize patient recruitment. *Can J Surg.* Canadian Medical Association; 2010 Jun;53(3):205-10.
261. McDonald AM, Knight RC, Campbell MK, Entwistle VA, Grant AM, Cook JA, et al. What influences recruitment to randomised controlled trials? A review of trials funded by two UK funding agencies. *Trials.*

2nd ed. 2006 Apr 7;7(1):1017-8.

262. Sully BGO, Julious SA, Nicholl J. A reinvestigation of recruitment to randomised, controlled, multicenter trials: a review of trials funded by two UK funding agencies. *Trials. BioMed Central*; 2013 Jun 9;14(1):166.
263. Jenkins V, Fallowfield L. Reasons for accepting or declining to participate in randomized clinical trials for cancer therapy. *Br J Cancer. Nature Publishing Group*; 2000 Jun;82(11):1783-8.
264. Cooley ME, Sarna L, Brown JK, Williams RD, Chernecky C, Padilla G, et al. Challenges of recruitment and retention in multisite clinical research. *Cancer Nurs. 2003 Oct*;26(5):376-84-quiz385-6.
265. LeBlanc TW, Lodato JE, Currow DC, Abernethy AP. Overcoming recruitment challenges in palliative care clinical trials. *J Oncol Pract. 2013 Nov*;9(6):277-82.
266. Fischer DJ, Burgener SC, Kavanaugh K, Ryan C, Keenan G. Conducting research with end-of-life populations: overcoming recruitment challenges when working with clinical agencies. *Appl Nurs Res. 2012 Nov*;25(4):258-63.
267. Cox K, McGarry J. Why patients don't take part in cancer clinical trials: an overview of the literature. *Eur J Cancer Care (Engl). 2003 Jun*;12(2):114-22.
268. Treweek S, Lockhart P, Pitkethly M, Cook JA, Kjeldstrøm M, Johansen M, et al. Methods to improve recruitment to randomised controlled trials: Cochrane systematic review and meta-analysis. *BMJ Open. British Medical Journal Publishing Group*; 2013;3(2):e002360.
269. Sygna K, Johansen S, Ruland CM. Recruitment challenges in clinical research including cancer patients and their caregivers. A randomized controlled trial study and lessons learned. *Trials. BioMed Central*; 2015 Sep 25;16(1):428.
270. Monaghan H, Richens A, Colman S, Currie R, Girgis S, Jayne K, et al. A randomised trial of the effects of an additional communication strategy on recruitment into a large-scale, multi-centre trial. *Contemp Clin Trials. 2007 Jan*;28(1):1-5.
271. Shelby-James TM, Hardy J, Agar M, Yates P, Mitchell G, Sanderson C, et al. Designing and conducting randomized controlled trials in palliative care: A summary of discussions from the 2010 clinical research forum of the Australian Palliative Care Clinical Studies Collaborative. *Palliat Med. 2012 Dec*;26(8):1042-7.
272. Watson JM, Torgerson DJ. Increasing recruitment to randomised trials: a review of randomised controlled trials. *BMC Med Res Methodol. BioMed Central*; 2006 Jul 19;6(1):34.
273. Valerie Harkins YH. Use of an Electronic Health Record to Optimize

- Site Performance in Randomized Clinical Trials. *J Clin Trials*. 2014;05(01):1-10.
274. Cowie MR, Blomster JI, Curtis LH, Duclaux S, Ford I, Fritz F, et al. Electronic health records to facilitate clinical research. *Clin Res Cardiol*. Springer Berlin Heidelberg; 2017 Jan;106(1):1-9.
 275. Callard F, Broadbent M, Denis M, Hotopf M, Soncul M, Wykes T, et al. Developing a new model for patient recruitment in mental health services: a cohort study using Electronic Health Records. *BMJ Open*. British Medical Journal Publishing Group; 2014 Dec 2;4(12):e005654.
 276. Dugas M, Lange M, Müller-Tidow C, Kirchhof P, Prokosch H-U. Routine data from hospital information systems can support patient recruitment for clinical studies. *Clin Trials*. 2010 Apr;7(2):183-9.
 277. McGregor J, Brooks C, Chalasani P, Chukwuma J, Hutchings H, Lyons RA, et al. The Health Informatics Trial Enhancement Project (HITE): Using routinely collected primary care data to identify potential participants for a depression trial. *Trials*. 4 ed. BioMed Central; 2010 Apr 15;11(1):39.
 278. Embi PJ, Jain A, Clark J, Bizjack S, Hornung R, Harris CM. Effect of a clinical trial alert system on physician participation in trial recruitment. *Arch Intern Med*. American Medical Association; 2005 Oct 24;165(19):2272-7.
 279. National Lung Cancer Audit pleural mesothelioma report 2016 (for the audit period 2014). 2018 Feb 6;:1-38.
 280. Roberts ME, Neville E, Berrisford RG, Antunes G, Ali NJ, BTS Pleural Disease Guideline Group. Management of a malignant pleural effusion: British Thoracic Society Pleural Disease Guideline 2010. Vol. 65 Suppl 2, *Thorax*. 2010. pp. ii32-40.
 281. Sears D, Hajdu SI. The cytologic diagnosis of malignant neoplasms in pleural and peritoneal effusions. *Acta Cytol*. 1987 Mar;31(2):85-97.
 282. Johnston WW. The malignant pleural effusion. A review of cytopathologic diagnoses of 584 specimens from 472 consecutive patients. *Cancer*. 1985 Aug 15;56(4):905-9.
 283. Hsu C. Cytologic detection of malignancy in pleural effusion: a review of 5,255 samples from 3,811 patients. *Diagn Cytopathol*. 1987 Mar;3(1):8-12.
 284. Chernow B, Sahn SA. Carcinomatous involvement of the pleura: an analysis of 96 patients. *Am J Med*. 1977 Nov;63(5):695-702.
 285. Salyer WR, Eggleston JC, Erozan YS. Efficacy of pleural needle biopsy and pleural fluid cytopathology in the diagnosis of malignant neoplasm involving the pleura. *Chest*. 1975 May;67(5):536-9.
 286. Muruganandan S, Alfonso H, Franklin P, Shilkin K, Segal A, Olsen N, et

- al. Comparison of outcomes following a cytological or histological diagnosis of malignant mesothelioma. *Br J Cancer*. 2017 Mar 14;116(6):703-8.
287. Jennings CJ, Walsh PM, Deady S, Harvey BJ, Thomas W. Malignant pleural mesothelioma incidence and survival in the Republic of Ireland 1994-2009. *Cancer Epidemiol*. 2014 Feb;38(1):35-41.
 288. Domen A, De Laet C, Vanderbruggen W, Gielis J, Hendriks JMH, Lauwers P, et al. Malignant pleural mesothelioma: single-institution experience of 101 patients over a 15-year period. *Acta Chir Belg*. 2017 Jun;117(3):157-63.
 289. Zahid I, Sharif S, Routledge T, Scarci M. What is the best way to diagnose and stage malignant pleural mesothelioma? *Interact Cardiovasc Thorac Surg*. Oxford University Press; 2011 Feb;12(2):254-9.
 290. Ryu J-S, Ryu HJ, Lee S-N, Memon A, Lee S-K, Nam H-S, et al. Prognostic impact of minimal pleural effusion in non-small-cell lung cancer. *J Clin Oncol*. 2014 Mar 20;32(9):960-7.
 291. Tsim S, MacLay J, Milroy RM, Laird B, Blyth KG. 88 Inflammation-based prognostic biomarkers in patients with malignant pleural mesothelioma in the West of Scotland. *Lung Cancer*. Elsevier Ireland Ltd; 2013 Apr 23;79:S31.
 292. Folkman J. Tumor angiogenesis: therapeutic implications. *N Engl J Med*. Massachusetts Medical Society; 1971 Nov 18;285(21):1182-6.
 293. Zetter BR. Angiogenesis and tumor metastasis. *Annu Rev Med*. 1998;49(1):407-24.
 294. Weidner N, Semple JP, Welch WR. Tumor angiogenesis and metastasis—correlation in invasive breast carcinoma. *New England Journal* 1991.
 295. Ellis LM, Fidler IJ. Angiogenesis and breast cancer metastasis. *Lancet*. 1995 Aug 12;346(8972):388-90.
 296. Weidner N, Carroll PR, Flax J, Blumenfeld W, Folkman J. Tumor angiogenesis correlates with metastasis in invasive prostate carcinoma. *AJPA*. American Society for Investigative Pathology; 1993 Aug;143(2):401-9.
 297. Yamazaki K, Abe S, Takekawa H, Sukoh N, Watanabe N, Ogura S, et al. Tumor angiogenesis in human lung adenocarcinoma. *Cancer*. 1994 Oct 15;74(8):2245-50.
 298. Edwards JG, Cox G, Andi A, Jones JL, Walker RA, Waller DA, et al. Angiogenesis is an independent prognostic factor in malignant mesothelioma. *Br J Cancer*. Nature Publishing Group; 2001 Sep 14;85(6):863-8.

299. Kumar-Singh S, Vermeulen PB, Weyler J, Segers K, Weyn B, Van Daele A, et al. Evaluation of tumour angiogenesis as a prognostic marker in malignant mesothelioma. *J Pathol.* 1997 Jun;182(2):211-6.
300. Folkman J. What is the evidence that tumors are angiogenesis dependent? *J Natl Cancer Inst.* 1990 Jan 3;82(1):4-6.
301. Menakuru SR, Brown NJ, Staton CA, Reed MWR. Angiogenesis in pre-malignant conditions. *Br J Cancer.* Nature Publishing Group; 2008 Dec 16;99(12):1961-6.
302. Folkman J, Watson K, Ingber D, Hanahan D. Induction of angiogenesis during the transition from hyperplasia to neoplasia. *Nature.* Nature Publishing Group; 1989 May 4;339(6219):58-61.
303. Hanahan D, Folkman J. Patterns and emerging mechanisms of the angiogenic switch during tumorigenesis. *Cell.* 1996 Aug 9;86(3):353-64.
304. Viacava P, Naccarato AG, Bocci G, Fanelli G, Aretini P, Lonobile A, et al. Angiogenesis and VEGF expression in pre-invasive lesions of the human breast. *J Pathol.* John Wiley & Sons, Ltd; 2004 Oct;204(2):140-6.
305. Chodak GW, Haudenschild C, Gittes RF, Folkman J. Angiogenic activity as a marker of neoplastic and preneoplastic lesions of the human bladder. *Ann Surg.* Lippincott, Williams, and Wilkins; 1980 Dec;192(6):762-71.
306. Merrick DT, Haney J, Petrunich S, Sugita M, Miller YE, Keith RL, et al. Overexpression of vascular endothelial growth factor and its receptors in bronchial dysplasia demonstrated by quantitative RT-PCR analysis. *Lung Cancer.* Elsevier; 2005 Apr;48(1):31-45.
307. McDonald DM, Choyke PL. Imaging of angiogenesis: from microscope to clinic. *Nat Med.* 2003 Jun;9(6):713-25.
308. Dreys J, Schneider V. The use of vascular biomarkers and imaging studies in the early clinical development of anti-tumour agents targeting angiogenesis. *J Intern Med.* Blackwell Publishing Ltd; 2006 Dec;260(6):517-29.
309. Jeswani T, Padhani AR. Imaging tumour angiogenesis. *Cancer Imaging.* 2005;5(1):131-8.
310. Turkbey B, Kobayashi H, Ogawa M, Bernardo M, Choyke PL. Imaging of Tumor Angiogenesis: Functional or Targeted? *American Journal of Roentgenology.* 2009 Aug;193(2):304-13.
311. Lee T-Y, Purdie TG, Stewart E. CT imaging of angiogenesis. *Q J Nucl Med.* 2003 Sep;47(3):171-87.
312. Yi CA, Lee KS, Kim EA, Han J, Kim H, Kwon OJ, et al. Solitary pulmonary nodules: dynamic enhanced multi-detector row CT study

- and comparison with vascular endothelial growth factor and microvessel density. *Radiology*. Radiological Society of North America; 2004 Oct;233(1):191-9.
313. Ohno Y, Koyama H, Matsumoto K, Onishi Y, Takenaka D, Fujisawa Y, et al. Differentiation of malignant and benign pulmonary nodules with quantitative first-pass 320-detector row perfusion CT versus FDG PET/CT. *Radiology*. Radiological Society of North America, Inc; 2011 Feb;258(2):599-609.
 314. Armato SG, Labby ZE, Coolen J, Klabatsa A, Feigen M, Persigehl T, et al. Imaging in pleural mesothelioma: a review of the 11th International Conference of the International Mesothelioma Interest Group. *Lung Cancer*. Elsevier; 2013 Nov;82(2):190-6.
 315. García-Figueiras R, Goh VJ, Padhani AR, Baleato-González S, Garrido M, León L, et al. CT perfusion in oncologic imaging: a useful tool? *AJR American journal of roentgenology*. American Roentgen Ray Society; 2013 Jan;200(1):8-19.
 316. Gill RR, Gerbaudo VH, Sugarbaker DJ, Hatabu H. Current trends in radiologic management of malignant pleural mesothelioma. *Semin Thorac Cardiovasc Surg*. 2009;21(2):111-20.
 317. Brooks PC, Clark RA, Cheresh DA. Requirement of vascular integrin $\alpha v \beta 3$ for angiogenesis. *Science*. 1994 Apr 22;264(5158):569-71.
 318. Robinson SD, Hodivala-Dilke KM. The role of $\beta 3$ -integrins in tumor angiogenesis: context is everything. *Curr Opin Cell Biol*. 2011 Oct;23(5):630-7.
 319. Barrett T, Brechbiel M, Bernardo M, Choyke PL. MRI of tumor angiogenesis. *J Magn Reson Imaging*. Wiley Subscription Services, Inc., A Wiley Company; 2007 Aug;26(2):235-49.
 320. Paldino MJ, Barboriak DP. Fundamentals of quantitative dynamic contrast-enhanced MR imaging. *Magn Reson Imaging Clin N Am*. 2009 May;17(2):277-89.
 321. Fusco R, Sansone M, Filice S, Carone G, Amato DM, Sansone C, et al. Pattern Recognition Approaches for Breast Cancer DCE-MRI Classification: A Systematic Review. *J Med Biol Eng*. Springer Berlin Heidelberg; 2016;36(4):449-59.
 322. Kim JK, Hong SS, Choi YJ, Park SH, Ahn H, Kim C-S, et al. Wash-in rate on the basis of dynamic contrast-enhanced MRI: usefulness for prostate cancer detection and localization. *J Magn Reson Imaging*. Wiley Subscription Services, Inc., A Wiley Company; 2005 Nov;22(5):639-46.
 323. Isebaert S, De Keyser F, Haustermans K, Lerut E, Roskams T, Roebben I, et al. Evaluation of semi-quantitative dynamic contrast-enhanced MRI parameters for prostate cancer in correlation to whole-mount

- histopathology. *Eur J Radiol*. Elsevier; 2012 Mar;81(3):e217-22.
324. Yacoub JH, Oto A, Miller FH. MR imaging of the prostate. *Radiol Clin North Am*. Elsevier; 2014 Jul;52(4):811-37.
 325. van den Boogaart VEM, de Lussanet QG, Houben RMA, de Ruyscher D, Groen HJM, Marcus JT, et al. Inter-reader reproducibility of dynamic contrast-enhanced magnetic resonance imaging in patients with non-small cell lung cancer treated with bevacizumab and erlotinib. *Lung Cancer*. Elsevier Ireland Ltd; 2016 Mar 1;93:20-7.
 326. Choi SH, Jung SC, Kim KW, Lee JY, Choi Y, Park SH, et al. Perfusion MRI as the predictive/prognostic and pharmacodynamic biomarkers in recurrent malignant glioma treated with bevacizumab: a systematic review and a time-to-event meta-analysis. *J Neurooncol*. 2016 Jun;128(2):185-94.
 327. Thukral A, Thomasson DM, Chow CK, Eulate R, Wedam SB, Gupta SN, et al. Inflammatory breast cancer: dynamic contrast-enhanced MR in patients receiving bevacizumab--initial experience. *Radiology*. Radiological Society of North America; 2007 Sep;244(3):727-35.
 328. Koh D-M, Burke S, Davies N, Padley SPG. Transthoracic US of the chest: clinical uses and applications. *Radiographics*. Radiological Society of North America; 2002 Jan;22(1):e1.
 329. Blyth KG, Groenning BA, Martin TN, Foster JE, Mark PB, Dargie HJ, et al. Contrast enhanced-cardiovascular magnetic resonance imaging in patients with pulmonary hypertension. *Eur Heart J*. 2005 Oct;26(19):1993-9.
 330. Benamore RE, O'Doherty MJ, Entwisle JJ. Use of imaging in the management of malignant pleural mesothelioma. *Clin Radiol*. 2005 Dec;60(12):1237-47.
 331. EVANS AL, Gleeson FV. *Radiology in pleural disease: State of the art. Respirology*. 2nd ed. Blackwell Science Pty; 2004 Aug 1;9(3):300-12.
 332. Helm EJ, Matin TN, Gleeson FV. *Imaging of the pleura. J Magn Reson Imaging*. Wiley Subscription Services, Inc., A Wiley Company; 2010 Dec;32(6):1275-86.
 333. Bellin M-F, Van Der Molen AJ. Extracellular gadolinium-based contrast media: An overview. *Eur J Radiol*. Elsevier; 2008 May 1;66(2):160-7.
 334. Lin S-P, Brown JJ. *MR contrast agents: physical and pharmacologic basics. J Magn Reson Imaging*. Wiley Subscription Services, Inc., A Wiley Company; 2007 May;25(5):884-99.
 335. Padhani AR, Dzik-Jurasz A. Perfusion MR imaging of extracranial tumor angiogenesis. *Top Magn Reson Imaging*. 2004 Feb;15(1):41-57.
 336. García-Figueiras R, Padhani AR, Beer AJ, Baleato-González S, Vilanova JC, Luna A, et al. *Imaging of Tumor Angiogenesis for*

- Radiologists--Part 1: Biological and Technical Basis. *Curr Probl Diagn Radiol*. Elsevier; 2015 Sep;44(5):407-24.
337. Chen W, Giger ML, Bick U, Newstead GM. Automatic identification and classification of characteristic kinetic curves of breast lesions on DCE-MRI. *Med Phys*. 2006 Aug;33(8):2878-87.
 338. Buckley DL, Drew PJ, Mussurakis S, Monson JRT, Horsman A. Microvessel density in invasive breast cancer assessed by dynamic gd-dtpa enhanced MRI. *Journal of Magnetic Resonance Imaging*. Wiley Subscription Services, Inc., A Wiley Company; 1997 May 1;7(3):461-4.
 339. Partridge SC, Stone KM, Strigel RM, DeMartini WB, Peacock S, Lehman CD. Breast DCE-MRI: influence of postcontrast timing on automated lesion kinetics assessments and discrimination of benign and malignant lesions. *Acad Radiol*. Elsevier; 2014 Sep;21(9):1195-203.
 340. O'Byrne K, Rusch V. *Malignant Pleural Mesothelioma*. Oxford University Press; 2006. 1 p.
 341. Coleman GC, Shaw PW, Balfour PC Jr., Gonzalez JA, Kramer CM, Patel AR, et al. Prognostic Value of Myocardial Scarring on CMR in Patients With Cardiac Sarcoidosis. *JACC: Cardiovascular Imaging*. 2017 Apr;10(4):411-20.
 342. Nagai T, Kohsaka S, Okuda S, Anzai T, Asano K, Fukuda K. Incidence and prognostic significance of myocardial late gadolinium enhancement in patients with sarcoidosis without cardiac manifestation. *Chest*. 2014 Oct;146(4):1064-72.
 343. Di Marco A, Anguera I, Schmitt M, Klem I, Neilan TG, White JA, et al. Late Gadolinium Enhancement and the Risk for Ventricular Arrhythmias or Sudden Death in Dilated Cardiomyopathy: Systematic Review and Meta-Analysis. *JACC Heart Fail*. 2017 Jan;5(1):28-38.
 344. Gulati A, Jabbour A, Ismail TF, Guha K, Khwaja J, Raza S, et al. Association of fibrosis with mortality and sudden cardiac death in patients with nonischemic dilated cardiomyopathy. *JAMA*. 2013 Mar 6;309(9):896-908.
 345. Doltra A, Amundsen BH, Gebker R, Fleck E, Kelle S. Emerging concepts for myocardial late gadolinium enhancement MRI. *Curr Cardiol Rev*. Bentham Science Publishers; 2013 Aug;9(3):185-90.
 346. Patel AM, Berger I, Wileyto EP, Khalid U, Torigian DA, Nachiappan AC, et al. The value of delayed phase enhanced imaging in malignant pleural mesothelioma. *J Thorac Dis*. 2017 Aug;9(8):2344-9.
 347. Boraschi P, Neri S, Braccini G, Gigoni R, Leoncini B, Perri G. Magnetic resonance appearance of asbestos-related benign and malignant pleural diseases. *Scand J Work Environ Health*. 1999 Feb;25(1):18-23.
 348. Alatas F, Alatas O, Metintas M, Ozarslan A, Erginel S, Yildirim H. Vascular endothelial growth factor levels in active pulmonary

- tuberculosis. *Chest*. 2004 Jun;125(6):2156-9.
349. Matsuyama W, Hashiguchi T, Matsumuro K, Iwami F, Hirotsu Y, Kawabata M, et al. Increased serum level of vascular endothelial growth factor in pulmonary tuberculosis. *Am J Respir Crit Care Med*. American Thoracic Society New York, NY; 2000 Sep;162(3 Pt 1):1120-2.
 350. Coolen J, Vansteenkiste J, De Keyzer F, Decaluwé H, De Wever W, Deroose C, et al. Characterisation of solitary pulmonary lesions combining visual perfusion and quantitative diffusion MR imaging. *Eur Radiol*. Springer Berlin Heidelberg; 2014 Feb;24(2):531-41.
 351. Kambadakone A, Yoon SS, Kim T-M, Karl DL, Duda DG, DeLaney TF, et al. CT perfusion as an imaging biomarker in monitoring response to neoadjuvant bevacizumab and radiation in soft-tissue sarcomas: comparison with tumor morphology, circulating and tumor biomarkers, and gene expression. *AJR American journal of roentgenology*. American Roentgen Ray Society; 2015 Jan;204(1):W11-8.
 352. Qin H-Y, Sun H, Wang X, Bai R, Li Y, Zhao J. Correlation between CT perfusion parameters and microvessel density and vascular endothelial growth factor in adrenal tumors. Chai KX, editor. *PLoS ONE*. Public Library of Science; 2013;8(11):e79911.
 353. Osimani M, Bellini D, Di Cristofano C, Palleschi G, Petrozza V, Carbone A, et al. Perfusion MDCT of prostate cancer: correlation of perfusion CT parameters and immunohistochemical markers of angiogenesis. *AJR American journal of roentgenology*. 2012 Nov;199(5):1042-8.
 354. Ohno Y, Nishio M, Koyama H, Miura S, Yoshikawa T, Matsumoto S, et al. Dynamic contrast-enhanced CT and MRI for pulmonary nodule assessment. *AJR American journal of roentgenology*. American Roentgen Ray Society; 2014 Mar;202(3):515-29.
 355. Vandemoortele T, Laroumagne S, Roca E, Bylicki O, Dales J-P, Dutau H, et al. Positive FDG-PET/CT of the pleura twenty years after talc pleurodesis: three cases of benign talcoma. *Respiration*. Karger Publishers; 2014;87(3):243-8.
 356. Nguyen NC, Tran I, Hueser CN, Oliver D, Farghaly HR, Osman MM. F-18 FDG PET/CT characterization of talc pleurodesis-induced pleural changes over time: a retrospective study. *Clin Nucl Med*. 2009 Dec;34(12):886-90.
 357. Maestrini V, Treibel TA, White SK, Fontana M, Moon JC. T1 Mapping for Characterization of Intracellular and Extracellular Myocardial Diseases in Heart Failure. *Curr Cardiovasc Imaging Rep*. Springer US; 2014;7(9):9287.
 358. Kellman P, Hansen MS. T1-mapping in the heart: accuracy and precision. *J Cardiovasc Magn Reson*. BioMed Central; 2014 Jan

4;16(1):2.

359. Qureshi NR, Gleeson FV. Imaging of Pleural Disease. *Clinics in Chest Medicine*. 2006 Jun;27(2):193-213.
360. Traill ZC, Davies RJ, Gleeson FV. Thoracic computed tomography in patients with suspected malignant pleural effusions. *Clin Radiol*. Elsevier; 2001 Mar;56(3):193-6.
361. Kim JS, Shim SS, Kim Y, Ryu YJ, Lee JH. Chest CT findings of pleural tuberculosis: differential diagnosis of pleural tuberculosis and malignant pleural dissemination. *Acta Radiologica*. SAGE PublicationsSage UK: London, England; 2014 Nov;55(9):1063-8.
362. Falaschi F, Battolla L, Zampa V, Cioni R, Cambi L, Antonelli A, et al. [Comparison of computerized tomography and magnetic resonance in the assessment of benign and malignant pleural diseases]. *Radiol med*. 1996 Dec;92(6):713-8.
363. Tynninen O, Aronen HJ, Ruhala M, Paetau A, Boguslawski Von K, Salonen O, et al. MRI enhancement and microvascular density in gliomas. Correlation with tumor cell proliferation. *Invest Radiol*. 1999 Jun;34(6):427-34.
364. Schlemmer H-P, Merkle J, Grobholz R, Jaeger T, Michel MS, Werner A, et al. Can pre-operative contrast-enhanced dynamic MR imaging for prostate cancer predict microvessel density in prostatectomy specimens? *Eur Radiol*. 2004 Feb;14(2):309-17.
365. Weidner N, Folkman J, Pozza F, Bevilacqua P, Allred EN, Moore DH, et al. Tumor angiogenesis: a new significant and independent prognostic indicator in early-stage breast carcinoma. *J Natl Cancer Inst*. 1992 Dec 16;84(24):1875-87.
366. Borre M, Offersen BV, Nerstrøm B, Overgaard J. Microvessel density predicts survival in prostate cancer patients subjected to watchful waiting. *Br J Cancer*. Nature Publishing Group; 1998 Oct;78(7):940-4.
367. Kadota K, Huang C-L, Liu D, Ueno M, Kushida Y, Haba R, et al. The clinical significance of lymphangiogenesis and angiogenesis in non-small cell lung cancer patients. *Eur J Cancer*. Elsevier; 2008 May;44(7):1057-67.
368. Hasan J, Byers R, Jayson GC. Intra-tumoural microvessel density in human solid tumours. *Br J Cancer*. Nature Publishing Group; 2002 May 20;86(10):1566-77.
369. Vermeulen PB, Gasparini G, Fox SB, Toi M, Martin L, McCulloch P, et al. Quantification of angiogenesis in solid human tumours: an international consensus on the methodology and criteria of evaluation. *Eur J Cancer*. 1996 Dec;32A(14):2474-84.
370. Martin L, Green B, Renshaw C, Lowe D, Rudland P, Leinster SJ, et al. Examining the technique of angiogenesis assessment in invasive

- breast cancer. *Br J Cancer*. Nature Publishing Group; 1997;76(8):1046-54.
371. Barbareschi M, Gasparini G, Morelli L, Forti S, Dalla Palma P. Novel methods for the determination of the angiogenic activity of human tumors. *Breast Cancer Res Treat*. 1995;36(2):181-92.
 372. Sullivan CAW, Ghosh S, Ocal IT, Camp RL, Rimm DL, Chung GG. Microvessel area using automated image analysis is reproducible and is associated with prognosis in breast cancer. *Hum Pathol*. Elsevier; 2009 Feb;40(2):156-65.
 373. Beliën JA, Somi S, de Jong JS, van Diest PJ, Baak JP. Fully automated microvessel counting and hot spot selection by image processing of whole tumour sections in invasive breast cancer. *J Clin Pathol*. BMJ Publishing Group; 1999 Mar;52(3):184-92.
 374. Edge SB, Compton CC. The American Joint Committee on Cancer: the 7th edition of the AJCC cancer staging manual and the future of TNM. *Ann Surg Oncol*. 7 ed. 2010 Jun;17(6):1471-4.
 375. Butchart EG, Ashcroft T, Barnsley WC, Holden MP. Pleuropneumectomy in the management of diffuse malignant mesothelioma of the pleura. Experience with 29 patients. *Thorax*. BMJ Publishing Group; 1976 Feb;31(1):15-24.
 376. Sugarbaker DJ, Strauss GM, Lynch TJ, Richards W, Mentzer SJ, Lee TH, et al. Node status has prognostic significance in the multimodality therapy of diffuse, malignant mesothelioma. *Journal of Clinical Oncology*. 1993 Jun;11(6):1172-8.
 377. Goldstraw P, Crowley J, Chansky K, Giroux DJ. Participating Institutions. The IASLC Lung Cancer Staging Project: proposals for the revision of the TNM stage groupings in the forthcoming (seventh) *J Thorac Oncol*; 2007.
 378. Boutin C, Rey F, Gouvernet J, Viallat JR, Astoul P, Ledoray V. Thoracoscopy in pleural malignant mesothelioma: a prospective study of 188 consecutive patients. Part 2: Prognosis and staging. *Cancer*. 1993 Jul 15;72(2):394-404.
 379. Negrini D, Moriondo A. Pleural function and lymphatics. *Acta Physiol (Oxf)*. 2013 Feb;207(2):244-59.
 380. Nowak AK, Francis RJ, Phillips MJ, Millward MJ, van der Schaaf AA, Boucek J, et al. A Novel Prognostic Model for Malignant Mesothelioma Incorporating Quantitative FDG-PET Imaging with Clinical Parameters. *Clin Cancer Res*. 2010 Apr 14;16(8):2409-17.
 381. Lee HY, Hyun SH, Lee KS, Kim B-T, Kim J, Shim YM, et al. Volume-based parameter of 18)F-FDG PET/CT in malignant pleural mesothelioma: prediction of therapeutic response and prognostic implications. *Ann Surg Oncol*. 2010 Oct;17(10):2787-94.

382. Labby ZE, Straus C, Caligiuri P, MacMahon H, Li P, Funaki A, et al. Variability of tumor area measurements for response assessment in malignant pleural mesothelioma. *Med Phys. American Association of Physicists in Medicine*; 2013 Aug;40(8):081916.
383. Chen M, Helm E, Joshi N, Gleeson F, Brady M. Computer-aided volumetric assessment of malignant pleural mesothelioma on CT using a random walk-based method. *Int J Comput Assist Radiol Surg. Springer International Publishing*; 2017 Apr;12(4):529-38.
384. Weber M-A, Bock M, Plathow C, Wasser K, Fink C, Zuna I, et al. Asbestos-related pleural disease: value of dedicated magnetic resonance imaging techniques. *Invest Radiol. 2004 Sep*;39(9):554-64.
385. Plathow C, Klopp M, Thieke C, Herth F, Thomas A, Schmaehl A, et al. Therapy response in malignant pleural mesothelioma-role of MRI using RECIST, modified RECIST and volumetric approaches in comparison with CT. *Eur Radiol. Springer-Verlag*; 2008 Aug;18(8):1635-43.
386. MD FJHB, PhD TMM, MBChB ID, de Fonseca MBChB D, S ASMBB, PhD JC, et al. A Novel Clinical Prediction Model for Prognosis in Malignant Pleural Mesothelioma Using Decision Tree Analysis. *Journal of Thoracic Oncology. Elsevier Inc*; 2016 Apr 1;11(4):573-82.
387. Edwards JG. Prognostic factors for malignant mesothelioma in 142 patients: validation of CALGB and EORTC prognostic scoring systems. *Thorax. 2000 Sep 1*;55(9):731-5.
388. Prodhomme O, Seguret F, Martrille L, Pidoux O, Cambonie G, Couture A, et al. Organ volume measurements: comparison between MRI and autopsy findings in infants following sudden unexpected death. *Arch Dis Child Fetal Neonatal Ed. BMJ Publishing Group*; 2012 Nov;97(6):F434-8.
389. Frauenfelder T, Tutic M, Weder W, Götti RP, Stahel RA, Seifert B, et al. Volumetry: an alternative to assess therapy response for malignant pleural mesothelioma? *Eur Respir J. European Respiratory Society*; 2011 Jul;38(1):162-8.
390. Sargent DJ, Rubinstein L, Schwartz L, Dancey JE, Gatsonis C, Dodd LE, et al. Validation of novel imaging methodologies for use as cancer clinical trial end-points. *Eur J Cancer. 2009 Jan*;45(2):290-9.
391. Liu F, Zhao B, Krug LM, Ishill NM, Lim RC, Guo P, et al. Assessment of therapy responses and prediction of survival in malignant pleural mesothelioma through computer-aided volumetric measurement on computed tomography scans. *J Thorac Oncol. 2010 Jun*;5(6):879-84.
392. Emirzeoglu M, Sahin B, Selcuk MB, Kaplan S. The effects of section thickness on the estimation of liver volume by the Cavalieri principle using computed tomography images. *Eur J Radiol. 2005 Dec*;56(3):391-7.
393. Milano MT, Zhang H. Malignant pleural mesothelioma: a population-

- based study of survival. *J Thorac Oncol*. 2010 Nov;5(11):1841-8.
394. Taioli E, Wolf AS, Flores RM. Meta-analysis of survival after pleurectomy decortication versus extrapleural pneumonectomy in mesothelioma. *Ann Thorac Surg*. 2015 Feb;99(2):472-80.
 395. Treasure T, Waller D, Tan C, Entwisle J, O'Brien M, O'Byrne K, et al. The Mesothelioma and Radical surgery randomized controlled trial: the Mars feasibility study. *J Thorac Oncol*. 2009 Oct;4(10):1254-8.
 396. Plathow C, Schoebinger M, Fink C, Hof H, Debus J, Meinzer H-P, et al. Quantification of lung tumor volume and rotation at 3D dynamic parallel MR imaging with view sharing: preliminary results. *Radiology*. Radiological Society of North America; 2006 Aug;240(2):537-45.
 397. Geets X, Lee JA, Bol A, Lonneux M, Grégoire V. A gradient-based method for segmenting FDG-PET images: methodology and validation. *Eur J Nucl Med Mol Imaging*. Springer-Verlag; 2007 Sep;34(9):1427-38.
 398. Kitajima K, Doi H, Kuribayashi K, Hashimoto M, Tsuchitani T, Tanooka M, et al. Prognostic value of pretreatment volume-based quantitative 18F-FDG PET/CT parameters in patients with malignant pleural mesothelioma. *Eur J Radiol*. 2017 Jan;86:176-83.
 399. Armato SG III, Li P, Husain AN, Straus C, Khanwalkar A, Kindler HL, et al. Radiologic-Pathologic Correlation of Mesothelioma Tumor Volume. *Lung Cancer*. 2015 Jan.
 400. Kircheva DY, Husain AN, Watson S, Kindler HL, Durkin A, Vigneswaran WT. Specimen weight and volume: important predictors of survival in malignant pleural mesothelioma. *Eur J Cardiothorac Surg*. 2016 Jun;49(6):1642-7.
 401. Armato SG, Nowak AK, Francis RJ, Kocherginsky M, Byrne MJ. Observer variability in mesothelioma tumor thickness measurements: defining minimally measurable lesions. *J Thorac Oncol*. 2014 Aug;9(8):1187-94.
 402. Curran D, Sahmoud T, Therasse P, van Meerbeeck J, Postmus PE, Giaccone G. Prognostic factors in patients with pleural mesothelioma: the European Organization for Research and Treatment of Cancer experience. *Journal of Clinical Oncology*. 1998 Jan;16(1):145-52.
 403. Herndon JE, Green MR, Chahinian AP, Corson JM, Suzuki Y, Vogelzang NJ. Factors predictive of survival among 337 patients with mesothelioma treated between 1984 and 1994 by the Cancer and Leukemia Group B. *Chest*. 1998 Mar;113(3):723-31.
 404. Kidd AC, McGettrick M, Tsim S, Halligan DL, Bylesjo M, Blyth KG. Survival prediction in mesothelioma using a scalable Lasso regression model: instructions for use and initial performance using clinical predictors. *BMJ Open Respir Res. Archives of Disease in childhood*; 2018;5(1):e000240.

405. Byrne MJ, Nowak AK. Modified RECIST criteria for assessment of response in malignant pleural mesothelioma. *Ann Oncol*. 2004 Feb;15(2):257-60.
406. Labby ZE, Armato SG, Kindler HL, Dignam JJ, Hasani A, Nowak AK. Optimization of response classification criteria for patients with malignant pleural mesothelioma. *J Thorac Oncol*. 2012 Nov;7(11):1728-34.
407. van Klaveren RJ, Aerts JGJV, de Bruin H, Giaccone G, Manegold C, van Meerbeeck JP. Inadequacy of the RECIST criteria for response evaluation in patients with malignant pleural mesothelioma. *Lung Cancer*. 2004 Jan;43(1):63-9.
408. Blayney JK, Ceresoli GL, Castagneto B, O'Brien MER, Hasan B, Sylvester R, et al. Response to chemotherapy is predictive in relation to longer overall survival in an individual patient combined-analysis with pleural mesothelioma. *Eur J Cancer*. 2012 Nov;48(16):2983-92.
409. Cheng L, Tunariu N, Collins DJ, Blackledge MD, Riddell AM, Leach MO, et al. Response evaluation in mesothelioma: Beyond RECIST. *Lung Cancer*. 2015 Dec;90(3):433-41.
410. Hu Z-D. Circulating biomarker for malignant pleural mesothelioma diagnosis: pay attention to study design. *J Thorac Dis*. 2016 Oct;8(10):2674-6.
411. Baldwin DR, Callister MEJ, Guideline Development Group. The British Thoracic Society guidelines on the investigation and management of pulmonary nodules. *Thorax*. 2015 Aug;70(8):794-8.
412. Murphy DJ, Gill RR. Volumetric assessment in malignant pleural mesothelioma. *Ann Transl Med*. 2017 Jun;5(11):241-1.